DOCTOR OF PHILOSOPHY

Endogenous neurosteroid actions at GABAA receptors during neuronal development

Brown, Adam R.

Award date:
2011

DOCTOR OF PHILOSOPHY

Endogenous neurosteroid actions at GABAA receptors during neuronal development

Adam R. Brown

2011

University of Dundee

Chapter 1

Introduction

1.1. GABA and the GABA receptors

1.1.1. GABA and the GABA receptors: a brief history

Gamma-aminobutyric acid, (GABA) is the major inhibitory transmitter in the mammalian central nervous system (CNS). However, for many years the concept that a small amino acid could have such a fundamental role in fast neuronal communication, proved controversial. In 1950 GABA was found to be present in the brain in considerable quantities and primarily in its free form following decarboxylation of glutamic acid, (Awapara *et al*., 1950; Roberts & Frankel, 1950; Udenfriend, 1950). These early biochemical studies made no suppositions pertaining to the inhibitory actions of GABA and were unconnected to the contemporaneous body of research seeking the chemical identity of the central neurotransmitters. The adrenergic and cholinergic control of the peripheral nervous system described in the 1930s, gave tantalizing clues into the possible mode of neurotransmission in the CNS, an area where investigation had been hampered by technical deficiencies. However, by using a pioneering intracellular microelectrode recording technique, J. C. Eccles was the first to successfully observe synaptic potentials inside spinal motor neurones (Brock *et al.,* 1951). This study confirmed the presence of a chemical rather than an electrical mechanism of information transfer from one neurone to another. Subsequently, efforts to identify the inhibitory chemical were greatly helped by Ernst Florey's work with a neuronal preparation derived from crayfish. Florey demonstrated that an unknown extract of the CNS, named 'Factor I', inhibited firing of the crayfish stretch receptor neurone (Florey, 1954). Soon, continued investigations involving the testing of numerous brain chemicals on this crayfish neurone preparation demonstrated that GABA mirrored all the actions observed with Factor I (Bazemore *et al.,* 1956). Despite these observations, further development of the GABA hypothesis was stalled by a

mixture of skepticism and negative findings. Florey himself dismissed GABA as the inhibitory transmitter, mainly because it could not be detected in chromatograms of Factor I (McLennan, 1958) and due to differences in action between Factor I and GABA on intestinal muscle (Florey & McLennan, 1959). Moreover, the topical application of GABA to exposed cortical tissue yielded inconclusive effects on the evoked potentials recorded by a crude silver wire electrode placed on the cortical surface (Iwama & Jasper, 1957; Purpura *et al*., 1957). However, further evidence of GABA's inhibitory action was inferred by microiontophoretic GABA application, a technique allowing a greater level of refinement by restricting the exposure of GABA to only a few cells. Eccles and colleagues used multi-barrelled delivery pipettes to systematically test the action of various amino acids upon neuronal activity in the spinal cord. They reported that GABA and β-alanine (a structurally related amino acid) reliably inhibited all types of spinal neurones (Curtis *et al.,* 1959). Yet the GABA-induced inhibition was not blocked by strychnine (at that time a recognized inhibitor of glycine-induced hyperpolarizing responses) and there remained no evidence that GABA had hyperpolarizing actions. As a result the authors deemed the effects of GABA to be 'non-specific', a conclusion that precipitated several years of stagnation with respect to GABA research. Eventually, decisive experiments were performed that sought to compare the properties of neurally-evoked inhibitory post synaptic potentials (IPSPs) and GABA-induced inhibition on the membrane potential. Using GABA iontophoresis, in conjunction with intracellular recording (thus allowing sensitive measurement of the membrane potential), two separate groups demonstrated that GABA application to either cortical neurones or neurones of the lateral vestibular nucleus, could closely imitate the hyperpolarising nature and associated Cl^- influx of IPSPs (Krnjevic & Schwartz, 1967; Obata *et al.,* 1967; Dreifuss *et al.,* 1969). Finally, it was proposed that GABA was the major inhibitory transmitter in the brain, a concept that was confirmed

by the selective block in cortex of GABA-evoked responses and IPSPs by bicuculline and picrotoxin (Curtis *et al.,* 1970). At approximately this time, GABA concentrations were shown to be much higher in inhibitory *vs* excitatory neurones and it was found that GABA release could be induced following stimulation of inhibitory neurones (Roberts *et al.*, 1970). In the 1970s mouse spinal neurone cultures were used extensively in conjunction with intracellular recording techniques to reveal that a diverse array of clinically relevant compounds could mimic (*i.e.* GABAmimetic), modulate or block the GABA response (see Section 1.1.8 regarding GABA pharmacology, Choh *et al*., 1977 Macdonald & Barker, 1977; Macdonald & Barker, 1978a; Macdonald & Barker, 1978b; Macdonald & Barker 1979a; Macdonald & Barker, 1979b). Application of the newly-refined patch clamp technique (Neher & Sakmann, 1976), allowed Hamill and colleagues, using spinal cord and hippocampal neurones maintained in cell culture, to demonstrate the existence of single, GABA activated, Cl^- channels that were blocked by bicuculline (Hamill *et al.*, 1983).

Advances in molecular biology resulted in the cloning of the subunits that form $GABA_A$Rs, an endeavor that revealed structural similarities to nicotinic acetylcholine (nACh) receptor subunits (Schofield *et al.,* 1987; Pritchett *et al*., 1989; see Section 1.1.3). The subsequent cloning of a diverse array of subunits uncovered a heterogeneity that is now known to give rise to multiple native $GABA_A$Rs (McKernan & Whiting 1996; Olsen & Sieghart, 2008). Each receptor subunit isoform shows distinct regional and even cellular expression patterns in the brain, a diversity that is mirrored by individual receptor subtypes with specific physiological and pharmacological profiles. $GABA_A$Rs are members of the Cys-loop ligand-gated ion channel (LGIC) superfamily that also includes strychnine sensitive glycine receptors, nicotinic ACh receptors and 5HT3 receptors (Olsen & Sieghart, 2008).

$GABA_A$Rs exhibit a rich pharmacology and are the target for many clinically relevant drugs (D'Hulst *et al*., 2009). Many of these compounds allosterically potentiate the GABA response (positive modulators) and include benzodiazepines, barbiturates, certain general anaesthetics as well as neurosteroids. On the other hand compounds that inhibit $GABA_A$Rs are convulsant and include the competitive antagonist bicuculline and the non-competitive antagonist picrotoxin (Hevers & Luddens, 1998; Johnston *et al*; 2005; D'Hulst *et al*., 2009). A detailed overview of $GABA_A$R subtypes with an emphasis on their expression, biophysics, pharmacology and contribution to certain behaviours is given in Sections 1.1.6 and 1.1.8.

In addition to the GABA-gated Cl^- permeable ion channel, further investigations highlighted a bicuculline-insensitive component of the GABA response, for example in sympathetic nerve terminals of rat aortic and vasa deferentia tissue (Bowery & Hudson, 1979). This led to the discovery of a second, slower mode of GABA transmission giving rise to the distinction between $GABA_A$ (bicuculline sensitive) and $GABA_B$ (bicuculline insensitive) receptors ($GABA_B$Rs, Bowery *et al*., 1980; Hill & Bowery, 1981). Although also activated by GABA, $GABA_B$ receptors utilize completely different transduction mechanisms to produce their cellular effect. As described above, the $GABA_A$Rs are members of the LGIC superfamily. By contrast, it is now known that $GABA_B$Rs belong to the class of 7-transmembrane spanning receptors linked to G-proteins which and have been shown to be present in almost all regions of the brain at both inhibitory and excitatory synapses (Ulrich & Bettler, 2007). At the presynaptic terminal, $GABA_B$Rs release G-protein subunits that block Ca^{2+} channels such that neurotransmitter release is suppressed (Mintz & Bean, 1993; Ulrich & Bettler, 2007) whereas at the postsynaptic cell, $GABA_B$Rs elicit a slow inhibitory post synaptic potential ($IPSP_B$) through activation of K^+ channels that hyperpolarize the membrane and shunt excitatory currents (Gähwiler & Brown, 1985; Ulrich & Bettler, 2007).

Alternatively, $GABA_BR$ activation may, via G-protein subunit dissociation, inhibit adenylate cyclase (Xu & Wojcik, 1986; Bowery, 1993) leading to reduced cAMP levels and a subsequent reduction of protein kinase A (PKA) activity, which in turn may influence the activity of many downstream targets (reviewed in Bowery & Enna, 2000; Ulrich & Bettler, 2007; Chalifoux & Carter, 2011).

A third class of GABA receptor, termed $GABA_CR$, was reported in 1984 based on the observation of a bicuculline- and baclofen-insensitive GABA binding site in neuronal membranes derived from rat cerebellum (Drew *et al*., 1984). The abundance of $GABA_CRs$ in the nervous system was found to be comparatively low, occurring at high levels most notably in the vertebrate retina and, to a lesser extent, at various CNS locations including the spinal cord and cerebellum (Cutting *et al*., 1991; Park *et al*., 1999; Rozzo *et al*., 2002). Subsequently, it was discovered that when mRNA isolated from bovine retina was injected into *Xenopus laevis* oocytes, functional GABA-gated chloride channels were expressed (*i.e.* now commonly termed $GABA_CRs$, but see below) that displayed GABA-induced Cl^- responses that were insensitive to bicuculline and the $GABA_BR$ agonist, baclofen and showed no modulation by barbiturates or benzodiazepines (Polenzani *et al*., 1991, for a description of the ρ subunit cloning process, see Section 1.1.3.2). Shortly after, the ρ subunit cDNA was cloned from a human retina cDNA library and, when expressed as a single subunit in *Xenopus* oocytes, recombinant homo- oligomeric GABA-gated Cl^- channels were formed that conferred the same insensitivity to bicucuclline and baclofen (Cutting *et al*., 1991; Shimada *et al*., 1992). It is now evident that there are three ρ subunit subtypes (ρ1-3), each showing a high level of sequence homology with other $GABA_AR$ subunits (Bormann, 2000).

1.1.2. GABA synthesis, metabolism, release and reuptake

1.1.2.1. Synthesis

The synthesis of GABA in the nervous system occurs by decarboxylation of the parent compound glutamate, by glutatamic acid decarboxylase (GAD; Awapara *et al*., 1950; Roberts & Frankel, 1950). In addition, a form of vitamin B6 called pyridoxal phosphate (PLP) is an essential co-factor for the conversion of glutamate to GABA. If PLP is removed, then GAD activity is suppressed, an effect that is readily reversed upon PLP replacement (Nicholls *et al*., 2001). Two isoforms of GAD exist which are denoted by their molecular masses, GAD 65 and GAD 67 (Wei & Wu, 2008). Despite having near identical amino acid sequences, the two GAD isoforms can be distinguished by their subcellular distribution. GAD 65 is found to be predominantly associated with synaptic vesicle membranes in nerve terminals, a location that may infer a role in fast, neurone-to-neurone GABA neurotransmission (Kaufman *et al*., 1991; Tian *et al*., 1999). By contrast, GAD 67 is found distributed evenly throughout the various cellular compartments, implicating this protein in providing GABA required for trophic or metabolic actions (Kaufman *et al*., 1991, Owens & Kriegstein, 2002). Moreover, evidence from a combination of biochemical and structural studies has confirmed GAD 67 to be constitutively active (holoenzymatic) such that it may establish a basal GABA pool. On the other hand GAD 65 is largely present in an inactive (apoenzyme) form and can be induced by neuronal activity to provide extra GABA for neurotransmission ‘on demand’ (Kaufmann *et al*., 1991; Martin *et al*., 1991; Fenalti *et al*., 2007).

1.1.2.2. Metabolism

GABA is metabolized to succinic semialdehyde by GABA α-oxoglutarate transaminase (GABA-T). In turn, succinic semialdehyde is converted to succinic acid and re-enters the Krebs cycle (Madsen *et al*., 2008). Alternatively, GABA that is not back-metabolized may be packaged into synaptic vesicles in preparation for endocytotic release (Madsen *et al*., 2008). This process requires GABA transporter proteins located in the vesicular membrane (VGATs; McIntire *et al*., 1997) that operate by secondary active transport, being energetically coupled to a proton gradient established by hydrogen ATP-ase pumps. Proton efflux *via* the vesicular GABA transporter is exchanged for GABA transport into the lumen in a 1:1 stoichiometry (Gasnier, 2004; Figure 1.1).

1.1.2.3. Release

In keeping with all other neurotransmitters, the principal mechanism of GABA release is exocytosis, following a rise in intracellular Ca^{2+} concentration. Briefly, synaptic vesicles loaded with GABA sit docked with the intracellular side of the pre-synaptic membrane from which transmitter release occurs. The exocytotic process appears to be conserved for all neurotransmitter classes and involves a finely orchestrated interplay between a group of proteins collectively termed SNAREs (Jahn & Scheller, 2006; Martens & McMahon, 2008). Initiation of this process begins when Ca^{2+}, upon entering the presynaptic bouton through N and P type voltage gated Ca^{2+} channels (VGCCs), binds to the vesicle-bound protein synaptotagmin, promoting the close association between a second vesicular-bound protein, synaptobrevin and the membrane-bound protein synaptotaxin (Jahn & Scheller, 2006; Martens & McMahon, 2008). This process brings the vesicle into close proximity with the nerve terminal membrane and precedes

vesicular fusion. Such a rapid release mechanism is facilitated by a tight spatial organization between the VGCCs and the docked vesicle meaning that release is near instantaneous (< 1 ms) following Ca^{2+} entry (Nicholls *et al*., 2001; Sudhof, 2004; Jahn & Scheller, 2006; Martens & McMahon, 2008). After discharging the stored GABA into the synaptic cleft, the empty vesicle is endocytosed back into the cytosol where it becomes part of a larger endosomal membrane from which new vesicles are made (Sudhof, 2004).

1.1.2.4. Re-uptake

Early investigations into the identity of the brain's inhibitory transmitter were clouded by the then dogma dictating that an essential property of a 'true' neurotransmitter was the existence of an enzymatic system responsible for the termination of neurotransmitter action - a mechanism that had been shown to be true in the case of acetylcholine esterase mediated metabolism of ACh (Krnjevic, 2005). This belief was dispelled in 1968 when GABA uptake in slices of rat cerebral cortex was observed, demonstrating the existence of high-affinity GABA transporters (Iversen & Neal, 1968). It is now known that in conjunction with GABA diffusion from the cleft (see Section 1.1.4), the termination of GABA-mediated synaptic events is aided, by the rapid removal of the released GABA by GABA transporters (traditionally termed GATs). GATs are located in the plasma membrane of GABA-ergic interneurones, in addition to being expressed in glia and are distinct to the GABA transporters required for vesicular storage described above. Along with cellular transporters for glycine, noradrenaline, 5-HT and dopamine, GATs are encoded for by corresponding members of the *SLC6* gene family and are 12-transmembrane spanning proteins that couple Na^+ influx with transmitter and Cl^- translocation (Table 1.1; Kanner, 2006). This process utilizes the energy derived

from the transport of Na^+ down its electrochemical gradient, a process that is therefore secondary to the energy required to maintain the Na^+ gradient (performed predominantly by Na^+-K^+ ATPase pumps). For each molecule of GABA transported, two Na^+ ions and one Cl^- ion enter the cytoplasm (Keynan & Kanner, 1988). To date, four distinct GABA transporters have been identified in the mouse; GAT1, GAT2, GAT3 and GAT4 consisting of 598, 614, 602 and 627 amino acids, respectively (Liu *et al.,* 1992, 1993). Each GAT subtype exhibits a differential apparent K_m for GABA transport (GAT1, 7 μM; GAT2, 79 μM; GAT3, 18 μM; GAT4, 0.7 μM) and GAT2 has been shown to have affinity for the osmolyte betaine. A betaine-GABA transporter (BGT-1) has also been cloned in rat, canine, and human and is homologous to the murine GAT2 (Yamauchi *et al*., 1992; Borden *et al*., 1995; Burnham *et al*., 1996). Unfortunately, a cloning process that has spanned at least three different species and performed by multiple laboratories has resulted in a confusing GABA transporter nomenclature (summarized in Table 1.1). As mice have been used in the present study, the murine terminology will be used unless otherwise stated.

In addition to the transportation of GABA, GAT3 and GAT4 transport β-alanine (K_m = 28 and 99 μM respectively) and taurine (K_m = 540 μM and 1.4 mM respectively, Liu *et al.*, 1993). These actions are of interest since both taurine and β-alanine can directly activate $GABA_A$Rs (Albrecht & Schousboe, 2005; Jia *et al*., 2008, see Section 1.1.5.2). Furthermore, extracellular levels of taurine and β-alanine are regulated by the taurine transporters (TauT1 and TauT2), which are additional members of the *SLC6* transporter family and show between 50-60% homology with the GABA transporters (Nelson *et al*., 1998). In recombinant expression systems, TauTs exhibit a K_m of 4.5 μM for taurine and 56 μM for β-alanine (Liu *et al.*, 1992).

Species	*Nomenclature*			
SLC6 gene	*SLC6a1*	*SLC6a12*	*SLCa13*	*SLCa11*
Mouse	GAT1	GAT2	GAT3	GAT4
Rat	GAT-1	BGT-1	GAT-2	GAT-3
Human	GAT-1	BGT-1	GAT-2	GAT-3
HUGO	**GAT1**	**BGT1**	**GAT2**	**GAT3**

Table 1.1. Summary of GABA transporter nomenclature. The nomeclaturefor three species is shown including a proposal by the HUGO Gene Nomenclature Committee. Table modified from Madsen *et al*., 2010.

A combination of studies using rodent, primate and human tissue have highlighted that GABA transporters display distinct cellular expression profiles in the brain. In particular, GAT1 is widely distributed (Durkin *et al*., 1995) and is primarily localized to pre-synaptic terminals (Conti *et al*., 1998; 2011). GAT2 expression has been reported both in the cortex and hippocampus where surprisingly it is not found in the vicinity of the GABA-ergic synapse but in extrasynaptic and predominantly astrocytic locations (Borden *et al*., 1995; Zhu & Ong, 2004). Moreover, GAT2 has a relatively weak affinity for GABA transport in comparison to the other GATs, a finding that has cast doubt over whether GAT2 has a major role in GABA reuptake. Alternatively, there is evidence suggesting that GAT2 has a specialized physiological function that is distinct from the other GATs, in particular involving the regulation of neuronal and astrocytic osmolarity following exocytotic injury (Zhu & Ong, 2004). GAT3 has more limited expression in the brain, being present early during development, in meningeal tissue and potentially at low levels at extrasynaptic sites in neurones and astrocytes (Liu *et al*., 1993; Conti *et al*., 2004; Madsen *et al*., 2010). GAT4 has been found to be localized mainly to distal astrocytic processes that are in direct contact with GABAergic interneurones (Durkin *et al*., 1995; Minelli *et al*., 1996). At the mRNA level, TauT1 is predominantly found in ocular neurones and the cerebellum (Vinnakota *et al.*, 1997), whereas TauT2 mRNA is highly expressed in the brain stem, striatum, thalamus, cerebellum, corpus callosum and anterior commisure (Liu *et al*., 1992; Smith *et al*., 1992). The processes involved in GABA release, re-uptake and metabolism are summarized in Figure 1.1.

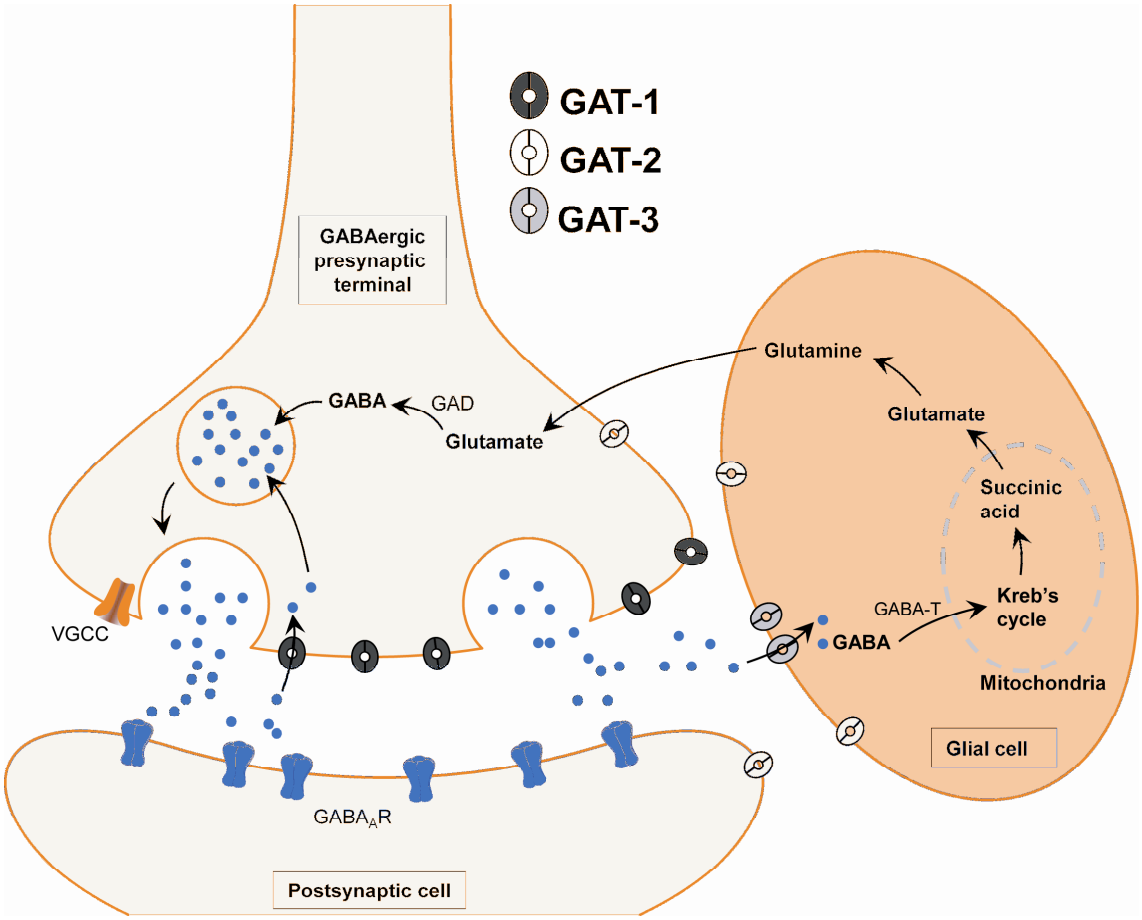

Figure 1.1. GABA release, reuptake and metabolism. A rudimentary schematic representation of the major events involved in GABA release, reuptake and metabolism at a cortical synapse. GABA is packaged into synaptic vesicles *via* VGATs. After vesicular docking with the pre-synaptic membrane, Ca^{2+} influx initiates the exocytosis of GABA into the cleft. GABA binding to $GABA_A$ (and $GABA_B$) receptors follows. Termination of the postsynaptic response is influenced by high-affinity GABA transporters (GATs), that exhibit distinct subcellular expression profiles. A highly simplified spatial organization is shown wherein GAT1 is putatively the predominant GABA transporter in the brain and is localized primarily to the pre-synaptic membrane. GAT3 displays a low level of expression in the mature brain, but may be present extrasynaptically in some neuronal populations, in addition to being expressed in distal astrocytic processes. Synaptic localization of GAT3 is sparse. GAT4 is largely confined to distal astrocytic processes with little, if any, existing neuronally. Note that the localization and role of GAT2 is not shown due to doubt over its role in GABA re-uptake. Following astrocytic reuptake, GABA is converted to glutamine which maybe transported back to the GABAergic neurone. Neuronal synthesis of GABA is achieved by decarboxylation of glutamate by GAD65/67. This Figure is modified from Conti *et al*., 2004. VGCC, voltage gated Ca^{2+} channel. GABA-T, GABA transaminase. GAD, glutamic acid decarboxylase.

Given that GABA transporters are crucial to the control of neuronal excitability, they represent a prospective therapeutic target for the treatment of disease states such as epilepsy, in which an inbalance in neuronal excitability is a pathophysiological feature (Madsen *et al*., 2010). To this end, GABA transporter blockers have been synthesized with differing degrees of potency and subtype selectivity. The best known of the GABA transporter inhibitors are nipecotic acid and guavacine, both of which were originally derived by chemical modification of the parent compound β-alanine (Clausen *et al*., 2006). Further chemical modification of these compounds led to the development of NO-771, SNAP-5114 and tiagabine – the latter being a licenced treatment for partial epileptic seizures (Madsen *et al*., 2010). Tiagabine and NO711 show selectivity for GAT1 (Clausen *et al*., 2006) however, nipecotic acid is non-specific and SNAP-5114 exhibits a preference for GAT2/3 (Kragler *et al.*, 2005).

1.1.3. $GABA_AR$ structure and heterogeneity

1.1.3.1. Molecular structure and activation

$GABA_ARs$ belong to the Cys-loop pentameric ligand gated ion channel (LGIC) super-family, which incorporates the strychnine-sensitive glycine gated chloride ion channel (GlyR; Breitinger & Becker, 2002), the nicotinic acetylcholine receptor (nAChR; Corringer *et al*., 2000), the ionotropic 5-HT3 receptor ($5\text{-}HT_3R$; Barnes *et al*., 2009), and the zinc-activated ion channel (ZAC; Hales & Peters, 2010). Of these members of the Cys-loop family, the $GABA_AR$ and GlyR are selective for anionic species (principally Cl^-) and therefore consequently in the majority of cases their activation exerts an inhibitory action (though see Section 1.1.4 regarding developmental Cl^- regulation).

Individual $GABA_AR$ subunits have a molecular mass ranging between 40 and 60 kDa resulting in pentameric receptors between 240 and 290 kDa (Hevers & Lüddens, 1998). Each subunit has a large extracellular, hydrophilic N-terminal domain containing the GABA-binding site in addition to a closed loop resulting from a 13 residue signature flanked by covalently bonded cysteines, features that are conserved across all members of the Cys-loop family (Simon *et al*., 2004; Olsen & Sieghart, 2008). This portion of the subunit precedes four hydrophobic transmembrane domains (TM1-4), and a relatively short extracellular C-terminus. The transmembrane domains display a large intracellular loop between the TM3 and TM4 region which contribute to the ion conduction pathway (Peters *et al*., 2005; Carland *et al*., 2009). In addition the intracellular domains of the β1-3 and γ2 subunits contain consensus regions for multiple protein kinases (Kittler & Moss, 2003; Jacob *et al*., 2008). Phosphorylation of serine and threonine residues located within the M3-M4 loop may serve as an important regulator of ion channel function (Hinkle & Macdonald, 2003; Houston *et al*., 2008). Moreover, the TM3-TM4 cytosolic loop contains target sites for protein-protein interactions that are of importance for sub-cellular trafficking and membrane clustering of the receptor (for detailed reviews concerning these processes see Kittler and Moss, 2003; Chen and Olsen, 2007; Jacob *et al.*, 2008; Vithlani *et al*., 2011; Lüscher *et al*., 2011). Individual $GABA_AR$ subunits are organized such that the ion channel lining is formed by the transmembrane α-helices from the second transmembrane domain while TM1, TM3 and TM4 form a lipid interface thereby protecting M2 from a hydrophobic environment (Connolly & Wafford, 2004).

The topographical organization of Cys-loop LGIC receptors has been most closely studied for the nACh receptor of the *Torpedo* electric organ (Unwin *et al*., 2003). Uniquely, this tissue provides a high density of nACh receptors in large

postsynaptic membrane sheets from which membranes with a surface lattice of receptors can be formed. Application of optical diffraction techniques has resulted in a low-resolution, three dimensional structure of the receptor molecule. These studies unequivocally confirmed a pentameric receptor assembly formed around a central, water filled, pore (Toyoshima & Unwin, 1988; Unwin, 1993). Subsequently, a similar approach verified that native porcine $GABA_AR$s also form pentameric membrane-spanning receptors in which the composite subunits assemble to create a central, ion-conducting pore (Nayeem *et al*., 1994).

A high resolution structure of the complete nAChR molecule together with the precise details of the conformational changes that take place following ligand binding, gating and desensitization, remains to be fully elucidated. Electron microscopy data from *Torpedo* nAChR preparations have provided a receptor structure with a 4 Å resolution (Miyazawa *et al*., 2003; Unwin, 2005). Furthermore, the collective findings of studies examining, at high resolution, various component parts of similar LGICs have provided additional insights. In particular, X-ray structures of the AChBP-binding protein from snail (a soluble protein homolog of the nAChR extracellular domain) at a resolution of up to 1.76 Å have been reported (Brejc *et al*., 2001; Sixma & Smit, 2003). Similarly, the crystal structure of the extracellular domain of the mouse nAChR α1 subunit bound to α-bungarotoxin has been revealed at a resolution of 1.94 Å (Dellisanti *et al*., 2007). Most recently, the identification of pentameric ligand-gated ion channel homologs in prokaryotes (Tasneem *et al*., 2005) has allowed the field to move to the atomic level. The advantage of using bacterial LGIC homologs, notably those found in *Gloeobacter violaceus* (named GLIC) and *Erwinia chrysanthemi* (named ELIC), is that they can be applied to the highly efficient *E.coli* expression system as a way of providing protein levels in amounts that are compatible with X-ray crystallography analysis (Bocquet *et al*., 2007; Corringer *et al*., 2010). Finally, the first X-ray structure

of a eukaryotic Cys-loop receptor - a glutamate gated chloride channel from *C. elegans* - has recently been described (Hibbs & Gouaux, 2011).

From these interconnecting avenues of research, a general hypothesis of ligand-induced receptor gating has emerged using the nicotinic receptor as a model template. Briefly, the ACh binding pocket is located in the subunit interface of the extracellular amino terminal domain and is constructed from 6 loops, A-F (Corringer *et al*., 2000). Residues implicated in ligand binding are situated in loops A, B and C of the β subunit, and loops D and E of the α subunit (Amin & Weiss, 1993; Corringer *et al*., 2000; Brejc *et al*., 2001; Boileau *et al*., 2002; Torres & Weiss 2002). Hence, combining electrophysiological and homology modeling evidence favours a direct interaction between GABA and loops A-E whereas the role of loop F is less clear, although it has been postulated to play a role in locking the agonist in place (Khatri & Weiss, 2010).

Upon ligand binding, a structural rearrangement is induced within the binding pocket, part of which results in closure of the C-loop – a process that may also serve to trap the ACh molecule in the binding pocket by a 'capping' motion (Hansen *et al*., 2005). This ligand-induced re-organization of the binding pocket is necessary to transmit the binding stage downstream to the M2 pore region to trigger channel opening (Miller & Smart, 2010). Investigation of the open and closed interface conformations of the GLIC and ELIC proteins revealed that the gating process involves a downwards motion of the β1-2 loop in the direction of the channel-forming M2 helices. At the same time, the M2-3 loops and the Cys-loop displace outwards, permitting retraction of the M2 helices into the outer protein wall (Unwin *et al*., 2005; Bocquet *et al*., 2009; Corringer *et al*., 2010). Hence, ligand binding leads to a series of conformational changes that destabilize the interactions underpinning the hydrophobic gate and trigger

the M2 α-helices to collapse, increasing the pore diameter and thus allowing ion permeation (Miyazawa *et al*., 2003; Unwin, 2003; Miller & Smart, 2010).

Recently, X-ray crystallography techniques have provided the first indication that inhibitory Cys-loop LGICs likely follow a similar gating procedure to that described above in the case of the nicotinic receptor (Hibbs & Gouaux, 2011). Briefly, Hibbs and Gouaux crystallized the *C.elegans* glutamate activated chloride channel (GluCl) protein in the presence of the allosteric partial agonist ivermectin and by doing so, captured the receptor in its activated state. Determination of the local structural changes following channel activation were then inferred by comparing GluCl with the crystal structure of GLIC captured in its resting state. This undertaking revealed that the global conformational change synonymous with channel opening is rooted in the 'splaying' apart of the MI and M3 helices. This then leads to the movement of the apical part of the M2 helices away from the channel axis and towards the periphery of the receptor leading to the open-pore conformation (Hibbs & Gouaux, 2011).

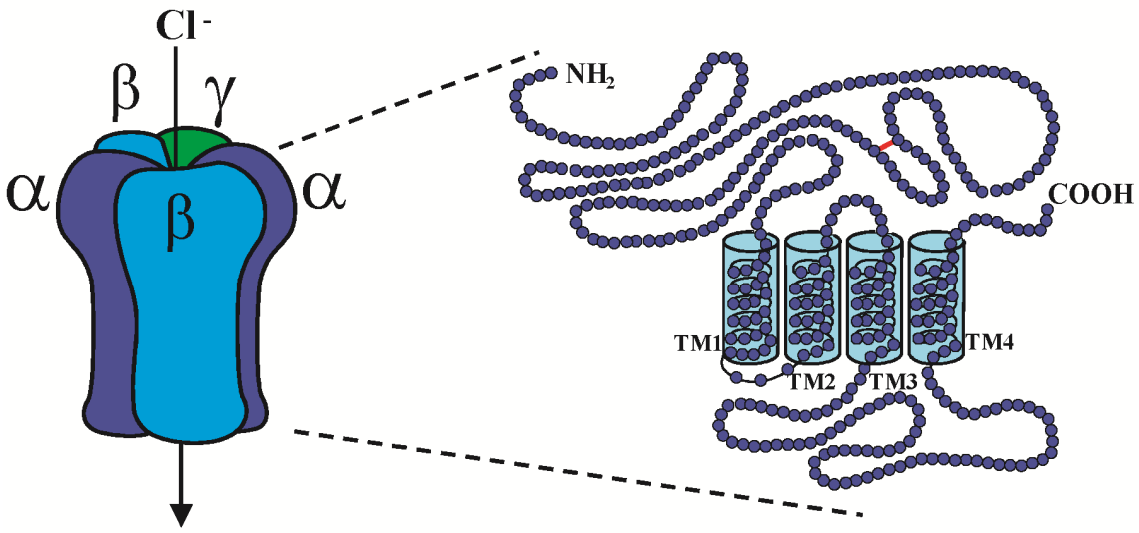

Figure1.2. $GABA_AR$ subunit assembly. Left: schematic illustration showing $GABA_AR$ assembly from five subunits (2α2β1γ) whereby a central Cl^- permeable pore is created. Right: schematic illustration of a $GABA_AR$ subunit showing the large extracellular N terminal domain containing the cysteine to cytseine disulphide bridge (shown in orange), four transmembrane spanning domains, the large intracellular loop between TM3 and TM4 and the short extracellular C terminal region.

1.1.3.2. Cloning of the $GABA_AR$ subunits

In the early 1980s the $GABA_AR$ was purified from bovine cerebral cortex by benzodiazepine-affinity chromatography and the subunits separated electrophoretically (for details regarding benzodiazepine pharmacology, see 1.1.6.1). The two resulting bands retained their pharmacological profile, binding GABA, muscimol and the benzodiazepine flunitrazepam with high affinity and with many similar properties exhibited by the receptors defined in membrane preparations and in crude soluble extracts (Sigel *et al*., 1983).

Soon after these studies, partial amino acid sequences were gleaned from the purified protein, from which appropriate nucleotide probes were constructed to screen a bovine cDNA library. The first two $GABA_AR$ subunits, termed α and β, were subsequently cloned (Schofield *et al*., 1987). Recombinant expression of α and β subunits in *Xenopus laevis* oocytes led to functional GABA-activated channels which

displayed many of the biophysical and pharmacological properties of native $GABA_A$Rs. However, the absence of the classical benzodiazepine sensitivity – a pharmacological hallmark of neural $GABA_A$Rs – led to speculation regarding the existence of additional $GABA_A$R subunits (Levitan *et al*., 1988). The possibility of more than two receptor subunits had not previously been anticipated because the purified receptors had been electrophoretically resolved into two distinct bands that satisfied the main pharmacological criteria displayed by native $GABA_A$Rs. Hence, Pritchett and coworkers predicted that the two principal bands derived from biochemical studies actually contained heterologous subunit compositions. Indeed, within six months the successful cloning of a further $GABA_A$R subunit, termed γ2, was announced from a human fetal brain cDNA library (Pritchett *et al*., 1989). Consistent with native $GABA_A$Rs, transfection of γ2 with α and β cDNAs resulted in functional receptors that exhibited benzodiazepine sensitivity (Pritchett *et al*., 1989). Sustained investigation over the following years revealed the existence of a diverse array of subunit genes. Complete sequencing of the human, and several other vertebrate, genomes has clarified that 19 genes exist that encode related but distinct subunits, thus bestowing $GABA_A$Rs with a considerable degree of subunit heterogeneity (Simon *et al*., 2004; Darlison *et al*., 2005; Olsen & Sieghart, 2008). In mouse, rat and human the $GABA_{A/C}$R genes correspond to 19 receptor subunits comprising 6α, 3β, 3γ, 1δ, 1ε, 1θ, 1π and 3ρ. Subunit heterogeneity is further increased by alternative exon-splicing. Of particular note, splice variants of the γ2 subunit, γ2S and γ2L, have been reported (Whiting *et al*., 1990; Kofuji *et al*., 1991). The only difference between γ2L and γ2S is the absence in the short variant of the 8-amino acid stretch in the large intracellular loop that contains a PKC consensus site, ser343 (Whiting *et al*., 1990; Moss *et al*., 1992). Both variants show differential expression patterns in the brain (Gutiérrez *et al*., 1994; Meier & Grantyn, 2004) and age-related differences in the ratio of γ2L and γ2S subunit

expression have been demonstrated in the hippocampus (Gutiérrez *et al*., 1996). Despite these differences between γ2L and γ2S distribution, their distinct physiological roles are poorly understood, as exemplified by the lack of any apparent phenotype of mice in which either the γ2L or the γ2S subunit has been genetically deleted (Wick *et al*., 2000). However, a recent study has demonstrated that γ2S is not only an integral $GABA_AR$ subunit, but can also exist alone on the cell surface (at least when recombinantly expressed in HEK293 cells) where it appears to act as an accessory protein that is able to modulate the zinc sensitivity of αβ receptors (Boileau *et al*., 2010).

Alternatively spliced variants of β2 and γ3 contain, like γ2L, consensus phosphorylation substrate sequences in the intracellular loop. Furthermore, alternative start sites create multiple mRNA species for α3, α5 and β3 and variants lacking one or more exons have been identified for ρ1, α4, β2 and ε subunits. To date, there is no evidence that any of these subunit variants exist in native $GABA_ARs$ (Simon *et al*., 2004; Olsen & Sieghart, 2008).

1.1.3.3. Cloning of the ρ subunits

Recombinant expression of ρ1/ρ2 hetero-oligomers has been demonstrated (Enz & Cutting, 1998) although a lack of antibody selectivity between ρ subtypes has precluded investigation of their existence in native neuronal tissue. On the other hand, there are several indications that ρ subunits can naturally co-assemble with other $GABA_AR$ subunits (Milligan *et al*., 2004; Pan & Qian, 2005; Harvey *et al.,* 2006) and some hippocampal and cerebellar Purkinje cells have been shown to display intermediate $GABA_C$ and $GABA_A$ pharmacological properties (Hartmann *et al*., 2004; Harvey *et al*., 2006). Due to structural similarity between the ρ and other $GABA_AR$ subunits and given that other $GABA_AR$ subtypes exhibit considerable variation in their pharmacological

profiles (for example, in case of benzodiazepine sensitivity), the IUPHAR Nomenclature Committee has incorporated ρ receptors into the $GABA_AR$ family and advised against the use of the term $GABA_C$ receptor to describe receptors composed solely of ρ subunits (Olsen & Sieghart, 2008). Irrespective of their preferred name, it is obvious that further research is needed to gain a better understanding of the physiological role of GABA receptors incorporating the ρ subunits.

1.1.3.4. Native $GABA_AR$ subtypes

Subsequent to the discovery of the considerable subunit repertoire underpinning the composition of the receptor, a substantial effort has been directed at delineating which receptor subtypes occur *in vivo*. Seminal studies designed to develop a better understanding of the relative expression of $GABA_AR$ subunits in the brain have been conducted at both the mRNA (Laurie *et al*., 1992a; Wisden *et al*., 1992) and protein level (Pirker *et al*., 2000). These studies have revealed that some subunits, for example α1, β2, γ2, are relatively common and are expressed almost ubiquitously throughout the brain, whereas others occur at much lower levels overall being confined to discrete brain regions where conversely, they may occur at high levels (Sieghart & Sperk, 2002). Moreover, the use of subunit-selective antibodies has provided convincing evidence that subunit expression profiles are not only region-specific, but indeed cell and domain specific such that specializations of synaptic $GABA_ARs$ are constructed in a process that is regulated by both pre- and postsynaptic mechanisms (Nusser *et al*., 1996a, 1996b; Somogyi *et al*., 1996; Klausberger *et al*., 2002; Serwanski *et al*., 2006; Klausberger & Somogyi, 2008). Finally, $GABA_AR$ distribution at distinct subcellular locations is differentially regulated in a subunit-composition dependent manner adding a further level of specificity (*i.e.* synaptic, perisynaptic, extrasynaptic; Nusser *et al*., 1996b;

Nusser *et al*., 1998a; Klausberger *et al*., 2002; Peng *et al*., 2004; Prenosil *et al*., 2006; Zhang *et al*., 2007; Herd *et al*., 2008; Kasugai *et al*., 2010). Despite the contention apparent in early literature surrounding $GABA_AR$ subunit stoichiometry (Backus *et al*., 1993), evidence now favours a scenario in which the vast majority of native $GABA_AR$ pentamers are composed of 2α, 2β and one of the remaining subunits, typically γ2 (Im *et al*., 1995; Tretter *et al*., 1997; Farrar *et al*., 1999). Investigation of concatenated receptors revealed that the majority are constructed in a γ-α-β-α-β arrangement (Minier & Sigel, 2004). Approximately 40-60% of all $GABA_ARs$ are composed of α1β2γ2, making this the most abundant receptor subtype in the brain (McKernan & Whiting, 1996; Möhler, 2006). Receptors composed of α2β3γ2 and α3β3γ2 are also relatively common but have more limited expression profiles, occurring most notably in limbic, forebrain and cortical structures (McKernan & Whiting, 1996). The remaining receptor isoforms represent only a small fraction of the total number of $GABA_ARs$, although such is the extent of the GABAergic system in the brain that these 'minor' subunits are probably expressed at levels comparable to receptors for other neurotransmitter systems (for example serotonin, dopamine and noradrenaline) and should therefore not be underestimated in their physiological relevance (Sieghart & Sperk, 2002; Olsen & Sieghart, 2008).

Generally, it appears that the two α and two β subunits are of the same subunit subtype (Sieghart & Sperk, 2002). However, there is evidence from immunoprecipitation and immunoaffinity chromatography studies indicating the coexistence of two different α subunits (Duggan *et al*., 1991; Lüddens *et al*., 1991; Mertens *et al*., 1993; Jechlinger *et al*., 1998; Benke *et al*., 2004) or two different β subunits (Li & De Blas, 1997; Jechlinger *et al*., 1998) within the same receptor complex, at least for some receptor isoforms. In disagreement with the perceived 2α, 2β, 1γ stoichiometry, a limited number of studies have reported the co-localisation of two γ

subunits in the same receptor complex, although different γ subunits in most studies were found not to be co-immunoprecipitated (reviewed in Sieghart & Sperk 2002; Whiting *et al*., 2003). Investigations of γ2 (Günther *et al*., 1995) and δ (Tretter *et al*., 2001) knockout mice have indicated the presence of receptors composed solely of α and β subunits. Since the γ2 subunit appears essential for synaptic clustering, an extrasynaptic location of αβ receptors on hippocampal pyramidal neurones has been proposed (Mortensen & Smart, 2006).

In summary, it has become evident that CNS imposes strict assembly rules and regional expression specificity that, collectively, severely curtails the number of functional native $GABA_AR$ subtypes. A recent IUPHAR $GABA_AR$ subtype classification (Olsen & Sieghart, 2008) has proposed the existence of 26 naturally occurring receptor isoforms, determined by analysis of the experimental evidence to date. However, 9 of the 26 isoforms have been currently categorized as 'tentative' due to a scarcity of definitive studies and it is envisaged that members of this category may exist as multiple distinct subtypes. Thus, the number of native oligomers will likely rise in the future.

1.1.4. GABA: a pioneer neurotransmitter during neurodevelopment

The initiation of GABA synthesis and signalling occurs during mid-gestation, long before the onset of synaptogenesis suggesting that GABA also serves a trophic role in the brain (Owens & Kriegstein, 2002; Di Cristo, 2007). Indeed, GABA signalling is implicated in numerous processes of neurodevelopment including cell proliferation, migration, and differentiation (Owens & Kriegstein, 2002; Ben-Ari *et al*., 2007). These actions involve the activation of $GABA_ARs$, which during early development, exert a depolarising action (Ben-Ari *et al*., 1989; Ben-Ari *et al*., 2007). Depolarizing GABA

responses occur as a consequence of the delayed expression of the Cl^- exporter KCC2. In immature neurones the transmembrane Cl^- gradient is determined largely by the Cl^- importer, NKCC1 resulting in a high intracellular, relative to the extracellular, Cl^- concentration. Hence, upon $GABA_AR$ activation the net movement of Cl^- out of the cell constitutes a depolarizing response (reviewed in Ben-Ari *et al*., 2007; Fiumelli & Woodin, 2007; Blaesse *et al*., 2009; Figure 1.3). GABA-induced depolarization activates voltage gated Ca^{2+} channels which can elicit long-lived increases in intracellular Ca^{2+} concentration ($[Ca^{2+}]_i$) leading to the activation of Ca^{2+}-dependent signalling pathways (Ben-Ari *et al*., 2007; Figure 1.3).

In rodents, GABA converts to its adult inhibitory role in the first two weeks of life upon the upregulation of KCC2 (Ben-Ari *et al*., 2007; Blaesse *et al*., 2009). However, trophic actions remain apparent during the juvenile and adolescent stages as evidenced by the role of GABA in inhibitory synapse formation (Chattopadhyaya *et al*., 2007; Huang, 2009; Figure 1.3).

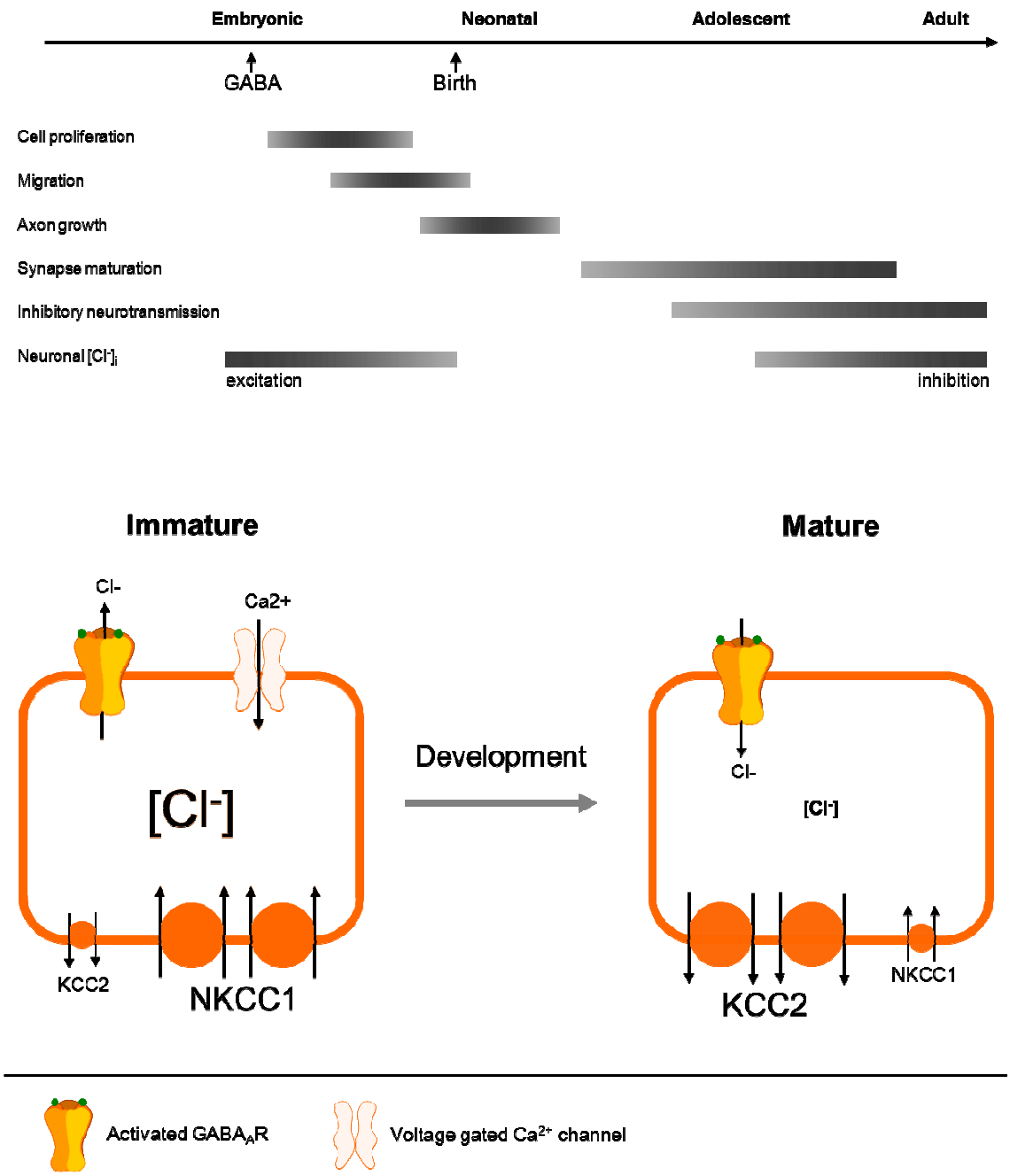

Figure 1.3. Developmental roles of GABA. Top: timecourse of the different developmental aspects involving GABA. At embryonic stages, before synapse formation, GABA is involved in cell proliferation, migration and axonal growth. Synapse formation begins before birth but does not become prominent until the second postnatal week when GABA is switching to an inhibitory role. Recreated and modified from Di Cristo, 2007. Bottom: schematic representation of developmental expression of neuronal Cl^- transporters and their effects of $GABA_AR$-mediated signaling. In immature neurones NKCC1 dominates resulting in a high $[Cl^-]_i$ relative to outside. This results in a depolarizing, Cl^- efflux upon $GABA_AR$ activation which is sufficient to activate VGCCs such that an increase in $[Ca^{2+}]_i$ ensues. In mature neurones the transmembrane Cl^- gradient is reversed due to an upregulation of KCC2. This leads to a domination of Cl^- export over Cl^- import. Under these conditions $GABA_AR$ activation causes a hyperpolarising Cl^- influx. Figure modified from Fiumelli & Woodin, 2007.

1.1.5. Forms of GABA mediated inhibition in the brain

1.1.5.1. Phasic inhibition

Synaptic $GABA_ARs$, typified by αβγ isoforms, primarily mediate inhibition in a 'phasic' manner, rapidly and precisely transducing presynaptic activity into a postsynaptic signal (Figure 1.4 A). Such receptors are clustered in the order of tens to hundreds at the postsynaptic membrane and briefly experience millimolar levels of GABA following presynaptic vesicular release (Edwards *et al*., 1990; Mody *et al*., 1994; Nusser *et al*., 1997). The GABA liberated from one vesicle binds to, and gates, a proportion of postsynaptic $GABA_ARs$ causing a near-synchronous activation (Farrant & Nusser, 2005 Figure 1.4 A). A salient feature of phasic inhibition is the short duration of the GABA transient in which rapid diffusion of GABA from the synaptic cleft, along with GABA re-uptake, terminates the phasic mode of $GABA_AR$ activation (Farrant & Nusser 2005). Hence, even though GABA may be liberated from a single vesicle at a concentration that would, under steady-state conditions, be saturating, the dominance of the rate of diffusion (and subsequent re-uptake) over the GABA binding rate means that receptor occupancy is not always maximal and can vary in a synapse-dependent manner (Frerking & Wilson, 1996; Nusser *et al*., 1997; Perrais & Ropert, 1999; Mozrzymas *et al*., 2003; reviewed in Barberis *et al*., 2011).

1.1.5.2. Tonic inhibition

Phasic receptor activation underpins the vast majority of fast, neurone-to-neurone information transfer in the brain. In addition, it is now recognized that in several discrete neuronal CNS populations, ambient levels of extracellular GABA are sufficient to tonically activate $GABA_ARs$, thus constituting a second form of neuronal inhibition

mediated by ionotropic $GABA_A$ receptors (Figure 1.4 C). The receptor subtypes that underlie tonic inhibition are often distant from the sites of synaptic GABA release being present in somatic, dendritic and axonal locations (Kullmann *et al*., 2005). A $GABA_AR$ mediated tonic conductance was first reported following voltage-clamp recordings performed on cerebellar granule cells and shortly after, from pyramidal cells of the somatosensory cortex, in the rat brain slice preparation (Kaneda *et al*., 1995; Brickley *et al*., 1996; Salin & Prince, 1996; Wall & Usowicz, 1997). The application of competitive $GABA_AR$ antagonists, in addition to abolishing spontaneously occurring IPSCs, shifted the holding current (an outward current) required to maintain the cell at a given membrane potential and reduced the current noise, thus reflecting a decrease in the number of open $GABA_AR$ channels (Kaneda *et al*., 1995; Brickley *et al*., 1996; Wall & Usowicz, 1997; Figure 1.4 C). In addition to CGCs, subsequent studies have confirmed the presence of $GABA_AR$- mediated tonic currents in a variety of neurones most notably in dentate gyrus granule cells (Nusser & Mody, 2002) and CA1 pyramidal cells (Bai *et al*., 2001) of the hippocampus and the thalamocortical relay neurones of the ventrobasal (Belelli *et al*., 2005; Cope *et al*., 2005a; Jia *et al*., 2005 - see section 1.1.7) and dorsal lateral geniculate nucleus (Bright *et al.*, 2007).

Analysis of solutes retrieved from *in vivo* microdialysis experiments (Lerma *et al*., 1986; Tossman *et al*., 1986; Kennedy *et al*., 2002; Xi *et al*., 2003; Nyitrai *et al*., 2006) coupled with theoretical considerations of GABA transporter stoichiometry (Attwell *et al*., 1993; Wu *et al*., 2007) have estimated that the free extracellular, 'ambient' GABA concentration varies between tens of nanomolar to a few micromolar – a range that emphasizes the likely existence of distinct spatial variations in ambient GABA concentration (Farrant & Nusser, 2005). The concentration of extracellular GABA will be primarily influenced by the balance of GABA releasing elements and GABA transporters. Indeed, pharmacological blockade of GABA transport (Wall &

Usowicz, 1997; Nusser & Mody, 2002; Semyanov *et al*., 2003) and genetic deletion of GAT-1 (Jensen *et al*., 2003) result in larger tonic currents as measured by electrophysiological techniques.

In addition to GABA, other endogenous agonists may exist that selectively and dynamically enhance the tonic conductance. Taurine is one such example and is known to exist extracellularly in low to high μM range (Lerma *et al*., 1986; Albrecht & Schoesboe, 2005). Extracellular taurine levels are regulated dynamically by TauT1/2 in response to certain stimuli including hyposmotic shock and depolarization (Albrecht & Schoesboe, 2005). Furthermore, when applied to thalamic brain slices, exogenous taurine has been found to augment the tonic conductance present in thalamocortical relay neurones whilst unaltering synaptic inhibition thus indicating a preferential interaction of taurine with δ-$GABA_A$Rs (Jia *et al*., 2008).

1.1.5.3. Spillover inhibition

Hence, two distinct modes of $GABA_A$R mediated inhibition exist whereby the temporally and spatially discrete nature of phasic inhibition contrasts starkly with the persistent and random activation of extrasynaptic receptors. However, it should be emphasized that these apparently overt distinctions may sometimes overlap and give rise to an additional mode of signaling, called spillover inhibition (Farrant & Nusser, 2005; Figure 1.4 B). Diffusion of GABA following phasic release may activate $GABA_A$Rs other than those located in close apposition, on the post synaptic membrane. The receptors involved in spillover inhibition may be localized to various nearby locations in the so called ‘perisynaptic’ environment which include beneath the same bouton - at regions that are distant from the release zone (Telgkamp *et al*., 2004); in the extrasynaptic membrane (Brickley *et al*., 2001); in presynaptic structures (Trigo *et al*.,

2008; Ruiz *et al*., 2010); or at adjacent synapses (Wei *et al*., 2003). Based on the observation that δ-$GABA_A$Rs, due to their high GABA affinity, putative modest desensitization properties and extrasynaptic localization, underlie the tonic conductance in several cell types, the widely held assumption is that δ-$GABA_A$Rs mediate both tonic and spillover inhibition (for example see Wei *et al*., 2003; Glykys & Mody, 2007; Figure 1.4 B). This idea has recently been challenged by the electrophysiological demonstration that δ-$GABA_A$Rs do not contribute to spillover inhibition in CGCs or thalamocortical neurones of the lateral geniculate nucleus (Bright *et al*., 2011). Adding further weight to this proposal, the authors showed that α4β2δ (the isoform present in thalamocortical neurones) when expressed recombinantly, rapidly desensitized to a steady state in the continued presence of 1 μM GABA (Bright *et al*., 2011). It is worth noting, however, that both these cell types exhibit glomerular synapses, the architecture of which may influence the lifetime and concentration of GABA in the cleft.

A further example of non-synaptic GABA signaling has been described by Olah and colleagues and relates to neurogliaform (NGF) cells of the hippocampus (Olah *et al*., 2009). Upon stimulation NGF cells release large amounts of GABA into the 'axonal cloud' in a synapse-independent manner. This GABA release, was found to reduced the excitatory output of the vast majority of surrounding neurones *via* a mechanism that involves δ-$GABA_A$Rs.

Volume transmission as mediated by NGF cells has been postulated to underlie a phasic current with intermediate features of synaptic and tonic inhibition. The so called $GABA_{Aslow}$ response has been reported in certain hippocampal interneurones as well as the inhibitory neurones of the reticular thalamus (Copogna & Pearce, 2011). It has been proposed that $GABA_{Aslow}$ is mediated by synaptically located high affinity $GABA_A$Rs (*e.g.* δ-$GABA_A$Rs) though a functional understanding of $GABA_{Aslow}$ currents remains in its infancy (Copogna & Pearce, 2011)

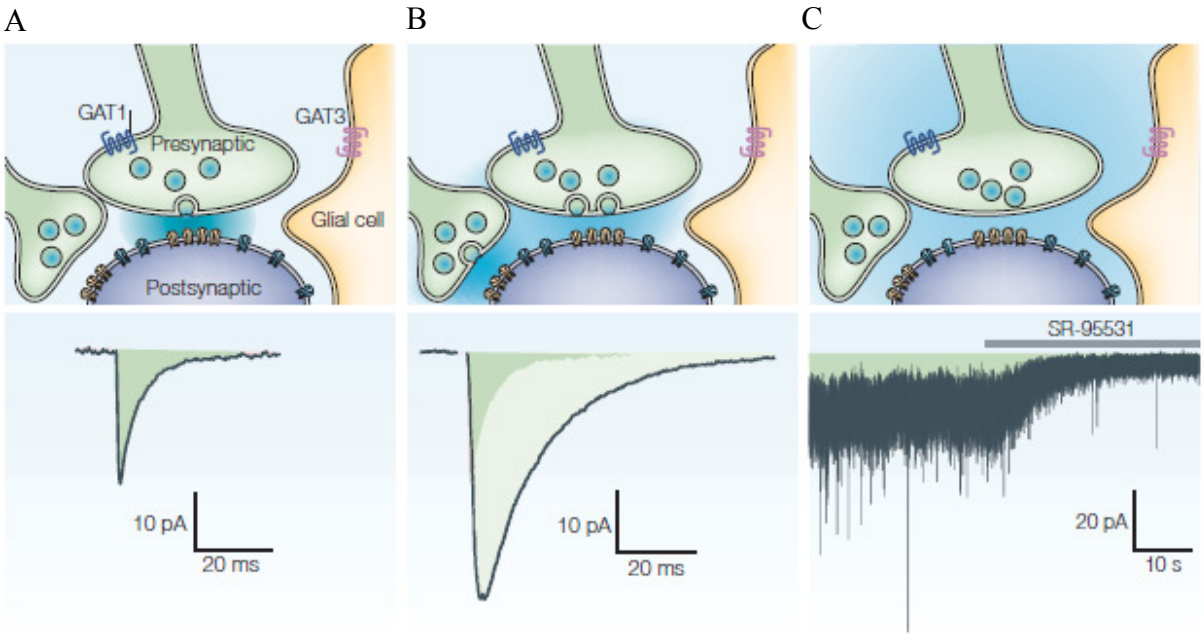

Figure 1.4. Forms of $GABA_AR$ inhibition A. Synaptic inhibition: presynaptic GABA release from a single vesicle activates those $GABA_ARs$ situated directly opposite on the postsynaptic membrane (depicted by the dark blue area). In whole-cell voltage clamp recordings this post-synaptic event is reflected by the mIPSC, a fast rising and bi-exponentially decaying current response. **B**. Spillover inhibition: at certain synapses, action potential dependent release can elicit spillover inhibition which involves the activation of synaptic $GABA_ARs$ as well as those located outside the immediate synaptic vicinity - at peri- or extra-synaptic locations. This is reflected as larger current waveform with a slower rise time and longer decay kinetics. Note the increased charge transfer relative to synaptic inhibition as demarcated by the shaded areas. **C**. Tonic inhibition: in neurones that express high affinity, slowly desensitizing $GABA_ARs$ at extrasynaptic locations (typically those which contain the δ or α5 subunit), ambient GABA concentrations can induce a persistent, 'tonic' form of inhibition. The current trace, shown on a much longer timescale relative to those shown in A and B, depicts the inward current response and reduction in baseline noise upon application of the $GABA_AR$ competitive antagonist SR-9553. Reproduced with permission from Farrant & Nusser, 2005.

1.1.6. Regulation of subunit composition: influence on $GABA_AR$ biophysics and cellular expression

1.1.6.1. The α subunits

The recombinant expression and subsequent electrophysiological assessment of $GABA_ARs$ composed of different subunit combinations has demonstrated that the type of α subunit influences GABA sensitivity, intrinsic deactivation and desensitization properties in addition to sensitivity to allosteric modulators (*e.g.* benzodiazepines– see below). A combination of *in situ* hybridization (Laurie *et al*., 1992a; Persohn *et al*., 1992; Wisden *et al*., 1992) and immunohistochemical (Zimprich *et al*., 1991; Fritschy *et al*., 1992; Fritschy & Mohler, 1995; Pirker *et al*., 2000) studies have confirmed α1 to be the most abundant subunit in the mature brain. Consequently, functional properties of receptors incorporating the α1 subunit have been studied in recombinant expression sysytems. The brief application of GABA to cells expressing recombinant α1β2γ2 $GABA_ARs$ resuled in currents with relatively fast decay kinetics compared to currents from equivalent cells expressing α3β2γ2 (Verdoorn, 1994). Subsequently, rapid agonist application techniques were used to reveal that the α1 subunit imposes a faster channel deactivation rate relative to α3 subunit when expressed recombinantly with the β1 and γ2 subunits but that the α subunit has no affect on the receptor desensitization kinetics (Lavoie *et al*., 1997, although see Gingrich *et al*., 1995).

The decay kinetics of IPSPs are similarly influenced by the type of α subunit present in the receptor complex. For example, in a variety of neurones the relatively long duration kinetics of mIPSCs observed in early postnatal development have been ascribed to α2/3 containing receptors, whereas the developmentally delayed incorporation of the α1 subunit to functional receptors contributes to a decrease of the

decay time of the synaptic events (Okada *et al*., 2000; Vicini *et al*., 2001; Jüttner *et al*., 2001; Goldstein *et al*., 2002; Bosman *et al*., 2005).

The α1 subunit it not always restricted to $GABA_AR$ isoforms expressed at synaptic locations as indicated by the anatomical and electrophysiological evidence supporting the existence of both extrasynaptic α1δ-containing receptors in interneurones of the dentate gyrus molecular layer that underlie the tonic currents observed in this region (Glykys *et al*., 2007). Furthermore, a recent quantitative immunocytochemical study on CA1 pyramidal neurones reported that approximately 60% of α1 subunit immuno-reactivity is present extrasynaptically. Whether the α1 subunit forms functional extrasynaptic $GABA_ARs$ or whether it is present extrasynaptically because of trafficking processes has yet to be determined (Kasugai *et al*., 2010)

The α4, α5 and α6 subunits are expressed, for the most part, at extra- or peri-synaptic locations, where they are perceived to form receptors that underlie tonic $GABA_AR$-mediated currents (Glykys & Mody, 2007; Belelli *et al*., 2009). In the mature brain these subunits have a restricted expression profile whereby the α4 and α6 subunits are primarily co-localized with the δ-subunit. In particular, the α4 subunit is expressed at relatively high levels in the cortex, striatum, thalamus and the dentate gyrus of the hippocampus (Laurie *et al*., 1992a; Huntsman *et al*., 1996; 1999a; Pirker *et al*., 2000), brain areas/neurones that are known to exhibit $GABA_AR$-mediated tonic currents (Nusser & Mody 2002; Belelli *et al*., 2005; Krook-Magnuson & Huntsman, 2005; Drasbek & Jensen, 2006; Ade *et al*., 2008; Kirmse *et al*., 2008). Moreover, the endogenous tonic conductance present in both dentate granule cells and thalamocortical cells is diminished in recordings from $\alpha4^{0/0}$ and $\delta^{0/0}$ mice (Chandra *et al*., 2006; Herd *et al*., 2008; 2009). The α6 subunit exists exclusively in cerebellar granule cells where it is incorporated into extrasynaptic receptors composed of α6β2/3δ and two synaptic isoforms α6β2/3γ2 and α1α6β2/3γ2 (Nusser *et al*., 1998a). Consistent with this

subcellular receptor compartmentalization, both tonic and synaptic inhibition mediated by α6-$GABA_A$Rs are present in cerebellar granule cells (Brickley *et al*., 1996). The α5 subunit is also primarily restricted to a few discrete brain regions, notably the hippocampus, olfactory bulb, striatum and cerebral cortex, where it may be incorporated into both synaptic and extrasynaptic $GABA_A$Rs (Sur *et al*., 1999; Brünig *et al*., 2002; Serwanski *et al*., 2006). A number of electrophysiological studies have reported a tonic inhibitory conductance in hippocampal pyramidal neurones and dentate gyrus granule cells that is mediated by α5-containing $GABA_A$Rs (Caraiscos *et al.*, 2004; Bonin *et al.*, 2007; Zhang *et al.*, 2007; Herd *et al.*, 2008). However, distinct from α4 and α6 subunits, α5 subunits do not appear to partner δ-containing receptors in the hippocampus. In particular, as hippocampal tonic currents mediated by α5-$GABA_A$Rs are enhanced by benzodiazepines the α5 subunit appears to co-assemble with a γ2 subunit (Bai *et al*., 2001; Caraiscos *et al*., 2004). Benzodiazepines and certain general anaesthetics (*e.g.* etomidate) elicit cognitive impairments including amnesia that are, in part, due to the potentiation of α5-$GABA_A$Rs (reviewed in Wang & Orser, 2011). The use of transgenic technology to either reduce the number, or completely 'knockout', α5-containing $GABA_A$Rs has revealed their role in hippocampal-dependent learning (Collinson *et al*., 2002; Crestani *et al*., 2002 Caraiscos *et al*., 2004, Cheng *et al*., 2006). Agents which selectively antagonise α5-$GABA_A$Rs have therapeutic potential as cognitive enhancers (Dawson *et al*., 2006; Ballard *et al*., 2009) and a possible cellular basis for this effect has recently been described (Martin *et al*., 2010). Specifically, Martin *et al* demonstrated that α5-$GABA_A$R activity attenuates the induction of LTP in the theta band of stimulation only, in a process that is independent of synaptic inhibition (Martin *et al*., 2010).

In the developing telencephalon and diencephalon α5 subunit expression is generally high from the perinatal to the juvenile stage then decreases at later

developmental stages (Laurie *et al*., 1992b). In keeping with this developmental profile, dopamine receptor 2 (DAR2) positive medium spiny neurones of the striatum exhibit tonic currents that are partially blocked by the α5 selective inverse agonist L655-708, in young, but not adult mice (Ade *et al*., 2008; Janssen *et al*., 2009; Santhakumar *et al*., 2010). Similarly, application of a low concentration (5 μM) of GABA to P2-4 mouse layer 5 pyramidal cells produced a relatively large inward current that was blocked by the α5-selective antagonist L655-708. This effect was substantially decreased by P7-10 (Sebe *et al*., 2010).

The α subunit may play a significant role in the targeting of $GABA_AR$ complexes to specific neuronal synapses (*e.g.* the axon initial segment or axo-dendritc synapses). For example, a direct interaction between the α2 subunit and the scaffolding protein gephyrin is capable of mediating the accumulation of $GABA_A$ receptor complexes to specific central inhibitory synapses *via* a gephyrin-dependent mechanism (Tretter *et al.*, 2008). Furthermore, a recent study has highlighted the role of the dystrophin glycoprotrin complex in regulating synapse specificity of $GABA_AR$ expression in CA1 pyramidal neurones of the hippocampus. Thus, here dystrophin stabilizes α1-$GABA_AR$ and the scaffolding protein neuroligin-2, but not gephyrin, in perisomatic postsynaptic densities (Panzanelli *et al*., 2011). The extensive array of $GABA_AR$ associated proteins that participate in $GABA_AR$ localization and membrane trafficking are reviewed in Chen & Olsen, 2007, Arancibia-Cárcamo & Kittler, 2009 and Lüscher *et al*., 2011.

1.1.6.2. The β subunits

Relative to the α subunits, the influence of the β subunit isoform on receptor function remains poorly understood owing in part to a lack of selective pharmacological tools to assess the impact of different β subunit subtypes on the biophysical properties of $GABA_ARs$. Current understanding has relied in part on the use of transgenic β subunit 'knock-out' and 'knock-in' mice. In comparison to WT, cortical neurones derived from $\beta3^{-/-}$ mice and maintained in cell culture exhibit a reduction in α2/3 subunit expression and display mIPSCs with a faster decay time, potentially due to a preponderance of α1-containing $GABA_ARs$. These observations may suggest a preferential co-assembly of particular isoforms of α and β (*i.e.* α2/3 and β3), which may then impart receptors with specific kinetic properties *cf* α1-$GABA_ARs$ (Ramadan *et al*., 2003). However, a later study conducted on thalamic neurones of the nucleus reticularis (nRT) revealed that the distinct kinetic profiles of two α3 containing $GABA_ARs$ are governed by the type of β subunit present in the receptor complex. By using loreclezole, a compound with some selectivity for β2/β3-$GABA_ARs$, α3-β1 containing isoforms were shown to exhibit a fast decay in comparison to α3-β3 containing receptors which exhibit a relatively slow decay time course (Huntsman & Huguenard, 2006).

As noted above, a region between M3 and M4 on the β subunit contains a consensus site that may be phosphorylated by a number of kinases, such as protein kinase A (PKA), protein kinase C (PKC), and Ca^{2+} calmodulin kinase II (CaMKII; Hinkle & Macdonald, 2003; Houston *et al*., 2008). This potential for post-translational modification raises the possibility that the phosphorylation state of the β-subunit regulates IPSC decay properties (Houston *et al*., 2008). Furthermore, the large intracellular β-subunit loop interacts with a variety of $GABA_AR$ proteins including Plic-1 (β1-3), HAP (β1), GRIF-1 (β2), PRIP-1 (β1-3) and BIG2 (β1-3) that are thought to be important for receptor trafficking, receptor stabilization, and regulating the receptor

phosphorylation status (Chen & Olsen, 2007; Lüscher *et al*., 2011). Therefore β-subunit phosphorylation/dephosphorylation by a variety of protein kinases and phosphatases, respectively, may provide a mechanism that is instrumental to trafficking different $GABA_AR$ subtypes to discrete subcellular locations (Michels & Moss, 2007; Lüscher *et al*., 2011). Consistent with this proposal, an electrophysiological study utilizing β2 subunit knock-in mice (β2N265S, Reynolds *et al*., 2003) in which β2-$GABA_ARs$ are rendered insensitive to the β2/3 preferring $GABA_AR$ modulator etomidate, have revealed that in thalamocortical relay neurones of the VB thalamus, the β2 subunit predominates at both synaptic and extrasynaptic locations (Belelli *et al*., 2005). In contrast, in hippocampal DGGCs a similar approach has revealed that the majority of synaptic receptors contain β3 (together with α1 and γ2) as opposed to the extrasynaptic $GABA_AR$ population which primarily incorporate β2 (together with α4 and δ, Herd *et al*., 2008).

1.1.6.3. The γ subunits

Localization of $GABA_ARs$ at the synapse is determined largely by the interaction between the γ-subunit and multiple accessory proteins of the $GABA_AR$ complex (Essrich *et al*., 1998; Chen & Olsen 2007; Arancibia-Cárcamo *et al*., 2009; Luscher *et al*., 2011). Proteins which interact directly with the γ2 subunit and are important for trafficking include GABARAP, PRIP-1 and GODZ. The γ2 subunit is also targeted by AP2 which facilitaes $GABA_AR$ access to the endocytotic pathway (for reviews see Chen & Olsen, 2007; Arancibia-Cárcamo *et al*., 2009; Luscher *et al*., 2011). The phosphatase calcineurin targets γ2 and blocking calcineurin to promote γ2 subunit phosphorylation results in IPSCs with a shorter duration of decay (Jones & Westbrook, 1997).

However, the presence of γ2 does not always necessitate a synaptic location as demonstrated by the evidence for extrasynaptic α5β2/3γ2 receptors which participate in tonic inhibition (Bai *et al*., 2001; Caraiscos *et al*., 2004; Ade *et al*., 2008). Furthermore, a recent quantitative immunocytochemcial study has revealed that approximately 60% of α1, α2 and β2 containing receptors are located in extrasynaptic regions (Kasugai *et al*., 2010). Assuming normal receptor construction (*i.e.* αβγ) this infers that a significant portion of γ subunits also exist extrasynaptically, although whether these receptors are involved in trafficking processes or whether they have a functional role has yet to be determined (Kasugai *et al*., 2010)

1.1.6.4. The δ subunits

The presence of a δ-subunit confers native $GABA_A$Rs with unique biophysical properties coupled with an extrasynaptic/perisynaptic cellular location making them ideally tailored to mediate a sustained Cl^- conductance underpinning tonic inhibition (Glykys & Mody, 2007; Belelli *et al*., 2009). With respect to the biophysical aspects, there are two general principles that appear necessary for extrasynaptic receptors to sustain an inhibitory conductance in response to ambient GABA concentrations. Firstly, the receptor should have a sufficiently high affinity for GABA such that activation occurs in the low-micromolar GABA concentration range that has been predicted to exist in the extracellular space (Nyitrai *et al*., 2006). However, constitutively active $GABA_A$Rs, for example those described for hippocampal pyramidal neurones, can also mediate tonic inhibition (McCartney *et a*l., 2007). Secondly, the receptor should exhibit little desensitization, a common property of many ligand gated ion channels which typically exhibit long periods of closed states following continued exposure to an agonist. Original investigations had suggested that both these criteria are satisfied by

recombinant receptors incorporating the δ-subunit in conjunction with α4, α6, α1 and β2-3. Thus, for example, δ-$GABA_A$Rs exhibited GABA EC50s in the tens of nanomolar range (Saxena & Macdonald, 1994; Wallner *et al*., 2003) and displayed minimal desensitization in the continued presence of an agonist (Haas & Macdonald, 1999; Wohlfarth *et al*., 2002; Bianchi & Macdonald, 2003). However, a recent study has demonstrated that δ-$GABA_A$Rs may exhibit a greater level of desensitization than previously anticipated (Bright *et al*., 2011 – discussed in Section 1.1.4).

In addition to these biophysical properties, another distinct characteristic of δ-$GABA_A$Rs is their extrasynaptic localization. It appears that in the absence of the γ2 subunit, δ-$GABA_A$Rs lose their synapse-finding ability. As a result they may be dispersed across the somatic, axonic or dendritc membrane at non-synaptic locations (Nusser *et al*., 1995; Nusser *et al*., 1998a; Wei *et al*., 2003). However, recent electrophysiological evidence has suggested that δ-$GABA_A$Rs may be present at mossy fibre boutons in the rat hippocampus where their activation may lead to depolarization and facilitation of synaptic transmission (Ruiz *et al*., 2010).

In the cerebellum, the δ subunit co-assembles with α6 and β2/3 subunits to form putative, extrasynaptic α6β2/3δ receptors that mediate a tonic conductance (Quirk *et al*., 1995; Brickley *et al*., 1996; Huh *et al*., 1996; Jechlinger *et al*., 1998; Nusser *et al*., 1998a; Brickley *et al*., 2001). In dentate gyrus granule cells, the δ subunit coassembles to form α4β2δ receptors which may be located peri- or extrasynaptically (Wei *et al*., 2003; Peng *et al*., 2004; Zhang *et al*., 2007; Herd *et al*., 2008). The tonic conductance present in DGGCs is due not only to δ-$GABA_A$Rs, as was originally proposed, but also involves a contribution from α5-$GABA_A$Rs. Similarly, the predominantly α5-$GABA_A$R mediated tonic current evident in CA1 pyramidal cells has been shown to include a δ-mediated component (Glykys *et al*., 2006; Glykys *et al*., 2008). In certain interneurones of the dentate gyrus, the δ-subunit has been found to coassemble with α1βx to form

another extrasynaptic $GABA_AR$ underlying a tonic conductance that displays a high sensitivity to modulation by ethanol (Glykys *et al*., 2007).

In addition, neurogliaform cells are a class of cortical interneurones that release enough GABA for 'volume transmission' within the 'axonal cloud' so that inhibitory responses, possibly mediated by δ-$GABA_ARs$, may be measured in the majority of surrounding cells in a synapse-independent manner (Olah *et al*., 2009; Copogna, 2011).

Studies examining the $GABA_AR$ distribution in the brain have consistently observed a co-expression of α4 and δ subunits in the thalamic sensory relay nuclei (Laurie *et al*., 1992a; Pirker *et al*., 2000). Indeed, thalamocortical relay neurones of both the ventrobasal complex and the dorsal lateral geniculate nucleus display a large tonic conductance (Belelli *et al*., 2005; Jia *et al*., 2005; Bright *et al*., 2007) that appears to be an important determinant of the thalamocortical oscillations underpinning certain attentional and vigilance states (Sherman & Guillery, 2002).

1.1.7. Tonic conductances mediated by δ-$GABA_A$Rs: physiological functions

Although current understanding is in its infancy regarding the physiological relevance of tonic inhibition, principles are emerging about how it may affect the information processing capacity of a neurone. Tonic currents mediated predominantly by δ-$GABA_ARs$ have been described in dentate gyrus granule cells (Nusser & Mody, 2002) where they are thought to lower interneuronal activity and provide a homeostatic control of network excitability (Semyanov *et al*., 2003; Farrant & Nusser *et al*., 2005). In CA1 pyramidal neurones of the hippocampus the tonic conductance is mediated, for the most part, by α5-$GABA_AR$ but also contain δ-$GABA_AR$ mediated component (Glykys *et al*., 2006). In these cells the tonic $GABA_AR$ activity primarily affects the 'offset' of the relationship between action potential generation and post synaptic excitation (*i.e.* the

left-to-right position of the input-output slope) and has only a minimal effect on the 'gain' (*i.e.* the gradient of the input-output slope – Semyanov *et al*., 2004; Pavlov *et al*., 2009). Hence, at least for CA1 neurones, the tonic conductance, as mediated by extrasynaptic $GABA_A$Rs, influences network excitability without affecting the neuronal sensitivity to changing inputs which may be of importance in learning and memory (Belelli *et al*., 2009; Pavlov *et al*.,, 2009). Moreover, the tonic δ-$GABA_A$R conductance in CA3 interneurones has been shown to functionally impact upon network dynamics such that it may modulate γ-oscillatory activity, a synchronization of neuronal activity thought to be involved in sensory encoding and memory storage/retrieval (Mann & Mody, 2010).

Granule cells of the cerebellum exhibit a tonic conductance mediated by α6β2/3δ receptors (Brickley *et al*., 1996, 2001, Wall & Usowicz, 1997) that has been demonstrated to be critically important in setting the gain for incoming information transfer through the cerebellar cortex. This action amplifies the signal-to-noise ratio and yields an increased cerebellar storage capacity (Hamann *et al*., 2002; Chadderton *et al*., 2004; Rancz *et al*., 2007).

In the lateral geniculate nucleus of the thalamus activation of a δ-$GABA_A$R mediated tonic current results in a perturbation of recurrent low threshold bursts. This observation indicates a role for δ-containing receptors in thalamocortical oscillations that underpin ceratin behavioural states (Bright *et al*., 2007). Moreover, an enhanced tonic inhibition in thlamocortical neurones of the ventrobasal nucleus has been found to be both necessary and sufficient for the full electrographic and behavioural expression of absence seizures (Cope *et al*., 2009).

In contrast to the apparent close association between δ-containing receptors and tonic inhibition, a recent study has provided evidence proposing the existence of pre-synaptic δ-containing receptors that, when activated, depolarize the presynaptic

membrane to facilitate glutamate release from hippocampal mossy fibres. This form of δ-$GABA_A$R mediated signaling may be important in learning and memory (Ruiz *et al*., 2010).

In addition, certain hippocampal interneurones can be excited by low ambient GABA levels due to a depolarized GABA reversal potential relative to the resting membrane potential. However, as the tonic $GABA_A$R conductance rises, the depolarizing and therefore excitatory effects of GABA are overpowered by the shunting inhibition resulting from an increased membrane conductance. Hence, in CA1 interneurones, a $GABA_A$R mediated tonic conductance exhibits a biphasic functionality that is dynamically regulated by the level of extracellular GABA (Song *et al*., 2011). Similarly, a depolarizing, yet inhibitory, δ-$GABA_A$R mediated conductance has recently been described in the auditory coincidence detector neurones of the chick nucleus laminaris (analagous to the mammalian medial superior olive). This conductance was found to be instrumental to sharpening auditory coincidence detection (Tang *et al*., 2011).

These findings add further tiers of complexity to the ways in which tonic conductances may modulate neuronal computations and serve to highlight their highly specialized roles in brain function.

1.1.8. $GABA_A$R pharmacology

The activity of the $GABA_A$R is modified by a chemically diverse range of drugs and endogenous modulators (Johnston, 2005; D'Hulst *et al*., 2009). Therapeutically, drugs that target this receptor are in widespread clinical use as general anaesthetics, anxiolytics, anticonvulsants, and sedative/hypnotics (D'Hulst *et al*., 2009). Such compounds facilitate $GABA_A$R chloride flux by either gating the channel directly, or by

augmenting the receptor's response to GABA. Compounds that exhibit the latter of these effects are termed positive allosteric modulators (D'Hulst *et al*., 2009). In addition, several compounds (*e.g*. certain general anaesthetics, barbiturates, neurosteroids) act as positive modulators at low concentrations but additionally, at greater concentrations, directly activate the $GABA_AR$ (*i.e.* a GABA-mimetic effect, Belelli *et al*., 1996). By contrast, negative allosteric modulators act to reduce the $GABA_AR$'s response to GABA. Because these compounds exhibit negative efficacy they are known as allosteric inverse agonists (Korpi *et al*., 2002a; Johnston, 2005). Lastly compounds that act allosterically but display neither positive or negative efficacy (such as flumazenil) can block the effects of allosteric modulators and these are called allosteric antagonists (Johnston, 2005).

An exhaustive account of the $GABA_AR$ pharmacophore is outside the scope of this thesis. Hence, the following section includes a focused discussion intended to emphasize the pharmacological diversity of the $GABA_AR$. Detailed reviews giving further information regarding $GABA_AR$ pharmacology include Hevers & Lüddens 1998; Korpi *et al*., 2002a, 2006; Johnston, 2005; Möhler, 2006; D'Hulst *et al*., 2009; Carter *et al*., 2010.

1.1.8.1. $GABA_AR$ agonists and antagonists

Because the overwhelming majority of native $GABA_ARs$ are ternary complexes composed of 2α, 2β and one other subunit (*e.g.* γ/δ), it follows that more than one GABA binding site exists *per* receptor. Concentration-response curves for GABA are sigmoidal with Hill coefficients between 1 and 2 (Sakmann *et al*., 1983; White, 1992) suggesting the necessity of at least two molecules of GABA for channel activation (Hevers & Lüddens, 1998). Functional studies of the $GABA_AR$ along with receptor

modeling based on the crystal structure of the AChBP have resulted in a structural model of the GABA binding site (Brejic *et al*., 2001; Cromer *et al*., 2002). This model comprises a pocket-like structure located at the α and β subunit interface of the extracellular amino terminal domain and is formed by 6 binding loops, A-F. The homology model further suggests that residues implicated in GABA binding are situated in loops A, B and C of the β subunit, and loops D and E of the α subunit (Cromer *et al*., 2002). Hence, evidence favours a direct interaction between loops A-E whereas the role of loop F (located on the α-subunt) is less clear, although it has been postulated to play a role in locking the agonist in place (Khatri & Weiss, 2010).

In addition to GABA, other endogenous agonists of the $GABA_AR$ exist. Taurine is one such example and occurs extracellularly in the low to high μM range (Lerma *et al*., 1986; Albrecht & Schoesboe, 2005). Extracellular taurine levels are regulated dynamically by the taurine transporters TauT1/2 in response to certain stimuli including depolarization (Albrecht & Schoesboe, 2005). Compared to GABA, taurine typically has a low affinity for the majority of $GABA_AR$ subtypes (Wu & Xu, 2003). However, exogenous taurine, when applied to thalamic brain slices, selectively augments the tonic conductance present in thalamocortical relay neurones (Jia *et al*., 2008). Specifically, Jia *et al*. found that application of taurine at concentrations within the proposed physiological range (10-100 μM) enhanced the tonic conductance of VB neurones in a concentration dependent manner. Moreover, this effect could be mimicked by selective blockade of taurine reuptake by guanidinoethyl sulfonate (GES, Jia *et al*., 2008).

4,5,6,7-tetrahydrosioxazolo[5,4-*c*] pyridine-3ol (THIP) is a GABA-site ligand that, at γ-$GABA_ARs$, acts as a low affinity partial agonist (Krogsgaard-Larsen *et al*., 2004). However, electrophysiological investigation of different combinations of recombinantly expressed $GABA_ARs$, demonstrated that THIP, at low concentrations, selectively activates receptors composed of α4βδ with a greater affinity than the native

ligand, GABA (Brown *et al*., 2002). Hence, the selectivity of THIP for δ-containing receptors presents the researcher with a valuable pharmacological tool for investigating the tonic currents mediated by δ-$GABA_A$Rs (Belelli *et al*., 2005; Farrant & Nusser, 2005; Glykys & Mody, 2007).

The channel gating properties of GABA and other GABA-site agonists can be competitively antagonized by gabazine (also referred to as SR-95531). Bicuculline, although routinely referred to as a competitive $GABA_A$R antagonist, actually exhibits a degree of intrinsic negative efficacy such that strictly, it should be considered an inverse agonist of $GABA_A$R function (McCartney *et al*., 2007). Finally picrotoxin non-competitively inhibits $GABA_A$Rs by blocking the associated Cl^- channel (Korpi *et al*., 2002a).

1.1.8.2. Benzodiazepines

Among the array of allosteric modulators that act at the $GABA_A$R, the benzodiazepines (BDZs) have attained major clinical relevance (Hevers & Lüddens, 1998; Rudolph & Knoflach, 2011). The powerful anxiolytic, anticonvulsant, muscle-relaxant, and sedative actions associated with BDZs were discovered by serendipity and at their time of introduction to the clinical setting in the early 1960s, very little was known about their mechanism of action. In fact, BDZs were in widespread clinical use for over 10 years before electrophysiological evidence began to accumulate showing their GABA enhancing properties (Polc *et al*., 1974; Polc & Haefely, 1976; Macdonald & Barker, 1978c). Further evidence favouring an interaction with the GABA receptor protein came from radioligand binding studies showing the binding of [^{3}H]-diazepam to specific binding sites – presumed to be 'benzodiazepine receptors' - in the brain (Möhler & Okada, 1977; Braestrup & Squires, 1978). Finally, the demonstration that in rat brain

membranes diazepam could increase the $GABA_A$Rs affinity for GABA and provided definitive evidence that the BDZ potentiation of the GABA response occurred through an interaction with the receptor complex (Skeritt *et al*., 1982). In contrast to other $GABA_A$R modulators (*e.g.* barbiturates, certain general anaesthetics, neurosteroids), BDZs do not affect Cl^- currents in the absence of GABA, thus demonstrating that BDZs are incapable of directly activating the $GABA_A$R, even at high concentrations (Choh *et al*., 1977; Study & Barker, 1981).

The classical benzodiazepines, for example chlordiazepoxide (Librium) and diazepam (Valium), are positive allosteric modulators of $GABA_A$R function (Rudolph & Knoflach, 2011). BDZs elicit a conformational change that favours the GABA-induced open state, thus increasing the apparent affinity of the receptor for GABA (Study & Barker, 1981; Macdonald & Twyman, 1992; Macdonald & Olsen, 1994).

Other ligands that interact with the BDZ binding site, for example RO 15-4513 and β-carboline-3-carboxylate (β-CCM) have negative modulatory effects on the GABA response and can be considered BDZ site inverse agonists. Finally, BDZ ligands may lack virtually any efficacy, as in the case of flumazenil, and are therefore termed BDZ-site antagonists (Rudolph & Knoflach, 2011).

These classifications, however, must be considered cautiously because the intrinsic efficacies of BDZs and BDZ-site compounds can vary depending on the $GABA_A$R isoform (Hevers & Lüddens, 1998). For example, the imidazopyridine zolpidem, although not a classical BDZ, is a positive allosteric modulator acting at the BDZ site (BDZ-site agonist) and is used clinically as a sedative. At relatively low concentrations zolpidem is selective for α1-$GABA_A$Rs whereas higher concentrations potentiate α2- and α3-containing receptors, with little or no action at α5-$GABA_A$Rs (Pritchett & Seeburg, 1990; Crestani *et al*., 2000). Furthermore, RO 15-4513 is

classified as an inverse agonist, but at α4 and α6 containing receptors acts as a positive modulator (Knoflach *et al*., 1996).

Typical BDZs are active at receptors incorporating a γ2 subunit (Pritchett *et al*., 1989) and to a lesser extent those receptors that contain a γ1 or γ3 subunit. Receptors incorporating δ, ε, θ, or π subunits are insensitive to BDZ modulation (Rudolph & Knoflach, 2011). The β subunit present in the receptor complex has little, if any, influence over BDZ sensitivity whereas the α subunit plays a major role (Korpi *et al*., 2002a). Hence, receptors that contain either the α1, α2, α3 or α5 subunits have nanomolar affinity for drugs such as diazepam and flunitrazepam whereas those that incorporate α4 or α6 are insensitive to modulation by BDZs (Rudolph & Knoflach, 2011). The molecular basis for this α-subunit selectivity was first deduced through the use of chimeric constructs to compose receptors of differing α1 (high BDZ affinity) and α6 (negligible BDZ affinity) subunit domains. This approach identified a single histidine residue in the α1 variant (replaced by an arginine in the α6) as a major determinant for high affinity binding of BDZs (Wieland *et al*., 1992). In addition to the importance of α1H101 for BDZ affinity, previous studies highlighted the necessity of a γ subunit in the receptor complex (Pritchett *et al*., 1989), a view confirmed by the studies on the γ2 knock-out mouse (Günther *et al*., 1995). Subsequently, a phenylalanine at position 77 and a methionine at position 130 on the γ2 subunit, were identified as playing a key role in conferring BDZ sensitivity (Buhr & Sigel, 1997). Collectively these studies revealed that the BDZ binding site is located at the interface between the γ2 and α1 subunit in the large extracellular N-terminal domain of α1β2γ2 $GABA_A$Rs, at a region homologous to the GABA binding site at the α-β interface (Sigel & Buhr, 1997; Sigel & Lüscher, 2011). This site has been confirmed recently using the crystallized AChBP as a structural model (Berezhnoy *et al*., 2009; Sigel & Lüscher, 2011).

The development of sophisticated molecular biological techniques led to the generation of four 'knock-in' transgenic mouse lines whereby the histidine crucial for BDZ action was replaced with arginine at the α1(H101R), α2(H101R), α3(H126R) and α5(H105R) subunits (for reviews see Rudolph and Möhler, 2004; Möhler, 2006; Zeilhofer *et al*., 2009; Atack, 2011a, 2011b; Möhler, 2011). Investigations utilising these mice have been highly informative in deciphering the role of $GABA_AR$ subtypes, and consequently particular brain circuitries, in specific behavioural actions. Receptors incorporating the α1 subunit, in conjunction with β and γ subunits appear to underlie the sedative, anterograde amnesic and antimyoclonic actions of diazepam (Rudolph *et al*., 1999), whereas αβγ2 receptors containing α2 and probably α3 subunits mediate the anxiolytic activity of diazepam (Low *et al*., 2000; Crestani *et al*., 2001; Atack, 2011a; Möhler, 2011). The muscle relaxant properties of diazepam appear to be mediated by a combination of α1-, α2-, α3- and α5-containing receptors (Low *et al*., 2000; Crestani *et al*., 2001, 2002). More recently, these 'knock-in' mice were utilized to deduce that α2- and α3-containing isoforms mediate the analgesic properties of diazepam in the spinal cord thus implicating α2- and α3-$GABA_ARs$ with a central role in the pain pathway (Knabl *et al*., 2008). Furthermore, by selectively enhancing the activity of α2- and α3-$GABA_ARs$ in rats, the investigators were able to observe a marked reduction in the brain activation evoked by noxious heat as measured by functional magnetic resonance imaging (Knabl *et al*., 2008).

The physiological insights gained from this approach have reinforced the search for subunit selective compounds that may impart desirable BDZ-like effects, but with a restricted spectrum of behavioral outcomes (D'Hulst *et al*., 2009). For example, compounds that preferentially act at α2- and α3-subunit containing receptors have proved effective non-sedative anxiolytics (McKernan *et al*., 2000; Mirza *et al*., 2008; Atack, 2011a). As previously indicated, α5 knock-out and knock-in mice display

improved cognitive abilities thus implicating receptors containing this subunit in learning and memory (Collinson *et al*., 2002; Crestani *et al*., 2002; Atack 2011b). Accordingly, α5-selective BDZ site inverse agonists can improve cognitive function (Atack *et al*., 2005; Dawson *et al*., 2006; Atack 2011b). Furthermore, aspects of the memory impairing effects of BDZs and the general anaesthetics etomidate and isoflurane have been attributed to enhancing the function of α5-$GABA_A$Rs (Bonin & Orser, 2008).

1.1.8.3. General anaesthetics: etomidate, propofol and barbiturates

Several compounds used clinically to induce general anaesthesia act primarily as positive modulators of $GABA_A$R function. Barbiturates, etomidate, propofol and neurosteroids (see Section 1.2) all exhibit GABA-enhancing properties, but, in contrast to the benzodiazepines, at higher concentrations they may also directly activate the receptor (Callachan *et al*., 1987; Peters *et al*., 1988; Hales *et al*., 1991; Pistis *et al*., 1997; Belelli *et al*., 1999a & b). These two actions are likely to require distinct regions of the receptor subunits (Hevers & Lüddens, 1998; Korpi *et al*., 2002a).

The anticonvulsant loreclezole and the structurally related intravenous anaesthetic, etomidate, exhibit selectivity for β2/3 containing receptors over those that contain the β1 subunit (Wingrove *et al*., 1994; Hill-Venning *et al*., 1997). Further studies on the β subunit selectivity of etomidate and loreclezole identified an amino acid residue located within the putative extracellular portion of the β subunit TM2 domain (Wingrove *et al*., 1994; Belelli *et al.,* 1997). Point mutation of this amino acid in β1-$GABA_A$Rs (β1S290N) renders an etomidate sensitive receptor, whereas the etomidate sensitivity is lost by the reverse mutation in β3-$GABA_A$Rs (β3N289S; Belelli *et al*., 1997). These mutations were utilized to generate two lines of knock-in mice one

harboring a β2N265S and the other a β3N265M point mutation (note that position 290 is equivalent to position 265 upon removal of the signal peptide (Jurd *et al.* 2003; Reynolds *et al*., 2003). For the β2N265S mouse the sedative effects of etomidate were eliminated and the hypnotic effects of this anaesthetic were reduced (Reynolds *et al*., 2003). Similarly, for the β3N265M mouse the hypnotic effects of etomidate were reduced, but additionally the immobilizing effect of this anaesthetic on the response to a noxious stimulus was lost (Jurd *et al*., 2003). These data reveal that the behavioural effects of this general anaesthetic are mediated by distinct $GABA_AR$ isoforms (reviewed in Drexler *et al*., 2011).

Distinct from both BDZs and etomidate, the intravenous anaesthetic propofol appears to exhibit little, if any, $GABA_AR$ subtype specificity (Sanna *et al*., 1995; Hill-Venning *et al.* 1997). However, recombinant receptor expression studies have demonstrated that the exchange of the critical β3 TM2 asparagine residue with methionine, in addition to influencing etomidate, also suppressed the GABA-enhancing actions of propofol (Siegwart *et al*., 2002). Indeed the β3N265M knock-in mouse is also insensitive to the immobilizing effects of propofol indicating that the binding sites for these intravenous anaesthetics may, to some extent, overlap with respect to β3-containing $GABA_ARs$ (Jurd *et al*., 2003; Zeller *et al*., 2007).

Barbiturates, typified by pentobarbitone and phenobarbitone also exhibit little $GABA_AR$ subtype specificity. In recombinant expression systems, $GABA_A$ receptors composed solely of α/β subunits or certain homomeric β subunit receptors, can respond to barbiturates suggesting that the γ subunit is not required for their action (Blair *et al.*, 1988; Levitan *et al.*, 1988). In contrast to etomidate and loreclezole, the isoform of the β subunit does not appear to be a critical determinant of barbiturate sensitivity

(Thompson *et al*., 1996). However, receptors containing the α_4 or α_6 subunit have a greater affinity for barbiturates than receptors incorporating the α_1, α_2 or α_3 subunits (Thompson *et al.*, 1996; Wafford *et al*., 1996). Of potential relevance to this, the potentiating actions of many modulators of the $GABA_AR$ including etomidate, pentobarbitone and propofol exhibit a greater efficacy at recombinantly expressed $\alpha_4\beta_3\delta$ receptors *cf* equivalent receptors incorporating the γ subunit (Brown *et al.*, 2002). Finally, at high concentrations (>50 μM) barbiturates may directly gate the channel, even in the absence of GABA and at even greater concentrations may elicit desensitization (Bormann, 1988; Peters *et al*., 1988) and/or channel block (Robertson, 1989), facets that may reflect the presence of several barbiturate interaction sites at $GABA_ARs$ (Sieghart *et al*., 1995).

1.2. Neurosteroids

1.2.1. Neurosteroids: a brief history

In 1941 the pioneering physiologist Hans Selye discovered that certain progesterone metabolites could induce rapid sedation and anaesthesia, on a time scale that ruled out a genomic locus of action (Selye, 1941). A molecular explanation for these overt behavioural changes remained unknown until Harrison and Simmonds demonstrated using extracellular recording from a rat brain slice preparation that the synthetic steroidal anaesthetic, alphaxalone, was a potent positive allosteric modulator of $GABA_AR$ function, with no effect on the functionally and genetically related glycine receptor (Harrison & Simmonds, 1984). Furthermore, this interaction was specific as the 3β-ol isomer of the anaesthetic (*i.e.* betaxolone), which is behaviourally inert, exhibited no such GABA-enhancing effect. Alphaxalone is structurally closely related to these endogenous progesterone metabolites studied by Selye. Consequently, the

authors presciently speculated that "endogenous steroids and their metabolites may also be able to modulate $GABA_AR$ function". This was confirmed only a few years later when it was shown using whole-cell voltage clamp and patch-clamp techniques that several endogenous steroids including the progesterone metabolites 5α-pregnan-3α-ol-20-one (5α3α) and 5β-pregnan-3α-ol-20-one (5β3α) and the deoxycorticosterone metabolite, 5α-pregnan-3α,21-diol-20-one (5α-THDOC), were potent (10-100 nM) positive allosteric modulators of $GABA_AR$ function (Callachan *et al*., 1987; Harrison *et al*., 1987; Peters *et al*., 1988). At the single channel level, these 'neuroactive' steroids were found not to affect the single-channel conductance of the $GABA_AR$, but instead achieve their GABA modulatory actions by increasing the probability that the channel would enter a naturally occurring long duration open state (Callachan *et al*., 1987; Barker *et al*., 1987; Twyman & Macdonald, 1992; Zhu & Vicini, 1997). Moreover, with a similarity to the described actions of barbiturates and the general anaesthetics etomidate and propofol (Section 1.1.6), higher concentrations (>100 nM) of these steroids were found to directly gate the receptor in a GABA-mimetic fashion (Callachan *et al*., 1987; Peters *et al*., 1988).

In common with other positive allosteric modulators, for example the benzodiazepines, these steroids when administered exogenously, not only induced hypnosis, sedation, and anaesthesia, but at lower concentrations were found to have anxiolytic, analgesic and anticonvulsant actions (Crawley *et al*., 1986; Kavaliers & Weibe, 1987; Belelli *et al*., 1989; Gasior *et al*., 1999; Rupprecht, 2003).

1.2.2. The brain is a steroidogenic organ

During the early studies in the late 1980's a major source of these "neuroactive" steroids was considered to be peripheral organs such as the adrenals and the ovaries (Purdy *et*

al., 1991; Paul & Purdy, 1992). In this scenario it was envisaged that peripherally derived "neuroactive" steroids would be produced under certain physiological situations *e.g.* during stress, or pregnancy, which would then cross the blood brain barrier to influence mood and behaviour (Purdy *et al*., 1991; Paul & Purdy, 1992). Such an endocrine role for these steroids is still considered to be of physiological importance. However, at approximately the same time as the GABA-modulatory actions of these steroids were being described, a number of laboratories began to investigate whether steroids could be synthesized in the CNS - a locus of origin that gave rise to the term "neurosteroids" (reviewed in Baulieu *et al*., 2001). Evidence in favour of this proposal came from the observation that the steroid levels in rat brain persisted long after adrenalectomy and gonadectomy. In particular, levels of progesterone (PROG), although reduced, persisted in such male rats, whereas as testosterone and corticosterone were no longer detectable. These data inferred that the surgical procedure had removed only the peripherally imported contribution to the overall steroid levels in the brain (Corpechot *et al*., 1981; 1983; 1993). Further evidence supporting the brain's "steroidogenic" capacity came from reports of circadian rhythm–dependent fluctuations in pregnenolone (PREG) and dehydroepiandosterone (DHEA) levels that were not synchronized with changes in peripheral steroid concentrations (Synguelakis *et al*., 1985; Robel *et al*., 1986). A series of subsequent findings indicated that the enzymatic machinery required for the *de novo* neurosteroid synthesis (*i.e.* from cholesterol) is present in certain CNS cell types, including neurones (see Section 1.2.4, Baulieu *et al*., 2001; Mellon, 2001; Mellon & Griffin, 2002; Agis-Balboa *et al*., 2006; Do Rego *et al*., 2009). These discoveries raised the possibility that, *via* their potentiating actions at $GABA_ARs$, neurosteroids may be able to locally and rapidly influence neuronal excitability in a paracrine, or indeed an autocrine fashion. Consistent with this proposal, GABA-modulatory concentrations of endogenous neurosteroids are known to occur

within the brain (Paul & Purdy, 1992; Mellon & Griffin, 2002). Furthermore, brain levels of GABA-modulatory steroids are dynamically regulated by various physiological conditions (*e.g.* pregnancy, puberty, stress) and perturbations in their levels are associated with certain neurological, psychiatric and pathophysiological conditions (*e.g.* certain forms of epilepsy, depression, schizophrenia, Alzheimer's – Reddy *et al*., 2010; Gunn *et al*., 2011; Luchetti *et al*., 2011).

1.2.3. The neurosteroid binding site(s)

Structure-activity studies have shown that certain chemical features are common to neurosteroids that are positive modulators of $GABA_AR$ function. Namely, such compounds possess a 5α- or 5β-reduced pregnane or androstane skeleton, a 3α-hydroxyl substituent and a hydrogen bond accepting (keto) group at either the C20 or the C17 position of the pregnane steroid side chain or androstane ring system, respectively (Majewska *et al*., 1986; Callachan *et al*., 1987 – Figure 1.5). Importantly steroids with a hydroxyl substituent at carbon 3 in the β conformation do not exert activity at $GABA_ARs$ (Figure 1.5).

Enantioselectivity of steroid action has also been demonstrated. In particular, the negative S(-) entantiomer of 5α3α exhibits a greatly reduced GABA-modulatory and anaesthetic potency relative to the endogenous positive R(+) enantiomer (Wittmer *et al*., 1996). As enantiomers exhibit identical physical properties and thus lipid solubility, these strict structural requirements provided compelling evidence of a neurosteroid interaction with a specific protein *cf.* lipid binding site on the $GABA_AR$ complex. Subsequent radioligand binding and functional studies indicated that that the neurosteroid enhancement of $GABA_AR$ function resulted from an interaction with a recognition site distinct from that of BDZs and barbiturates (Callachan *et al*., 1987; Gee *et al*., 1988; Peters *et al*., 1988; Belelli *et al*., 1996).

Application of modern molecular biological techniques has revealed the identity of critical residues involved in neurosteroid binding (Hosie *et al*., 2006). This accomplishment was initially aided by the electrophysiological demonstration that neurosteroid access to the $GABA_AR$ requires lateral diffusion across the membrane thus inferring that the neurosteroid binding pocket is located in the transmembrane spanning domains of the receptor complex (Akk *et al.*, 2005). Specifically, Akk *et al*. showed that during a cell attached recording in which a tight seal is formed between the pipette and cell thus isolating the activity of receptors in the patch of membrane directly under the pipette (see Materials & Methods), bath application of neurosteroid still resulted in $GABA_AR$ potentiation as determined by a change in the kinetics of GABA-activated single channel events (Akk *et al*., 2005). This observation suggests that the neurosteroid either accesses the $GABA_AR$ by partitioning into the membrane followed by lateral diffusion or, that it accesses the receptor *via* the membrane from an intracellular route. Utilizing excised patch experiments and a membrane impermeant GABA-modulatory steroid, they subsequently demonstrated that steroid enhancement of $GABA_AR$ function only occurred when this steroid was presented to the inner membrane leaflet *i.e.* steroid application to the outer leaflet had no GABA enhancing effect. Collectively, these findings suggest that a steroid-potentiating site, probably located at transmembrane regions of the protein, is readily accessible *via* the inner membrane leaflet (Akk *et al*., 2005).

Subsequently, chimeric α1 and β2 receptor subunits were constructed that contained the transmembrane regions from the relatively neurosteroid insensitive *Drosophila melanogaster* RDL GABA receptor (αR and βR chimera, respectively). For the invertebrate RDL receptor, neurosteroids exhibit a greatly reduced GABA-modulatory action and have no GABA-mimetic properties. Hence, the αR and βR chimeras were generated such that the TM1 and TM2 regions (previously implicated in

neurosteroid potentiation – Rick *et al*., 1998), were substituted with homologous sections of the RDL receptor. Recombinant expression and subsequent functional analysis of αRβγ and αβRγ receptors revealed that the GABA-modulatory and GABA-mimetic actions of 5α3α and 5α-THDOC were abolished in the αR, but not the βR, receptor, thus highlighting a region between TM1 and TM2 on the α1 subunit as crucial to neurosteroid actions at $GABA_A$Rs (Hosie *et al*., 2006). Substitution by site directed mutagenesis of the polar residues within this transmembrane region of the α1 subunit with the homologous hydrophobic residues found in the RDL receptor revealed T236 to be critical for steroid activation, whereas Q241 influenced both potentiation and activation (Hosie *et al*., 2006). Serial mutagenesis of Q241 indicated that H-bonding residues were crucial to retain neurosteroid modulation thus implicating Q241 with a direct role in neurosteroid binding. Based on this concept, a modeling strategy identified further residues in TM4 of the α1 subunit (N407 and Y410) that are ideally placed for H-bonding with the opposite end of the neurosteroid molecule. A similar approach for the activation site yielded an additional residue in TM3 of the β2 subunit (Y284) thus suggesting the activation site spans the α/β interface (Hosie *et al*., 2006). Another important feature that emerged from the study by Hosie *et al* was the necessity for both the activation and the potentiation sites to be occupied in order for maximal neurosteroid activation whereas potentiation of GABA responses was shown not to require neurosteroid occupation of both sites (Hosie *et al*., 2006).

However, subsequent electrophysiological studies have provided evidence to suggest a more complex picture of the steroid binding pocket. For example, potentiating actions of two steroids (5β-3α-hydroxy-18-norandrostane-17b-carbonitrile, and the synthetic enantiomer of etiocholanolone) are differentially influenced by mutations of the residues implicated in steroid potentiation by Hosie *et al*. Hence, additional residues or indeed additional binding sites may contribute to modulatory actions in a manner

dependent on steroid structure (Li *et al*., 2006, 2007; Akk *et al*., 2008; 2010). Nevertheless, the putative identification of transmembrane steroid binding sites has reinforced the proposal of Akk *et al*. that GABA-modulatory steroids may access the receptor *via* membrane lateral diffusion (Akk *et al*., 2005). Extending this observation, membrane accumulation of neurosteroid is proposed to be an important determinant of neurosteroid potency at $GABA_A$Rs (Shu *et al*., 2004, 2007; Akk *et al*., 2009; Chisari *et al*., 2009; Olsen & Li, 2011).

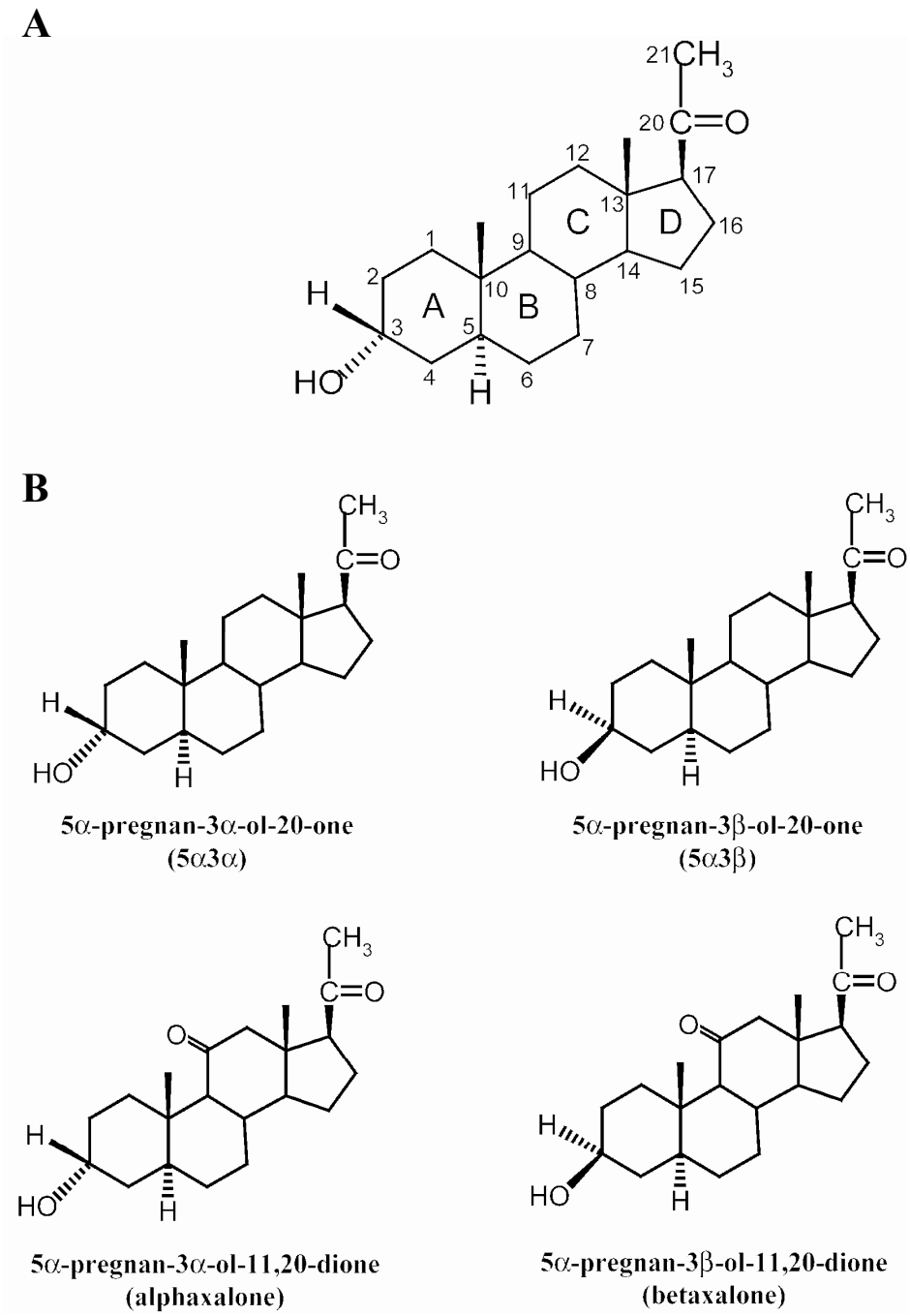

Figure 1.5. Steroid action at $GABA_A$Rs is stereospecific. **A**. Chemical structure of 5α3α showing the cyclopentanophenanthrene nucleus composed of three 6 member rings and one 5 member ring, lettered A-D. The carbon backbone forming the steroid ring system is shown according to the conventional numbering system. Substituents projecting above (solid wedges) and below (broken wedges) the ring system are in the β and α configuration respectively. **B.** Stereoisomeric pairs of active (left) and inactive (right) GABA-modulatory steroids. The hydroxyl group at C3 and the side chain at C17 must be in the α and β configuration respectively for activity at $GABA_A$ receptors.The androstane ring system contains a keto group instead of the side chain at C17.

1.2.4. Neurosteroid biosynthesis

The first step of neurosteroidogenesis is the transport of cholesterol from the outer to the inner mitochondrial membrane by the 18 kDa translocator protein TSPO (formerly called the peripheral benzodiazepine receptor, Rupprecht *et al*., 2010) which functions together with the steroidogenic acute regulator protein (stAR; Sierra, 2004). This translocation of cholesterol is the rate-limiting step in the synthesis of PREG, a reaction that is catalyzed by the mitochondrial enzyme cholesterol side chain cleavage P450scc (Mellon *et al*., 2001; Rupprecht *et al*., 2010). Once PREG is synthesized it may be converted to a number of steroidal end products depending on the type of enzymes present in the cell and/or by substrate competition between enzymes (for reviews see Compagnone & Mellon, 2000; Mellon *et al*., 2001; De Rego *et al*., 2009). Here, I will focus on the synthesis of the GABA-modulatory neurosteroid 5α3α. The synthesis of 5α3α is achieved by the sequential action of three cytosolic enzymes and proceeds as follows, 1) PREG, once synthesized, leaves the mitochondria and is converted to PROG by 3β-hydroxysteroid dehydrogenase (3β-HSD), 2) PROG is converted to 5α-dihydroprogesterone (5α-DHP) by 5α-reductase (5α-R) and 3) 5α-DHP is converted to 5α3α by 3α- hydroxysteroid dehydrogenase (3α-HSD, Mellon *et al*., 2001; Figure 1.6). In addition, 3α-HSD may exist, at least in the rat brain, in two distinct forms – a cytosolic form that favours the reductive reaction to form 5α3α and a membrane bound form that can act in the reverse direction, oxidizing 5α3α to 5α-DHP (Li *et al*., 1997). Differential regional expression of these two forms of 3α-HSD has been shown to locally regulate neurosteroid levels in a manner that affects $GABA_AR$ activity (described further below).

Immunohistochemical approaches have been utilized to investigate the cellular localization of the neurosteroidogenic enzymes in the rodent brain. Initial studies conducted on rat brain tissue revealed 5α-R immunoreactivity to be abundantly

expressed in glial cells (Pelletier *et al*., 1994; Tsuruo *et al*., 1996; Kiyokage *et al*., 2005). However, a similar approach in mouse brain tissue found 5α-R immunoreactivity to be exclusively restricted to neuronal populations, a finding that was reproduced at the mRNA level for both 5α-R and 3α-HSD (Agis-Balboa *et al*., 2006). The reasons for the apparent discrepancy between rat and mouse are unclear but species specific differences provide a possible explanation. Interestingly, immunohistochemical investigation of the 5α3α distribution in adult rat brain reported this neurosteroid to be localized predominantly to principal neurones thus supporting a neuronal and not glial site of neurosteroidogenesis (Saalmann *et al*., 2007). In addition, *de novo* neurosteroidogenesis in cerebellar Purkinje cells (*i.e.* GABA-ergic) has been well-defined and appears to be conserved in mammals (Tsutsui, 2008).

Although the apparent differences between rats and mice concerning 5α-R expression have yet to be resolved, the proposal that neurosteroids are manufactured primarily in glutamatergic cell populations would favour an autocrine (rather than paracrine) action. Such a "self-governing" mechanism of neurosteroid synthesis is an attractive possibility as it may allow the neurone to "fine-tune" its' inhibitory response following changes in excitatory input. Indirect support for an autocrine mechanism of action has come from the visualization of fluorescently-tagged neurosteroids partitioning into the cell membrane (Akk *et al*., 2005). In particular, in hippocampal neuronal cultures a strong membrane and intracellular fluorescence was observed. This pattern of steroid distribution within a neurone suggests that the intracellular compartment may act as a neurosteroid reservoir that could influence the neurosteroid-$GABA_AR$ interaction (Akk *et al*., 2005).

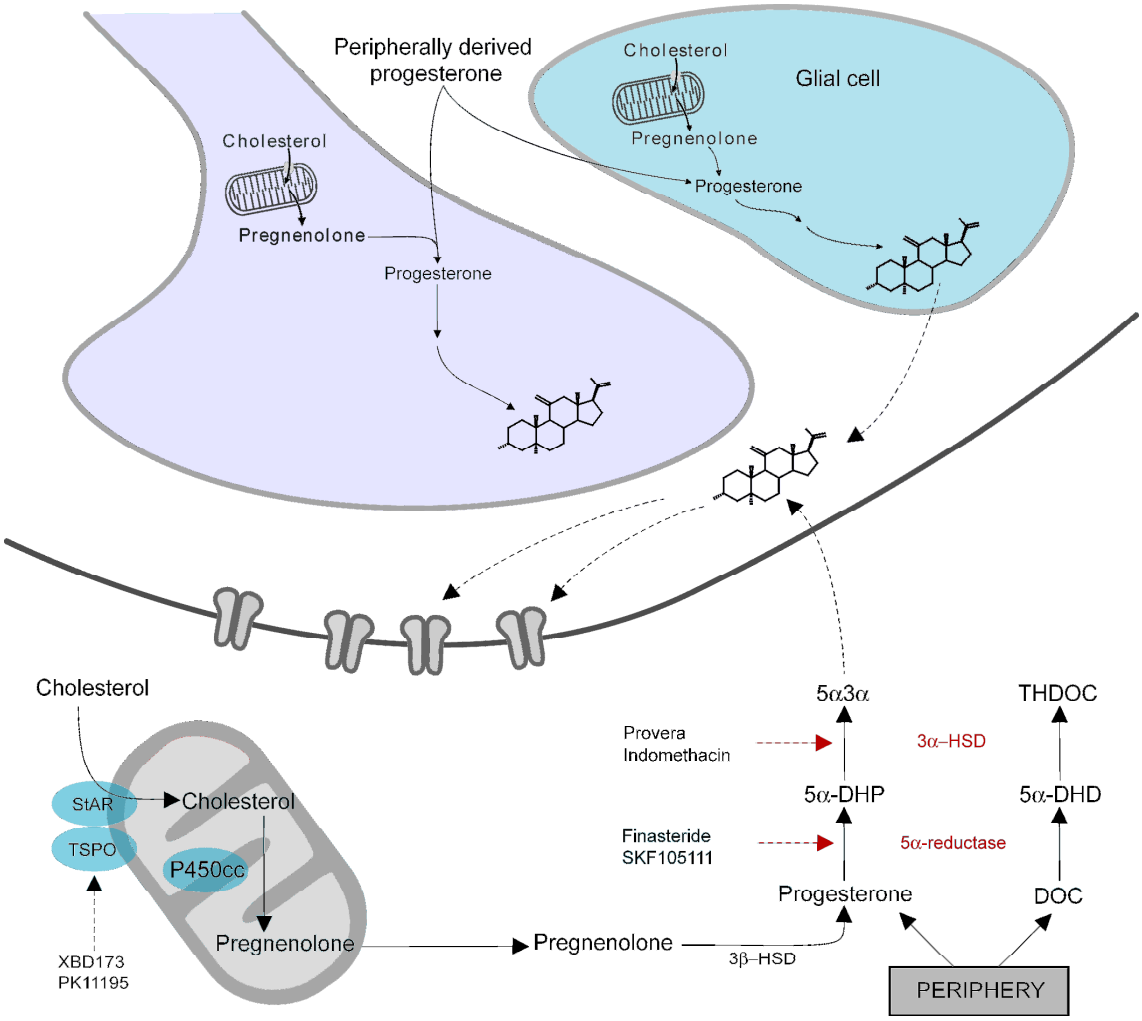

Figure 1.6. Neurosteroidogenesis. *De novo* neurosteroid production requires translocation of cholesterol from the outer- to the inner-mitochondrial membrane by TSPO and its accessory proteins such as STAR. The TSPO complex is targeted by the drugs XBD173 (activator) and PK11195 (inhibitor). P450scc converts cholesterol to pregnenolone which then diffuses into the cytosol. Pregnenolone is converted to progesterone by 3β-HSD. In turn, 5α-R converts progesterone to 5α-DHP which is then converted by 3α-HSD to 5α3α. These latter two enzymes may also act on peripherally derived progesterone or deoxycorticosterone (DOC). Interaction of DOC with 5α-R produces 5α-DHD which is converted to the GABA-active 5α-THDOC by 3α-HSD. Note that 5α-R may be blocked by drugs such as finasteride and SKF 105111 whereas 3α-HSD activity may be blocked by provera and indomethacin. The enzymes required for synthesis of GABA-modulatory neurosteroids have been demonstrated to exist in both neurones and glia meaning that the neurosteroid/$GABA_AR$ interaction may be paracrine or indeed autocrine in nature.

1.2.5. Neurosteroid modulation of synaptic $GABA_ARs$

1.2.5.1. Presynaptic

In certain neurones, the probability of neurotransmitter release is regulated by pre-synaptic $GABA_A$ autoreceptors (reviewed in Kullmann *et al*., 2005). Using the whole-cell voltage clamp technique, a change in pre-synaptic release probability can be measured by the corresponding change in the frequency of post-synaptic currents (Vautrin *et al*., 1993). In contrast to the classical neurosteroid augmentation of inhibitory Cl^- influx, an enhancement of pre-synaptic $GABA_ARs$ by neurosteroids has been shown to increase the IPSC frequency in certain neurones (reviewed in Herd *et al*., 2007). This effect can be accounted for by the differential transmembrane Cl^- gradient at terminal boutons such that pre-synaptic $GABA_AR$ activation leads to Cl^- efflux from the cell. Under these conditions, neurosteroid potentiation of pre-synaptic $GABA_ARs$ enhances Cl^- efflux which further depolarizes the terminal membrane and activates VGCCs leading to an increased transmitter release (Haage & Johansson, 1999; Haage *et al*., 2002, 2005; Kullman *et al*., 2005; Ruiz *et al*., 2010).

1.2.5.2. Postsynaptic

The principal neurosteroid effect on IPSCs recorded from *in situ* synapses, is to prolong their decay time course (Herd *et al*., 2007). The causes for this effect have been investigated in studies in which IPSCs were artificially mimicked using rapid application of saturating GABA concentrations to neuronal nucleated membrane patches of CGCs (Zhu & Vicini, 1997). Under these non-equilibrium conditions the neurosteroid acts primarily to slow the recovery of $GABA_ARs$ from desensitization, a perturbation that could produce a prolongation of the GABA-evoked currents (Zhu &

Vicini, 1997). Specifically, 5α-THDOC was shown to increase the probability of the channel being in the open state by increasing the number of delayed channel openings. Moreover, in support of the importance of desensitization to the effect of the neurosteroid on the $GABA_AR$, 5α-THDOC failed to potentiate the whole-cell current response to taurine - a low affinity agonist that was shown not to induce desensitization (Zhu & Vicini, 1997).

Electrophysiological investigation of a wide variety of neurones has unanimously confirmed the IPSC-prolonging properties of neurosteroids (reviewed in Herd *et al*., 2007, Mitchell *et al*., 2008). However, an interesting feature that has emerged from these studies is that the neurosteroid effect on synaptic $GABA_ARs$ is neurone specific. For example, the duration of mIPSCs recorded from cerebellar Purkinje neurones (Cooper *et al*., 1999), cerebellar granule cells (Vicini *et al*., 2002) and hippocampal CA1 neurones (Harney *et al*., 2003) are sensitive to low, nanomolar neurosteroid concentrations, whilst those recorded from hypothalamic magnocellular neurones (Koksma *et al*., 2003) require micromolar neurosteroid concentrations to elicit an equivalent response. Hence, these comparisons suggest that the native interaction between neurosteroids and native synaptic $GABA_ARs$ is highly selective and specific to individual brain regions and even individual neurones. The following Section describes three important factors that influence neurosteroid sensitivity – phosphorylation, local metabolism and subunit composition.

1.2.6. Regulators of neurosteroid sensitivity

1.2.6.1. Phosphorylation

The phosphorylation status of the $GABA_AR$ complex has been shown by a number of laboratories to dynamically regulate the interaction of neurosteroids with $GABA_ARs$

(Hodge *et al*., 1999, 2002; Fancsik *et al*., 2000; Harney *et al*., 2003). An elegant physiological model of the role of phosphorylation has emerged from studies examining the excitability of magnocellular oxytocin-releasing neurones of hypothalamic supraoptic nucleus (SON) in rats, before and after parturition (Brussaard *et al*., 1997, 2000; Koksma, 2003). Specifically, in pregnant rats the spontaneous IPSCs (sIPSCs) recorded from SON magnocellular neurones are neurosteroid sensitive until 1 day prior to giving birth. However, once parturition commenced, levels of circulating neurosteroids greatly decreased, and in tandem, the synaptic $GABA_A$Rs of magnocellular neurones became insensitive to neurosteroids. A switch from α1- to α2-subunit containing $GABA_A$Rs was originally postulated to account for the neurosteroid insensitivity observed (Brussaard *et al*., 1997; Brussaard & Herbison, 2000). However, subsequent investigation suggested that this form of synaptic plasticity was regulated by changes in the activity of protein kinases and phosphatases (Brussaard *et al*., 2000; Koksma *et al*., 2003). Specifically, in pregnant rats stimulation of protein kinase C (PKC) or inhibition of phosphatases led to sIPSCs that were no longer prolonged by 5α3α. Moreover, in postpartum rats blocking PKC or stimulating phosphatase activity conferred neurosteroid sensitivity to sIPSCs. These observations are of physiological importance to the onset of parturition since oxytocin released from magnocellular neurones was found to stimulate PKC thereby reducing the contribution of neurosteroids to synaptic inhibition such that further oxytocin release was promoted (Koksma *et al*., 2003).

Investigations into the role of phosphorylation in other brain regions have revealed that, in contrast to magnocellular neurones of the SON, phosphorylation of the $GABA_A$R complex imparts a greater neurosteroid sensitivity. For example, in CA1 hippocampal neurones, inhibition of PKC reduced the prolongation of mIPSCs by 5α3α, whereas in DGGCs PKC stimulation enhanced the mIPSC prolonging actions of 5α3α

(Harney *et al*., 2003). Moreover, PKC isoform ε has been shown to influence neurosteroid sensitivity. In particular, muscimol stimulated $^{36}Cl^-$ uptake in the presence of alphaxalone was found to be enhanced in cortical microsacs derived from PKCε knock-out mice (Hodge *et al*., 2002).

Thus, phosphorylation plays a complex and incompletely understood role in influencing neurosteroid sensitivity at the $GABA_AR$. In order to move towards a better understanding, more specific information is required pertaining to the particular kinase and phosphatase isoforms involved and the location of their action, be it on the receptor itself or one of the many accessory proteins.

1.2.6.2. Metabolism

The enzymatic machinery required for neurosteroid synthesis exhibits a differential expression profile within the CNS (Melon *et al*., 2001; Do Rego *et al*., 2009). This finding raises the possibility that local differences in neurosteroid synthesis and metabolism could provide a mechanism for the tight spatial control of neurosteroid action on $GABA_ARs$ (Belelli & Lambert, 2005).

Evidence in favour of this idea has come from experiments using the anaesthetic steroid ganaxolone - a synthetic 5α3α analogue. By virtue of a 3β-methyl group, the crucial 3α-hydroxy group on the steroid A ring is protected from metabolism thus rendering ganaxolone metabolically stable, without affecting its GABA modulatory properties (Carter *et al*., 1997). DGGCs were shown to display mIPSCs that were more sensitive to ganaxolone prolongation than they were to 5α3α, thus implicating neurosteroid metabolism in this differential sensitivity (Belelli & Herd, 2003). In particular, the membrane bound form of 3α-HSD (that favours the reverse oxidative reaction) is prevalent in DGGCs (Li *et al*., 1997) and blockade of this enzyme with

either indomethacin or methoxyprogesterone acetate (Provera) enhanced the sensitivity of DGGC mIPSCs to exogenous application of 5α3α (100 nM, Belelli & Herd, 2003). Therefore, the regulation of 3α-HSD expression can metabolically influence the concentration of GABA-modulatory neurosteroid that the $GABA_AR$ experiences. Another interesting finding of the Belelli & Herd study was that when applied alone to the brain slice, both indomethacin and Provera caused a modest increase in both the mIPSC decay time and the bicuculline sensitive tonic current, observations that infer the existence of a resident neurosteroid tone at DGGCs (Belelli & Herd, 2003).

The strategy of using an inhibitor of neurosteroid synthesis to unveil the effects of endogenous neurosteroids has provided further insights. In particular, injection of mice with the 5α-R inhibitor SKF 105111 produced a substantial decrease in brain 5α3α levels within 30 mins post injection. In behavioural studies this perturbation was accompanied by a decreased sensitivity to the muscimol-induced loss of righting reflex. Furthermore, whole-cell voltage-clamp studies of cortical neurons obtained from such treated mice revealed the sIPSCs to exhibit faster decay kinetics when compared to control mice. Collectively, these observations support the existence of an endogenous neurosteroid tone (Pinna *et al*., 2000; Puia *et al*., 2003).

In CA1 hippocampal neurones, the 5α-R inhibitor finasteride had no effect on the mIPSC decay kinetics when applied alone. However, bath application of PROG (1 μM) to the brain slice led to a slowly developing, and finasteride sensitive, prolongation of the sIPSC decay time course (Sanna *et al*., 2004). These results may suggest that CA1 neurones do not ordinarily experience an endogenous neurosteroid tone but that the enzymes required to synthesize neurosteroids from PROG (*i.e.* 5α-R and 3α-HSD) are present and active (Sanna *et al*., 2004).

As described in Section 1.2.4, the initial (and rate-limiting) step in neurosteroid synthesis is the translocation of cholesterol into the inner mitochondrial membrane by TSPO. Therefore, if a cell contains the full complement of enzymes required to manufacture neurosteroids *de novo*, and they are present in their active form, then stimulation of TSPO-mediated cholesterol translocation should raise neurosteroid levels. The anxiolytic drug etifoxine, in addition to acting as an allosteric modulator of $GABA_AR$ function, stimulates TSPO and thereby elevates the cortical production of 5α3α, an effect that contributes to the behavioural actions of the drug (Verleye *et al*., 2005). The selective TSPO activator XBD-173 prolongs the decay time of mIPSCs recorded from cortical neurones, in a manner that is blocked by finasteride (Rupprecht *et al*., 2009). Furthermore, XBD-173 was effective in behavioral tests that are predictive of anxiolytic action, and these actions could be blocked by the TSPO "antagonist" PK11195 (Rupprecht *et al*., 2009). The anxiolytic potential of XBD-173 was confirmed in humans, suggesting TSPO is a viable target that could be exploited to produce anxiolytic compounds with a reduced side effect profile compared to BDZs (Rupprecht *et al*., 2009, 2010). Interestingly, reduced levels of 5α3α in the cerebrospinal fluid are associated with some forms of depression (Uzunova *et al*., 1998). Clinically, the time course of therapeutic efficacy of SSRIs such as fluoxetine (Prozac), correlates with a return to normal neurosteroid levels (Uzunova *et al*., 1998). Similarly, the defecit in brain neurosteroid levels observed in the socially isoalated mouse model of depression can be rectified by fluoxetine treatment (Pinna *et al*., 2004; Matsumoto *et al*., 2007). The molecular mechanisms that mediate the SSRI-induced increase in neurosteroid levels remain to be identified in full, although an allosteric interaction with 3α-HSD has been suggested (Pinna *et al*., 2010).

Collectively these findings indicate that the synthesis and metabolism of neurosteroids are important factors in regulating the neurosteroid-$GABA_AR$ interaction.

Furthermore, pharmacological manipulations that stimulate the neurosteroid manufacturing process may have therapeutic potential for the treatment of certain psychiatric conditions, including anxiety disorders (Belelli & Lambert, 2005; Rupprecht *et al*., 2010).

1.2.6.3. Subunit composition

As detailed in Section 1.1.8, the $GABA_AR$ subunit composition can confer distinct pharmacological properties. By contrast, the subunit composition has only a modest impact on neurosteroid action. However, differences in sensitivity may be important considering the proposed physiological neurosteroid concentration range (Belelli & Lambert, 2005; Herd *et al*., 2007). Specifically, recombinant α1β1γ2 and α3β1γ2 receptors display sensitivity to relatively low concentrations (~ 3 nM) of 5α3α, whilst analogous receptors incorporating α2, α4, α5 or α6 subunits require 10-30 fold higher concentrations to elicit equivalent GABA-modulatory effects (Belelli *et al*., 2002).

Perhaps the most salient finding regarding the influence of subunit composition upon neurosteroid actions is that the magnitude of the neurosteroid effect is significantly greater for recombinant receptors incorporating the δ-subunit *cf.* the γ2 subunit (Belelli *et al*., 2002; Brown *et al*., 2002; Wohlfarth *et al*., 2002; Glykys *et al*., 2007). This finding raises the possibility that endogenous neurosteroids may selectively enhance a δ-$GABA_AR$ mediated tonic inhibition, a proposal that is discussed below.

1.2.7. Extrasynaptic $GABA_ARs$: a target for endogenous neurosteroids?

The first indication that δ-$GABA_ARs$ may provide an important molecular target for neurosteroid action came from the behavioral evaluation of δ knock-out mice.

Specifically, these mice showed a blunted response to the anxiolytic, anaesthetic/hypnotic and pro-convulsant (*i.e.* absence-like) action of the pregnane steroids (Mihalek *et al*., 1999).

Consistent with this finding, electrophysiological studies revealed that neurosteroids including 5α3α and 5α-THDOC greatly enhanced GABA activation of recombinantly expressed α1βδ, α4βδ and α6βδ receptors relative to equivalent receptors containing a γ subunit (Belelli *et al*., 2002; Brown *et al*., 2002; Wohlfarth *et al*., 2002; Glykys *et al*., 2007). Subsequently, it was shown that the low efficacy of GABA acting at δ-$GABA_A$Rs could be shifted to a high-efficacy mode by neurosteroids, thus accounting for the preferential interaction of neurosteroids with these receptors (Bianchi & Macdonald, 2003).

Subsequent whole-cell voltage clamp studies performed on brain slices has further supported this proposal. For example, the tonic conductance recorded from adult mouse CGCs and DGGCs has been reported to be enhanced by a low concentration (10 nM) of 5α-THDOC, without the steroid affecting the kinetics of their synaptic currents recorded from these neurones (Stell *et al*., 2003). Furthermore, the tonic currents recorded from DGGCs and CGCs derived from $\delta^{0/0}$ mice exhibited a blunted response to 5α-THDOC thus implicating receptors incorporating the δ subunit in mediating this effect (Stell *et al*., 2003).

Other evidence has provided a rather more complicated indication of the nature of the neurosteroid/δ-$GABA_A$R interaction (Shen *et al*., 2007). Specifically, the enhancement of recombinant α4β2δ and α4β3δ receptors by 30 nM 5α3α was found to be dependent on the direction of Cl^- flux through the $GABA_A$R. Thus, upon manipulation of the internal Cl^- concentration such that GABA evoked an outward current response, 5α3α ceased to enhance and instead inhibited the GABA response at α4β2δ receptors. However, this effect was absent at α1β2δ, α4β3δ and α4β2

recombinant receptor subtypes where 5α3α retained a GABA-enhancing effect (Shen *et al*., 2007). These results may be of physiological importance when the transmembrane Cl^- gradient favours an outward Cl^- flux *i.e.* a depolarizing effect in response to GABA, for example during development (see Section 1.1.4). Moreover, receptors composed of α4βδ subunits occur in thalamocortical neurones and DGGCs (Porcello *et al*., 2003; Stell *et al*., 2003; Belelli *et al*., 2005; Chandra *et al*., 2006; Herd *et al*., 2008; Herd *et al*., 2009).

Considering the studies discussed above, it would appear that δ-$GABA_A$Rs are major targets for low concentrations (in the nM range) of neurosteroids, levels which are known to occur physiologically (Paul & Purdy, 1992; Mellon & Vaudry, 2001; Mellon & Griffin, 2002). However, several lines of evidence have indicated that the situation is far more complicated. For example, simply relating the behavioural findings from $\delta^{0/0}$ to an absence of neurosteroid/δ-$GABA_A$R interactions is potentially problematic because the genetic deletion may cause widespread plasticity changes (Vicini *et al*., 2002; Spigelman *et al*., 2003 *c.f*. Stell *et al*., 2003, for review see Herd *et al*., 2007). Other studies have revealed that not all neuronal extrasynaptic $GABA_A$Rs are sensitive to low concentrations of neurosteroids. For example, thalamocortical (TC) neurones of the ventrobasal thalamus (VB) exhibit a considerable tonic conductance mediated by α4β2δ receptors (Porcello *et al*., 2003; Belelli *et al*., 2005; Cope *et al*., 2005a; Jia *et al*., 2005; Chandra *et al*., 2006; Herd *et al*., 2009). Application of 250 nM 5α-THDOC had no effect on this conductance whereas electrically evoked IPSCs were significantly prolonged (Porcello *et al*., 2003). Furthermore, the tonic conductance in juvenile rat DGGCs is not affected by 100 nM 5α3α (Belelli & Herd, 2003). In adult rat DGGCs 5α3α (10-30 nM) induced only a modest increase in the membrane noise and had no affect on the holding current (Mtchedlishvilli & Kapur, 2006). Similarly, the tonic conductance in adult rat CGCs was only marginally enhanced by 100 nM 5α-

THDOC (Hamann *et al*., 2002). Similar discrepancies are apparent for studies investigating the sensitivity of tonic conductances mediated by α5-$GABA_A$Rs to neurosteroid modulation and are reviewed in Herd *et al*., 2007.

Collectively, these *in vitro* studies demonstrate that the high neurosteroid efficacy consistently exhibited by recombinant δ-$GABA_A$Rs does not necessarily translate in to a similar action at native δ-$GABA_A$Rs. As described above, additional factors are known to influence neurosteroid sensitivity of neurones (*i.e.* phosphorylation status, local metabolism) and it remains a possibility that these contribute to the regulation of the neurosteroid/δ-$GABA_A$R interaction (Herd *et al*., 2007). Moreover, the levels of neurosteroids are dynamically regulated by a variety of physiological and pathophysiological conditions (Belelli & Lambert 2005; Herd *et al*., 2007; Mitchell *et al*., 2008; Gunn *et al*., 2011). With respect to the current study, evidence supporting a role for neurosteroids in neuronal development is considered below.

1.2.8. Trophic neurosteroid actions during development

A number of neurosteroids, including PREG, PROG, DHEA and 5α3α, have been implicated in playing a role in CNS development (reviewed in Mellon, 2007; Melcangi *et al*., 2011). With respect to the current study, the actions of 5α3α will be focused upon with an emphasis on how $GABA_A$R modulation by this neurosteroid may contribute to certain developmental processes.

Brain 5α3α levels have been shown to be developmentally regulated (Pomata *et al*., 2000; Grobin & Morrow, 2001). For example, in the rat cortex 5α3α levels have been quantified from embryonic through to postnatal development using radioimmunoassay. These studies have revealed that 5α3α levels are relatively high during gestation, peaking at approximately embryonic day 18 (E18) before falling

sharply immediately prior to parturition (E20-E21, Grobin & Morrow, 2001). After birth cortical 5α3α levels continue to decline until, between postnatal days 10 and 14 (P10-14), a secondary elevation in 5α3α levels occurs (Grobin & Morrow, 2001). By P15, however, cortical 5α3α levels decreased to a steady state level until sex differences in 5α3α levels become apparent on and after P25 (Grobin & Morrow, 2001). These developmental variations in cortical 5α3α levels correlate well with changes in brain expression of 5α-R and 3α-HSD (Kellogg & Frye, 1999; Melcangi *et al*., 1998; Griffin *et al*., 2004). Given these developmental changes in both the levels of 5α3α and the expression of the 5α3α-synthesizing enzymes, a role in brain development and plasticity might be anticipated. Indeed, treatment of neonatal rats at either P1 or P5 with 5α3α resulted in abnormalities in interneurone localization in the prefrontal cortex in adults (Grobin *et al*., 2003). Videomicroscopy studies of cultured hippocampal neurones reveal inhibition of neurite extension within 40 mins of incubation with 5α3α (1 μM, Brinton *et al*., 1994). Furthermore, in two independent studies 5α3α was shown to increase proliferation of rat hippocampal neuroprogenitors, CGCs and human cortical-derived neural stem cells at a concentration range consistent with those required for enhancement of $GABA_AR$ function (0.1-1 μM - Keller *et al*., 2004a; Wang *et al*., 2005).

The mechanisms by which 5α3α mediates these neurodevelopmental actions are incompletely understood, and metabolism to genome-active precursors are likely. However, the developmental actions described for 5α3α may involve an interaction with $GABA_ARs$. As described in Section 1.1.4, GABA evokes depolarizing responses in the immature brain due to the delayed expression of KCC2 Cl^- co-transporter (reviewed in Blaesse *et al*., 2009). Under these developmental conditions, $GABA_AR$ activation has been shown to raise intracellular Ca^{2+} levels ($[Ca^{2+}]_i$) by activation of VGCCs (Cherubini *et al*., 1991; Yuste & Katz, 1991; reviewed in Ben-Ari *et al*., 2007). Hence, it is possible that potentiation by 5α3α of $GABA_AR$ function during development

augments $[Ca^{2+}]_i$ giving rise to the possibility that Ca^{2+} sensitive signaling pathways become activated. Indeed, blocking VGCCs with nifedipine prevented the 5α3α-induced increase in the proliferation of neural progenitors (Keller *et al*., 2004a; Wang *et al*., 2005). Subsequently, using Ca^{2+} imaging techniques on cultured rat hippocampal neurones, a developmentally regulated increase in $[Ca^{2+}]_i$ in response to 5α3α (500 nM) has been reported (Wang & Brinton, 2008). This effect could be prevented by picrotoxin thus implicating $GABA_A$Rs in mediating at least a portion of the developmental actions of 5α3α (Wang & Brinton, 2008).

Another indication of the importance of 5α3α to normal brain development has come from investigations of a mouse model of Niemann-Pick disease type C. Caused by mutations in the NPC1 gene, this neurodegenerative disease is characterized by dysfunctional trafficking and intracellular accumulation of cholesterol. The disease onset typically begins in childhood and is fatal by adolescence (Griffin *et al*., 2004). The naturally occurring NP-C mouse recapitulates many of the cellular deficits seen in humans (*e.g.* demyelination, Purkinje cell degeneration, loss of motor function) and also results in premature death (Griffin *et al*., 2004). In this study Griffin *et al.* demonstrated that neonatal (P7) 5α3α treatment markedly prolonged the NP-C mouse lifespan, delayed the appearance of neurological symptoms and increased Purkinje cell survival. Furthermore, 5α3α but not the $GABA_A$R-inactive 3β-ol isomer, increased survival of NP-C Purkinje neurones maintained in cell culture in a manner that was blocked by bicuculline thus implicating $GABA_A$Rs in mediating this effect (Griffin *et al*., 2004). Together with highlighting the promising therapeutic potential of 5α3α and related analogues, the effects observed in this study following P7 5α3α application suggest that this steroid may be involved in processes crucial to normal brain development that occur before the end of the first week of life (Griffin *et al*., 2004).

1.2.9. $GABA_AR$-mediated currents during development: a role for neurosteroids?

The evidence described so far primarily concerns the influence of 5α3α on morphological and cytoarchitectural processes during development. However, a common functional feature of synaptic development is that the decay of postsynaptic currents becomes faster with maturity (Takahashi, 2005). Indeed, this form of synaptic plasticity has been described for postsynaptic currents mediated by NMDA-Rs (Takahashi *et al*., 1996), AMPA-Rs (Taschenberger & von Gersdorff, 2000), nACHRs (Sakmann & Brenner, 1978), GlyRs (Takahashi *et al*., 1992) as well as $GABA_ARs$. With respect to $GABA_ARs$ a developmental speeding of IPSC kinetics has been reported in CGCs (Brickley *et al*., 1996; Tia *et al*., 1996), cerebellar Purkinje cells (Pouzat & Hestrin, 1997), DGGCs (Draguhn & Heinemann, 1996; Hollrigel & Soltesz, 1997), hypothalamic magnocellular oxytocin neurones (Brussaard *et al*., 1997), cortical neurones (Dunning *et al*., 1999), laterodorsal thalamic neurones (Okada *et al*., 2000) and ventrobasal thalamic neurones (Peden *et al*., 2008). Physiologically, a shortening of IPSC decay time is thought to contribute to the increased demand for temporal precision - a prerequisite for the development of complex network activity (Takahashi, 2005). Evidence to date has indicated that the developmental decrease of the duration of postsynaptic currents is due primarily to switches in postsynaptic receptor subunit composition so that receptors with intrinsically faster decay kinetics become more prevalent with maturity. For example, the postsynaptic $GABA_ARs$ expressed in laterodorsal thalamic neurones exhibit a delayed incorporation of the α1 subunit, a finding that has been proposed to underlie the faster IPSC decay kinetics observed during development (Laurie *et al*., 1992b; Fritschy *et al*., 1994; Okada *et al*., 2000). Despite the influence of receptor subunit composition, other factors are also known to influence the decay kinetics of postsynaptic currents. For example, changes in neurotransmitter release probability, GAT expression, post translational-modifications

of postsynaptic proteins or alterations of the cytoskeleton could impact upon mIPSC kinetics (Jones & Westbrook, 1997; Petrini *et al*., 2003; Mozrzymas, 2004; Takahashi, 2005; Chen & Olsen, 2007; Barberis *et al*., 2011)

Given that neurosteroid levels are known to be relatively high around the perinatal period (Grobin & Morrow, 2001; Grobin *et al*., 2003) it is conceivable that $GABA_AR$ currents may be positively modulated by endogenous neurosteroids early in development and consequently prolong the duration of mIPSC. In support of this proposal, observations made in spinal neurones during neonatal development indicate the presence of a neurosteroid tone (Keller *et al*., 2004b). Specifically, in lamina II (LII) neurones of the dorsal horn, the decay kinetics of $GABA_AR$-mediated mIPSCs exhibit developmental speeding (Ma *et al*., 1993; Keller *et al*., 2001) in the absence of any change in $GABA_AR$ subunit composition (Poulter *et al*., 1992; Bohlhalter *et al*., 1996). However, by applying PK11195 and finasteride (a TSPO inhibitor and a 5α-R inhibitor, respectively) to young (< P23) LII dorsal horn neurones in the spinal slice preparation, the $GABA_AR$ mediated mIPSCs became faster in their decay time thus unveiling a tonic presence of 5α-reduced neurosteroids in LII neurones (Keller *et al*., 2004b). Conversely, mIPSCs from adult LII neurones were unaffected by inhibitors of 5α-reductase and TSPO but were prolonged by pharmacological stimulation of TSPO by diazepam thus indicating that adult neurones may retain a fully functional complement of neurosteroidogenic enzymes but do not produce GABA-modulatory levels of neurosteroids under normal conditions (Keller *et al*., 2004b). Further investigations revealed that the neurosteroidogenic pathway present in adult LII dorsal horn neurones can be reactivated in an experimental model of inflammatory pain (Poisbeau *et al*., 2005). In particular, peripheral inflammation induced by intraplantar injection of carrageenan resulted in $GABA_AR$-mediated mIPSCs that were prolonged compared to control an effect that could be blocked by finasteride, or by PK11195 (Poisbeau *et al*.,

2005). In a behavioural assessments of pain thresholds, pretreatment with finasteride before the induction of inflammation resulted in an increase in inflammation-induced hyperalgesia to heat. Hence, it has been proposed that an upregulation in 5α-reduced neurosteroid synthesis in response to peripheral inflammation may represent a mechanism for the modulation of antinociceptive control in LII dorsal neurones (Poisbeau *et al*., 2005; Schlicter *et al*., 2006). Finally, extension of these studies into inhibitory transmission in LIII/IV revealed lamina specific differences in the endogenous neurosteroid tone experienced by synaptic $GABA_ARs$ (Inquimbert *et al*., 2007). In 10-15 day old rats, finasteride had no effect on the mIPSCs from LIII/IV neurones (*c.f* LII). However, preincubation (>1hr) with 1 μM PROG or sub-cutaneous injection (75 mg/kg) of PROG (followed by ex vivo recording from spinal cord slice preparartions) resulted in prolonged LIII/IV mIPSCs whereas mIPSCs recorded from LII neurones were unaffected by these treatments. These results demonstrate how localised differences in neurosteroidogenesis can impact on mIPSC duration. Furthermore, the fact that progesterone did not further prolong LII mIPSCs suggests that $GABA_ARs$ expressed by these neurones are maximally prolonged by endogenous neurosteroids between P10 and P15 (Inquimbert *et al*., 2007).

As described previously, certain neurones and glia in the brain have a neurosteroidogenic capacity. Therefore, it is conceivable that in addition to LII dorsal horn neurones, select supraspinal locations could exhibit a developmentally regulated tonic neurosteroid production that may influence $GABA_AR$ function. Clearly, to investigate this possibility it would be beneficial to study a neuronal class where the developmental profile of $GABA_AR$ subtype expression is well defined. One such class of neurones are the thalamocortical (TC) cells of the ventrobasal (VB) nucleus, a thalamic brain region that is a primary focus on the current investigation. As such, the

developmental $GABA_AR$ expression of VB neurones is described in the accompanying Section.

1.2.10. $GABA_AR$ expression in the VB nucleus during development

A recent study on mouse VB neurones that combined whole-cell voltage clamp recordings and immunohistochemical techniques has revealed the developmental changes in the α subunit identity in synaptic $GABA_ARs$ (Peden *et al*., 2008). In particular, at P8-11 synaptic $GABA_ARs$ expressed on VB neurones are predominantly composed of α2-containing receptors based on the findings that 1) α2, but not α1, immunostaining was high at this time. 2) α3 subunit immunostaining was absent in the VB nucleus throughout development. 3) P8-11 mIPSCs were not prolonged by low, α1-$GABA_AR$ selective concentrations (*i.e.* 100 nM) of zolpidem. 4) the prolongation of P8-11 mIPSC decay time to relatively high (α2/3-$GABA_AR$ affecting concentrations *i.e.* 1 μM) of zolpidem was lost in α2H101R mice. 5) P8-11 mIPSC properties were unaffected in VB neurones derived from $\alpha1^{0/0}$ mice. 6) α4 subunit immunofluorescence did not co-localise with gephyrin clusters – a marker of inhibitory synapses (Peden *et al*., 2008). Hence, at this developmental time point it is possible to deduce that all synaptic $GABA_ARs$ expressed by VB neurones contain the α2-subunit. However, Peden and colleagues found that over the subsequent 10 days of development there occurred a synaptic re-organization of α subunits such that virtually all synaptic $GABA_ARs$ contained the α1 subunit by P20 (Peden *et al*., 2008). The importance of the α1 subunit to synaptic transmission in more mature VB neurones (P15-20) was dramatically demonstrated by VB recordings from the $\alpha1^{0/0}$ mouse. Although in VB neurones, $\alpha1^{0/0}$ P8-11 VB mIPSCs exhibited unchanged mIPSC properties relative to WT, the majority

of VB neurones fell "silent" with respect to mIPSCs by P15-22 *i.e.* no synaptic activity was evident (Peden *et al*., 2008).

Therefore the α-subunit expression profile of synaptic $GABA_A$Rs during VB development is relatively straightforward. Before P15 $GABA_A$Rs primarily contain the α2 subunit, after P15 they primarily, if not exclusively, contain the α1 subunit. Mice that harbour an F77I point mutation on the γ2 subunit result in mIPSCs that display a severely attenuated sensitivity to enhancement by zolpidem indicating that this drug selectively activates γ2 containing receptors (in addition to α1-, α2-, α3- and α5-$GABA_A$Rs - Cope *et al*., 2005b). Thus, at P8-11 the sensitivity of mIPSCs recorded from VB neurones towards non-selective concentrations of zolpidem infers the presence of the γ2 subunit in synaptic $GABA_A$Rs (Peden *et al*., 2008). Collectively, these findings suggest that the major synaptic $GABA_A$R isoform at immature (P8-14) VB neurones is α2βγ2.

Identification of synaptic $GABA_A$R isoforms expressed by more mature VB neurones has been achieved by an accumulation of evidence from several studies. Immunohistochemical methods indicate the presence of α1, α4, β2, γ2 and δ subunits in the adult ventrobasal nucleus (Pirker *et al*., 2000). Miniature inhibitory postsynaptic currents (mIPSCs) recorded from VB neurones (12-21 day old) exhibit relatively fast decay kinetics and, in WT but not α1H101R mice, are sensitive to modulation by benzodiazepines (Sohal *et al*, 2003). Furthermore, WT VB neurones display sensitivity to low (100 nM) α1-subunit selective concentrations of zolpidem (Peden *et al*., 2008). Deletion of the β2 subunit reduces the frequency and amplitude of VB mIPSCs and the effect of etomidate to prolong VB mIPSC kinetics is lost in the β2N265S mouse thus implicating $GABA_A$R incorporating the β2 subunit within the synapse (Belelli *et al*., 2005). By contrast, deletion of the β3 subunit does not affect VB mIPSC properties (although it severely disrupts the properties of mIPSCs recorded from neurones of the

nucleus reticularis – Huntsman *et al*., 1999). Collectively, these studies have established that the synaptic $GABA_ARs$ receptors in juvenile (P15+) to adult VB neurones are composed of α1, β2 and γ2 subunits.

VB neurones examined in a brain slice preparation display a considerable endogenous tonic current that can be augmented by THIP concentrations (< 1μM) selective for δ-$GABA_ARs$ and blocked by $GABA_AR$ antagonists (Belelli *et al*., 2005; Cope *et al*., 2005a; Jia *et al*., 2005). The tonic-enhancing properties of β2/3 selective concentrations of etomidate are diminished in the β2N265S mouse (Belelli *et al*., 2005) and the tonic current present in WT VB neurones is severely attenuated upon deletion of the α4 (Chandra *et al*., 2006), β2 (Belelli *et al*., 2005) or δ subunit (Porcello *et al*., 2003; Herd *et al*., 2009) . Taken together, these studies have deduced that, in VB neurones, the majority of extrasynaptic $GABA_AR$ are composed of α4, β2 and δ subunits.

1.2.11. $GABA_AR$ expression in the cortical L2/3 pyramidal neurones during development

Relative to VB neurones, L2/3 pyramidal neurones of the cortex display a rather more complex and less well defined expression profile of $GABA_AR$ subtypes during development. Specifically, detailed studies combining electrophysiological and immunohistochemical methods (as exist for VB neurones) are lacking. In light of this, evidence form different avenues of research will be assessed and a developmental profile of $GABA_ARs$ expressed by L2/3 neurones will be put forward.

At the mRNA level for the whole cortex, during the first week of life α1 subunit expression is low, but nevertheless evident, whereas after this time-point the levels of α1 mRNA increase such by the end of the second postnatal week it becomes the most abundant of the α subunits - a feature that is maintained into adulthood (Gambarana *et*

al., 1990, 1991; Laurie *et al*., 1992b; Van Eden *et al*., 1995). An essentially opposite mRNA expression profile has been reported for the α2 and α3 subunits, which exhibit relatively high levels in the first ~ two weeks, before a decrease in their relative expression occurs such that low levels persist throughout life (MacLennan *et al*., 1991; Araki *et al*., 1992; Laurie *et al*., 1992b). Hence, unlike the VB neurones of the thalamus, a significant proportion of α2/α3 subunit expression remains in adult cortical neurones indicating the existence of a heterogenous population of $GABA_A$Rs with respect to the α-subunit (MacLennan *et al*., 1991; Araki *et al*., Laurie *et al*., 1992b). These developmental patterns in cortical α subunit mRNA expression have been confirmed at the protein level by immunohistochemical approaches (Fritschy *et al*., 1994; Pirker *et al*., 2000). Furthermore, Fritschy *et al*. reported that the developmental loss of α2 subunit protein occurred uniformly across all immunoreactive cells and did not represent a loss of staining in a subset thus indicating that the switch from an α2 to an α1 subunit is likely to be a general developmental process intrinsic to all neuronal types (Fritschy *et al*., 1994). The α4 and α5 subunit subtypes may also show developmental changes in their cortical expression levels. In particular α5 subunit mRNA levels have been detected at relatively high levels during neonatal development but decreases to undetectable levels after approximately two weeks (Laurie *et al*., 1992b). The α4 subunit mRNA is detectable at modest levels from birth to adult whereas the α6 mRNA is absent at every developmental stage (Laurie *et al*., 1992b)

The ontogenic $GABA_A$R subunit expression in the cortex displays considerable topographical specificity. In particular, the maturation of α1 and α2 subunits was demonstrated to be both area and layer specific whereby in cortical regions (*e.g.* the primary visual cortex) the α2 to α1 subunit switch occurred prior to other regions (*e.g.* association areas - Fritschy *et al*., 1994; Hornung & Fritschy, 1996; Paysan *et al*., 1997). Regarding the β subunit composition of cortical $GABA_A$Rs, β2 and/or β3 subunit

proteins exhibit a prominent expression during neuronal maturation, suggesting that these subunits are present to a similar extent in both perinatal and adult animals (Fritschy *et al*., 1994). Due to a lack of β subunit antibody specificity (Fritschy *et al*., 1994; Pirker *et al*., 2000) and conflicting findings from *in situ* hybridization studies (Gambarana *et al*., 1991; Poulter *et al*., 1993; Laurie *et al*., 1992b) the developmental maturation of the β subunit proteins is not well-defined. Studies using antibodies that recognize β2/3 subunits (but are unable to discriminate between them) have reported similar levels of immunostaining with this antibody throughout development (Fritschy *et al*., 1994). In addition, analysis of β subunit mRNA levels during development generally supports the prominence of β2/3 subunit expression over β1 (Gambarana *et al*., 1991; Laurie *et al*., 1992b; Poulter *et al*., 1993). Relative to γ1 and γ3 subunit mRNAs, high levels of γ2 subunit mRNA expression have been reported in widespread cortical regions and these levels vary little with development (Gambarana *et al.,* 1991; Laurie *et al*., 1992b). Finally, δ subunit mRNA has been detected in the developing cortex, initially at low levels in the first few days after birth but then increasing to moderate levels in the second week of life and into maturity (Laurie *et al*., 1992b).

Functional studies have provided additional insights into the receptor subunit composition of cortical $GABA_A$Rs. Developmental investigations of cortical neurones maintained in culture and in the brain slice preparation have been performed using pharmacological and electrophysiological methods (Dunning *et al*., 1999). In broad agreement with anatomical investigations these studies revealed that a switch in the relative abundance of the α1 subunit occurs. Specifically, mIPSCs were found to shorten in duration with development and this profile was remarkably similar for whole cell voltage clamp recordings performed on both cultured and brain slice (LIV/V) cortical neurones (Dunning *et al*., 1999). After 5-7 days in vitro (DIV) mIPSCs from cultured cortical neurones exhibited a modest prolongation in response to high

concentrations of zolpidem (300 nM), whereas this prolongation was markedly enhanced by 22-28 DIV. The increase in zolpidem sensitivity correlated with an increased α1 subunit signal following RT-PCR analysis of cortical tissue, observations that collectively are consistent with a developmental increase in α1-$GABA_A$Rs (Dunning *et al*., 1999). Furthermore, Dunning *et al*. measured the developmental expression of cortical α5 subunit expression using RT-PCR techniques. In agreement with the developmental α5 subunit expression profile as measured by mRNA detection, the α5 subunit was found to be abundant during the first week of life then decreased substantially with maturity (Dunning *et al*., 1999). The α5 subunit is known to form an extrasynaptic $GABA_A$R population in certain mature neurones (Brünig *et al*., 2002; Glykys & Mody, 2007). A recent study utilizing a brain slice preparation reported that 5 μM GABA induced a substantial tonic conductance in neonatal (P2-4) cortical pyramidal neurones. This current, which dissipated substantially by P30, could be partially blocked by L655-708, a selective α5-$GABA_A$R antagonist (Sebe *et al*., 2010). Thus, early in development α5-$GABA_A$Rs may form an extrasynaptic population of receptors in cortical pyramidal neurones that are sensitive to relatively low concentrations of GABA (Sebe *et al*., 2010). A component of this tonic current was found to be additionally sensitive to THIP action thus implicating a role for δ-$GABA_A$Rs early in cortical development. Indeed, western blot analysis revealed a relative ontogenic progression whereby the δ subunit protein is initially high (P3) but decreases with development (P30 – Sebe *et al*., 2010). Nevertheless, P14-19 L2/3 cortical neurones have been shown to exhibit a tonic current that is mediated by $GABA_A$Rs containing the δ subunit, probably in conjunction with α4 and β2/3 subunits (Drasbek & Jansen, 2006; Drasbek *et al*., 2007).

With respect to the β subunit composition of cortical $GABA_A$Rs during development, there is less functional evidence with which to compare information

gleaned form anatomical studies. In cortical cultures derived from $\beta3^{0/0}$ mice, mIPSCs presented with faster decay kinetics and a higher sensitivity to zolpidem (100 nM) compared with mIPSCs from corresponding WT cultures whereas sensitivity to loreclezole (10 μM - β2/3-$GABA_AR$ selective) was unchanged (Ramadan *et al*., 2003). Immunohistochemical analysis has revealed that deletion of the β3 subunit resulted in concomitant decreases in the levels of α2 and α3, but not α1 subunit staining (Ramadan *et al*., 2003). These results may indicate the co-existence, at least in cell culture, of α1 and β2 subunits that form receptors underling fast (mature) IPSC kinetics whereas α2/3, in conjunction with β3 mediate slow-decaying (immature) IPSCs (Ramadan *et al*., 2003).

The zolpidem sensitivity exhibited by mIPSCs of mature cortical neurones and, to a lesser extent, immature cortical neurones (Dunning *et al*., 1999; Ramadan *et al*., 2003) suggest that the γ2 subunit is present in the majority of synaptic cortical $GABA_ARs$ throughout the ontogenic period - a finding that is consistent with the anatomical investigations described above.

Taken together these anatomical and functional studies performed on multiple cortical regions allow tentative speculation concerning the synaptic $GABA_AR$ isoforms expressed by neurones of L2/3. During the first week of life it appears that α2/3β3γ2 receptors predominate with a more modest proportion of receptors composed of α1β2γ2. This situation essentially reverses with maturity so that α1β2γ2 becomes the primary $GABA_AR$ subtype whereas a smaller contribution from α2/3β3γ2 receptors persists. This proposed profile of synaptic L2/3 $GABA_AR$ must be viewed as a generalization since other subunit subtypes, although existing at lower levels, show developmental variations in their expression and are likely to form distinct $GABA_AR$ complexes (Laurie *et al*., 1992b; Olsen & Sieghart, 2008).

Chapter 2

Materials & Methods

2.1. Patch-clamp technique: a historical perspective

To measure the ionic flux through a single ion channel a technique with a resolution in the picoampere range is required. This considerable technical obstacle was overcome in the early 1970's by Ernst Neher and Bert Sakmann whose co-development of the patch-clamp technique led to them being awarded a Nobel Prize for Physiology or Medicine in 1991. For the first time investigators could directly measure in real time, and with high amplitude acuity, the activity of individual ion-permeable channels in biological membranes. Such a feat represented a major advance in the field of biophysics and paved the way for a new era in ion-channel research.

Using an enzymatically cleansed denervated frog muscle preparation, Sakmann and Neher proposed that isolating a few nAChRs in a small patch of membrane under a non-conductive glass pipette would provide a high-resistance seal sufficient to prevent single channel current activity from being drowned out by the background noise. Early experiments failed, by two orders of magnitude, to achieve the seal resistances required. Nevertheless by modifying the pipette properties to increase the seal resistance to an adequate level (> 50 MΩ) signals began to emerge that could be reliably interpreted as single-channel currents (Neher & Sakmann, 1976). The properties of these currents, square pulses of equal amplitude and varying open durations, confirmed previous indirect measures of nACHR channel activity using noise analysis methods (Katz & Miledi, 1972).

Despite the groundbreaking findings this technique revealed, the necessity to have two voltage-clamping electrodes in addition to the recording electrode limited early experiments to large cells such as frog muscle fibres, molluscan neurones and the squid giant axon. Moreover, routinely accomplishing a high enough seal resistance remained a problem and the resolution was still inadequate to measure channels of

lower unitary conductance. A serendipitous discovery a few years later resolved these shortcomings in addition to providing further advantages. Investigators found that by applying a small amount of suction to the pipette interior, tight pipette-membrane seals with resistances of 10 – 100 GΩ could be reliably obtained. The so called "giga-seal", in conjunction with significant improvements to the amplifier electronics, reduced the background noise by approximately tenfold thus permitting a patch of membrane to be voltage clamped without the need for separate electrodes. This advance unlocked a plethora of different cell types amenable to patch-clamp manipulation, a considerable advantage given that previously it was limited to a few large excitable cells (Sigworth & Neher 1980; Hamill *et al.,* 1981; Fenwick *et al.,* 1982).

The mechanical stability of the giga-ohm seal was found to be such that the seal between the membrane and pipette was maintained even when the pipette was pulled away from the cell. As a result the patch clamp technique evolved to incorporate a number of configurations; cell-attached, whole-cell, inside-out patch and outside-out patch (Hamill *et al.,* 1981). The simplest and least invasive, the cell-attached configuration involves the formation of a seal between pipette and cell-surface and permits the measurement of clusters of single ion-channels or alternatively frequency of action potentials. Removal of the pipette from the cell surface whilst in the cell attached format results in the an outside-out patch whereby the cytosolic region of the membrane is exposed to the extracellular solution allowing investigation of how intracellular signalling cascades impact on channel function (Figure 2.1). Alternatively, if a brief pulse of negative pressure is applied to the electrode during the cell-attached mode, the membrane under the pipette becomes disrupted giving a low resistance access to the interior of the cell. This whole-cell configuration allows the sum of ionic currents in the cell to be measured. Initially, however, it was found that the rapid diffusional exchange that takes place upon rupture of the cell membrane led to the dialysis of the intracellular

milieu meaning that signalling molecules were lost and cell function compromised. Modification of the pipette solution minimised this problem and presented the opportunity to control the cell's internal environment. Finally, once access to the whole cell is established, withdrawal of the pipette from the cell results in the formation of an outside-out patch. Here, the membrane becomes inverted within the end of the pipette such that the exterior region of the cell membrane is exposed to the extracellular environment. The outside-out configuration allows the effects of ligand binding to the extracellular protein domain to be investigated (Hamill *et al.,* 1981; Figure 2.1).

As a result of the 1981 landmark paper by Hamill and colleagues, patch-clamp methods became widely utilised by researchers interested in answering a whole spectrum of ion-channel associated questions arising from diverse fields of biology. Increasingly investigators sought to apply the patch clamp technique to more physiological, *in situ*, cell preparations. For example in areas of high structural complexity, such as the CNS, it is clearly desirable to measure ion-channel activity in a preparation that retains functional synapses. Not only does this allow investigation of native structural properties, such as receptor subunit composition, the functional roles of these proteins in neuronal communication can also be studied in discrete CNS regions. Accordingly, patch clamp methods for thin slice preparations of mammalian brains were developed and first described in 1989 (Edwards *et al.,* 1989).

Today the patch-clamp technique has evolved to incorporate a number of other techniques including single-cell RT-PCR (Sucher & Deitcher, 1995) and fluorescent cell labelling permitting the molecular and visual classification of populations of neurones, respectively, for targeted investigation (Suter *et al.,* 2000). Furthermore, dual-recording of connected neurones has been described (Cobb *et al.,* 1995) and remarkably, recent advances have resulted in the ability to record single cell electrical activity from the intact brain of freely moving rats (Lee *et al.,* 2006). Hence not only do

traditional patch-clamp methods remain the gold-standard for studying ion-channel function, their application in tandem with other techniques has confirmed the position of this versatile and highly sensitive approach at the very forefront of biophysical research.

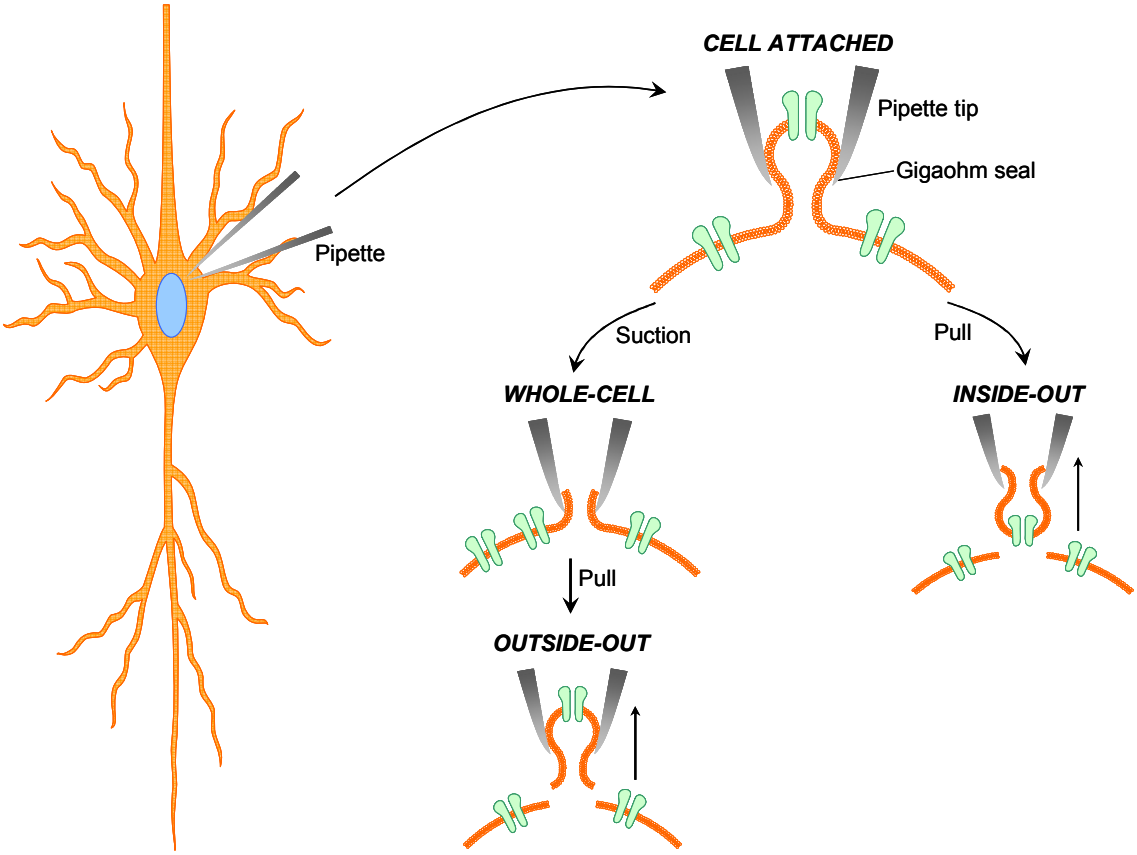

Figure 2.1. Patch clamp configurations. Schematic representation of the procedures necessary to establish the various patch-clamp configurations. Cell attached is the starting point for all other patch clamp formats and achieved by forming contact between the pipette and the cell before brief application of negative pressure to produce a gigaohm seal ("giga-seal"). Withdrawal of the electrode from the cell generates an inside-out excised patch. Alternatively, further suction results in whole cell configuration, a low-resistance electrical access to the cell's interior. Withdrawal of the pipette from here results in an outside-out patch. Figure based on the original illustrations of Hamill *et al*., 1981.

In the present study the patch clamp technique has been employed to explore neurosteroid-$GABA_AR$ interactions in brain slices derived from wild type and transgenic mice engineered to be devoid of certain $GABA_AR$ subunits. Whole cell voltage clamp methods and pharmacological manipulation allow the researcher to target specific aspects of neuronal transmission. For example, to study inhibitory

neurotransmission as mediated by $GABA_A$Rs, it is necessary to block excitatory, glutamatergic transmission so that the remaining currents can be interpreted as exclusively $GABA_A$R-mediated. Here, cessation of excitatory neurotransmission was readily achieved by supplementing the ECS with 2 mM kynurenic acid, a non-specific blocker of ionotropic glutamate receptors. When recording in the whole-cell voltage clamp mode, the resulting currents are termed spontaneous inhibitory postsynaptic currents (sIPSCs) as they arise from spontaneous GABA release from numerous presynaptic boutons. However, due to differences in conduction velocities between presynaptic fibres, action-potential driven (and hence multi-vesicular) GABA release can be somewhat asynchronous. Accordingly, the synaptic currents that comprise the summated sIPSC rise and decay slightly out of time (Mody *et al*., 1994). Such variability in the timing of individual currents that form the sIPSC makes it difficult for the researcher to interpret pharmacological properties of postsynaptic receptors. For example benzodiazepines exert their modulatory action solely by perturbing $GABA_A$R channel kinetics yet along with prolonging the sIPSP decay time course, benzodiazepines also increase sIPSC amplitude despite apparent receptor saturation. One solution is to isolate currents which arise solely from mono-vesicular release of GABA. These events are termed miniature IPSCs (mIPSCs) and although smaller and less frequent than sIPSCs serve as the preferred inhibitory event in this study for pharmacological evaluation of postsynaptic $GABA_A$R function. To obtain recordings that exclusively contain mIPSCs, 0.5 μM TTX was included in the recording ECS to block voltage gated sodium channels thereby preventing action potential propagation.

2.2. Breeding and housing of transgenic mice

The $\delta^{0/0}$ and $\alpha4^{0/0}$ mice used in this study were generated on C57BL/6J-129Sv/SvJ background at the University of Pittsburgh as has been previously described (Mihalek *et al.*, 1999; Chandra *et al*., 2006). Similarly the $\alpha1^{0/0}$ mice were generated on a mixed C57BL6-129SvEv background at the Merck Sharpe & Dohme Laboratories, Harlow (see Sur *et al.*, 2001). GAD 67-GFP knock-in mice were generated on a C57BL/6J-ICR background as has been described previously (Tamamaki *et al*., 2003).

Electrophysiological experiments were performed on brain slices prepared from the first 2-3 generations of wild type (WT), $\delta^{+/+}$, $\alpha4^{+/+}$, $\delta^{0/0}$ and $\alpha4^{0/0}$ breeding pairs derived from the corresponding heterozygous ($^{+/0}$) mice bred at the University of Dundee. Since no differences were observed in mIPSC properties from WT, $\delta^{+/+}$or $\alpha4^{+/+}$ mice, all data from these strains were pooled. For GAD 67-GFP mice electrophysiological experiments were conducted on brain slices prepared from mice that came from first 2-3 generations of heterozygous breeding pairs.

All mice were housed under 12 hour light/dark conditions and had access to food and water *ad libitum*. On or after postnatal day 14, mice were genotyped by taking ear tissue biopsies on which DNA extraction and subsequent PCR analysis was performed using the Extract-N-Amp Tissue PCR Kit (Sigma Aldrich, MO, USA). The oligonucleotide primers used for genotyping the different mouse strains are detailed below. For experiments in which GAD 67-GFP mice were used that were under 2 weeks old, phenotyping of mice was achieved by visually examining the mice 1-2 days after birth with “miner’s-lamp” goggles equipped with a fluorescent light source and green emission filters (FHS/F-01, BLS, Budapest, Hungary). Heterozygotic mice were readily distinguished by vivid green fluorescence that could be visualized through the skull

$\alpha 4^{0/0}$

WT:	*Forward*	5' CTGATGTTGAAATGGTAGGTATCTG 3'
	Reverse	5' AAGCGAGAAACCGGATCACTG 3'
TAR:	*Forward*	5' TGACTCTGGGCTAAACATTC 3'

$\delta^{0/0}$

WT:	*Forward*	5' ATGACTGTGTTCCTGCATCA 3'
	Reverse	5' AGCCCCTCCCTGAAAGCTAG 3'
TAR:	*Forward*	5' ATGACTGTGTTCCTGCATCA 3'
	Reverse	5' TTGTCTGTTGTGCCCAGTCA 3'

$\alpha 1^{0/0}$

WT:	*Forward*	5' ATTAATGGAGAGTGTGGTAATCT 3'
	Reverse	5' ACCATGGCTGTCCTTACCTCATG 3'
TAR:	*Forward*	5' ATTAATGGAGAGTGTGGTAATCT 3'
	Reverse	5' GGATGCGGTGGGCTCTATGGCTTCTGA 3'

GAD 67-GFP

WT:	*Forward*	5' GGCACAGCTCTCCCTTCTGTTTGC 3'
	Reverse	5' GCTCTCCTTTCGCGTTCCGACAG 3'
TAR:	*Reverse*	5' CTGCTTGTCGGCCATGATATAGACG 3'

2.3. Brain slice preparation

Thin brain slices were prepared from WT or transgenic mice. Animals were killed by cervical dislocation in accordance with Schedule 1 of the UK Government Animals (Scientific Procedures) Act, 1986. The brains were dissected and placed in oxygenated ice-cold oxygenated (95% O_2/5%CO_2) artificial cerebrospinal fluid (aCSF). For cortical preparations aCSF contained 225 mM sucrose, 2.95 mM KCl, 1.25 mM NaH_2PO_4, 26 mM $NaHCO_3$, 0.5 mM $CaCl_2$, 10 mM $MgSO_4$, 10 mM glucose (Osmolarity 328-330 mOsm). For thalamic preparations the sucrose content was increased to 234 mM as it

was found that the associated increase in osmolarity (335-340 mOsm) improved the viability of thalamic relay neurones.

Brain slices were obtained using a Vibratome series 1000 PLUS Sectioning System (Intracell, Royston, Hertfordshire, UK). For experiments concerning cortical layer II and III neurones, slices were cut in the coronal plane whereas thalamic preparations were cut horizontally. Regardless of brain region under investigation, slices were cut at 300-350 μm for mice of post natal day 15 (P15) or older, and 400 μM for younger animals. Slices were immediately transferred on to a nylon mesh platform housed within a chamber containing circulating oxygenated extracellular solution (in mM: 126 NaCl, 26 $NaHCO_3$, 2.95 KCl, 1.25 NaH_2PO_4, 2 $MgCl_2$, 2 $CaCl_2$, 10 glucose [306-309 mOsm]) and allowed to rest at room temperature for a minimum of one hour prior to recording.

2.4. Visualisation of neurones

Neurones were visually identified for investigation using an infra-red sensitive black and white CCD camera (Hitachi Denshi, Japan) connected to an upright Olympus BX50WI microscope (Olympus, Southall, UK) equipped with IR-DIC optics. Brain regions were identified using x10 water immersion optics before single cells were targeted within the desired region at x40. An additional x1.6 magnification was gained using a magnification chamber. To aid visualisation, microscope images were displayed on a video monitor (VM-1720E, Hitachi Denshi, Japan).

2.4.1. Identification of L2/3 pyramidal neurones of the neocortex

Pyramidal neurones belonging to layer 2 and 3 (L2/3) of the neocortex were identified based on their location and morphology. Layer I resides closest to the pial surface and contains very few cell bodies. Layers 2/3 on the other hand, have a high cell density such that a clear border between layer I and L2/3 is evident. Pyramidal cells are the principal output cells of the cortex and account for approximately 80% of the neuronal population with the remainder comprising inhibitory interneurones. Moreover they display a distinctive cyto-architecture whereby the cell body is pyramidal shaped and projects a prominent apical dendrite perpendicular to the surface of the brain. Morphological differences between pyramidal cells of different cortical layers also exist. In particular L2/3 pyramidal cells are small to medium relative to those found in deeper layers. Together these criteria enable L2/3 pyramidal neurones to be easily distinguished by visual inspection.

2.4.2. Identification of L2/3 interneurones of the neocortex

GABAergic interneurones from cortical L2/3 were identified in brain slices derived from glutamic acid decarboxylase–green fluorescence protein (GAD67-GFP) knock-in mice. This mouse line has been engineered to co-express GFP with the GABA-synthesising, 67 kDa GAD 67, enzyme (Tamamaki *et al*., 2003). Co-localisation studies confirmed that the three major interneurone classes present in mouse neocortex, (*i.e.* calretinin-, parvalbumin- or somatostatin-expressing) are all GFP-positive (GFP+, Tamamaki *et al*., 2003). Hence, visual identification of L2/3 GFP+ cells, using epifluorescence microscopy, enabled reliable identification of GABAergic interneurones. To identify GFP+ neurones the microscope was connected to a mercury

lamp (Olympus U-RFL-T - Southall, UK) and fitted with the appropriate filter to provide the correct wavelengths of light for GFP illumination (excitation/emission = 488 nm/509 nm). Once a GFP+ neurone was selected, whole-cell patch clamp recordings were obtained using the conventional infra-red differential interference microscopy techniques as described above.

2.4.3. Identification of VB neurones

Thalamocortical (TC) relay neurones of the ventrobasal (VB) complex were identified by locating the nucleus reticularis (nRT) at a magnification of x10. In the horizontal plane, the nRT is situated medial to the dense band of fibres that form the internal capsule. The VB complex is medial to the nRT and can be subdivided into ventral posterolateral (VPL) and ventral posteromedial (VPM) nuclei (Figure 1.2 A). Visually the VB complex appears as a distinctive striated region formed by bands of axon collaterals running perpendicular to the nRT. Medial to the VB complex lies the posterior nucleus (Po, Figure 1.2 A). Compared with VB, the Po exhibits a less dense fibrous network resulting in a much lighter appearance. Once the location of the VB complex was confirmed using these anatomical markers, optics were switched to x40 and the relatively large TC cells were readily identified by their round, smooth appearance and diffuse distribution.

A B

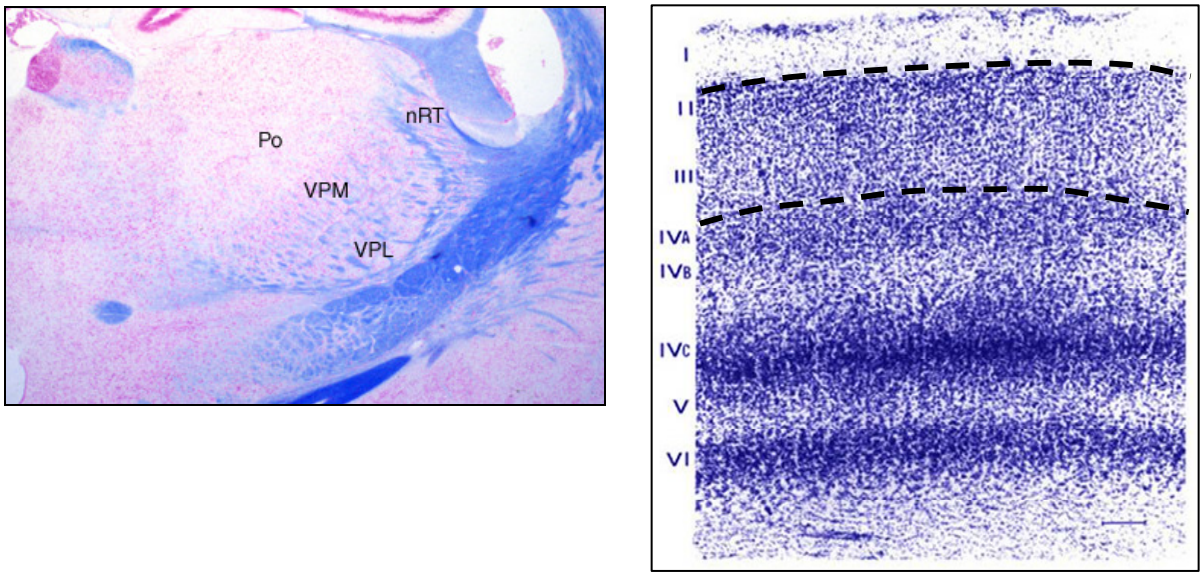

Figure 2.2 Anatomical location of the VB nucleus (thalamus) and L2/3 (cortex). A. Coronal thalamic section (Kluver-Barrera stain) showing the VPM and VPL which collectively comprise the VB nucleus. Note that the VB nucleus is encased by the nRT. Figure taken from: www.crulrg.ulaval.ca/pages_perso_chercheurs/deschenes_m/indexAG.html **B.** Coronal section of the mouse somatosensory cortex (Nissl stain) illustrating the distinctive cortical laminar organisation in which L2/3 are demarcated by the broken black lines. Figure taken from: http://webvision.med.utah.edu/imageswv/nissl2.jpg.

2.5. Patch-clamp electrophysiological recordings

Patch pipettes with a resistance of 2-6 MΩ were pulled from thick-wall borosilicate glass (0.95 mm I.D., 1.55 mm E.D., Garner Glass Co., Claremont, CA) using a Narashige PC-10 electrode puller (Narashige, Japan). Pipettes were filled with intracellular solution (ICS) containing, in mM, 135 CsCl, 10 HEPES, 10 EGTA, 2 $MgCl_2$, 1 $CaCl_2$, 2 Mg-ATP and 5 QX-314 (pH 7.2-7.3, 290-300 mOsm). For thalamic experiments, the CsCl content was adjusted to 140 mM. The presence of CsCl provided K^+ conductance block whereas QX-314 (Cal-Tag Med Systems, Buckingham, UK) was added to block Na^+ leak currents, both measures serving to minimise electronic filtering

of recorded currents. Mg-ATP was included to minimise channel rundown associated with the loss of essential cytostolic components caused by dilution into the pipette.

Positioning of the patch pipette on to the cell was accomplished using an MX7600R micromanipulator (SD Instruments, Oregon, USA) affording coarse and high precision control on three axes. Whole-cell voltage clamp recordings were acquired at -60 mV using an Axopatch 1D amplifier (Molecular Devices, CA, USA) connected to a CV-4 headstage, and filtered at 2 kHz using an eight-pole low-pass Bessel filter. Data acquisition and digitisation was performed using a NIDAQ mx card (National Instruments, TX, USA) and stored to a personal computer hard-drive using WinEDR software (Strathclyde University, UK). Data acquisition was simultaneously performed using a DTR 1204 digital tape recorder (Biologic Scientific Instruments, France) serving as a secondary, "back-up" data store. Real time observation of current recordings was achieved using a digital storage oscilloscope (Tektronix, Beaverton, OR, USA) and also by using the WinEDR "record to disk" interface. Typically, series resistance values for L2/3 pyramidal cells and thalamocortical VB neurones were between 4-20 MΩ, with up to 80% compensation. Recordings were considered void if values of series resistance changed by more than 20% during the experiment or if they exceeded 20 MΩ.

2.6. mIPSC Analysis

Offline analysis of digitised data was conducted using WinEDR/WinWCP software (Strathclyde University, UK). Detection of mIPSCs was carried out using an alogorithmic detection protocol involving the following criteria: amplitude threshhold (typically -4 pA); the duration greater than threshold (typically 2 ms); and the dead time

over which period no events were detected (typically 30 ms). However, since this study involved two distinct neuronal populations (*i.e.* VB *vs* L2/3) at varying developmental ages, values for each of these criteria were adjusted accordingly to optimally detect events from intrinsically variable mIPSC durations, amplitudes and frequencies. A small proportion of mIPSCs were found to have a rise time greater than 1 ms which most likely reflected mIPSCs arising in spatially distant dendritic locations. Given the distance between dendrites and cell soma, dendritic mIPSCs undergo unquantifiable electronic filtering. Hence, detected mIPSCs were subjected to filtering protocol whereby events were discarded if they fell outside the limits of a Gaussian distribution or had rise times greater than 1 ms. After individual mIPSC inspection, and deletion of spurious events, data from typically 50 or more mIPSCs was accepted for detailed kinetic analysis. Note at the early developmental age of P7/8, L2/3 neurones were found to have a particularly low frequency meaning that sometimes, fewer than 50 mIPSCs were analysed. mIPSCs were analysed with respect to their peak amplitude, rise time (10-90%), charge transfer (area under the mIPSC) and time taken for events to decay by 50% (T50) and 90% (T90). Subsequently, mIPSCs were averaged by alignment with mid-point of the rising phase and the resulting averaged mIPSC was fitted with either an mono- ($y(t)=Ae^{(-t/\tau)}$) or bi-exponential ($y(t)=A_1e^{(-t/\tau1)} + A_2e^{(-t/\tau2)}$) decay function where y(t) is the current amplitude at any given time t, A is the current amplitude at time zero and τ is the decay time constant. To assess which function best fitted the averaged mIPSC in question and to reveal whether the decay phase of the mIPSC was mono- or bi-exponentially decaying, the standard deviation of the residuals were measured and an F test applied. For the vast majority of mIPSCs analysed, the decay was best described by a bi-exponential decay function. Accordingly, a mean weighted decay constant (τw) was calculated to depict the relative contribution of each decay component. Values for τ_W were derived from the following equation,

$$\tau_w = \tau_1 P_1 + \tau_2 P_2$$

where τ_1 and τ_2 are the decay time constants for the first and second exponential functions, and P_1 and P_2 are the proportions of current amplitude described by each component i.e.,

$$P1 = \frac{A1}{A1+A2} \qquad P2 = \frac{A2}{A1+A2}$$

Where relevant, mIPSC parameters are expressed as percentage change relative to control. Specifically, for paired experiments in which mIPSC properties were compared before and after drug application, the drug induced change was calculated as percentage of control for individual cells and these values averaged to give the mean percentage change. For the comparison of unpaired mIPSC parameters, for example WT *vs* KO, the percentage change was calculated from the average WT control.

Frequency analysis of mIPSCs was conducted for each cell by running an event detection protocol over a minimum of 30 seconds of recording. The selected recording period was visually inspected such that mIPSCs missed by the automated detection process were inserted and spurious noise that satisfied the detection criteria omitted.

The total charge mediated by synaptic currents was calculated using the equation: Phasic charge = f_{mIPSC} x Q_{mIPSC}, where f is the number of events per second (*i.e.* the frequency) and Q is the average charge transfer associated with an individual mIPSC.

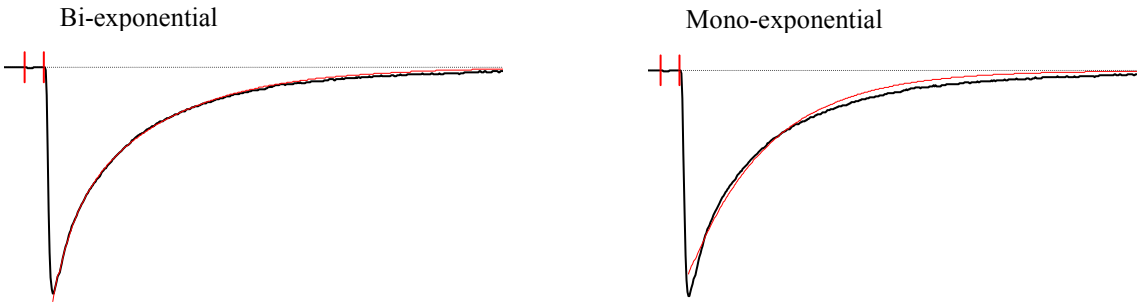

Figure 2.3. Examplar mIPSCs. mIPSCs are depicted with superimposed decaying bi-exponential (red line, left) and mono-exponential (red line, right) fits. The mono-exponential decay function is described by ($y(t)=Ae^{(-t/\tau)}$) and bi-exponential ($y(t)=A_1e^{(-t/\tau1)} + A_2e^{(-t/\tau2)}$). For mIPSCs best fitted by a bi-exponential function the weighted decay time constant, τw, was calculated by: $\tau_w = \tau_1P_1+\tau_2P_2$

2.7. Tonic and drug evoked inward current analysis

Estimation of the tonic and drug-evoked inward current was calculated by the difference in holding current after 30 μM bicuculline methobromide and drug application, respectively. The mean DC current and RMS (standard deviation) of a 30 sec to 60 sec current section, 25.6 ms to 102.4 ms epochs were visually examined, depending on the mIPSC frequency of the cell. At the sampling rate of 10 kHz, 256 or 1024 baseline points for each 25.6 ms or 102.4 ms of current trace respectively, provided one data point. Epochs containing mIPSCs or those which exhibited an unstable baseline were

discarded. To divorce between modest drug effects and temporal 'drift' of the baseline holding current, currents were interpreted as genuine if the DC shift was greater than twice the standard deviation of the control baseline holding current. Where small responses to drug application were observed, pooled data from three 10-15 second periods of control were compared with pooled data from three 10-15 second periods of drug section.

2.8. Drug and solution application

Unless stated otherwise, all salts used were purchased from VWR (West Chester, Pennsylvania, USA). Bicuculline (Axxora, Nottingham, UK), strychnine, (Sigma Chemicals, St Louis, MO, USA), TTX (Tocris, Bristol, UK), 4,5,6,7-tetrahydroisoxazolo[4,5-c]pyridine-3-ol (THIP) (generous gift of B. Ebert) were prepared as concentrated stock solutions in distilled water. The neurosteroid 5α-pregnan-3α-ol-20-one (5α3α; gift from Dr K. Gee, UC Irvine, CA, USA), the 5α-reductase inhibitor finasteride (Steraloids, USA) and the delta-subunit selective compound, DS2 (gift from K.Wafford, formerly of Merck Sharp & Dohme, Harlow, UK) were prepared as concentrated stocks (1000x) in DMSO. Drugs made up as stock solutions were diluted to the final required concentration in ECS: Bicuculline, 30 μM; TTX, 0.5 μM; strychnine, 0.5 μM; THIP, 1 μM; 5α3α, 300 nM/1 μM; finasteride, 50 μM; DS2, 10 μM. Kynurenic acid (Ascent Scientific, Bristol, UK) was dissolved directly into ECS at a concentration of 2 mM. Likewise, α- and γ-cyclodextrin (Sigma-Aldrich, St Louis, MO, USA) were dissolved directly into the extracellular and intracellular solution (final concentration 1 mM and 0.5 mM, respectively).

Slices were superfused with ECS using a gravity based perfusion system set to a flow rate of 3-5 ml/min and recycled to a 50 ml reservoir using a peristaltic pump (Minipuls 3, Gilson, UK). Drugs dissolved in ECS were applied to the slice from separate reservoirs. At the stated flow rate, solution exchange (*e.g.* from standard ECS to ECS + drug) was complete 2 – 3 minutes after the reservoirs were switched. During drug exchange the solution flowing out of the slice chamber ran to waste. Slices were exposed to solutions heated to 35 °C achieved using a feedback heating system whereby a temperature controller (School of Pharmacy, London, UK) monitored solution temperature at the slice and simultaneously controlled an in-line heat exchanger (G23, UCL, London, UK) positioned between the solution reservoirs and slice chamber.

2.9. Statistical analysis

All data are expressed as the arithmetic mean value ± SEM (standard error of the mean). To calculate statistical significance, Student's t-tests (paired or unpaired, Microsoft Excel), ANOVA (followed *post-hoc* by Newman-Keuls, SigmaStat), or one way repeated measures ANOVA (followed *post-hoc* by Newman-Keuls, SigmaStat) were used as appropriate. To compare the cumulative probability distributions of individual mIPSC properties within a cell (e.g. before and after drug application), the Kolmogorov-Smirnoff (KS) test was used (SPSS software, IL, USA). Finally, to calculate correlations, a linear fit analysis routine was implemented using Origin 7.0 (OriginLab, MA, USA) to obtain R and *p* values. In all cases $p < 0.05$ was considered to be significant.

Chapter 3

A pharmacological investigation of $GABA_A$ receptor - mediated inhibition in VB neurones

3.1. An investigation of inhibitory neurotransmission in WT P17-24 VB neurones

As a preface to investigating the putative actions of endogenous neurosteroids on GABA-ergic transmission during development, initial experiments sought to establish the properties of GABA-mediated inhibition in VB neurones at a post-neonatal age range of P17-P25. In particular, the relative contribution of both synaptic and tonic forms of $GABA_AR$-mediated inhibition was assessed using a combination of $GABA_AR$ subunit-deficient mice and pharmacological approaches.

3.1.1. The properties of mIPSCs recorded from VB neurones

$GABA_A$ receptor ($GABA_AR$) mediated mIPSCs recorded from thalamic VB neurones of wild type mice displayed similar characteristics to those reported previously (Belelli *et al*., 2005; Peden *et al*., 2008). In common with these previous studies, all recordings were performed in the presence of 0.5 μM TTX and 2 mM kynurenic acid, a holding potential of -60 mV and with near symmetrical chloride between intracellular and extracellular compartments. Accordingly, mIPSCs presented as transient inward current deflections that could be readily distinguished from the baseline noise (Figure 3.1 A and B). Addition of 30 μM bicuculline, a competitive $GABA_A$ receptor antagonist, abolished all mIPSCs (Figure 3.1 C) and moreover caused an outward shift in the holding current (Figure 3.4). With respect to the synaptic events, mIPSCs recorded from a total of 54 VB neurones, from mice of either sex, exhibited relatively fast rise times (0.5 ± 0.1 ms), mean peak amplitudes of -68 ± 2 pA, relatively rapid decay kinetics (τ_W = 3.3 ± 0.1 ms) and occurred at a relatively high frequency (12 ± 1 Hz). The majority of WT VB neurones (51/54) displayed mIPSCs with decay components that were well

described by a bi-exponential decay function, for which the weighted decay time constant, τ_W, was calculated to quantify the decay time course (see Methods). However, a minority of mIPSCs (3/54 neurones) were fitted best with a mono-exponential decay function for which the decay time constant, tau (τ) was determined. Values for τ and τ_W were pooled and regarded as synonymous entities. Henceforth, the term τ_W is used to describe the decay time constant for both bi- and mono-exponentially decaying mIPSCs. A quantitative comparison of VB neurone mIPSC properties with those from mIPSCs recorded under identical conditions from other CNS locations is detailed in Table 3.1. Of particular note is the similarity in decay times between mIPSCs measured from VB neurones and those recorded from cerebellar Purkinje cells. This probably reflects a commonality between the composition of synaptic $GABA_A$ receptors in these two neuronal populations ($\alpha1\beta2\gamma2$; see Discussion). As demonstrated in Figure 3.2, the peak amplitude distribution for any given cell was found to be skewed towards larger peak amplitude values, a feature shared by many CNS synapses (Edwards *et al*., 1990, 1995; Llano & Gerschenfeld, 1993). In addition, for every VB neurone analysed, no statistically significant relationship was observed between peak amplitude and rise time indicating that dendritic filtering did not overtly affect mIPSC properties (for example see Figure 3.2).

	Thalamic VB (n = 54)	Cortical L2/3 (n = 25)	Thalamic nRT (n = 28*†)	Dentate GCs (n = 65*†)	Cerebellar Purkinje (n = 33#)
Rise Time (ms)	0.5 ± 0.1	0.5 ± 0.1	0.4 ± 0.1	0.4 ± 0.1	0.4 ± 0.1
Peak Amplitude (pA)	-68 ± 2	-42 ± 2	-61 ± 3	-65 ± 2	-127 ± 7
% τ_{Slow}	27 ± 2	47 ± 4	69 ± 3	47 ± 1	23 ± 1
τ_W (ms)	3.3 ± 0.1	5.4 ± 0.2	16.0 ± 1	8.6 ± 0.2	3.1 ± 0.1
Charge Transfer (pC)	-259 ± 12	-221 ± 11	-815 ± 42	-529 ± 21	ND
Frequency (Hz)	12 ± 1	12 ± 1	11 ± 2	3 ± 0	13 ± 2

Table 3.1. Properties of mIPSCs recorded from five different mouse CNS cell types between P16-25. For all stated values, mIPSCs were recorded in the host lab under identical conditions (intra/extracellular chloride ~ 135 mM, 35°C, voltage clamped at -60 mV). Cell types from left to right: thalamocortical neurones of the ventrobasal nucleus; cortical layer 2/3 pyramidal cells; thalamic neurones of the nucleus reticularis; hippocampal dentate gyrus granule cells; cerebellar Purkinje neurones. * Data provided by Dr M. Herd. † Data provided by Dr D. Peden. # Data provided by Dr A. Haythornthwaite (PhD Thesis 2004). ND, not determined.

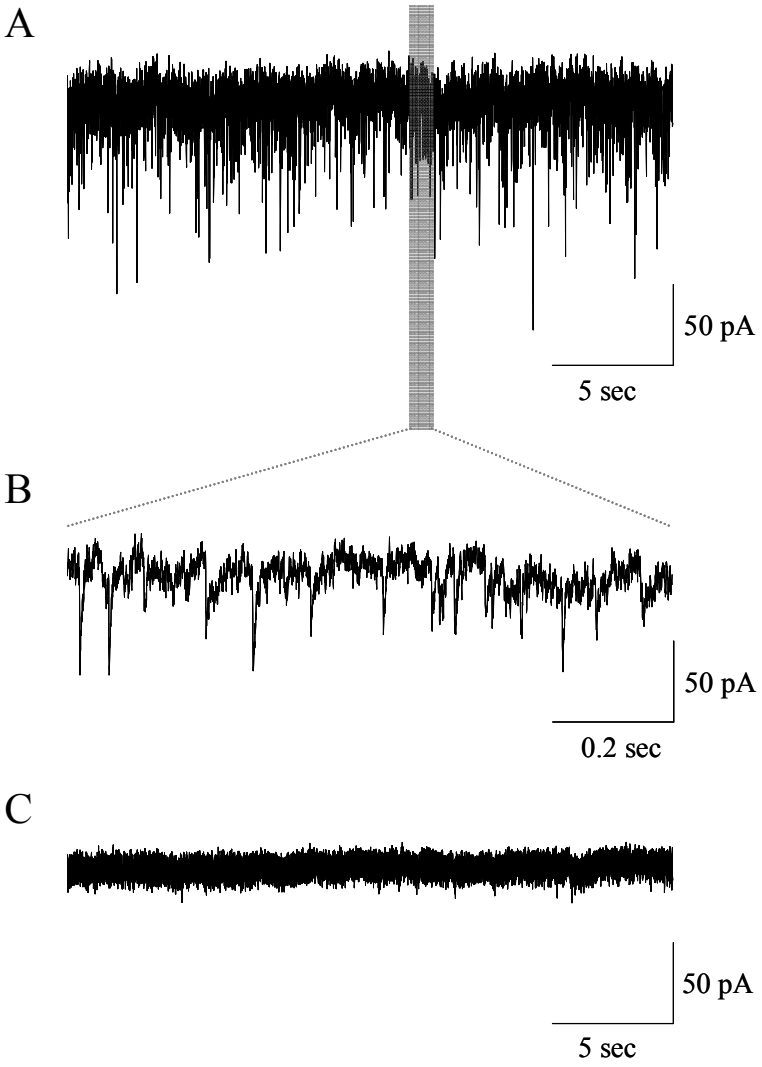

Figure 3.1. Representative current trace from a WT VB neurone. **A**. A 25 second section of current recording from a representative VB neurone voltage clamped at -60 mV and recorded in the presence of 0.5 μM TTX and 2 mM kynurenic acid. Note the relatively high frequency of mIPSCs (downward deflections) emerging from a noisy baseline. **B**. A 1 second sample of the same recording on an expanded time scale. **C**. The application of bicuculline abolishes mIPSCs and leads to a reduction in the baseline noise as denoted by a decrease in RMS values.

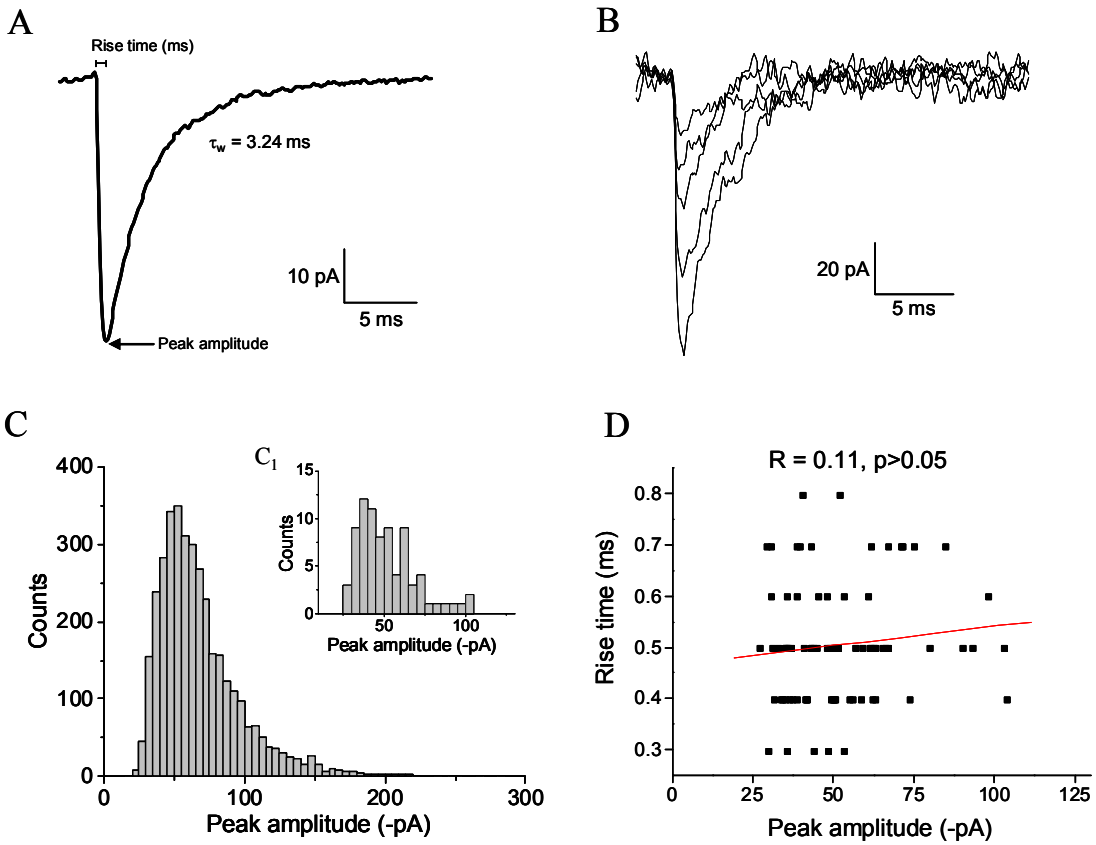

Figure 3.2. The properties of mIPSCs from WT VB neurones. A. An averaged mIPSC composed from 78 individual events extracted from one representative recording. Note the relatively fast rise time and fast decay kinetics. **B.** Superimposed individual mIPSCs from the same recording showing intra-cell variation in the peak amplitude. Note the 'noisy' appearance of individual mIPSCs. **C.** A peak amplitude histogram compiled from 3636 mIPSCs recorded from 54 WT VB neurones illustrating that the Gaussian distribution is skewed towards mIPSCs with larger peak amplitudes. **C_1.** Peak amplitude histogram derived from mIPSC recorded from the same representative cell (referred to in A, B and D). **D.** An X-Y plot of rise time *vs* peak amplitude for the individual mIPSCs recorded from the same VB neurone. The linear fit (grey line) shows the absence of any correlation between rise time and peak amplitude indicating that recorded mIPSCs were not affected by dendritic filtering.

3.1.2. The effect of postnatal age on the properties of mIPSCs recorded from WT P17-P24 VB neurones

As has been reported for several classes of ligand gated ion channels, $GABA_AR$ structure and function are influenced by age (reviewed by Takahashi, 2005). Therefore, in the present study the effect of postnatal age upon the mIPSCs recorded from VB neurones was examined for the juvenile age range, P17-24. Over this developmental period, a small but significant decrease was observed in peak amplitude ($R = -0.28$, $p < 0.05$, Figure 3.3 A) and rise time ($R = -0.41$, $p < 0.05$, Figure 3.3 B, Table 3.2), coupled with an acceleration of the decay kinetics as indicated by a decrease in τ_W ($R = -0.39$, $p < 0.05$, Figure 3.3 C). The frequency of mIPSCs did not change between P17-24 ($R = 0.04$, $p > 0.05$, Figure 3.3 D, Table 3.2). The effect of development upon the properties of mIPSCs recorded from VB neurones is investigated in detail in Chapter 4.

	P17-18 (n = 19 cells)	P20-21 (n = 16 cells)	P23-24 (n = 7 cells)
Peak amplitude (pA)	73 ± 4	69 ± 4	62 ± 4
Rise time (ms)	0.6 ± 0.1	0.5 ± 0.1	0.5 ± 0.1*
τ_W (ms)	3.5 ± 0.2	3.4 ± 0.1	2.9 ± 0.1*
T50 (ms)	2.5 ± 0.1	2.4 ± 0.1	1.9 ± 0.1**
Frequency (Hz)	13 ± 2	10 ± 2	15 ± 4

Table 3.2. A summary of the mIPSC properties recorded from WT P17-24 VB neurones. * $p < 0.05$, **, $p < 0.01$, *vs* P17-18, Student's unpaired t-test.

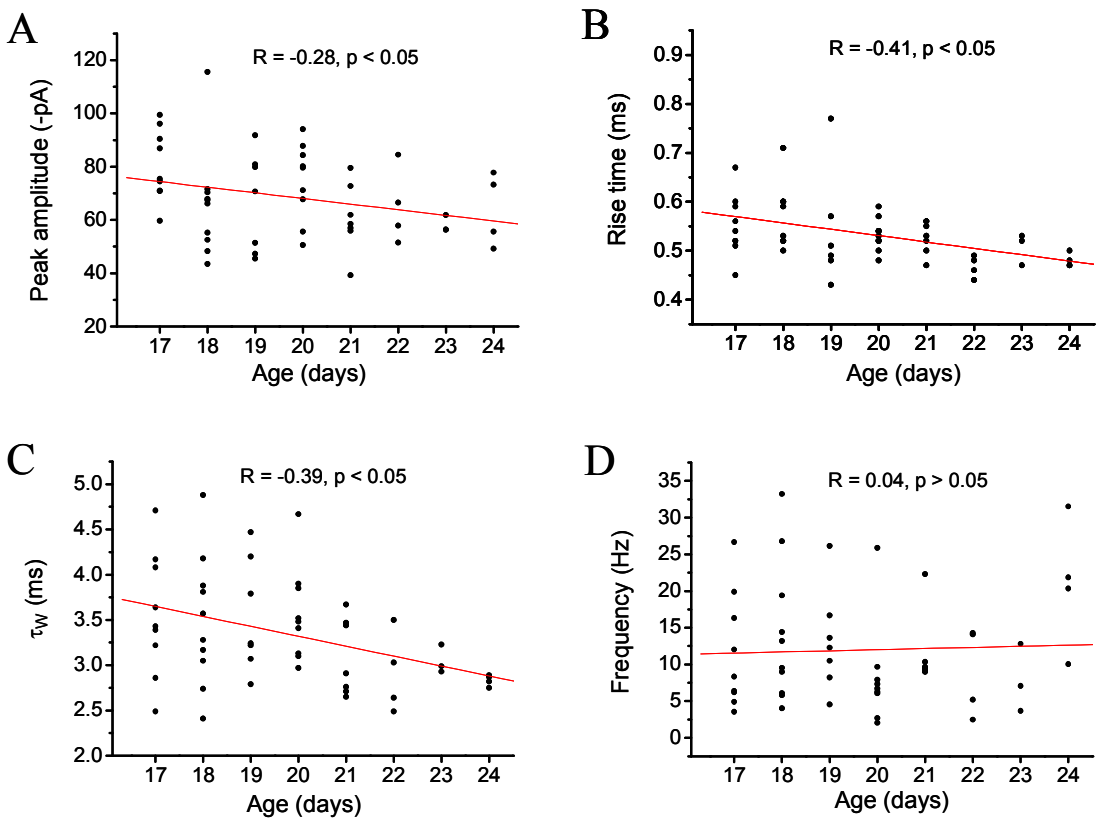

Figure 3.3. The effect of age on the properties of mIPSCs from P17-24 WT VB neurones. A-D. Scatter plots fitted with linear regressions (grey lines) for peak amplitude (A), rise time (B), τ_W (C), and frequency of mIPSCs (D). Note the significant correlations for peak amplitude, rise time and τ_W, all of which decrease with maturity. In contrast, age has no effect on the frequency of mIPSCs between P17-24.

3.1.3. The lack of effect of gender on the properties of mIPSCs recorded from WT P17-24 VB neurones.

Consistent with other ligand gated ion channels, $GABA_AR$ structure and function are influenced by gender (Chudomel *et al*., 2009). Therefore, in the present study the effect of sex was analysed upon the mIPSCs recorded from VB neurones of mice between 17 and 24 days old. Importantly, no differences between gender were observed for any of the mIPSC parameters measured (see Table 3.3).

	Male (n=33 neurones)	**Female (n=21 neurones)**
Peak amplitude (pA)	-67 ± 3	-71 ± 4
Rise time (ms)	0.5 ± 0.1	0.5 ± 0.1
Charge transfer (pC)	-248 ± 14	-276 ± 23
T50 (ms)	2.3 ± 0.1	2.4 ± 0.1
τ_W (ms)	3.3 ± 0.1	3.4 ± 0.2
Frequency (Hz)	12 ±1	12 ± 2

Table 3.3. A summary comparing the properties of WT mIPSCs from VB neurones of male and female mice. Statistical analysis revealed no significant difference between gender for any of mIPSC properties listed above. In all cases $p > 0.05$, Student's unpaired t-test).

3.1.4. The properties of the extrasynaptic, tonic conductance of VB neurones

Addition of 30 μM bicuculline to brain slices derived from P17-24 wild type mice of either sex resulted in a robust outward shift in the holding current (96 ± 9 pA, $p < 0.001$ *vs* control, Student's paired t-test, n = 27) and a reduction in the baseline noise as indicated by measurements of RMS (control: 7.6 ± 0.3 pA *vs* bicuculline (30 μM): 5.1 ± 0.3 pA, $p < 0.05$ Student's paired t-test, n = 28; Figure 3.4). Analysis of the tonic conductance recorded from VB neurones derived from P17-24 male and female mice showed no sex-dependent effects on either the holding current or the RMS before and after bicuculline application (Figure 3.5, Table 3.4). Differences in the size of tonic currents in VB neurones have previously been observed at distinct developmental age groups (Peden *et al*., 2008). In this study, no correlation was observed between the endogenous tonic current/baseline noise and age for this limited developmental range (P17-24, Table 3.4). Hence, all data was pooled regardless of sex and age. The large outward current revealed by bicuculline, observed in the presence of TTX and in well-superfused brain slices, infers that VB neurones display a considerable and persistent $GABA_AR$-mediated tonic conductance. Similar observations have been reported previously for both mice and rats (Belelli *et al.,* 2005; Cope *et al.,* 2005a, 2009; Chandra *et al*., 2006; Herd *et al.,* 2009).

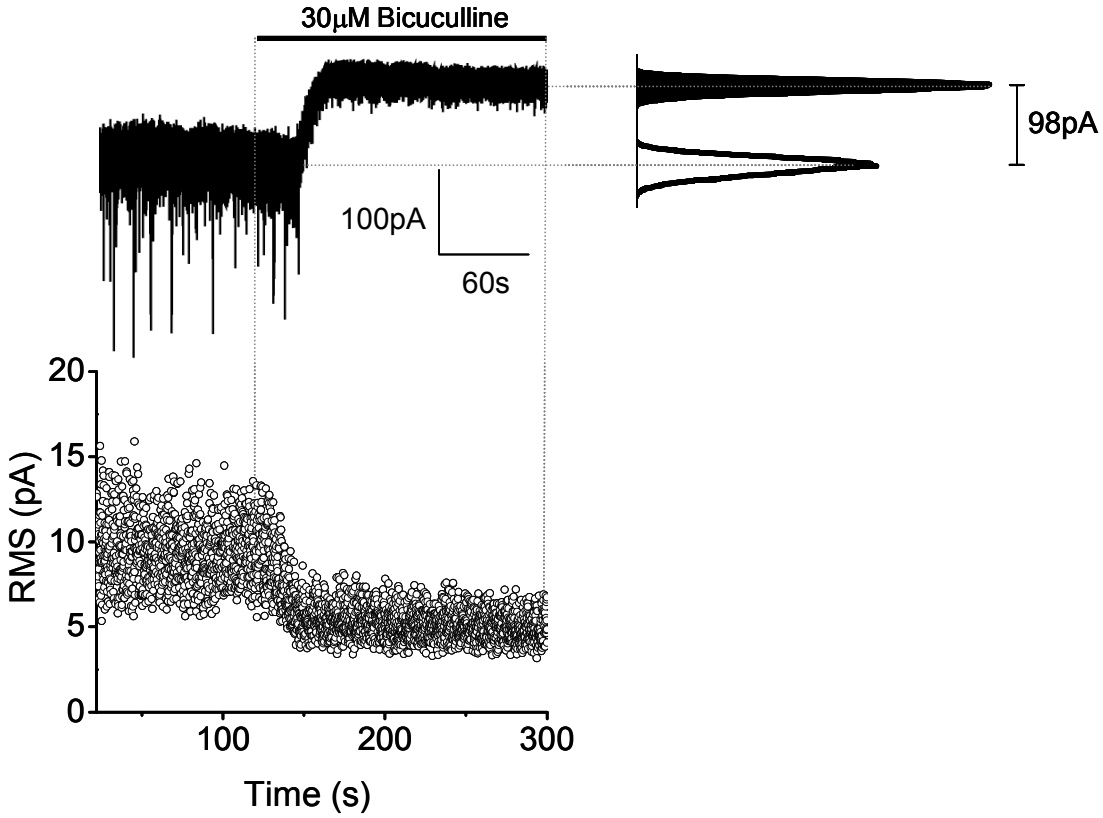

Figure 3.4. Thalamic VB neurones display a large endogenous tonic current. Top left: a representative VB neurone current recording illustrating that the application of 30 μM bicuculline reveals a robust tonic current. This is indicated by an outward shift in the baseline holding current coupled with a decrease in the baseline noise. The corresponding all points histogram is shown on the right illustrating the bicuculline-induced outward shift in holding current. Bottom left: the corresponding scatter plot of RMS *vs* time in which application of bicuculline is associated with a decrease in RMS. Values of RMS are plotted approximately every 0.075 seconds for 300 seconds of the recording before and after application of 30 μM bicuculline.

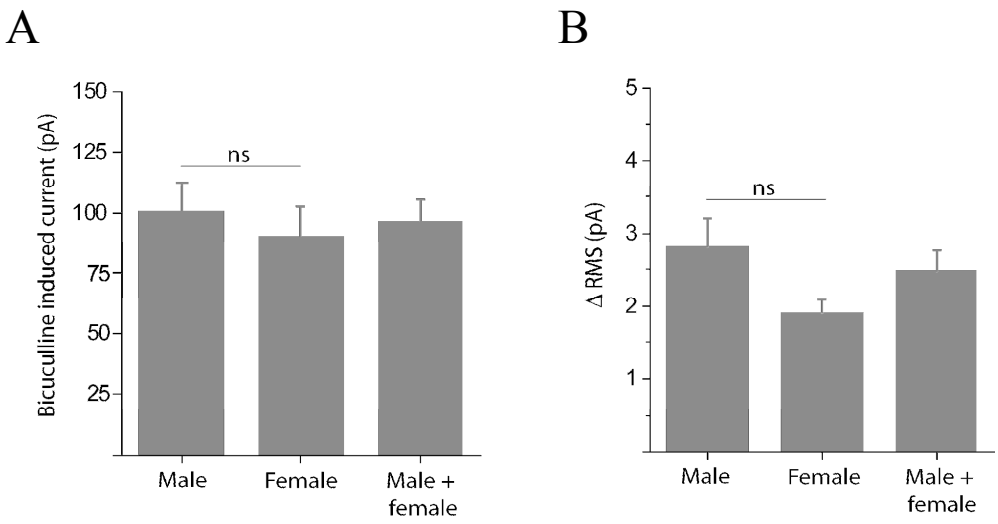

Figure 3.5. Gender does not influence the magnitude of the $GABA_AR$-mediated tonic current. **A.** A bar graph illustrating the tonic current induced by 30 μM bicuculline. No statistically significant differences were observed for the tonic current recorded from VB neurones derived from male (n = 17) or female mice (n = 10; p > 0.05, Student's unpaired t-test) **B**. A bar graph showing the change in RMS induced by 30 μM bicuculline. Note that although the change in RMS appeared marginally greater for male (n = 17) *vs* female (n = 10) VB neurones, the difference was not statistically significant (p > 0.05, Student's unpaired t-test).

	Male (n=17)	**Female** (n=10)	**Male + Female** (n=27)
Tonic current (pA)	100 ± 12	90 ± 13	96 ± 9
Δ RMS (pA)	2.8 ± 0.4	1.9 ± 0.2	2.5 ± 0.3
Tonic current density (pA/pF)	2.2 ± 0.3	1.9 ± 0.3	2.1 ± 0.2

Table 3.4. Gender does not influence the $GABA_AR$-mediated extrasynaptic conductance of P17-24 WT VB neurones. For all parameters stated, no significant difference was observed between male and female. In all cases, p > 0.05, Student's unpaired t-test.

3.2. A characterisation of $GABA_AR$-mediated inhibition in VB neurones of the $\alpha4^{0/0}$ mice

The α4 subunit has a relatively limited expression profile in the CNS, the thalamus being one area where this relatively rare subunit is present at notable levels (Wisden *et al*., 1992; Khan *et al*., 1996; Pirker *et al*., 2000; Chandra *et al*., 2006; Halonen *et al*., 2009). Indeed, in thalamocortical relay neurones of the VB, functional α4-containing receptors are ostensibly found outwith the synapse based on the observation that α4-subunit deletion abolishes the VB tonic current whilst reportedly unaltering mIPSC properties (Chandra *et al.,* 2006). Here, my preliminary experiments aimed to corroborate these earlier findings by assessing the relative contribution of α4-subunit containing receptors to inhibitory transmission in the VB.

3.2.1. Synaptic inhibition

The biophysical properties of mIPSCs recorded from $\alpha4^{0/0}$ VB neurones were investigated. Compared to WT, the mIPSCs recorded from VB neurones of $\alpha4^{0/0}$ mice exhibited a faster decay time course, as shown by a small, yet significant, decrease in τ_W (WT: 3.3 ± 0.1 ms, n = 54, *vs* $\alpha4^{0/0}$: 3.0 ± 0.1 ms, n = 49, $p < 0.01$, Student's unpaired t-test, Figure 3.7 B and D). In addition, the peak amplitude of mIPSCs recorded from $\alpha4^{0/0}$ VB neurones was modestly greater than WT (WT: -68 ± 2 pA, n = 54, *vs* $\alpha4^{0/0}$: -79 ± 3 pA, n = 49, $p < 0.001$, Student's unpaired *t*-test, Figure 3.7 A, C and E), although the overall charge transfer of individual mIPSCs was unchanged (WT: 260 ± 12 fC, n = 54 *vs* $\alpha4^{0/0}$: 270 ± 12 fC , n = 49, $p > 0.05$, Student's unpaired t-test). Finally, the frequency of mIPSCs recorded from $\alpha4^{0/0}$ VB neurones was substantially increased compared to WT (WT: 12 ± 1 Hz, n = 54, *vs* $\alpha4^{0/0}$: 24 ± 2 Hz, n = 49, $p < 0.001$,

Student's unpaired t-test; Figure 3.7 G, for a full summary of mIPSC properties see Table 3.5). Interestingly, some characteristics of mIPSCs recorded from $\alpha4^{0/0}$ VB neurones are shared by mIPSCs obtained from VB neurones of $\delta^{0/0}$ mice in recordings acquired in the host laboratory. In particular, consistent with VB recordings from $\alpha4^{0/0}$ mice, mIPSCs obtained from VB neurones of $\delta^{0/0}$ mice exhibited a greater mean peak amplitude (δWT: -66 ± 2 pA, n = 19; $\delta^{0/0}$ = -82 ± 3 pA, n = 25, $p < 0.001$, Student's unpaired t-test, Table 3.5) and faster decay kinetics as illustrated by a reduced average τ_W (δWT: 3.8 ± 0.1 ms, n = 19, *vs* $\delta^{0/0}$: 3.2 ± 0.1 ms, n = 25, $p < 0.001$, Student's unpaired t-test, Table 3.5). However, in contrast to the large increase in mIPSC frequency observed in VB neurones from $\alpha4^{0/0}$ mice, the mIPSC frequency of $\delta^{0/0}$ VB neurones was not statistically different to δWT controls (δWT: 17 ± 0.1 Hz, n = 19, *vs* $\delta^{0/0}$: 22 ± 0.1 Hz, n = 25, $p > 0.05$, Student's unpaired t-test, Table 3.5, δWT and $\delta^{0/0}$ data provided by Dr M. Herd, University of Dundee).

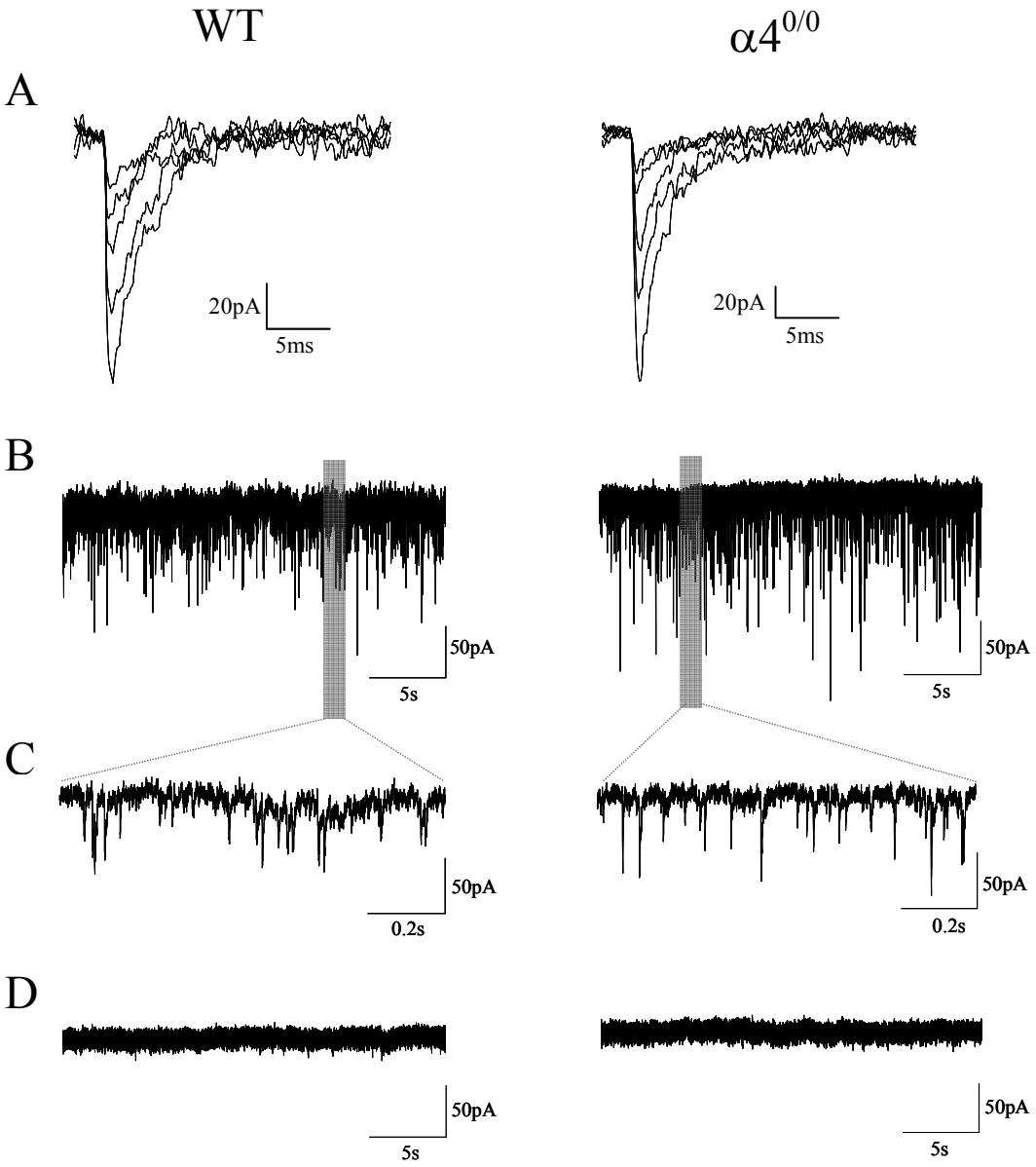

Figure 3.6. Representative current recordings from VB neurones of WT and $\alpha4^{0/0}$ mice. **A**. Superimposed individual mIPSCs recorded in the presence of 0.5 μM TTX and 2 mM kynurenic acid illustrating the intra-cell variation in peak amplitude for a representative WT (left) and $\alpha4^{0/0}$ (right) VB neurone. **B**. 25 seconds of a typical current recording from a WT (left) and an $\alpha4^{0/0}$ (right) VB neurone. Note the relatively high frequency of mIPSCs (downward deflections). **C.** A 1 second sample of the same recordings illustrated above, shown on an expanded time scale for a WT (left) and $\alpha4^{0/0}$ (right) VB neurone. Note that the 'noisy' baseline evident in WT VB neurones is reduced in VB neurones derived from $\alpha4^{0/0}$ mice. **D.** Application of 30 μM bicuculline abolishes mIPSCs for both WT and $\alpha4^{0/0}$ VB neurones and reduces the background noise to similar levels.

	WT (n=54 neurones)	$\alpha4^{0/0}$ (n=49 neurones)	δWT (n=19 neurones†)	$\delta^{0/0}$ (n=25 neurones†)
Peak amplitude (pA)	-68 ± 2	-79 ± 3**	-66 ± 2	-82 ± 3***
Rise time (ms)	0.5 ± 0.1	0.5 ± 0.1	0.5 ± 0.1	0.5 ± 0.1
τ_W (ms)	3.3 ± 0.1	3.0 ± 0.1**	3.8 ± 0.1	3.2 ± 0.1***
T50 (ms)	2.4 ± 0.1	2.0 ± 0.1***	2.9 ± 0.1	2.3 ± 0.1***
Charge transfer (pC)	-259 ± 12	-269 ± 12	-263 ± 11	-296 ± 15
Frequency (Hz)	12 ± 1	24 ± 2***	17 ± 2	22 ± 2

Table 3.5. A summary of the properties of mIPSCs recorded from VB neurones of WT, $\alpha4^{0/0}$, δWT and $\delta^{0/0}$ mice. ** $p < 0.01$, *** $p < 0.001$, *vs* WT control, Student's unpaired t-test. † Data provided by Dr M. Herd (Dundee University).

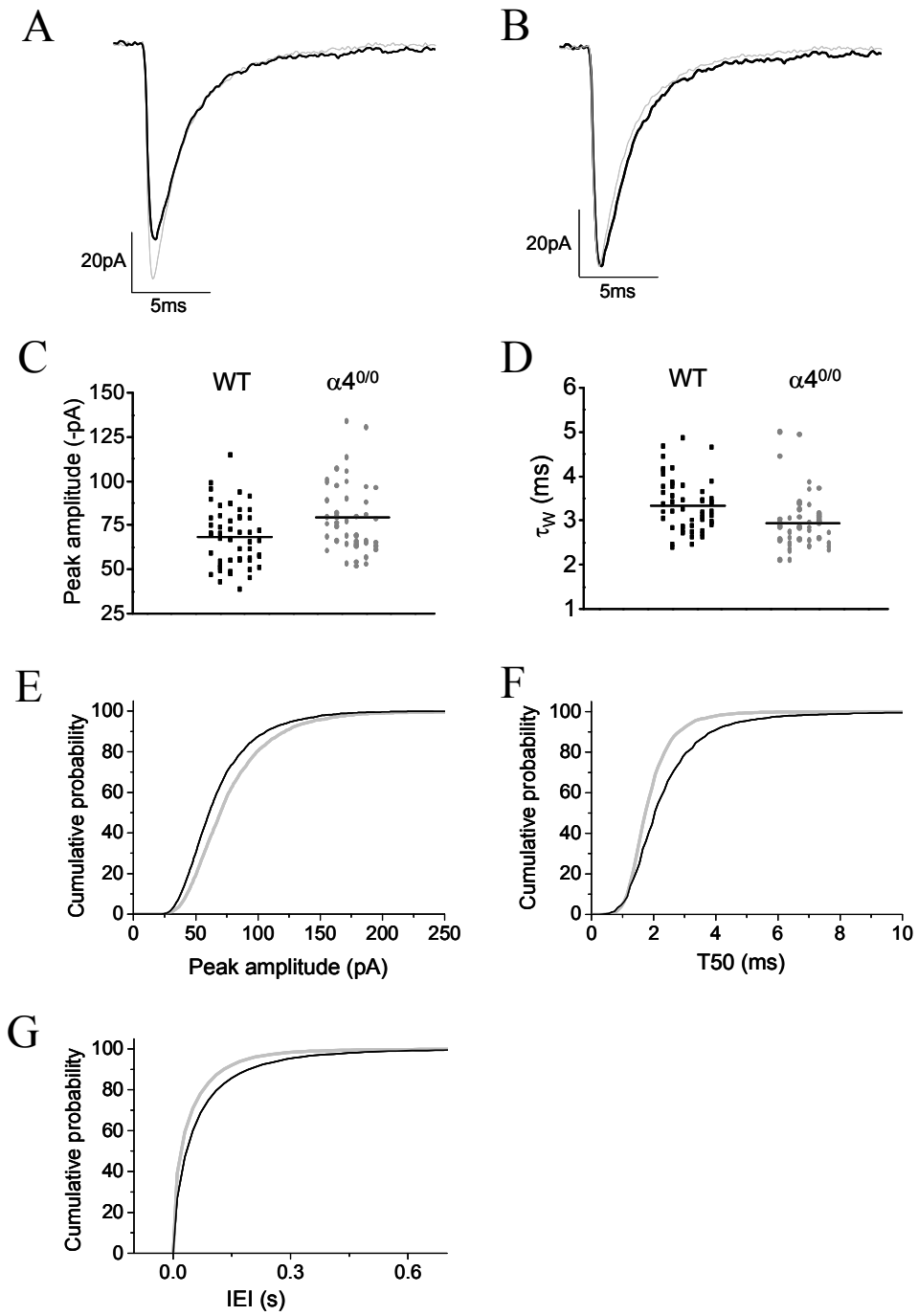

Figure 3.7. A comparison of the mIPSCs recorded from WT and $\alpha4^{0/0}$ VB neurones. A. Averaged overlayed mIPSCs recorded from a representative WT (black line) and an $\alpha4^{0/0}$ (grey line) VB neurone. Note the larger amplitude for the $\alpha4^{0/0}$ VB mIPSC. **B**. Overlayed, averaged traces of the same recordings shown in A normalised with respect to peak amplitude. Note the modest decrease in the decay time course for mIPSCs recorded from $\alpha4^{0/0}$ VB neurones. **C** and **D**. Scatter plots of the mean peak amplitude (C) and τ_W values (D) from 54 WT and 49 $\alpha4^{0/0}$ neurones. The average values are denoted by horizontal bars. **E.** A cumulative probability plot of peak amplitude for 3636 WT events (54 cells; black line) and 4394 $\alpha4^{0/0}$ events (49 cells; grey line). Note the apparent rightward shift in the peak amplitude distribution for mIPSCs recorded from $\alpha4^{0/0}$ VB neurones indicating that these neurones display mIPSCs with a greater mean peak amplitude compared with WT VB neurones ($p < 0.001$, KS test). **F**. A cumulative probability plot showing a leftward shift in the T50 cumulative probability plot for mIPSCs recorded from $\alpha4^{0/0}$ VB neurones (grey line) indicating that these neurones display faster decay kinetics compared with WT VB neurones (black line, $p < 0.001$, KS test). **G**. A cumulative probability plot showing the apparent leftward shift in the inter-event interval (IEI) distribution for mIPSCs recorded from $\alpha4^{0/0}$ VB neurones (grey line) indicating that these neurones display higher frequency of mIPSCs compared with WT VB neurones (black line, $p < 0.001$, KS test).

3.2.2. Tonic inhibition

Deletion of the α4-subunit dramatically reduced the tonic conductance (Figure 3.8). Specifically, WT VB neurones displayed a mean outward shift in holding current of 96 ± 9 pA shift in holding current upon 30 μM bicuculline administration (n = 27, $p < 0.001$ *vs* control, Student's paired t-test, Figure 3.8 C_1), whereas recordings obtained from $\alpha4^{0/0}$ VB neurones exhibited a mean outward shift of 13 ± 4 pA (n = 12, $p < 0.05$ *vs* control, Student's paired t-test, Figure 3.8 C_1). In addition, the background noise, as measured by the mean RMS, was decreased in $\alpha4^{0/0}$ VB neurones (WT: 7.6 ± 0.3 pA, n = 27, *vs* $\alpha4^{0/0}$: 4.9 ± 0.3 pA, n = 12, $p < 0.001$, Student's unpaired t-test, Figure 3.6 C, Figure 3.8 C_2). Application of 30 μM bicuculline to WT VB neurones decreased the RMS (7.6 ± 0.3 pA *vs* 5.1 ± 0.3 pA, $p < 0.001$, n = 27, Student's paired t-test) but had no effect on the mean RMS measurements obtained from $\alpha4^{0/0}$ VB neurones (4.9 ± 0.3 pA *vs* 4.6 ± 0.3 pA, n = 12, $p > 0.05$, Student's paired t-test). Hence, following bicuculline application the background noise, as indicated by mean RMS measurements, was similar in both strains (WT: 5.1 ± 0.3 pA, n = 27, *vs* 4.6 ± 0.3 pA, n = 12, $p > 0.05$, Student's unpaired t-test, Figure 3.6 D). These data reveal that α4-subunit containing $GABA_A$Rs play a major role in mediating an extrasynaptic conductance in VB neurones. With respect to the synapse, deletion of the α4-subunit induced modest changes in the biophysical properties of mIPSCs, effects that were concomitant with a marked increase in mIPSC frequency (Figure 3.7, Table 3.6). To develop a better understanding of $GABA_A$R-mediated transmission that is present in VB neurones, we now sought to establish how α4-subunit deletion impacted on the pharmacology of various ligands that are commonly regarded to preferentially target extrasynaptic $GABA_A$ receptors. Namely these comprised the neurosteroid 5α-pregnan-3α-ol-20-one (5α3α, Belelli *et al*., 2002; Stell *et al*., 2003), the δ-subunit preferential

agonist THIP (Brown *et al*., 2002; Stórustovu & Ebert., 2006; Herd *et al*., 2009), and the δ-subunit selective allosteric modulator, DS2 (Wafford *et al*., 2009).

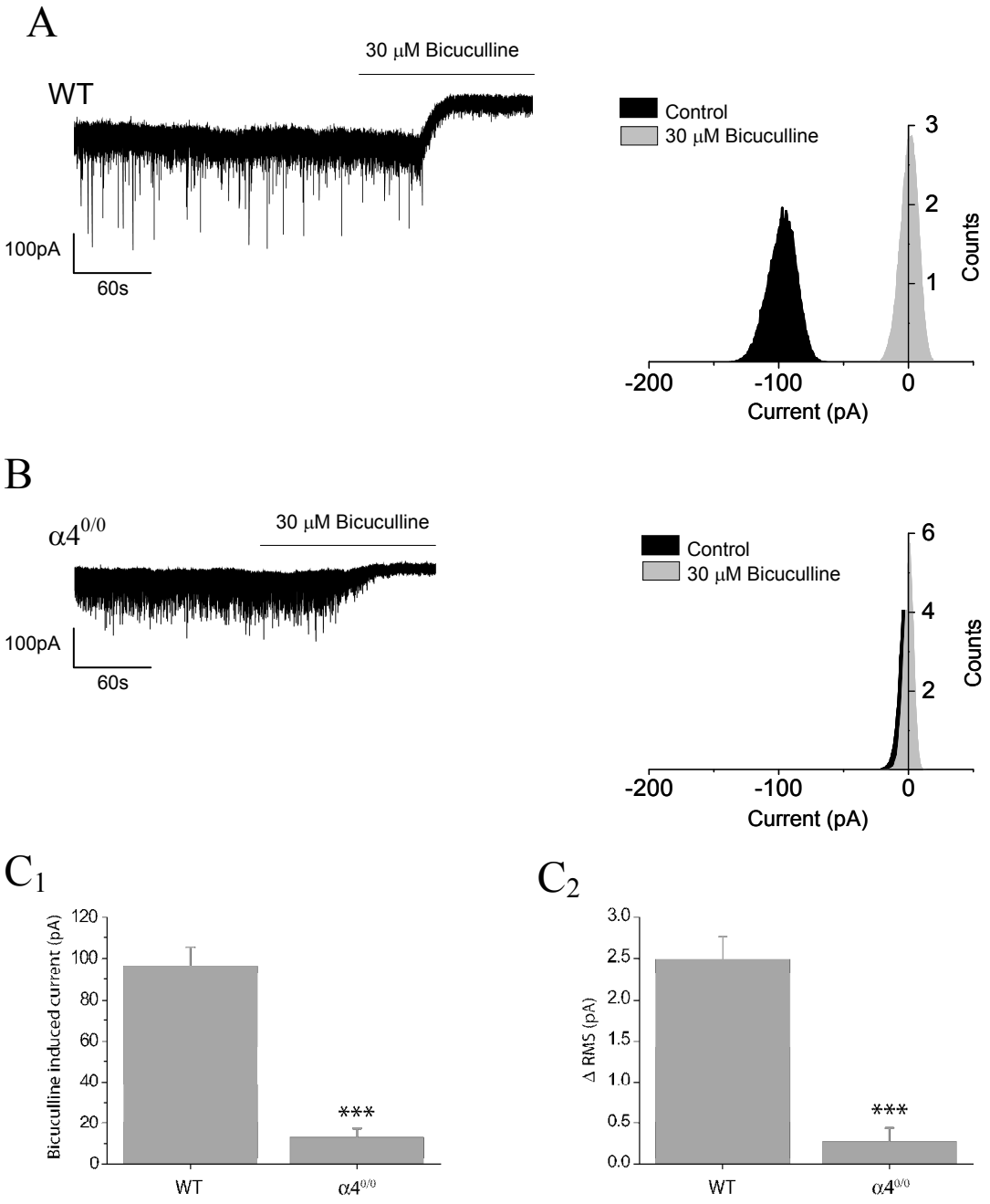

Figure 3.8. The deletion of the α4 subunit greatly diminished the $GABA_AR$-mediated tonic conductance of VB neurones. A. A current trace recorded from a representative WT VB neurone depicting the outward shift in the holding current coupled with a reduction in the baseline noise in response to 30 μM bicuculline application. Right panel: quantification of the shift in holding current is provided by the all points histogram (normalised to bicuculline) revealing an endogenous tonic current of 98 pA for the representative cell shown. **B.** A current trace recorded from a representative $\alpha4^{0/0}$ VB neurone. In contrast to WT neurones, application of 30 μM bicuculline to VB neurones derived from $\alpha4^{0/0}$ mice led to a greatly reduced outward shift in the holding current. Right panel: quantification of the shift in holding current is provided by the all-points histogram (normalised to bicuculline) revealing an endogenous tonic current of 6 pA for the representative cell shown. **C**. Bar graphs illustrating the impact of α4-subunit deletion on the tonic conductance in VB neurones. **C_1.** Application of 30 μM bicuculline to WT VB neurones elicited a mean inward current of 96 ± 9 pA (n = 27). In equivalent experiments performed on $\alpha4^{0/0}$ VB neurones the effect of 30 μM bicuculline on the holding current was substantially diminished, although the modest inward current was still significant (13 ± 5 pA, n = 12, $p < 0.05$ *vs* control, Student's paired t-test).**C_2.** Moreover, WT VB neurones displayed a reduction in baseline noise in response to 30 μM bicuculline application (Δ RMS WT: 2.5 ± 0.3 pA). This effect was greatly blunted in experiments performed on VB neurones derived from $\alpha4^{0/0}$ mice (Δ RMS $\alpha4^{0/0}$: 0.3 ± 0.2 pA, $p > 0.05$ *vs* control, Student's paired t-test). *** $p < 0.001$ *vs* WT, Student's unpaired t-test

3.3. The contribution of δ subunit containing $GABA_A$Rs to inhibitory transmission in VB neurones

3.3.1. A comparison of the actions of THIP on WT and $\alpha4^{0/0}$ VB neurones: synaptic and extrasynaptic $GABA_A$Rs

To investigate further the bicuculline-sensitive tonic currents observed in VB neurones, the extrasynaptic conductance was challenged with THIP. This compound preferentially activates $GABA_A$Rs containing the δ-subunit, where it displays a greater efficacy than GABA (Brown *et al*., 2002; Storustovu & Ebert, 2006). In recordings from WT VB neurones, 1 μM THIP had no effect on any of the mIPSC parameters analysed (Table 3.6, Figure 3.9). Conversely, 1 μM THIP evoked a large inward current in WT VB neurones (304 ± 41 pA, n = 8, $p < 0.001$ *vs* control, Student's paired t-test, Figure 3.10 A), an effect reversed by 30 μM bicuculline. In contrast, THIP elicited a greatly reduced, albeit significant, inward current in VB neurones derived from $\alpha4^{0/0}$ mice (8 ± 2 pA, n = 8, $p < 0.05$, Student's paired t-test, Figure 3.10 B).

	WT (n = 6 cells)		**α4$^{0/0}$** (n = 11 cells)	
	Control	**1 μM THIP**	**Control**	**1 μM THIP**
Peak amplitude (pA)	-85 ± 5	-96 ± 6	-78 ± 4	-80 ± 6
Rise time (ms)	0.5 ± 0.1	0.5 ± 0.1	0.5 ± 0.1	0.5 ± 0.1
τ_W (ms)	3.7 ± 0.3	3.8 ± 0.3	2.8 ± 0.1	2.9 ± 0.1
Frequency (Hz)	11 ± 4	9 ± 3	20 ± 5	15 ± 3

Table 3.6. A summary of the effects of 1 μM THIP on mIPSCs recorded from WT and α4$^{0/0}$ VB neurones. For both genotypes, 1 μM THIP had no statistically significant effects on mIPSC peak amplitude, rise time, τ_W or frequency. In all cases, $p > 0.05$ *vs* control, Student's paired t-test.

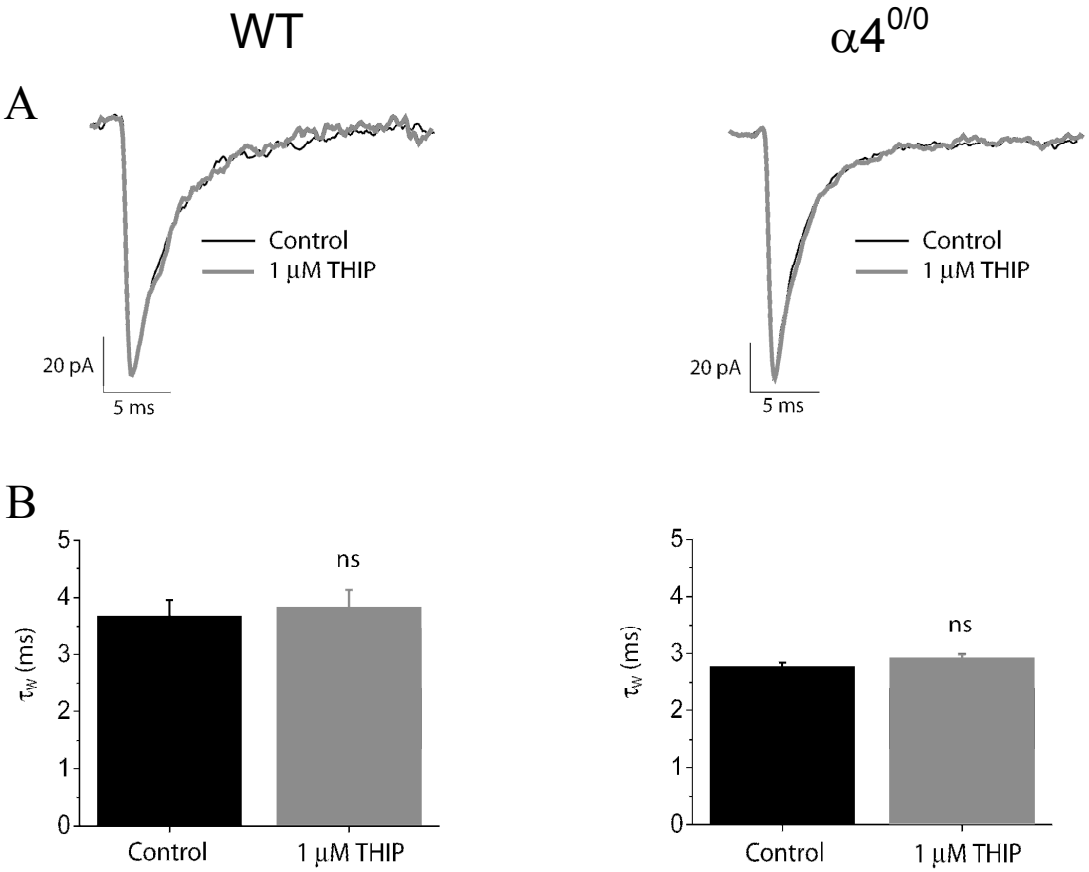

Figure 3.9. The influence of 1 μM THIP on WT and α4$^{0/0}$ VB mIPSCs: A. Superimposed, normalised average mIPSC recorded from a representative WT (left) and α4$^{0/0}$ (right) VB neurone before (black line) and after (grey line) bath application of 1 μM THIP. Note the absence of any effect on the mIPSC decay time constant, τ_W, for both genotypes. **B.** Bar graphs summarising the lack of effect of 1 μM THIP upon the decay kinetics of WT (left) and α4$^{0/0}$ (right) VB neurones. $p > 0.05$ *vs* control, Student's paired t-test.

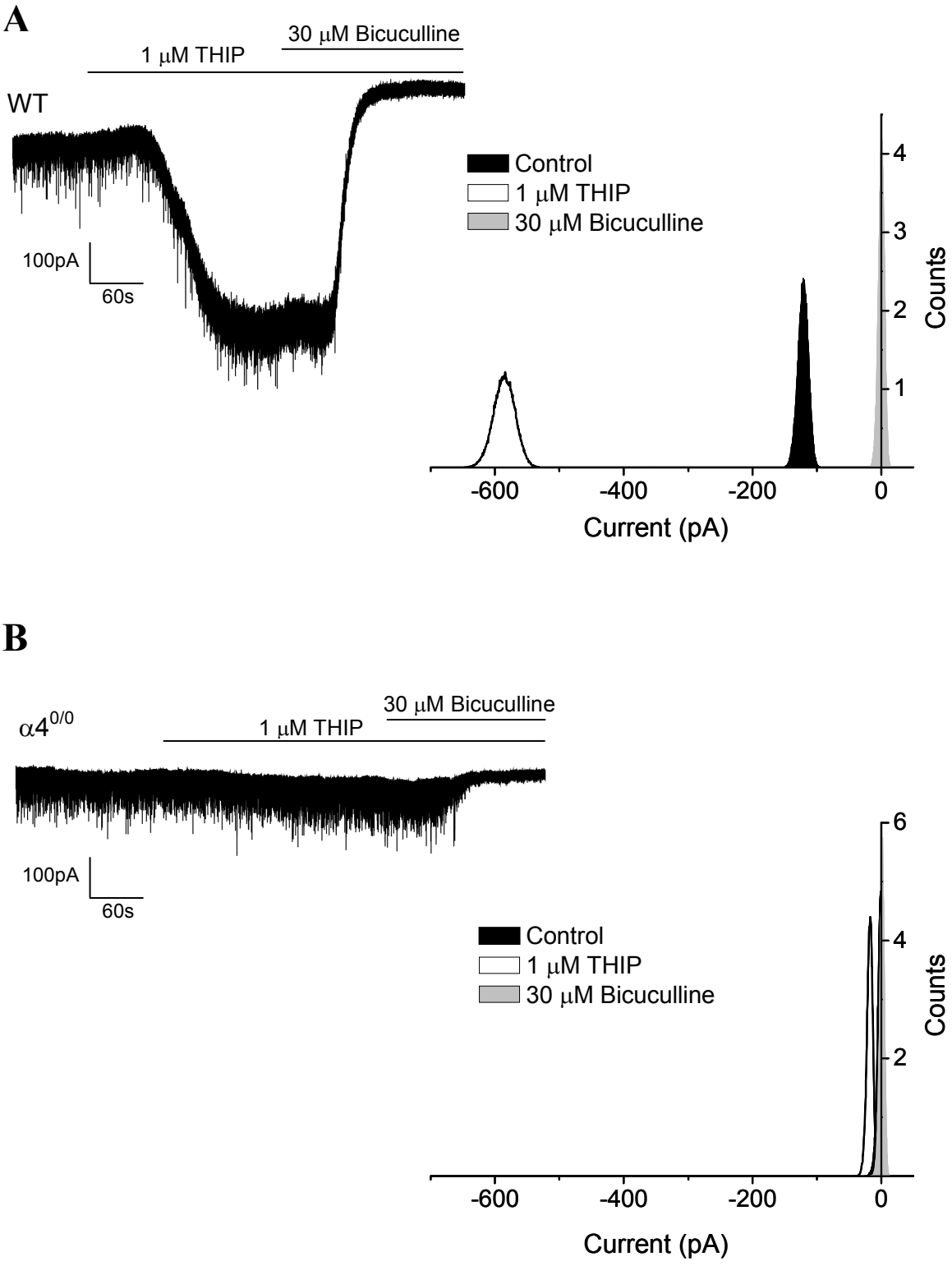

Figure 3.10. THIP induces a large inward current tonic for WT, but not for $\alpha4^{0/0}$, VB neurones. A. A current recording from a representative WT VB neurone showing the large inward current generated by 1 μM THIP, an effect subsequently reversed by 30 μM bicuculline. Right panel: the corresponding all-points histogram (normalised to bicuculline) showing a -463 pA inward current shift in response to 1 μM THIP, whereas 30 μM bicuculline induced a 122 pA outward shift relative to the control holding current. **B**. A current recording from a representative $\alpha4^{0/0}$ VB neurone showing that the inward current induced by 1 μM THIP is almost abolished. Right panel: the accompanying all-points histogram (normalised to bicuculline) showing a -16 pA inward current deviation in response to 1 μM THIP followed by a 3 pA outward shift when 30 μM bicuculline is applied.

3.3.2. A comparison of the actions of DS2 on WT and $\delta^{0/0}$ VB neurones: synaptic and extrasynaptic $GABA_ARs$

4-chloro-N-[2-(2-thienyl)imidazo[1,2-a]pyridine-3-yl benzamide (DS2) is a recently developed synthetic ligand that acts as a selective positive modulator of recombinant δ-$GABA_A$Rs (Wafford *et al.,* 2009). Furthermore, DS2 has been shown to augment the tonic conductance of VB neurones whilst having no effect on mIPSCs (Wafford *et al.,* 2009). Consistent with this report, 10 μM DS2 had no effect on VB mIPSCs (Table 3.7, Figure 3.11). However, 10 μM DS2 elicited a mean inward current of -115 ± 15 pA (n = 6, $p < 0.001$ *vs* control, Student's paired t-test). Often, the inward current induced by DS2 developed slowly but, once established, was well maintained until challenged with the $GABA_A$R antagonist, bicuculline (*e.g.* see Figure 3.12 A). Under these circumstances tonic current determinations were calculated 8 – 11 minutes after 10 μM DS2 was applied to the slice. Hence, the average value for the change in holding current observed with DS2 application may be an underestimate of the true effect. Nevertheless, the mean magnitude of the inward current observed with 10 μM DS2 in this study is in agreement with that reported previously (Wafford *et al*., 2009). To verify that the observed DS2-induced enhancement of VB tonic conductance is mediated by δ-$GABA_A$ receptors, 10 μM DS2 was applied to VB neurones derived from $\delta^{0/0}$ mice. These experiments revealed that the DS2-induced inward current is greatly diminished, and indeed not significant relative to the control holding current, when the δ-subunit gene is deleted (DS2-induced inward current: 11 ± 7 pA, n = 5, $p > 0.05$ *vs* control, Student's paired t-test, $p < 0.001$ *vs* WT DS2-induced current, Student's unpaired t-test, Figure 3.12 B).

	WT (n = 5)		**$\delta^{0/0}$** (n = 5)	
	Control	**10 μM DS2**	**Control**	**10 μM DS2**
Peak amplitude (pA)	-60 ± 3	-68 ± 4	-82 ± 6	-85 ± 4
Rise time (ms)	0.5 ± 0.1	0.5 ± 0.1	0.5 ± 0.1	0.5 ± 0.1
T50 (ms)	1.9 ± 0.1	1.9 ± 0.1	1.8 ± 0.1	1.9 ± 0.1
τ_W (ms)	2.6 ± 0.1	2.8 ± 0.3	2.6 ± 0.1	2.8 ± 0.1

Table 3.7. A summary of the effects of 10 μM DS2 on mIPSCs recorded from WT and $\delta^{0/0}$ VB neurones. For both genotypes, 10 μM DS2 had no statistically significant effects on any of the mIPSC parameters listed relative to control. In all cases $p > 0.05$ *vs* control, Student's paired t-test.

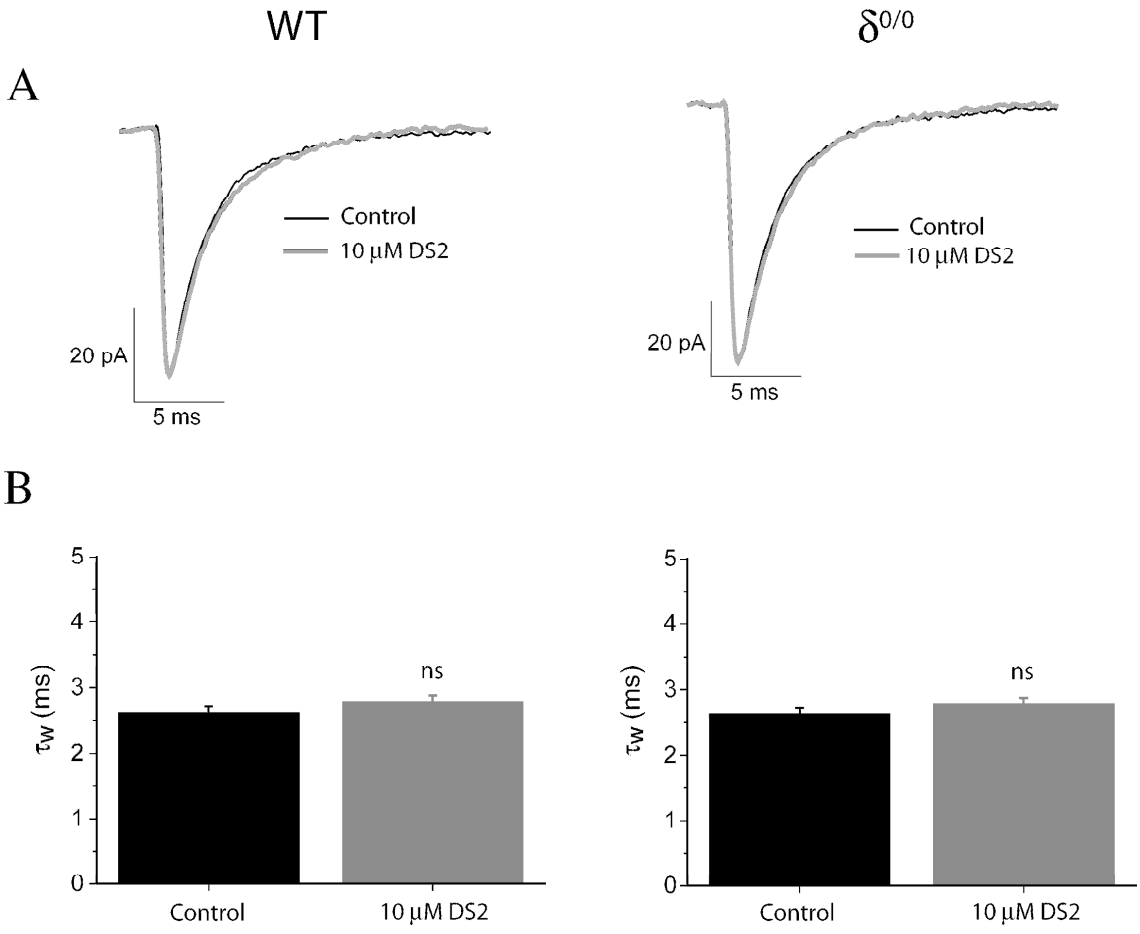

Figure 3.11. The influence of 10 μM DS2 on WT and $\delta^{0/0}$ VB mIPSCs: A. Superimposed and normalised wild type averaged mIPSCs recorded from a representative WT (left) and $\delta^{0/0}$ (right) VB neurone before (black line) and after (grey line) the bath application of 10 μM DS2. Note the absence of any effect on the mIPSC decay time. **B.** Bar graphs summarising the lack of effect of 10 μM DS2 upon mIPSC decay kinetics of WT (left) and $\delta^{0/0}$ (right) VB neurones. $p > 0.05$ *vs* control, Student's paired t-test.

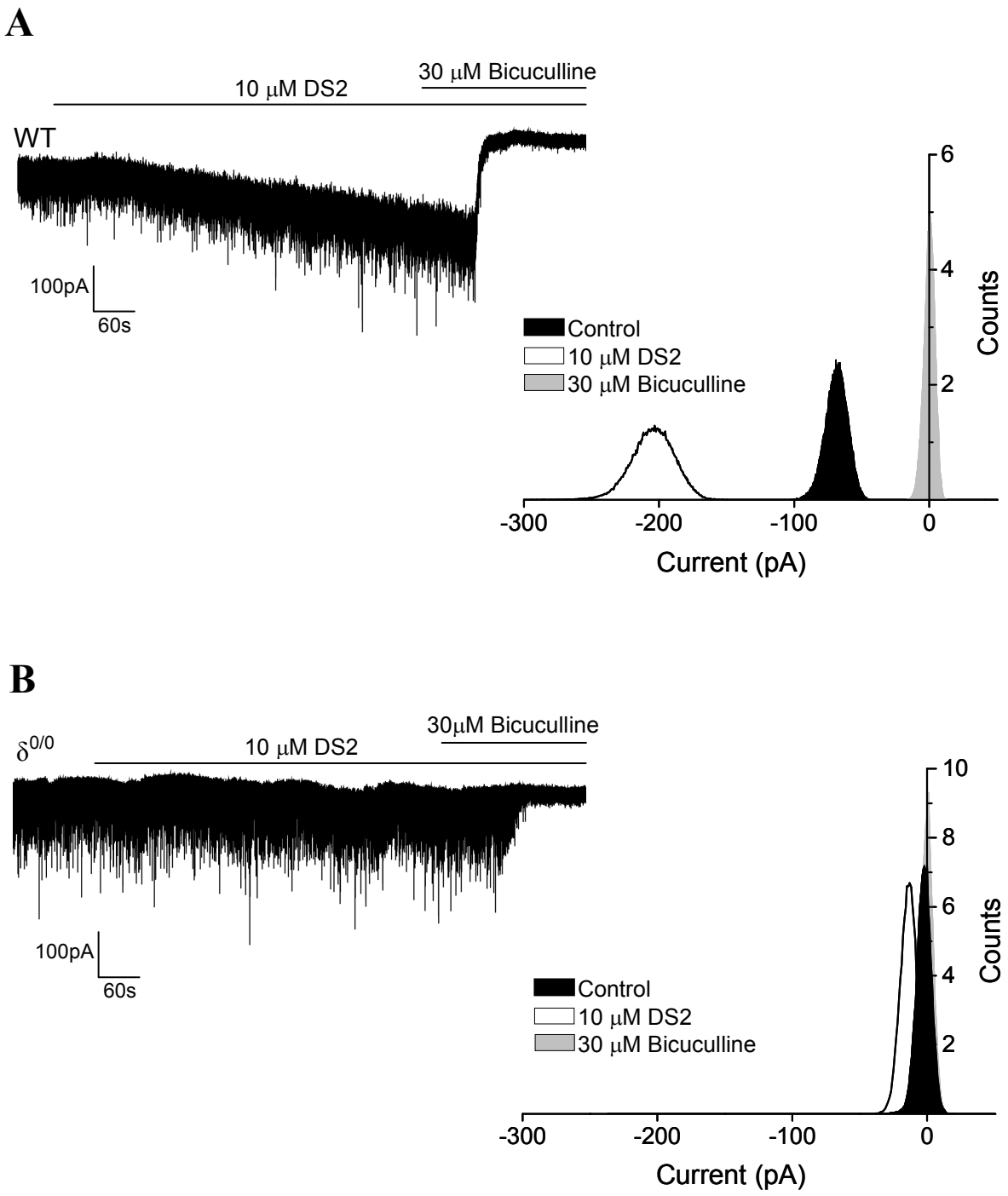

Figure 3.12. DS2 (10 μM) greatly enhances the tonic conductance of WT, but not $\delta^{0/0}$, VB neurones. **A.** A current recording from a representative WT VB neurone showing the inward current generated by 10 μM DS2 as demonstrated by an inward shift in the holding current that is reversed by 30 μM bicuculline. Note that bicuculline also reveals the endogenous tonic conductance. Right panel: the corresponding all points histogram (normalised to bicuculline) showing a -83 pA inward current in response to 10 μM DS2 whereas the subsequent application of 30 μM bicuculline induced an 89 pA outward current relative to the control holding current. **B**. A current recording from a representative $\delta^{0/0}$ VB neurone showing that the inward current induced by 10 μM DS2 is attenuated in VB neurones derived from $\delta^{0/0}$ mice. Right panel: the accompanying all points histogram (normalised to bicuculline) showing a -15 pA inward current in response to 10 μM DS2 followed by a 7 pA outward shift when 30 μM bicuculline is subsequently applied.

3.3.3. A comparison of the actions of 5α-pregnan-3α-ol-one on WT and α4$^{0/0}$ VB neurones: synaptic and extrasynaptic GABA$_A$Rs

Metabolites of progesterone and deoxycorticosterone such as 5α-pregnan-3α-ol-20-one (5α3α) and 5α-pregnan-3α,21-diol-20-one (THDOC) respectively, are established as being potent endogenous modulators of GABA$_A$R function (Belelli & Lambert, 2005; Gunn *et al*., 2011). For recombinant GABA$_A$Rs incorporating the γ-subunit (*i.e.* those which are abundantly expressed at synaptic locations) nanomolar concentrations of 5α3α and THDOC act with apparent promiscuity, indiscriminately augmenting GABA$_A$R function (Belelli *et al*., 2002). In addition, the GABA-evoked currents mediated by recombinantly expressed δ-containing GABA$_A$Rs are highly sensitive to 5α3α and 5α-THDOC (Belelli *et al.,* 2002; Brown *et al*., 2002; Wohlfarth *et al.,* 2002), and the behavioural effects of ganaxolone (a synthetic GABA-modulatory neurosteroid) are attenuated in δ$^{0/0}$ mice (Mihalek *et al*., 1998). These studies have prompted much speculation surrounding the physiological relevance of the GABA-modulatory neurosteroid actions on δ-GABA$_A$R mediated tonic inhibition. Here, the actions of 5α3α upon synaptic and tonic inhibition in VB neurones have been evaluated in brain slices obtained from both WT and α4-subunit deficient mice. Application of 100 nM 5α3α to WT VB neurones prolonged mIPSCs by 25 ± 6 % (τ_W control: 3.8 ± 0.1 ms, τ_W 100 nM 5α3α: 4.5 ± 0.1 ms, n = 11, $p < 0.01$, Student's paired t-test, Figure 3.13, Table 3.8). Similarly, when applied to α4$^{0/0}$ VB neurones, 100 nM 5α3α resulted in a prolongation of the decay time course as demonstrated by a 15 ± 4 % increase in τ_W (control: 3.5 ± 0.2 ms, 100 nM 5α3α: 4.1 ± 0.3 ms, n = 10, $p < 0.05$, Student's paired t-test, Figure 3.13, Table 3.8). Moreover, the percentage prolongation of τ_W by 5α3α was not significantly different between the two strains ($p > 0.05$, one way repeated measures ANOVA). For both WT and α4$^{0/0}$ recordings, 100 nM 5α3α did not affect the peak

amplitude, rise time or frequency of mIPSCs (in each case $p > 0.05$ *vs* control, Student's paired t-test).

Application of 1 μM 5α3α to VB neurones also prolonged the decay time course of control mIPSCs. Specifically, 1 μM 5α3α increased the τ_W by 39% ± 16 (control: 3.7 ± 0.2 ms, 1 μM 5α3α: 5.1 ± 0.3 ms, $n = 5$, $p < 0.05$, Student's paired t-test) although the percentage-prolongation was not significantly different *vs* the prolongation induced by 100 nM 5α3α ($p > 0.05$, one way repeated measures ANOVA). Considering that δ-$GABA_A$Rs have been highlighted as a significant molecular target for physiological neurosteroid levels (10-100 nM), the effects of 5α3α on tonic inhibition were investigated in WT VB neurones. Relative to 1 μM THIP, application of 100 nM 5α3α caused only a modest enhancement of the endogenous tonic current (100 nM 5α3α: -32 pA ± 4 pA, $n = 11$, $p < 0.001$ *vs* control, Student's paired t-test, Figure 3.14 A). Furthermore, 1 μM 5α3α induced an inward current (1 μM 5α3α: -55 ± 20 pA, $n = 6$, $p < 0.05$ *vs* control, Student's paired t-test, Figure 3.14 B) although this was not significantly different to the current generated by 100 nM 5α3α ($p > 0.05$, Student's unpaired t-test). In contrast to WT VB recordings, addition of 100 nM 5α3α to $\alpha4^{0/0}$ VB neurones had no appreciable effect on the holding current (100 nM 5α3α: -4 ± 3 pA, $n = 5$, $p > 0.05$ *vs* control, Student's paired t-test; $p < 0.01$, *vs* WT 100 nM 5α3α-induced current, Student's unpaired t-test, Figure 3.14 C).

	WT (n = 11)		**α4$^{0/0}$** (n = 10)	
	Control	**100 nM 5α3α**	**Control**	**100 nM 5α3α**
Peak amplitude (pA)	-60 ± 5	-64 ± 5	-68 ± 5	-67 ± 4
Rise time (ms)	0.6 ± 0.1	0.6 ± 0.1	0.6 ± 0.1	0.6 ± 0.1
τ_W (ms)	3.8 ± 0.1	4.5 ± 0.1**	3.5 ± 0.2	4.1 ± 0.3*
Frequency (Hz)	14 ± 3	15 ± 3	23 ± 4	22 ± 5

Table 3.8. A summary of the effects of 100 nM 5α3α on mIPSCs recorded from WT and α4$^{0/0}$ VB neurones. For both genotypes, 100 nM 5α3α had no statistically significant effects on the mIPSC peak amplitude, rise time or mIPSC frequency. Conversely, for both WT and α4$^{0/0}$ recordings, 100 nM 5α3α significantly prolonged the decay time constant τ_W. * $p < 0.05$, ** $p < 0.01$, *vs* control, Student's paired t-test. Note that all data displayed in this table are from paired recordings (before and after the neurosteroid).

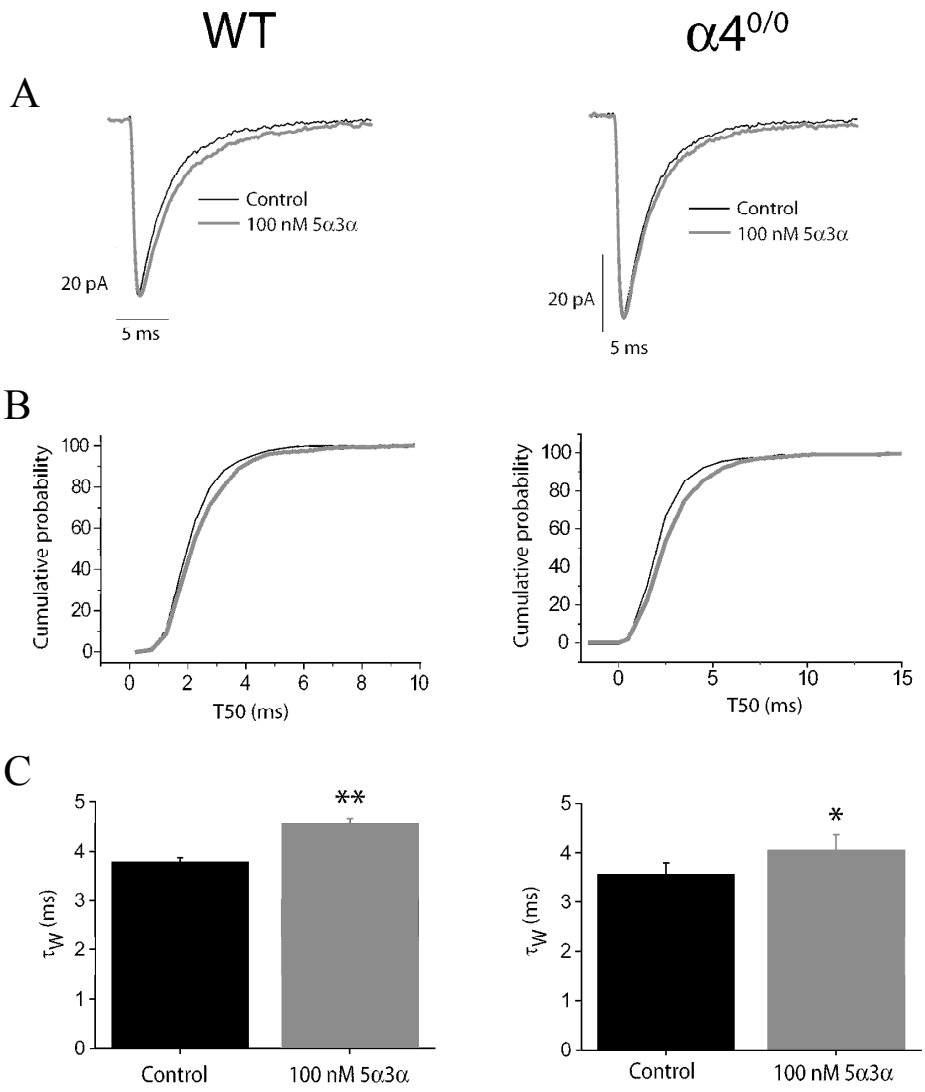

Figure 3.13. The neurosteroid 5α3α (100 nM) modestly prolongs mIPSCs of WT VB neurones. A. Representative, overlayed and averaged mIPSCs recorded from WT (left) and $\alpha4^{0/0}$ (right) VB neurones. Note that the small prolongation of the decay time course in the presence of 100 nM 5α3α. **B**. Cumulative probability plots of T50 for mIPSCs recorded from WT (left, control = 508 mIPSCs, 100 nM 5α3α = 521 mIPSCs from 7 cells) and $\alpha4^{0/0}$ VB neurones (right, control = 814 mIPSCs, 100 nM 5α3α = 680 mIPSCs from 10 cells). Note the small rightward shift in the T50 cumulative probability plot upon 100 nM 5α3α application (grey line) for both WT and $\alpha4^{0/0}$ VB neurones, indicating a prolongation of the mIPSC decay time irrespective of strain (in both cases, $p < 0.05$ *vs* control, KS test) **C.** Bar graphs illustrating the effects of 100 nM 5α3α on the weighted decay time constant, τ_W. Note the increase in τ_W when treated with 100 nM 5α3α. * $p < 0.05$, ** $p < 0.01$ *vs* control, Student's paired t-test.

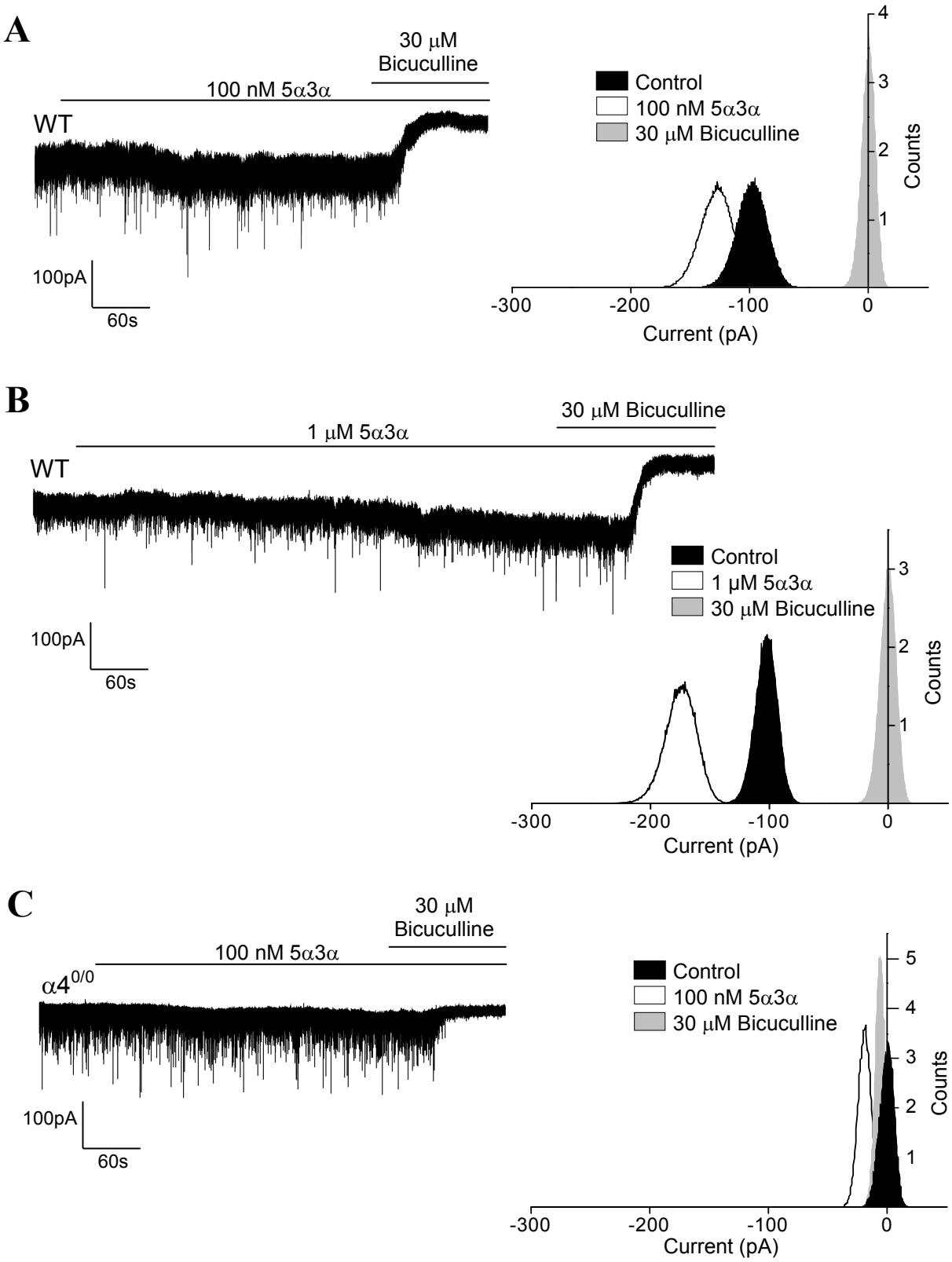

Figure 3.14. The neurosteroid 5α3α enhances the tonic conductance of WT, but not α4$^{0/0}$, VB neurones. A and B. Current recordings from representative WT VB neurones (left) and corresponding all-points histograms (normalised to bicuculline; right) showing that the application of 100 nM (A) and 1 μM 5α3α (B) caused a -30 pA and -70 pA inward shift in the holding current respectively. In both cases this effect was reversed by 30 μM bicuculline indicating that 5α3α potentiates a $GABA_AR$-mediated tonic conductance in VB neurones. Note in both cases bicuculline additionally reveals the presence of an endogenous tonic current **C**. A current recording from a representative α4$^{0/0}$ VB neurone (left) and the corresponding all-points histogram (normalised to bicuculline; right) showing that in contrast to WT neurones, application of 100 nM 5α3α to α4$^{0/0}$ VB neurones had little effect on the holding current.

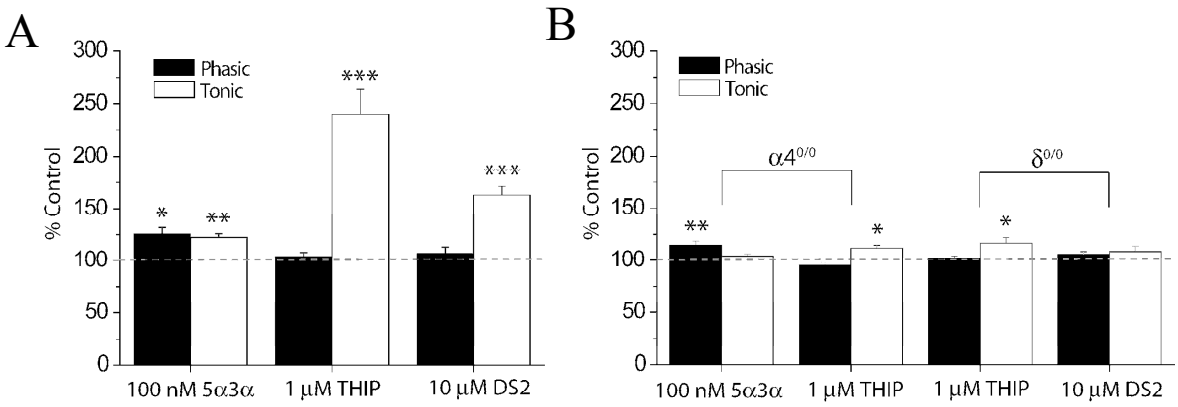

Figure 3.15. The differential effects of 5α3α, DS2 and THIP on phasic *vs* tonic inhibition in VB neurones. **A**. A bar graph illustrating the percentage change in both mIPSC τ_W (phasic, black bars) and holding current (tonic, white bars) for WT VB neurones in response to 100 nM 5α3α (mIPSCs, n = 7 cells; tonic, n = 8 cells), 10 μM DS2 (mIPSCs, n = 5 cells; tonic, n = 5 cells) and 1 μM THIP (mIPSCs, n = 6 cells; tonic, n = 8 cells) relative to drug-free control (normalised to 100%; dashed grey line). Note that 100 nM 5α3α elicits a modest but significant enhancement of both forms of inhibition, whereas 10 μM DS2 and 1 μM THIP selectively enhance tonic, but not synaptic, inhibition. **B**. A bar graph illustrating the percentage change in both mIPSC τ_W and holding current for VB neurones derived from $GABA_AR$-subunit α4 or δ knockout mice in response to 100 nM 5α3α (mIPSCs, n = 10 cells; tonic, n = 5 cells), 10 μM DS2 (mIPSCs, n = 5 cells; tonic, n = 5 cells) and 1 μM THIP ($\alpha4^{0/0}$: mIPSCs, n = 11 cells; tonic, n = 8 cells; $\delta^{0/0}$: mIPSCs, n = 7 cells; tonic, n = 7 cells) relative to drug-free control (normalised to 100%; dashed grey line). Note that the effects of all three compounds on the mIPSC decay time constant, τ_W, are unchanged compared to WT recordings. Conversely, the enhancement of the tonic conductance by 100 nM 5α3α and 10 μM DS2 that is evident in WT recordings, is absent in recordings from $\alpha4^{0/0}$ and $\delta^{0/0}$ VB neurones, respectively. Similarly, the tonic-enhancing action of 1 μM THIP is severely blunted in $\alpha4^{0/0}$ and $\delta^{0/0}$ VB neurones, although a small, statistically significant enhancement remains in both cases. * $p < 0.05$ *vs* control, ** $p < 0.01$ *vs* control , *** $p < 0.001$ *vs* control, one-way repeated measures ANOVA.

3.4. A comparison of the effects of co-application of DS2 and THIP on the tonic conductance of WT VB neurones

As previously detailed, DS2 and THIP are δ-$GABA_AR$ preferring compounds. Given that DS2 is a positive allosteric modulator of δ-$GABA_AR$ function, whereas THIP is an agonist at this receptor isoform, it is conceivable that when THIP is applied in the presence of DS2, the THIP response should be augmented due to allosteric modulation. To examine this hypothesis, DS2 was administered to WT thalamic slices and the actions on VB tonic inhibition determined. Subsequently 1 μM THIP was applied to the preparation. Consistent with experiments described in section 3.4.2, 10 μM DS2 induced a significant inward shift in the holding current (-105 ± 21 pA, n = 4, $p < 0.05$ *vs* control, Student's paired t-test, Figure 3.16, Figure 3.18 A). Moreover, the subsequent application of 1 μM THIP in the presence of DS2, induced a considerable inward current (-577 ± 28 pA, n = 4, $p < 0.001$ *vs* control, Student's paired t-test, Figure 3.16, Figure 3.18 A). Deducting the DS2–alone induced current yields a -473 ± 43 pA (n = 4, $p < 0.001$ *vs* control, Student's paired t-test) inward current response to 1 μM THIP, a value that is significantly larger than for experiments evaluating the effects of 1 μM THIP alone (-304 ± 41 pA, n = 8, $p < 0.05$, Student's unpaired t-test, Figure 3.18 C).

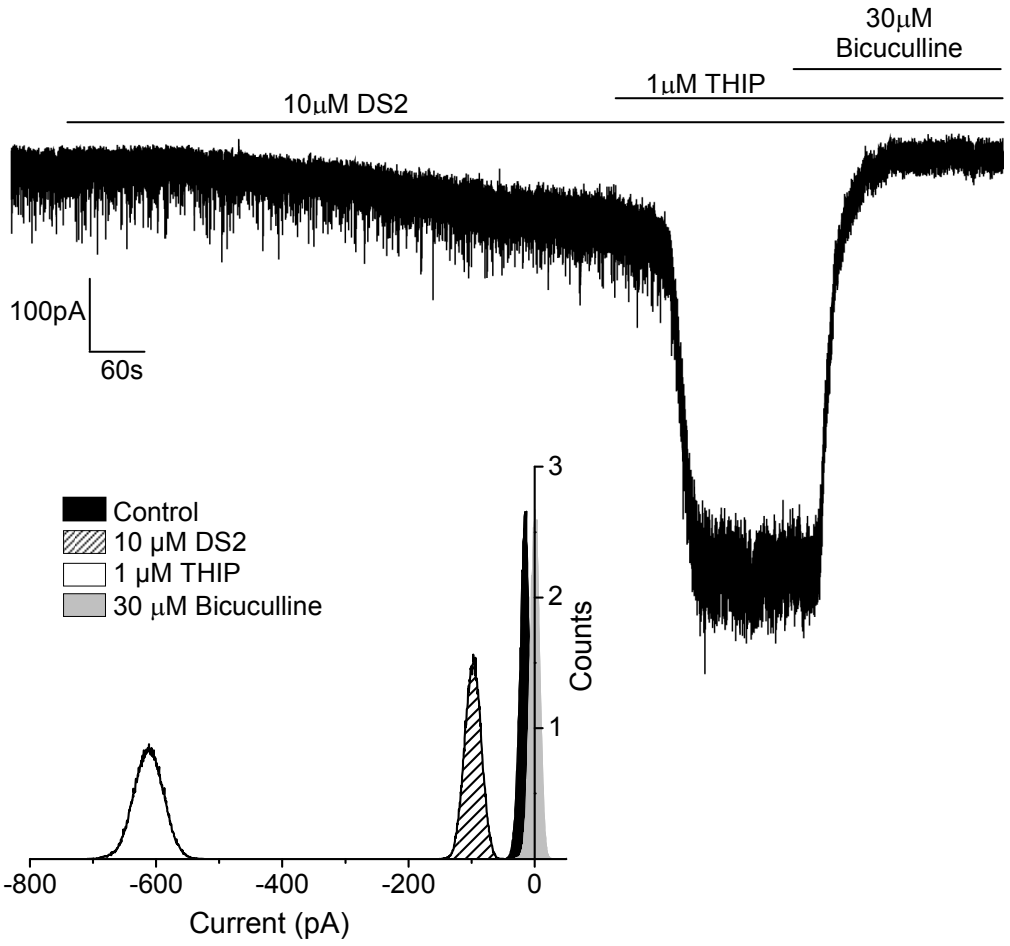

Figure 3.16. The tonic conductance induced by 1 μM THIP is greatly enhanced in the presence of 10 μM DS2 for WT VB neurones. A current recording from a representative WT VB neurone showing the inward current following 10 μM DS2 addition. The subsequent application of 1 μM THIP in the presence of 10 μM DS2 elicited a substantial inward current, an effect reversed by 30 μM bicuculline. Note that bicuculline application additionally reveals a resident tonic conductance. Illustrated below is the corresponding all-points histogram (normalised to bicuculline) in which the shift in holding current generated by 10 μM DS2, 1 μM THIP and 30 μM bicuculline are -82, -596 and 17 pA, respectively, relative to control.

3.5. A comparison of the effects of co-application of 5α3α and THIP on the tonic conductance of WT VB neurones

Given that THIP is established to selectively activate δ-$GABA_A$Rs at low micromolar concentrations (Brown *et al.,* 2002; Stórustovu & Ebert, 2006), the enhancement of the THIP-induced current by DS2 in VB neurones described here provides additional evidence that DS2 exerts this effect by an interaction with δ-$GABA_A$Rs. Hence, it is postulated that this method can be used as an additional approach to δ-subunit knockout mice to verify whether inward current responses to 5α3α are primarily mediated by δ-$GABA_A$Rs. With respect to this, 100 nM 5α3α was applied to WT thalamic slices and the actions on VB tonic current determined. Subsequently, 1 μM THIP was applied to the preparation. Similar to those results described in Section 3.4.3, 100 nM 5α3α application alone resulted in a modest augmentation of the tonic current as illustrated by a small, but significant, inward current (-29 ± 6 pA, n = 3, $p < 0.05$, *vs* control, Student's paired t-test, Figure 3.17, Figure 3.18 B). The subsequent application of 1 μM THIP resulted in a robust inward current (-251 ± 27 pA, n = 3, $p < 0.05$ *vs* control, Student's paired t-test, Figure 3.17). Therefore, deducting the current induced by 100 nM 5α3α, leaves a THIP-induced inward current of -223 ± 22 pA (n = 3, $p < 0.01$ *vs* 100 nM 5α3α). However, the magnitude of this THIP-induced inward current relative to the holding current after 100 nM 5α3α application was not statistically different to determinations of the inward current following 1 μM THIP treatment alone (1 μM THIP alone: -304 ± 41 pA, n = 8, $p > 0.05$ *vs* 1 μM THIP relative to 100 nM 5α3α, Student's unpaired t-test, Figure 3.17, Figure 3.18). This observation, that a physiological concentration of the neurosteroid 5α3α, does not augment the inward current in response to 1 μM THIP, corroborates the findings described in Section 3.3.3 and

provides further evidence that the extrasynaptic conductance in VB neurones is only modestly sensitive to modulation by exogenous neurosteroids.

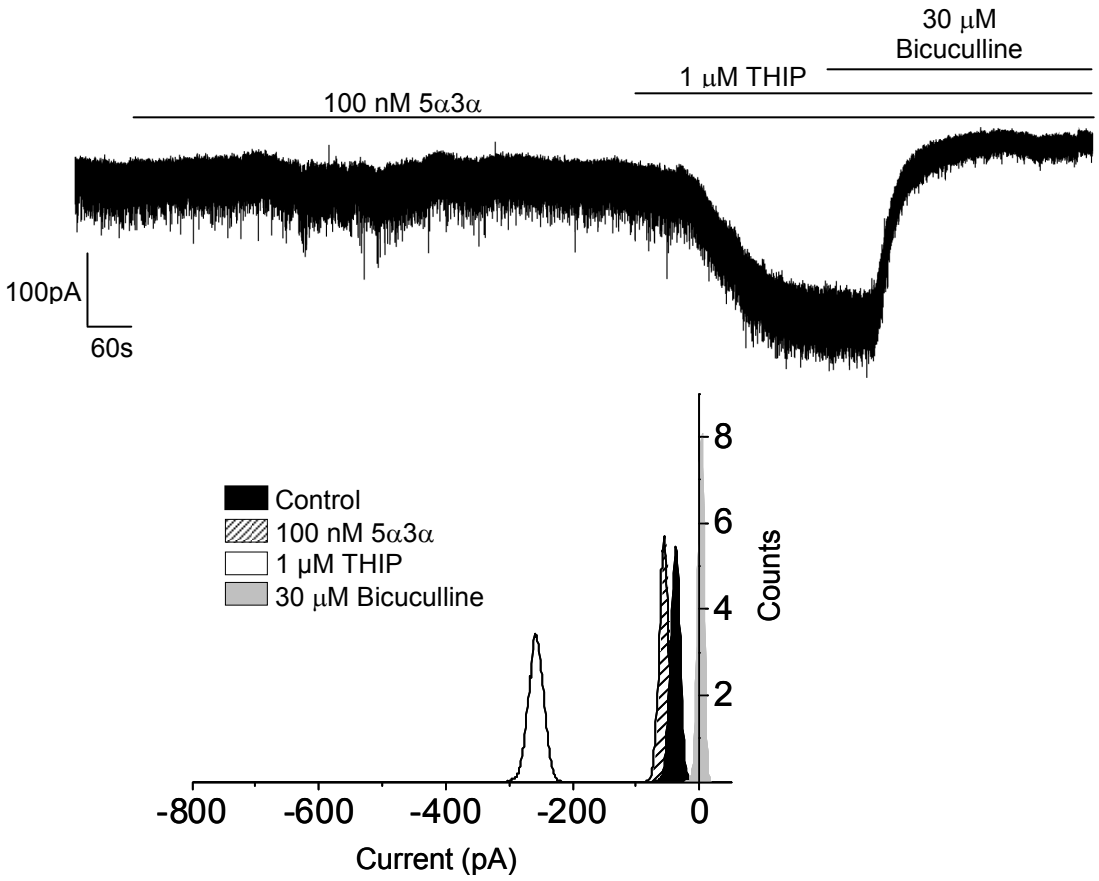

Figure 3.17. The tonic conductance induced by 1 μM THIP is not enhanced in the presence of 100 nM 5α3α for WT VB neurones. A current recording from a representative WT VB neurone showing that the addition of 100 nM 5α3α has only a modest effect on the holding current. The subsequent application of 1 μM THIP in the presence of 100 nM 5α3α elicited a robust inward current. However, compared to 1 μM THIP application alone, this effect was not statistically significant ($p > 0.05$, Student's unpaired t-test). The inward current generated by 5α3α and THIP was reversed by 30 μM bicuculline. Illustrated below is the corresponding all-points histogram (normalised to bicuculline) in which the shift in holding current generated by 100 nM 5α3α, 1 μM THIP and 30 μM bicuculline are -18, -220 and 40 pA, respectively, relative to control.

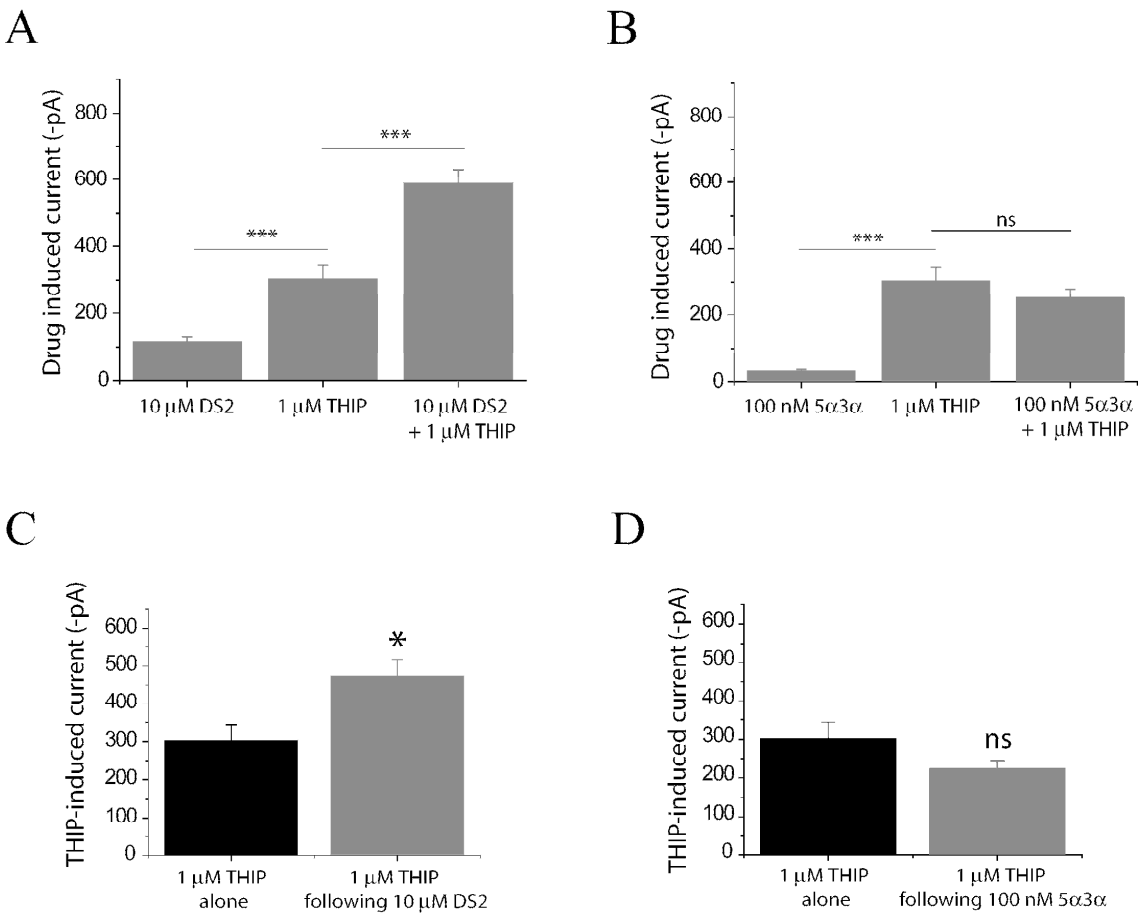

Figure 3.18. The effect of THIP (1 μM) co-application with DS2 (10 μM) or 5α3α (100 nM). A. Summary bar graph depicting the inward current induced by DS2 (10 μM) alone, THIP (1 μM) alone, and DS2 (10 μM) and THIP (1 μM) co-applied. **B.** Summary bar graph depicting the inward current induced by 5α3α (100 nM) alone, THIP (1 μM) alone, and 5α3α (100 nM) and THIP (1 μM) co-applied. **C.** Summary bar graph showing the increased inward current generated by THIP (1 μM) following 10 μM DS2 application. **D.** Summary bar graph depicting the lack of effect of 5α3α co-application on the THIP (1 μM) – induced inward current.

Chapter 4

Endogenous neurosteroid interactions with $GABA_A$ receptor-mediated inhibition in VB neurones during postnatal development.

4.1. The effect of postnatal age on the properties of mIPSCs recorded from WT VB neurones

Numerous studies, conducted on thalamic, cerebellar, cortical and hippocampal neurones have uniformly indicated that during development an increased expression of synaptic $GABA_AR$s incorporating the α1 subunit contributes to the decrease in the time course of synaptic $GABA_AR$ mediated currents (Rovira & Ben-Ari 1993; Tia *et al*., 1996; Hollrigel & Soltesz 1997; Dunning *et al*., 1999; Okada *et al*., 2000; Vicini *et al*., 2001; Ortinski *et al*., 2004; Bosman *et al*., 2005; Peden *et al*., 2008). However, electrophysiological studies performed on brain slices, or neurones maintained in cell culture, derived from $\alpha1^{0/0}$ mice have consistently reported that although the developmental alteration to the IPSC decay kinetics is attenuated, deletion of the α1 subunit does not completely prevent these changes (Vicini *et al*., 2001; Ortinski *et al*., 2004; Peden *et al*., 2008). Immunohistochemical studies probing the presence of 5α3α across the adult rodent brain using a specific antibody to this neurosteroid, have highlighted endogenous 5α3α immunolabelling on VB neurones (Herd & Belelli, unpublished observations; Saalmann *et al*., 2007). Hence, the present study investigated the possibility that neurosteroid levels impact upon mIPSC decay kinetics during development. A precedent for such a scenario had been offered by Peden and colleagues who reported that most of the developmental speeding of mIPSC decay kinetics in VB neurones occurs between P8-9 and P10-11 by a mechanism that is independent of the α1-subunit (Peden *et al*., 2008). Therefore, as a prelude to investigating whether during postnatal development endogenous neurosteroids impact on $GABA_AR$-mediated inhibition in VB neurones, I first sought to establish the properties mIPSCs at distinct developmental time-points (P7, P8, P10 and P20-24). Thalamocortical (TC) neurones of the VB nucleus are particularly amenable for the study of inhibitory transmission during

development. This is due in part to the relatively high frequency of mIPSCs evident even at early neonatal (*i.e.* P7) ages. Furthermore, the developmental transition of α subunits is well characterised and after P14 synaptic inhibition is mediated primarily, if not exclusively by α1-$GABA_A$Rs (Peden *et al*., 2008). Specifically, the mIPSCs recorded from VB neurones of $\alpha1^{0/0}$ mice display normal characteristics until ~P14 at which point these cells become devoid of mIPSCs (Peden *et al*., 2008). Considered together with anatomical evidence demonstrating an absence of α2 and abundance of α1 in the mature thalamus (Laurie *et al*., 1992a; Wisden *et al*., 1992, Peden *et al*., 2008) there most likely occurs a rapid and complete switch to α1 subunit-containing $GABA_A$Rs in VB neurones at P14 (Peden *et al*., 2008).

Analysis of mIPSCs recorded from WT VB neurones derived from neonatal (P7, P8, P10) to juvenile (P20-24) mice revealed developmental differences in their biophysical properties. Specifically, at P7, P8 and P10 significant decreases in peak amplitude (P7: -82 ± 4 pA *vs* P20-24: -66 ± 3 pA, $p < 0.001$, Student's unpaired t-test), rise time (P7: 0.6 ± 0.1 ms *vs* P20-24: 0.5 ± 0.1 ms, $p < 0.001$, Student's unpaired t-test) and τ_W (P7: 8.5 ± 0.4 ms *vs* P20-24: 3.2 ± 0.1 ms, $p < 0.001$, Student's unpaired t-test, Figure 4.1) were observed (for all values see Table 4.1). On the other hand, the frequency increased from 3.9 ± 0.5 Hz at P7 to 10.9 ± 1.4 Hz at P20-24 (Figure 4.1 A and C, Table 4.1). These effects are consistent with previous studies concerning the developmental profile of mIPSC properties conducted on several neuronal types in the CNS (Cohen *et al*., 2000; Okada *et al*., 2000; Ortinski *et al*., 2004; Peden *et al*., 2008). I next investigated whether endogenous GABA-modulatory neurosteroids may influence the developmental changes in mIPSC parameters described for WT VB neurones.

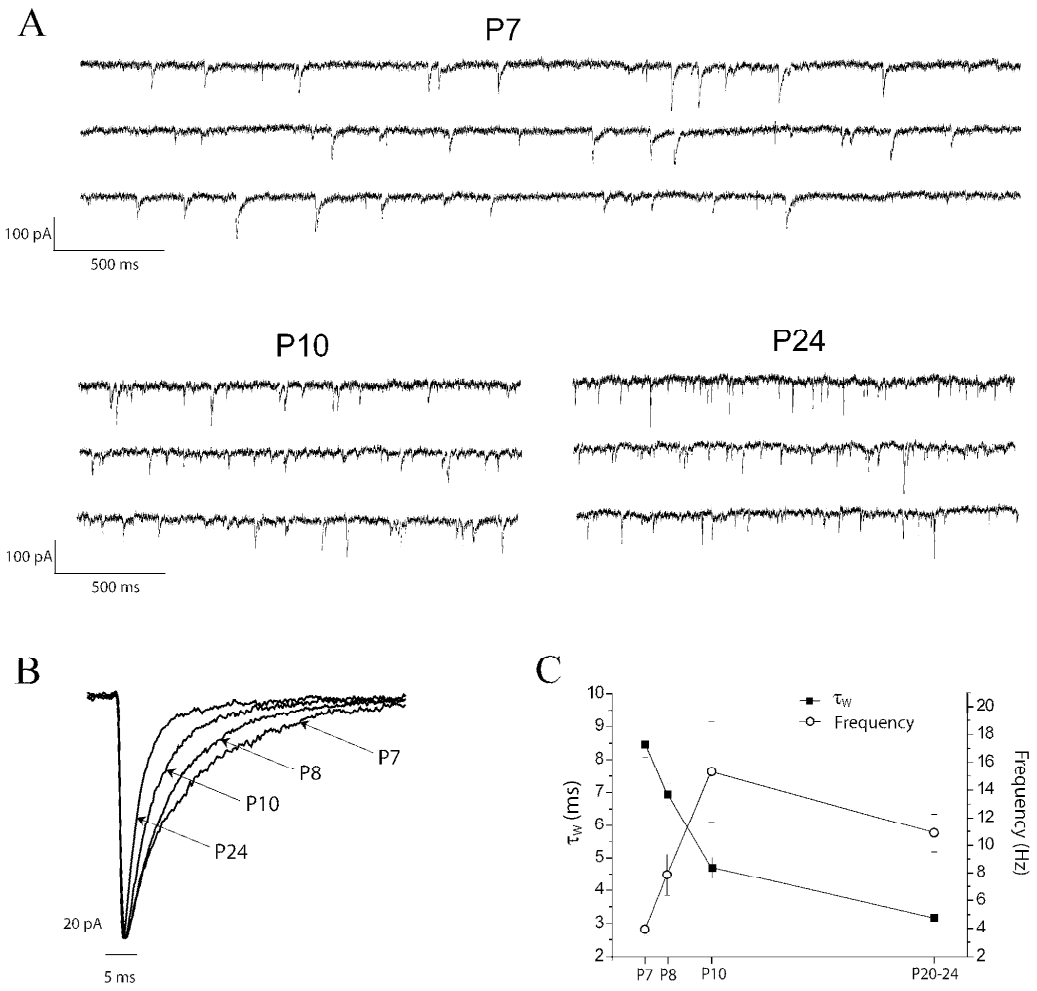

Figure 4.1. The properties of mIPSCs recorded from VB neurones during postnatal development. **A.** Traces showing typical current recordings from VB neurones derived from WT mice at P7, P10 and P24. As development progresses, the frequency of events increases whereas the decay time and peak amplitude decreases. **B**. Averaged, overlayed mIPSCs normalised with respect to peak amplitude, recorded from four representative WT VB neurones from brain slices derived from P7, P8, P10 and P24 mice. Note the progressive decrease in the mIPSC decay time with age. **C**. A superimposed line graph showing the progressive decrease in mIPSC τ_W, and the concomitant increase in their frequency, during development.

	P7 (n = 15 cells)	P8 (n = 9 cells)	P10 (n = 7 cells)	P20-24 (n = 28 cells)
Peak amplitude (pA)	-82 ± 4***	-92 ± 6***	-93 ± 9***	-66 ± 3
Rise time (ms)	0.6 ± 0.1***	0.6 ± 0.1***	0.6 ± 0.1***	0.5 ± 0.1
τ_W (ms)	8.5 ± 0.4***	6.9 ± 0.3***	4.7 ± 0.3***	3.2 ± 0.1
Frequency (Hz)	3.9 ± 0.5**	7.9 ± 1.5	15.3 ± 3.6	10.9 ± 1.4

Table 4.1. The properties of mIPSCs recorded from WT VB neurones at different stages of development. ** $p < 0.01$, *** $p < 0.001$ *vs* P20-24

4.2. The effects of finasteride pre-treatment on mIPSCs from P7 WT VB neurones

To assess whether endogenous neurosteroids impact upon properties of mIPSCs during VB neuronal development, thalamic brain slices from 7-day old WT mice were pre-treated with the 5α-reductase inhibitor finasteride (50 μM). Inhibition of 5α-reductase prevents the conversion of progesterone (PROG) to 5α-dihydroprogesterone (5α-DHP) and deoxycorticosterone (DOC) to 5α-dihyrodeoxycorticosterone (5α-DOC), the immediate precursors of 5α3α and THDOC, respectively (see Introduction Figure 1.6). Compared with mIPSCs obtained from control recordings, pre-incubation with 50 μM finasteride resulted in mIPSCs with significantly faster decay kinetics as indicated by a decrease in τ_W (P7 control: 8.5 ± 0.4 ms, n = 15, *vs* 50 μM finasteride: 6.0 ± 0.3 ms, n = 8, $p < 0.001$, Student's unpaired t-test, Figure 4.2, Figure 4.6, Table 4.3). In contrast, the mIPSC rise time and peak amplitude were unaffected by finasteride treatment (in both cases, $p > 0.05$ *vs* control, Student's unpaired t-test, Table 4.3). By contrast, the mIPSC frequency was significantly increased following finasteride pre-treatment (control: 3.9 ± 0.5 Hz, n = 15, *vs* 50 μM finasteride: 10.2 ± 3.4 Hz, n = 8, $p < 0.05$, Student's unpaired t-test, Table 4.3).

The observed decrease in the rate of decay following treatment with the 5α-reductase inhibitor, finasteride, suggests that VB neurones may be subject to an endogenous neurosteroid tone at P7 that is sufficient to prolong the mIPSC decay time course. This proposal is supported by the finding that finasteride (1-50 μM) does not affect biophysical mIPSC properties by direct interaction with the receptor complex (Sanna *et al*., 2004, Peden & Belelli, unpublished observations).

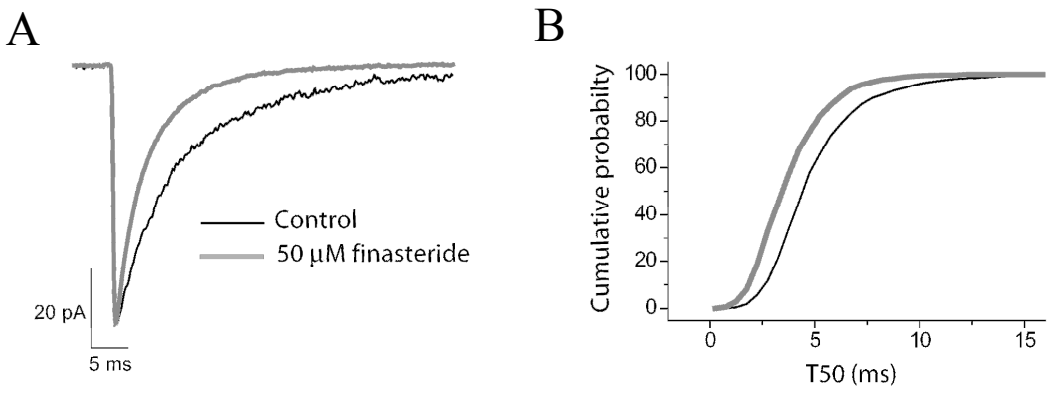

Figure 4.2. The effect of finasteride (50 µM) pre-incubation on the decay kinetics of mIPSCs recorded from P7 VB neurones. A. Overlayed, averaged mIPSCs normalised with respect to peak amplitude from representative control (black line) and 50 µM finasteride pre-treated (>4 hours, grey line) P7 VB neurones. Note that the finasteride treatment resulted in an average mIPSC with a faster decay time course. **B**. A cumulative probability plot of T50 for 2092 control events (pooled from 15 cells; black line) and 768 events from P7 VB neurones pre-treated with 50 µM finasteride (pooled from 8 cells; grey line). Note the leftward shift in the T50 distribution indicating that all finasteride pre-treated cells exhibited faster decay kinetics compared with control ($p < 0.001$, KS-test).

4.3. The effects of α- and γ-cyclodextrin pre-incubation on mIPSCs from P7 WT VB neurones

To further investigate this proposal I attempted to remove any endogenous neurosteroid from the brain-slice tissue by using the steroid-scavenger, γ-cyclodextrin (γ-CD; Shu *et al*., 2004; Shu *et al*., 2007). This compound comprises 8 oligosaccharides arranged in a cyclical fashion such that a lipophilic, and a 'steroid-preferring', inner-cavity is created (see Introduction Fig 1.6). Indeed, the ability of γ-cyclodextrin to sequester neurosteoids and thereby prevent their modulatory actions at $GABA_ARs$ has been shown in both recombinant expression systems and neuronal cultures (Shu *et al*., 2004; Shu *et al*., 2007), but γ-CD has not been used to determine whether neurosteroids are playing an endogenous role. In the present study, thalamic brain slices obtained from 7 day old WT mice were pre-incubated for a minimum of 1 hour and a maximum of 4 hours, with 1 mM γ-CD. Subsequently, voltage-clamp recordings were acquired with 1 mM γ-CD in the extracellular solution (ECS) and 0.5 mM γ-CD included in the intracellular solution (ICS). These conditions will henceforward be referred to as 'γ-CD pre-incubation'. Following γ-CD pre-incubation, the mIPSCs from P7 VB neurones were unchanged with respect to the rise time and the peak amplitude ($p > 0.05$ *vs* control, Student's unpaired t-test, Table 4.3), however, the decay kinetics were significantly faster than those of mIPSCs obtained from control recordings (τ_W control: 8.5 ± 0.4 ms, n = 15, *vs* τ_W γ-CD pre-treated: 5.8 ± 0.3 ms, n = 9, $p < 0.001$, Student's unpaired t-test, Figure 4.3 A, Table 4.3). Moreover, the mIPSC frequency was significantly increased following γ-CD pre-incubation (control: 3.9 ± 0.5 Hz, n = 15, *vs* γ-CD pre-incubation: 7.4 ± 1.6 Hz, n = 9, $p < 0.05$, Student's unpaired t-test, Table 4.3).

The magnitude of the effect on τ_W observed with γ-CD treatment was similar to that produced by finasteride pre-incubation (γ-CD pre-treatment: 5.8 ± 0.3 ms *vs* finasteride: 6.0 ± 0.3 ms, $p > 0.05$, Student's unpaired t-test). To address the specificity of γ-CD's neurosteroid-sequestering action I pre-incubated P7 WT thalamic slices with α-cyclodextrin (α-CD). This compound differs from γ-CD only by containing one less oligosaccharide in the ring structure, thus rendering the lipophilic inner cavity too small to house steroid molecules (Shu *et al*., 2007). In parallel to experiments with γ-CD, brain slices were pre-incubated for a minimum of 1 hour and a maximum of 4 hours, in the presence of 1 mM α-CD. Furthermore, during recordings 1 mM α-CD was present in the ECS and the ICS was supplemented with 0.5 mM α-CD. Under these conditions (referred to henceforward as 'α-CD pre-incubation'), VB neurones exhibited mIPSCs with decay kinetics that were indistinguishable from control mIPSCs (τ_W control: 8.5 ± 0.4 ms, $n = 15$, *vs* τ_W α-CD pre-incubated: 8.8 ± 0.7 ms, $n = 7$, $p > 0.05$, Student's unpaired t-test, Figure 4.3, C & D, Figure 4.6 C, Table 4.3). In addition, the peak amplitude and rise time were unaltered by α-CD pre-incubation (in both cases, $p > 0.05$ *vs* control, Table 4.3).

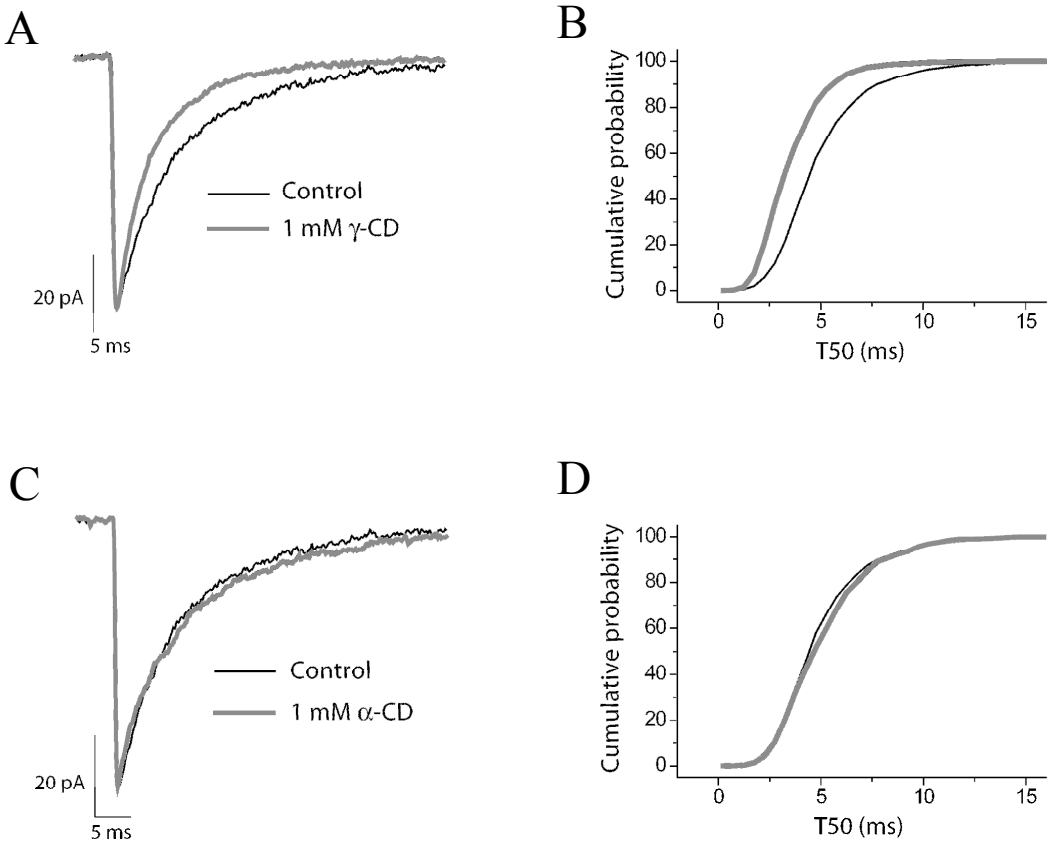

Figure 4.3. The effect of γ- and α-cyclodextrin pre-incubation (1 mM) on the decay kinetics of mIPSCs recorded from P7 VB neurones. A. Overlayed, averaged mIPSCs normalised with respect to peak amplitude from representative control (black line) and 1 mM γ-CD pre-treated (> 1 hour, grey line) P7 VB neurones. Note that the γ-CD treatment resulted in an average mIPSC with a faster decay time course. **B**. A cumulative probability plot of the T50 for 2092 control events (pooled from 15 cells; black line) and 1403 events from P7 VB neurones pre-treated with 1 mM γ-CD (pooled from 9 cells; grey line). Note the leftward shift in the T50 distribution indicating that all γ-CD pre-treated cells exhibited faster decay kinetics compared with control ($p < 0.001$, KS-test). **C**. Overlayed, averaged mIPSCs normalised with respect to peak amplitude from representative control (black line) and 1 mM α-CD pre-treated (> 1 hour, grey line) P7 VB neurones. Compared to γ-CD, pre-treatment with α-CD had no effect on the average mIPSC decay time course. **D**. A cumulative probability plot of T50 for 2092 control events (pooled from 15 cells; black line) and 992 events from P7 VB neurones pre-treated with 1 mM α-CD (pooled from 8 cells; grey line). Compared to γ-CD, note the absence of leftward shift in the T50 distribution indicating that α-CD pre-treatment had no effect on the mIPSC T50 ($p > 0.05$ *vs* control, KS-test).

4.4. The effects of γ-cyclodextrin pre-incubation on mIPSCs from WT VB neurones during development

In order to further investigate the observed reduction in decay time following either finasteride or γ-CD treatment, experiments were performed to assess whether VB neurones of later developmental stages were similarly sensitive to γ-CD. Following γ-CD pre-incubation, mIPSCs recorded from P8 VB neurones had significantly faster decay kinetics compared with control as indicated by a reduction in τ_W (control: 6.9 ± 0.3 ms, n = 9, *vs* γ-CD pre-incubation: 5.5 ± 0.3 ms, n = 9, $p < 0.01$, Student's unpaired t-test, Figure 4.4, table 4.2). By P10, γ-CD pre-incubation ceased to have any effect on the mIPSC decay time course ($p > 0.05$ *vs* control, Student's unpaired t-test, Figure 4.4, Table 4.2). Similarly, γ-CD pre-incubation had no effect on the decay time of mIPSCs recorded from P20-24 VB neurones ($p > 0.05$ *vs* control, Student's unpaired t-test, Figure 4.4, Table 4.2). In addition, neither the mIPSC rise time nor the peak amplitude was affected by γ-CD pre-incubation, regardless of age (in all cases $p > 0.05$ *vs* control, Student's unpaired t-test, Table 4.2). For the mIPSCs recorded from P8, P10 and P20-24 VB neurones no effect of γ-CD pre-incubation was observed on the mIPSC frequency (in each case $p > 0.05$ *vs* control, Student's unpaired t-test). However, an increase in mIPSC frequency following γ-CD pre-incubation was observed at P7 (control: 3.9 ± 0.5 Hz, n = 15, *vs* γ-CD pre-incubation: 7.4 ± 1.6 Hz, n = 9, $p < 0.05$, Student's unpaired t-test, Table 4.2). Collectively, these findings provide further evidence in favour of an endogenous neurosteroid presence early in development that dissipates with maturity in VB neurones.

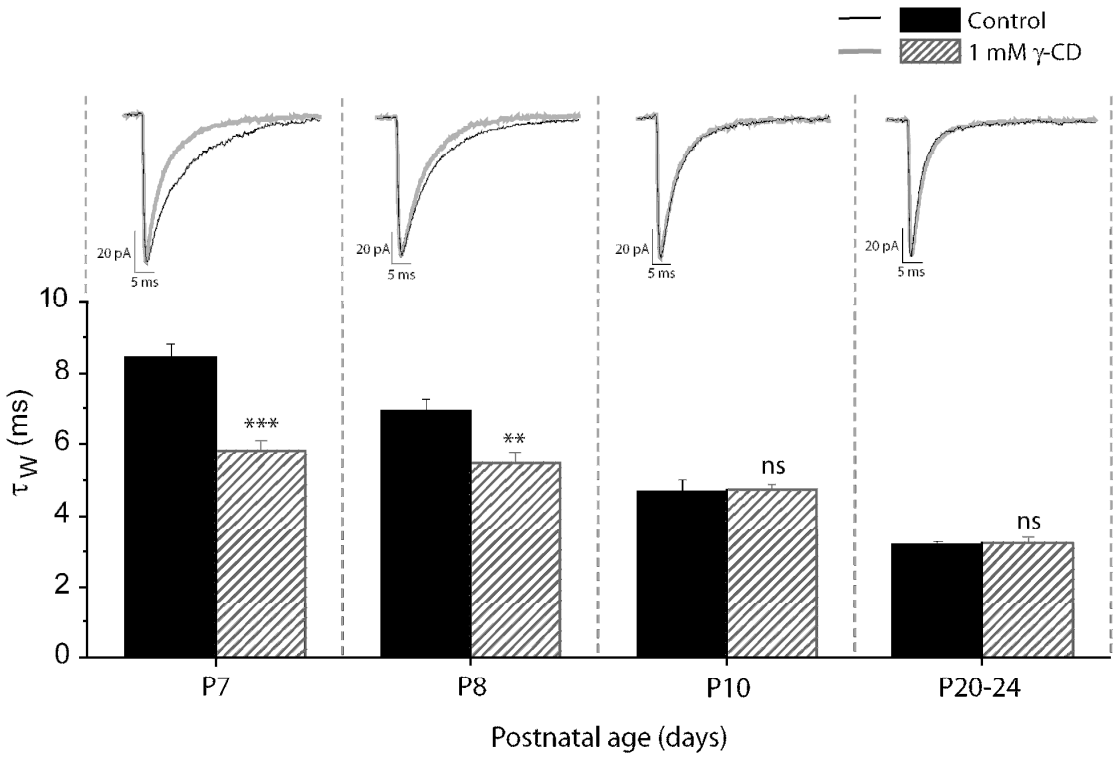

Figure 4.4. The effect of γ-CD pre-incubation (1 mM) on the τ_W of mIPSCs recorded from VB neurones during development. A bar graph depicting the effect of γ-CD pre-incubation (1mM) on the τ_W of mIPSCs recorded from WT VB neurones at P7, P8, P10 and P20-24. Illustrated above are the corresponding averaged and overlayed mIPSCs, normalised with respect to peak amplitude, taken from representative VB neurones in the absence (control, black line) and following 1 mM γ-CD pre-incubation (grey line). Note that at P7 and P8 γ-CD pre-incubation results in a significant reduction in τ_W, whereas at later developmental stages (P10 and P20-24) this effect is lost. *** $p < 0.001$, ** $p < 0.01$ *vs* control, Student's unpaired t-test.

	P7		P8		P10		P20-24	
	Control (n = 15 cells)	**1 mM γ-CD (n = 9 cells)**	**Control (n = 9 cells)**	**1 mM γ-CD (n = 9 cells)**	**Control (n = 7 cells)**	**1 mM γ-CD (n = 6 cells)**	**Control (n = 28 cells)**	**1 mM γ-CD (n = 9 cells)**
Peak amplitude (pA)	-82 ± 4	-90 ± 5	-92 ± 6	-92 ± 3	-93 ± 9	-86 ± 5	-66 ± 3	-71 ± 6
Rise time (ms)	0.6 ± 0.1	0.6 ± 0.1	0.6 ± 0.1	0.6 ± 0.1	0.6 ± 0.1	0.6 ± 0.1	0.5 ± 0.1	0.5 ± 0.1
τ_W (ms)	8.5 ± 0.4	5.8 ± 0.3***	6.9 ± 0.3	5.5 ± 0.3**	4.7 ± 0.3	4.7 ± 0.1	3.2 ± 0.1	3.2 ± 0.2
Frequency (Hz)	3.9 ± 0.5	7.4 ± 1.6*	7.9 ± 1.5	7.8 ± 1.4	15.3 ± 3.6	13.8 ± 2.2	10.9 ± 1.4	10.8 ± 2.5

Table 4.2. A summary of the impact of development and γ-CD pre-incubation (1 mM) on the properties of mIPSCs recorded from WT VB neurones. * $p < 0.05$, ** $p < 0.01$, *** $p < 0.001$, *vs* control, Student's unpaired t-test.

4.5. The effects of intracellular application of γ-CD on mIPSCs from P7 WT VB neurones.

Pre-treatment of P7/8 thalamic slices with finasteride (50 μM), or γ-CD (1 mM), resulted in VB neurones that displayed mIPSCs with markedly faster decay kinetics compared with those from control recordings. Next, I investigated the effects of γ-CD when applied solely to the intracellular environment *(i.e.* with no pre-incubation period and standard ECS) with a view to assessing the cellular localisation of the perceived neurosteroid tone. Accordingly for such experiments, the ICS was supplemented with 0.5 mM γ-CD (referred to henceforth as γ-CD ICS). Under these conditions P7 mIPSCs presented with faster decay kinetics, as indicated by a reduction in the τ_W (control: 8.5 ± 0.4 ms, n = 15, *vs* γ-CD ICS: 5.9 ± 0.3 ms, n = 8, $p < 0.001$, Student's unpaired t-test, Figure 4.5 A). Moreover, intracellular application of γ-CD resulted in P7 mIPSCs with decay kinetics that were indistinguishable from the decay kinetics of mIPSCs recorded from P7 VB neurones following finasteride, or γ-CD pre-incubation (in all cases $p > 0.05$, Student's unpaired t-test, Figure 4.6, Table 4.3). In contrast, supplementing the ICS with 0.5 mM α-CD, had no impact on the decay kinetics (as assessed by measurements of τ_W) or indeed the rise-time, peak amplitude or mIPSC frequency (in all cases $p > 0.05$ *vs* control, Student's unpaired t-test, Figure 4.5, Figure 4.6, Table 4.3). Importantly, previous studies have established that γ-CD does not interact directly with $GABA_A$Rs (Shu *et al*., 2004; 2007 but see Pytel *et al*., 2006). In agreement, the finding in the present study that γ-CD pre-incubation had no effect at later developmental time points (*i.e.* P10 and P20-24), provides further evidence that there is no direct interaction between γ-CD and $GABA_A$Rs. Moreover, this specificity is supported by the lack of effect at P7, of α-CD, a structurally similar molecule to γ-CD (albeit without steroid scavenging properties).

Hence, the observation that for P7 VB neurones, the intracellular application of the steroid scavenger γ-CD is sufficient to decrease the decay time of $GABA_AR$-mediated mIPSCs, supports the proposal of a neurosteroid tone during neonatal development. This idea is substantiated further by the similarity of action between the 5α-reductase inhibitor finasteride, and γ-CD. Therefore it appears that, for VB neurones at least, the progressive acceleration of mIPSC decay times with maturity is initially primarily due to a loss of GABA-modulatory neurosteroids before the second week of life. The continued decrease in the mIPSC decay time after P8 is most likely due to an α2 to α1 subunit switch (Peden *et al*., 2008).

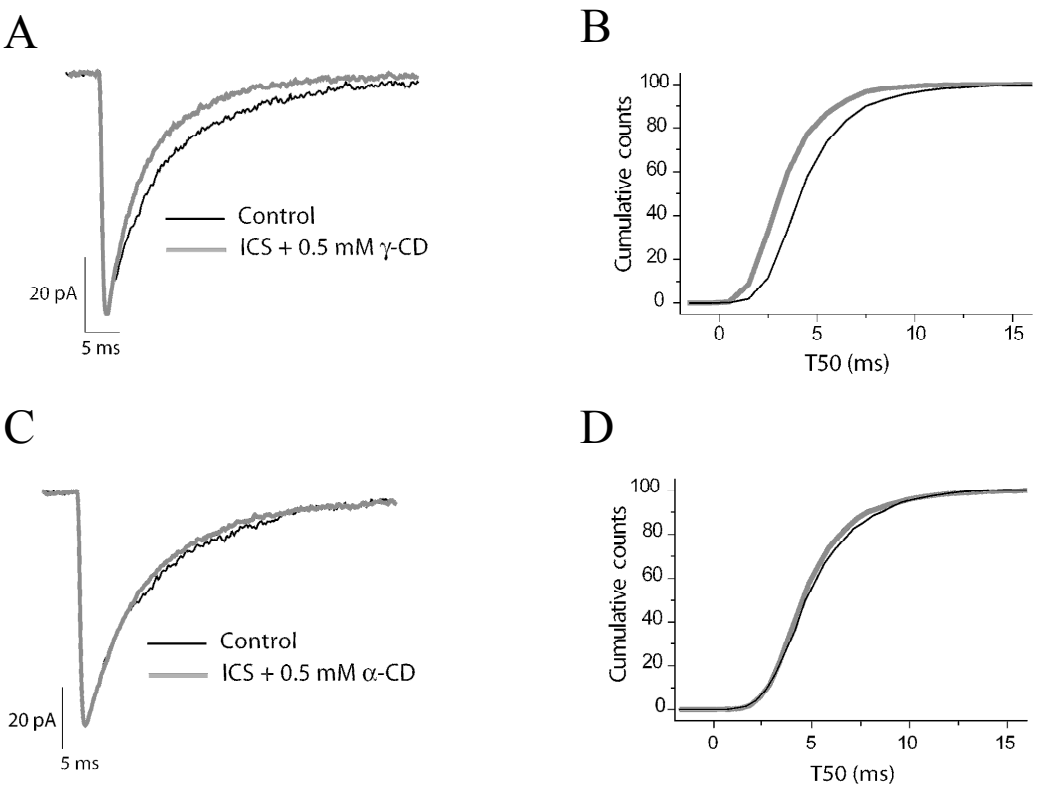

Figure 4.5. The effect of intracellular γ-CD or α-CD (0.5 mM) on the decay kinetics of mIPSCs recorded from P7 VB neurones. A. Overlayed, averaged mIPSCs normalised with respect to peak amplitude from a representative control WT VB neurone (black line) and a WT VB neurone in which the intracellular solution contained 0.5 mM γ-CD (grey line). Note that the intracellular γ-CD treatment resulted in an average mIPSC with a faster decay time course compared with control. **B**. A cumulative probability plot of the T50 for 2092 control events (pooled from 15 cells; black line) and 1358 events from P7 VB neurones in which the intracellular solution contained 0.5 mM γ-CD (pooled from 8 cells; grey line). Note the leftward shift in the T50 distribution indicating that all cells in which γ-CD was present only in the intracellular environment, exhibited faster decay kinetics compared with control ($p < 0.001$, KS-test). **C**. Overlayed, averaged mIPSCs normalised with respect to peak amplitude from a representative control WT VB neurone (black line) and a WT VB neurone in which the intracellular solution contained 0.5 mM α-CD (grey line). Note that, in contrast to intracellular γ-CD, intracellular α-CD did not affect the mIPSC decay time course. **D**. A cumulative probability plot of the T50 for 2092 control events (pooled from 15 cells; black line) and 875 events from P7 VB neurones in which the intracellular solution contained 0.5 mM α-CD (pooled from 8 cells; grey line). Compared to intracellular γ-CD, note the absence of leftward shift in the T50 distribution indicating that the intracellular α-CD treatment had no effect on the mIPSC T50 ($p > 0.05$ *vs* control, KS-test).

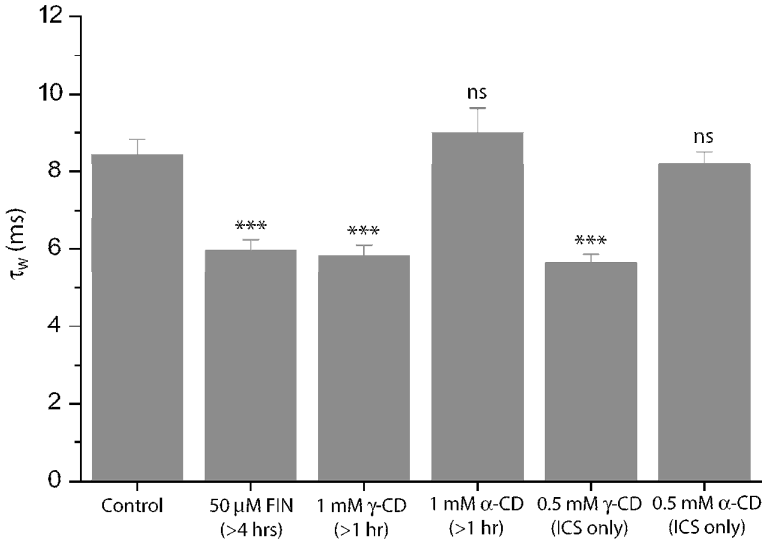

Figure 4.6. The effects of finasteride (50 µM), γ-CD and α-CD on the τ_W of mIPSCs recorded from WT P7 VB neurones. A bar graph depicting 1) the effects of 50 µM finasteride pre-incubation (FIN, >4 hrs), 2) 1mM γ/α-CD pre-incubation (>1 hr) and 3) the effects of only supplementing the ICS with 0.5 mM γ/α-CD. Note that finasteride and both γ-CD treatments led to a significant and similar reduction in τ_W whereas the α-CD treatments were inert in this respect. *** $p < 0.001$, Student's unpaired t-test.

	Control (n = 15 cells)	**50 μM Finasteride (n = 8 cells)**	**1 mM γ-CD (n = 9 cells)**	**1 mM α-CD (n = 7 cells)**	**0.5 mM γ-CD ICS only (n = 8 cells)**	**0.5 mM α-CD ICS only (n = 8 cells)**
Peak amplitude (pA)	-82 ± 4	-80 ± 7	-90 ± 5	-93 ± 3	-74 ± 8	-83 ± 5
Rise time (ms)	0.6 ± 0.1	0.6 ± 0.1	0.6 ± 0.1	0.6 ± 0.1	0.6 ± 0.1	0.6 ± 0.1
T50 (ms)	5.8 ± 0.3	4.5 ± 0.3*	3.9 ± 0.2***	5.5 ± 0.5	3.9 ± 0.2***	5.6 ± 0.2
τ_W (ms)	8.5 ± 0.4	6.0 ± 0.3***	5.8 ± 0.3***	8.8 ± 0.7	5.9 ± 0.3***	8.2 ± 0.3
Frequency (Hz)	3.9 ± 0.5	10.2 ± 3.4*	7.4 ± 1.6*	5.1 ± 1.2	3.8 ± 1.2	3.8 ± 1.2

Table 4.3. A summary of the effects of finasteride (50 μM), γ-CD (1 mM pre-incubated/0.5mM ICS only) and α-CD (1 mM pre-incubated/0.5 mM ICS only), upon the properties of the mIPSCs of VB neurones derived from 7 day old mice. * $p < 0.05$, *** $p < 0.001$, *vs* control, Student's unpaired t-test.

4.6. Defining the temporal profile of intracellular γ-CD action

Application of γ-CD (0.5 mM) to the intracellular compartment of P7 VB neurones resulted in markedly faster decay kinetics compared with standard ICS, or ICS supplemented with α-CD (Figure 4.5, 4.6, Table 4.3). To further investigate the temporal aspects of this effect, experiments were performed wherein recordings were obtained shortly after the whole-cell configuration was acquired. The effects of 0.5 mM γ-CD ICS were then compared to standard ICS and 0.5 mM α-CD ICS. Due to the relatively high frequency of mIPSCs in P6/7 VB neurones, it was possible to obtain sufficient events to allow mIPSC analysis over relatively short time periods (≤ 2 mins). For P6/7 VB neurones, following the intracellular 'break-in' and the subsequent delivery of γ-CD to the intracellular compartment, a time-dependent decrease in τ_W occured (Figure 4.7, Table 4.4). Specifically, compared to standard ICS or α-CD (0.5 mM) ICS, no significant difference in the τ_W was observed after 0-2 mins with γ-CD (0.5 mM) ICS ($p > 0.05$, one-way ANOVA, Figure 4.7, Table 4.4). However, at 3-5 mins, 6-8 mins, and 10-16 mins post "break-in", intracellular application of γ-CD resulted in mIPSCs that were significantly faster than corresponding experiments performed with standard ICS or indeed ICS supplemented with α-CD (in all cases $p < 0.05$, one-way ANOVA, Figure 4.7, Table 4.4). In addition, no significant differences were observed between τ_W values obtained using standard ICS and ICS supplemented with α-CD (0.5 mM) at any time point after "break-in" examined (in each case $p > 0.05$, one-way ANOVA, Figure 4.7, Table 4.4). To summarise, the majority of the decrease in the mIPSC τ_W occurred 3-5 minutes after the whole-cell configuration was attained and a plateau for this effect is evident by 6-8 minutes. These data corroborate the proposal that a native neurosteroid tone exerts a modulatory action on synaptic $GABA_ARs$ in P6/7 VB neurones. The relatively fast-acting actions of intracellular γ-CD (*i.e.* the effect

is complete 3-5 mins after “break-in”) infers that this steroid-scavenger molecule is able to access and sequester endogenous neurosteroids (and thereby prevent neurosteroid-$GABA_AR$ interaction) on a timescale that is consistent with estimates of the rate of equilibrium between the pipette and the cell interior (Marty & Neher, 1995).

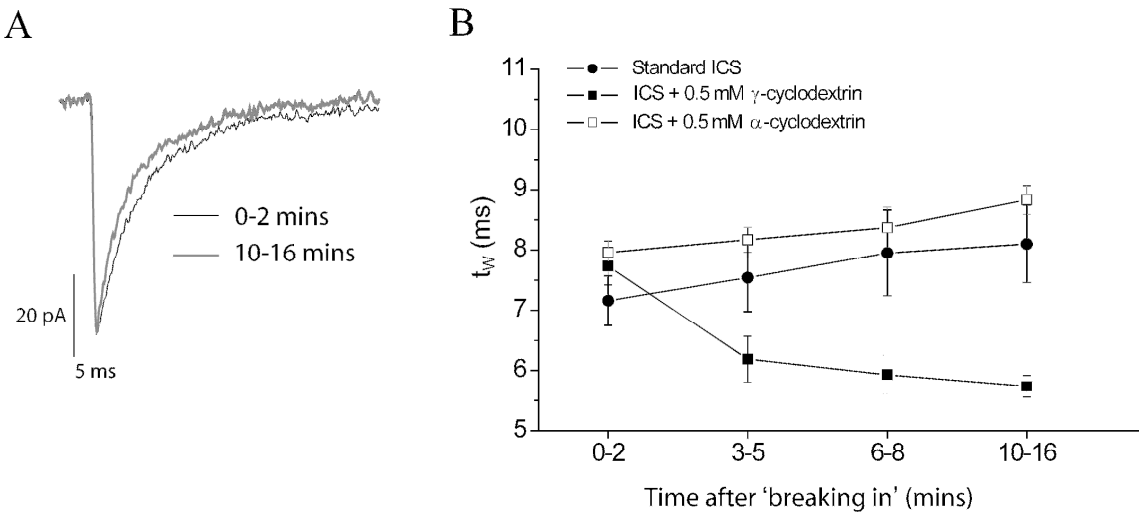

Figure 4.7. The time-dependent effects of intracellular γ-cyclodextrin (0.5 mM) on the τ_W of WT P6/7 VB neurones. A. An overlayed mIPSC normalised with respect to peak amplitude illustrating the time-dependent effects of intracellular γ-CD (0.5 mM) application. Specifically, mIPSCs recorded 10-16 mins after 'break-in' presented with faster decay kinetics compared to those obtained 0-2 mins after the whole cell configuration was attained. **B.** A line graph illustrating the effects of standard ICS, ICS + 0.5 mM γ-CD and ICS + 0.5 mM α-CD, following the acquisition of the whole-cell configuration. Note that when the ICS is supplemented with 0.5 mM γ-CD, there is a time-dependent decrease in τ_W. This effect is absent when recordings were performed with standard ECS or ECS + 0.5 mM α-CD.

	0-2 mins			3-5 mins			6-8 mins			10-16 mins		
	Standard ICS (n=8 cells)	**ICS+0.5 mM α-CD (n=6 cells)**	**ICS + 0.5 mM γ-CD (n=8 cells)**	**Standard ICS (n=5 cells)**	**ICS+0.5 mM α-CD (n=4 cells)**	**ICS + 0.5 mM γ-CD (n=8 cells)**	**Standard ICS (n=4 cells)**	**ICS+0.5 mM α-CD (n=5 cells)**	**ICS + 0.5 mM γ-CD (n=8 cells)**	**Standard ICS (n=7 cells)**	**ICS+0.5 mM α-CD (n=7 cells)**	**ICS + 0.5 mM γ-CD (n=8 cells)**
τ_W (ms)	7.2 ± 0.4	8.0 ± 0.2	7.7 ± 0.3	7.5 ± 0.6	8.2 ± 0.2	6.2 ± 0.4*	8.0 ± 0.7	8.4 ± 0.3	5.9 ± 0.3**	8.1 ± 0.6	8.8 ± 0.2	5.7 ± 0.2**

Table 4.4. A summary of the effects of time after 'breaking-in' on the mIPSC τ_W when the intracellular solution was standard, supplemented with α-CD (0.5 mM), or supplemented with γ-CD (0.5 mM). * $p < 0.05$, ** $p < 0.01$, *vs* standard ICS, one-way ANOVA.

4.7. The effect of exogenous 5α3α application upon the mIPSCs recorded from P7 WT VB neurones

By P10, pre-incubation with γ-CD ceases to affect the decay kinetics of mIPSCs recorded from VB neurones (Figure 4.4, Table 4.2). This insensitivity could be caused by a decline in the level of endogenous neurosteroid to below that which is required to influence synaptic $GABA_ARs$ (assuming that γ-CD treatment results in a complete removal of the neurosteroid), or alternatively may result from a change in the neurosteroid sensitivity of the synaptic $GABA_ARs$ (Brussaard *et al*., 1997). To assess whether P7 VB neurones retain sensitivity to exogenous neurosteroid application, recordings were obtained following bath application of 1 μM 5α3α. In the presence of 1 μM 5α3α, mIPSCs recorded from P7 VB neurones presented with prolonged decay times compared with control (τ_W control, 8.5 ± 0.9 ms, n = 15, *vs* τ_W 1 μM 5α3α: 12.0 ± 0.3 ms, n = 3, $p < 0.05$, Student's paired t-test, Figure 4.8). As described in Chapter 3 (section 3.3.3), application of 1 μM 5α3α prolonged P17-24 VB mIPSCs from 3.7 ± 0.2 ms to 5.1 ± 0.1 ms (n = 5, $p < 0.05$, Student's paired t-test). This constituted a 48 ± 22 % increase in the τ_W at P17-24 compared with 39 ± 16 % increase at P7 ($p > 0.05$, one way repeated measures ANOVA). Hence, despite the modulatory influence of the putative endogenous steroid tone, mIPSCs recorded from P7 VB neurones retain sensitivity to exogenous 5α3α.

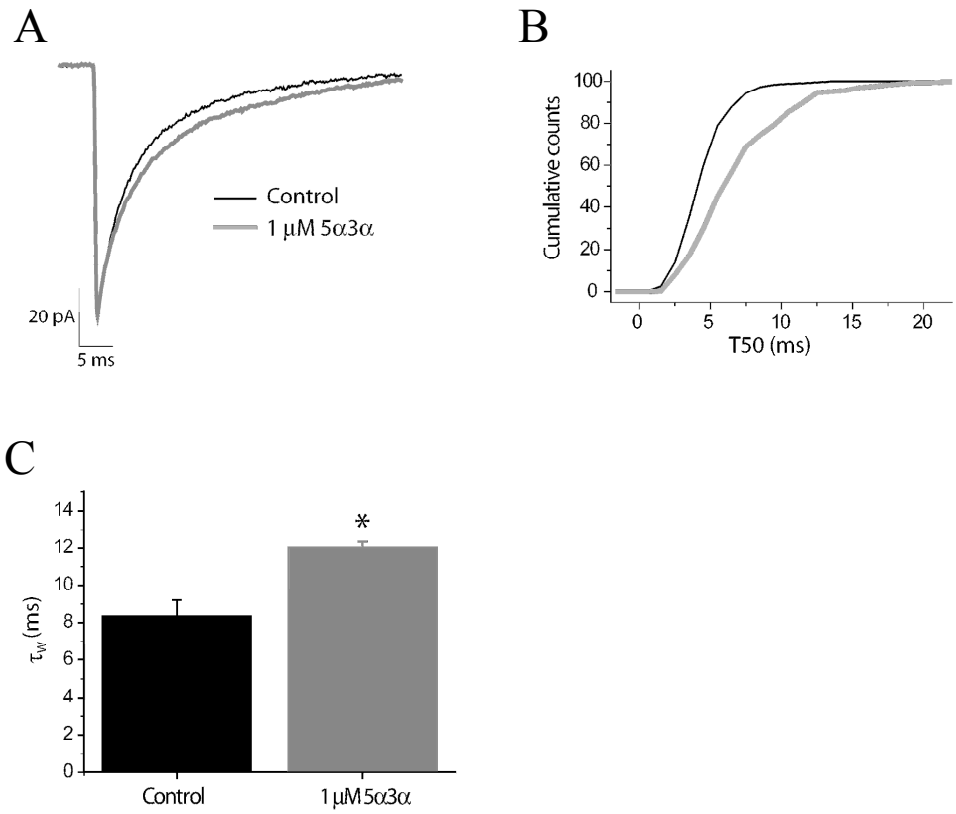

Figure 4.8. The effect of 5α3α (1 μM, bath applied) on the decay kinetics of mIPSCs recorded from WT P7 VB neurones. A. Overlayed, averaged mIPSC normalised with respect to peak amplitude from a representative WT P7 VB neurone before (control, black line) and after 1 μM 5α3α application (grey line). Note that, in the presence of 1 μM 5α3α, the mIPSC decay time course is prolonged compared with control. **B**. A cumulative probability plot of T50 for 703 control events (black line) and 372 events following 1 μM 5α3α application (grey line). Note the rightward shift in the T50 cumulative probability plot indicating that, in the presence of 1 μM 5α3α, all mIPSCs, exhibited slower decay kinetics compared with control ($p < 0.001$, KS-test). **C**. A bar graph illustrating the effect of 1 μM 5α3α application on the decay time, τ_W, of WT P7 VB mIPSCs. Note that, relative to control, the decay time constant, τ_W, is increased following 5α3α application. * $p < 0.05$ vs control, Student's paired t-test.

4.8. The effects of 5α-dihydroprogesterone pre-incubation on mIPSCs recorded from P20-24 WT VB neurones

Pre-incubation with γ-CD significantly decreased the τ_W of mIPSCs recorded from P7 and P8 VB neurones but had no effect on those recorded from VB neurones derived from P10 or P20-24 mice (Figure 4.4, Table 4.2). Taken together with the observation that P17-24 mIPSCs retain sensitivity to 100 nM 5α3α (see Section 3.3.3), it would appear that a neurosteroid tone is no longer resident at later developmental stages. One possibility is that post P8 the enzymes required to synthesize endogenous neurosteroids are no longer expressed or active. Therefore, I investigated whether the thalamic slice preparation (P20-24) could convert the $GABA_AR$-inert neurosteroid 5α-dihydroprogesterone (5α-DHP - the immediate precursor of 5α3α) to the $GABA_AR$-active metabolite 5α3α (see Introduction, Figure 1.6). This process is governed by 3α-hydroxysteroid dehydrogenase (3α-HSD), which together with 5α-reductase has been found to be present in certain glutamatergic cell populations of the adult mouse thalamus (Agis-Balboa *et al*., 2006). In initial experiments with P20-24 VB neurons, mIPSCs were recorded before, and after, the acute application of 3 μM 5α-DHP to assess whether this neurosteroid (which displays structural similarity to 5α3α) has a direct modulatory action at synaptic $GABA_ARs$. These experiments confirmed that 5α-DHP is inert in this respect (see Table 4.5). Subsequently, thalamic brain slices were pre-incubated with 3 μM 5α-DHP for either a relatively short (30-60 mins) or long (> 120 mins) incubation period. Whole-cell voltage-clamp recordings were then performed with 3 μM 5α-DHP present in the ECS and standard ICS. Following the short incubation period (30-60 mins), 5α-DHP had no effect on any of the mIPSC parameters measured (in all cases $p > 0.05$ *vs* control, Student's unpaired t-test, Figure 4.9, Table 4.5). By contrast, when pre-incubated for greater than 120 mins with 3 μM DHP, the

mIPSC decay time course was substantially prolonged as inferred by an increase in the decay time constant, τ_W (control: 3.3 ± 0.1 ms, n = 54, *vs* 3 μM 5α-DHP long pre-incubation: 7.9 ± 0.5 ms, n = 10, $p < 0.001$, Student's unpaired t-test, Figure 4.9, Table 4.6). To verify that the prolonged τ_W following the long, >120 mins, incubation with 5α-DHP, was due to the conversion of 5α-DHP to the GABA-active neurosteroid, 5α3α, thalamic slices were first incubated with 30 μM indomethacin (a 3α-HSD inhibitor) for 30 mins before 3 μM 5α-DHP was added subsequently for a minimum of 120 mins. Under these conditions, a blunted effect on the mIPSC decay time was observed compared to 5α-DHP alone (τ_W: 4.2 ± 0.3 ms, n = 8, $p < 0.001$ *vs* 3 μM 5α-DHP long incubation, Student's unpaired t-test, Figure 4.9 C, Table 4.6). However, it should be noted that the increase in τ_W that occurred in the presence of indomethacin was significant compared to control ($p < 0.001$, Student's unpaired t-test, Table 4.6), suggesting that the indomethacin treatment had not completely inhibited the activity of the 3α-HSD. Collectively, these observations illustrate that the enzyme 3α-HSD is functionally active in the thalamic brain slice preparation at P20-24 and that the developmental loss of neurosteroid tone at synaptic $GABA_ARs$ is likely due to a paucity in the supply of the 5α3α precursor, 5α-DHP.

	control (n = 7)	**3 µM 5α-DHP (n = 7 cells)**
Peak amplitude (pA)	-74 ± 7	-74 ± 5
Rise time (ms)	0.6 ± 0.1	0.6 ± 0.1
τ_W (ms)	3.7 ± 0.3	3.8 ± 0.4

Table 4.5. The acute application of 3 µM 5α-DHP has no effect on the peak amplitude, rise time or τ_W of mIPSCs recorded from P20-24 VB neurones. In all cases $p > 0.05$ *vs* control, Student's paired t-test.

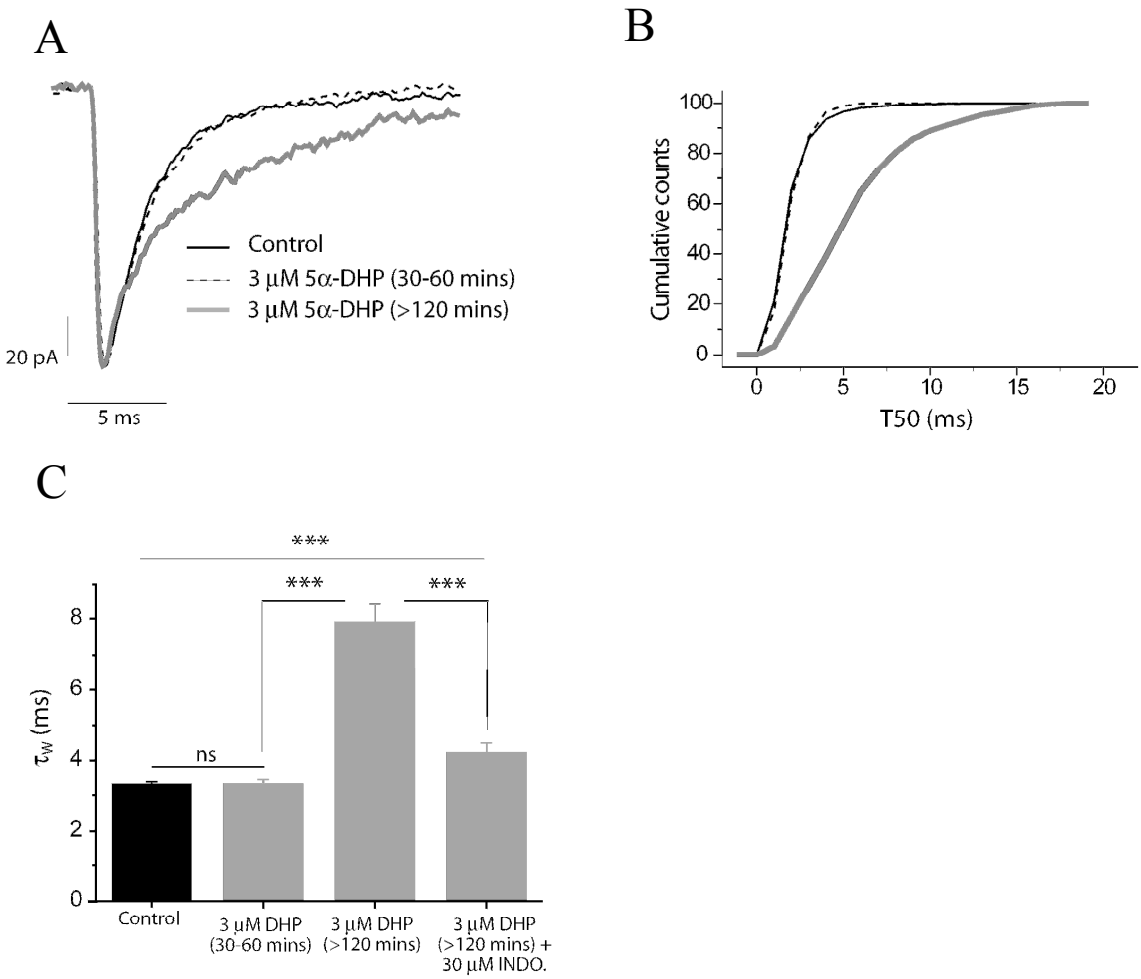

Figure 4.9. The effect of 5α-DHP pre-incubation (3 μM) on the decay kinetics of mIPSCs recorded from WT P20 VB neurones. **A.** Overlayed, averaged mIPSCs normalised with respect to peak amplitude from 3 representative WT P20 VB neurones in the absence of 5α-DHP (control, black line), following 30-60 mins exposure to 3 μM 5α-DHP (black-dashed line), and following greater than 120 mins exposure to 3 μM 5α-DHP (grey line). Note that, after 30-60 mins in the presence of 3 μM 5α-DHP, the mIPSC decay time course is indistinguishable from the control mIPSC. However, when the slice is pre-incubated for > 120 mins, the mIPSC decay time is substantially prolonged. **B**. A cumulative probability plot of T50 for 3636 control events (pooled from 54 cells, black line), 522 events following 30-60 mins pre-incubation with 3 μM 5α-DHP (pooled from 7 cells, black-dashed line), and 534 events following > 120 mins pre-incubation with 3 μM 5α-DHP (pooled from 10 cells, grey line). Note the similarity in the T50 cumulative probability plot for mIPSCs obtained under control conditions and those obtained from slices pre-incubated for 30-60 mins with 3 μM 5α-DHP. However, pre-incubating the slice for > 120 mins with 3 μM 5α-DHP resulted in a rightward shift in the cumulative probability plot indicating that all mIPSCs displayed an increased T50 compared with control and 30-60 mins 3 μM 5α-DHP pre-incubation (in both cases, $p < 0.001$, KS-test). **C**. A bar graph illustrating the effect on the mean τ_W, of both short and long 5α-DHP pre-incubation periods. The effect of pre-incubation with 5α-DHP for > 120 mins with 30 μM indomethacin (INDO) is also shown. Note the significant increase in τ_W following > 120 mins, but not 30-60 mins, 5α-DHP pre-incubation. Additionally, the effect on τ_W of pre-incubating for > 120 mins with 5α-DHP is significantly attenuated when 30 μM indomethacin is present. *** $p < 0.001$ *vs* control, Student's unpaired t-test.

	control (n = 54 cells)	**3 µM 5α-DHP 30-60 mins** (n = 7 cells)	**3 µM 5α-DHP >2 hrs** (n = 10 cells)	**3 µM 5α-DHP + 30 µM INDO. >2 hrs** (n = 8 cells)
Peak amplitude (pA)	-68 ± 2	-68 ± 6	-73 ± 7	-63 ± 3
Rise time (ms)	0.5 ± 0.1	0.6 ± 0.1	0.6 ± 0.1	0.6 ± 0.1
τ_W (ms)	3.3 ± 0.1	3.3 ± 0.1	7.9 ± 0.5***	4.2 ± 0.3***

Table 4.6. A > 2 hr, but not a 30-60 min, incubation with 3 µM 5α-DHP significantly prolonged the τ_W of mIPSCs recorded from P20-24 VB neurones. In addition, a > 2 hr 5α-DHP incubation resulted in a significantly longer mIPSC rise time. Note that pre-incubating with 3 µM DHP for >2 hrs in the presence of 30 µM indomethacin (INDO) resulted in a much reduced effect on the mIPSC decay time albeit the reduced effect was still significant *vs* control. Additionally note that for this condition the rise time was significantly increased, compared to control. *** $p < 0.001$ *vs* control, Student's unpaired t-test.

Chapter 5

Endogenous neurosteroid interactions with $GABA_A$ receptor-mediated inhibition in cortical layer 2/3 neurones during postnatal development.

5.1. The effect of postnatal age on the properties of mIPSCs recorded from WT L2/3 pyramidal neurones

During development, the decay time of mIPSCs recorded from VB neurones becomes progressively faster. In order to explain the increased rate of mIPSC decay as a function of development in VB neurones, past studies have focused on the subunit composition of the receptor complex (Peden *et al*., 2008). In the present study, however, evidence from experiments using a steroid-scavenger molecule, γ-CD, infers that until the end of the first week of life the acceleration in decay kinetics is dominated by the potentiating effects of an endogenous neurosteroid tone influencing synaptic $GABA_AR$s. One important question regarding this finding concerns the regional specificity of this effect. To explore the extent of the neurosteroid tone and its impact on $GABA_AR$-mediated inhibition during development, I investigated the properties of synaptic $GABA_AR$s of layer 2/3 (L2/3) pyramidal neurones of the frontal cortex. These neurones receive input from layer IV pyramidal neurones which in turn are innervated directly by thalamocortical relay neurones (Sherman & Guillery, 2002; Bannister, 2005). In addition L2/3 pyramidal neurones have been identified as expressing enzymes required for the conversion of progesterone to 5α3α (Agis-Balboa *et al*., 2006).

Analysis of mIPSCs recorded from WT L2/3 pyramidal neurones derived from neonatal/juvenile (P7, P8, P9, P10, P15) to adolescent (P20-24) mice revealed developmental differences in their biophysical properties. To summarise, the mIPSC frequency increased with age, with the largest increase in frequency occurring between P10 (2.2 ± 0.3 Hz) and P15 (12.9 ± 2.0 Hz, Figure 5.1 C, Table 5.1). Indeed, at earlier time-points (P7-10) the mIPSC frequency remained low. At P7 the frequency was extremely low (0.5 Hz ± 0.1, Figure 5.1, Table 5.1), although this value can be considered an overestimate since a proportion of P7 L2/3 pyramidal neurones exhibited

so few mIPSCs that they were discarded before analysis. The mIPSC rise time was also found to decrease with age (P7 *vs* P20-24, $p < 0.001$, Student's unpaired t-test, Table 5.1), an observation that has been made previously with respect to mIPSCs from hippocampal CA1 neurones (Cohen *et al*., 2000). However, since the temporal resolution is limited to 0.1 ms because of the 10 kHz acquisition rate, the decrease in rise time with development described here needs to be viewed cautiously. The mIPSC peak amplitude remained similar between P7 and P20-24 apart from at P9 and P15 when mIPSCs presented with significantly larger peak amplitudes ($p < 0.001$ and $p < 0.01$, respectively, *vs* P20-24, Student's unpaired t-test, Table 5.1). The decay time of mIPSCs, as inferred by measurement of the weighted decay time constant, τ_W, generally decreased with development. One exception to this occurred at P10 when a secondary increase in decay time was observed relative to P9. Specifically, P7 L2/3 pyramidal neurones exhibited mIPSCs with long decay kinetics (τ_W: 12.9 ± 0.6 ms) although by P9, these had become significantly faster (τ_W: 8.9 ± 0.2 ms, $p < 0.001$ *vs* P7, Student's unpaired t-test, Figure 5.1 C, Table 5.1). However, at P10, a secondary increase in mIPSC decay kinetics was observed (τ_W: 10.5 ± 0.5 ms, $p < 0.01$ *vs* P9, Student's unpaired t-test, Figure 5.1 C, Table 5.1). As development progressed beyond P10 the mIPSC decay time decreased substantially to 6.5 ± 0.3 ms at P15 and further to 5.4 ± 0.2 ms by P20-24 (Figure 5.1 C, Table 5.1). With the profile of mIPSC decay kinetics between P7 and P20-24 now established, investigations were focused on whether mIPSCs from L2/3 pyramidal neurones are influenced by an endogenous neurosteroid tone.

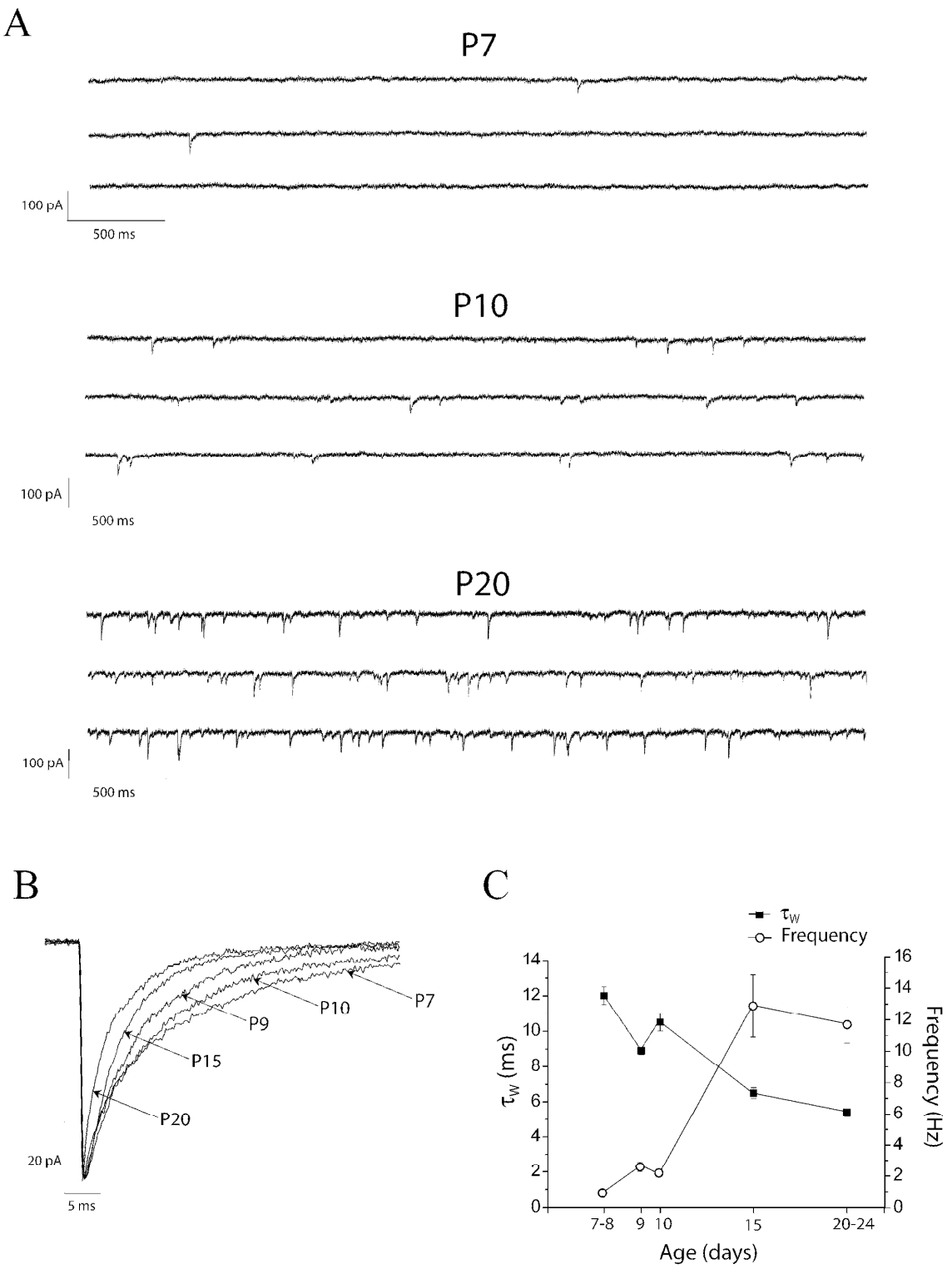

Figure 5.1. The properties of mIPSCs recorded from WT L2/3 pyramidal neurones during postnatal development. A. Traces showing typical current recordings from L2/3 pyramidal neurones derived from WT mice at P7 (top), P10 (middle) and P20 (bottom). Note the increase in the frequency of events with development **B**. Averaged, overlayed mIPSCs normalised with respect to peak amplitude, recorded from four representative WT L2/3 pyramidal neurones from brain slices derived from P7, P9, P10, P15 and P20 mice. Note the progressive decrease in decay time with development apart from at P10 when mIPSCs present with a relatively prolonged decay *vs* P9. **C**. A superimposed line graph showing the net decrease in τ_W, and the concomitant increase in mIPSC frequency, during development.

	P7 (n = 23 cells)	P8 (n = 19 cells)	P9 (n = 18 cells)	P10 (n = 20 cells)	P15 (n = 14 cells)	P20-24 (n = 25 cells)
Peak amplitude (pA)	-44 ± 2	-46 ± 7	-57 ± 3***	-46 ± 2	-54 ± 3**	-42 ± 2
Rise time (ms)	0.6 ± 0.1***	0.6 ± 0.1***	0.6 ± 0.1***	0.6 ± 0.1***	0.5 ± 0.1**	0.5 ± 0.1
τ_W (ms)	12.9 ± 0.6***	11.0 ± 0.6***	8.9 ± 0.2***	10.5 ± 0.5***	6.5 ± 0.3**	5.4 ± 0.2
Frequency (Hz)	0.5 ± 0.1***	1.4 ± 0.3***	2.6 ± 0.3***	2.2 ± 0.3***	12.9 ± 2.0	11.7 ± 1.2

Table 5.1. The properties of mIPSCs recorded from WT cortical L2/3 pyramidal neurones at different stages of development. **p < 0.01, *** p < 0.001, Student's unpaired t-test.

5.2. The effects of finasteride pre-treatment on mIPSCs recorded from P7 WT L2/3 pyramidal neurones

Pre-incubation of P7/8 WT cortical brain slices with 50 μM finasteride for longer than 4 hours resulted in L2/3 pyramidal neurones exhibiting mIPSCs with significantly faster decay times (τ_W control: 12.0 ± 0.4 ms, n = 42, *vs* τ_W 50 μM finasteride: 8.5 ± 0.3 ms, n = 7, $p < 0.01$, Student's unpaired t-test, Figure 5.2). Additionally, a significant increase in the mIPSC frequency was observed following finasteride treatment (control: 0.9 ± 0.2 Hz, n = 42, *vs* 50 μM finasteride: 1.8 ± 0.4 Hz, n = 7, $p < 0.05$, Student's unpaired t-test). The decrease in decay time following 50 μM finasteride treatment suggests that, in common with VB neurones, mIPSCs from P7 L2/3 cortical neurones are prolonged by a resident neurosteroid tone. To investigate this possibility further, experiments were performed using the steroid scavenger, γ-CD.

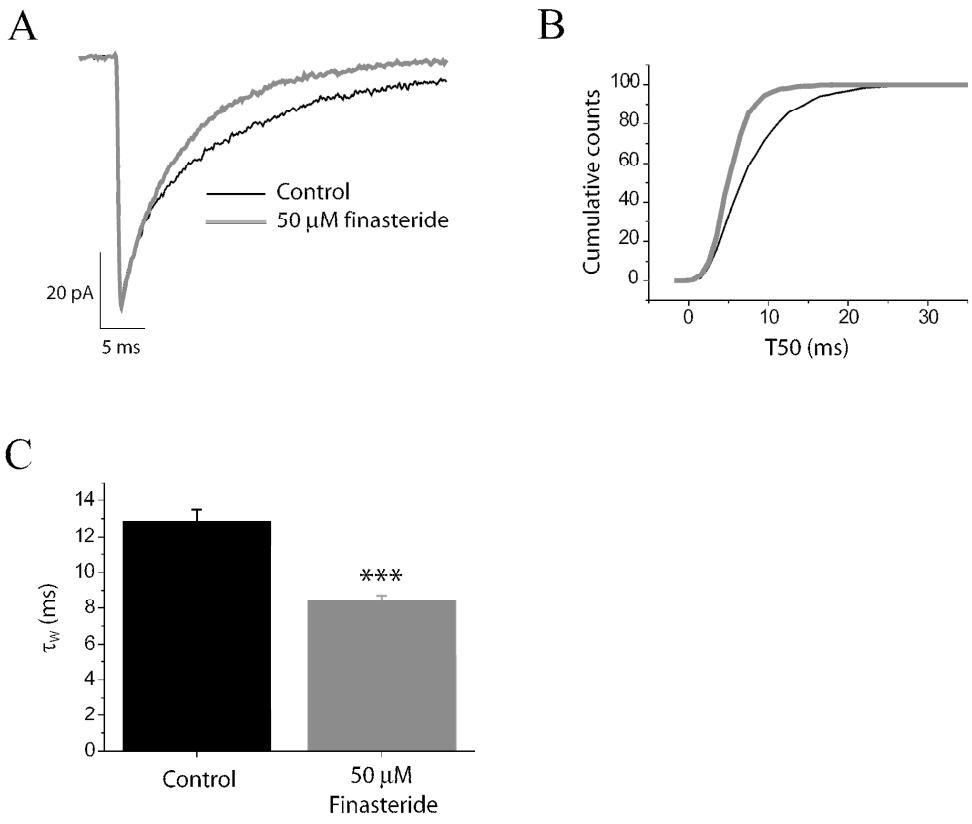

Figure 5.2. The effect of finasteride (50 µM) pre-incubation on the decay kinetics of mIPSCs recorded from P7 WT L2/3 pyramidal neurones. **A.** Overlayed, averaged mIPSC normalised with respect to peak amplitude from representative control (black line) and 50 µM finasteride pre-treated (> 4 hours, grey line) P7 pyramidal neurones. Note that the finasteride treatment resulted in an average mIPSC with a faster decay time course. **B**. A cumulative probability plot of T50 for 1125 control events (pooled from 23 cells; black line) and 601events from P7 VB neurones pre-incubated with 50 µM finasteride (pooled from 7 cells; grey line). Note the leftward shift in the T50 distribution indicating that all finasteride pre-treated cells exhibit faster decay kinetics compared with control ($p < 0.001$, KS-test). **C**. A bar graph depicting the average τ_W values for control (n = 23 cells) and following pre-incubation with 50µM finasteride (n = 7 cells). Note that treatment with finasteride caused a significant decrease in the τ_W. *** $p < 0.001$ *vs* control, Student's unpaired t-test.

5.3. The effects of α- and γ-cyclodextrin pre-incubation on mIPSCs recorded from P7/8 WT L2/3 pyramidal neurones

Cortical brain slices obtained from 7 and 8 day old WT mice were pre-incubated for a minimum of 1 hour (and a maximum of 5 hours) with 1 mM γ-CD. Subsequently, voltage-clamp recordings were acquired with 1 mM γ-CD in the extracellular solution (ECS) and 0.5 mM γ-CD in the intracellular solution (ICS). These conditions will henceforward be referred to as 'γ-CD pre-incubation'. Following γ-CD pre-incubation, mIPSCs exhibited significantly faster decay kinetics compared with those obtained from control recordings (τ_W control: 12.0 ± 0.4 ms, n = 42, *vs* τ_W γ-CD pre-treated: 8.5 ± 0.3 ms, n = 20, $p < 0.001$, Student's unpaired t-test, Figure 5.3, Table 5.1). This effect was indistinguishable from that observed following 50 μM finasteride treatment (τ_W γ-CD pre-treated: 8.5 ± 0.3 ms, n = 20, *vs* τ_W 50 μM finasteride: 8.5 ± 0.3 ms, n = 7, $p > 0.05$, Student's unpaired t-test, Figure 5.6). In contrast, the mIPSCs from P7/8 L2/3 neurones were unchanged with respect to the peak amplitude and frequency following γ-CD pre-incubation (in both cases $p > 0.05$ *vs* control, Student's unpaired t-test, Table 5.1).

In parallel to the experiments with γ-CD, cortical brain slices were pre-incubated for a minimum of 1 hour (and a maximum of 5 hours) in the presence of 1 mM α-CD. Furthermore, 1 mM α-CD was present in the ECS and the ICS was supplemented with 0.5 mM α-CD. Under these conditions (referred to henceforward as 'α-CD pre-incubation'), L2/3 pyramidal neurones exhibited mIPSCs with decay kinetics that were indistinguishable from control mIPSCs (τ_W control: 12.0 ± 0.4 ms, n = 42, *vs* τ_W α-CD pre-incubated: 11.5 ± 1.3 ms, n = 8, $p > 0.05$, Student's unpaired t-test, Figure 5.3, Table 5.1). Furthermore, the peak amplitude and rise time were also unaltered by α-CD pre-incubation (in both cases, $p > 0.05$ *vs* control).

Hence, mIPSCs from L2/3 pyramidal neurones display faster decay kinetics following γ-CD, but not α-CD, pre-incubation. When considered together with the effects of finasteride described in section 5.2, these observations support the notion of an endogenous neurosteroid tone at P7 that is sufficient to prolong $GABA_AR$ mediated mIPSCs in L2/3 pyramidal neurones. Moreover, there is a clear similarity between the actions of finasteride, γ-CD and α-CD on mIPSCs from cortical L2/3 and thalamic VB neurones (see Chapter 4).

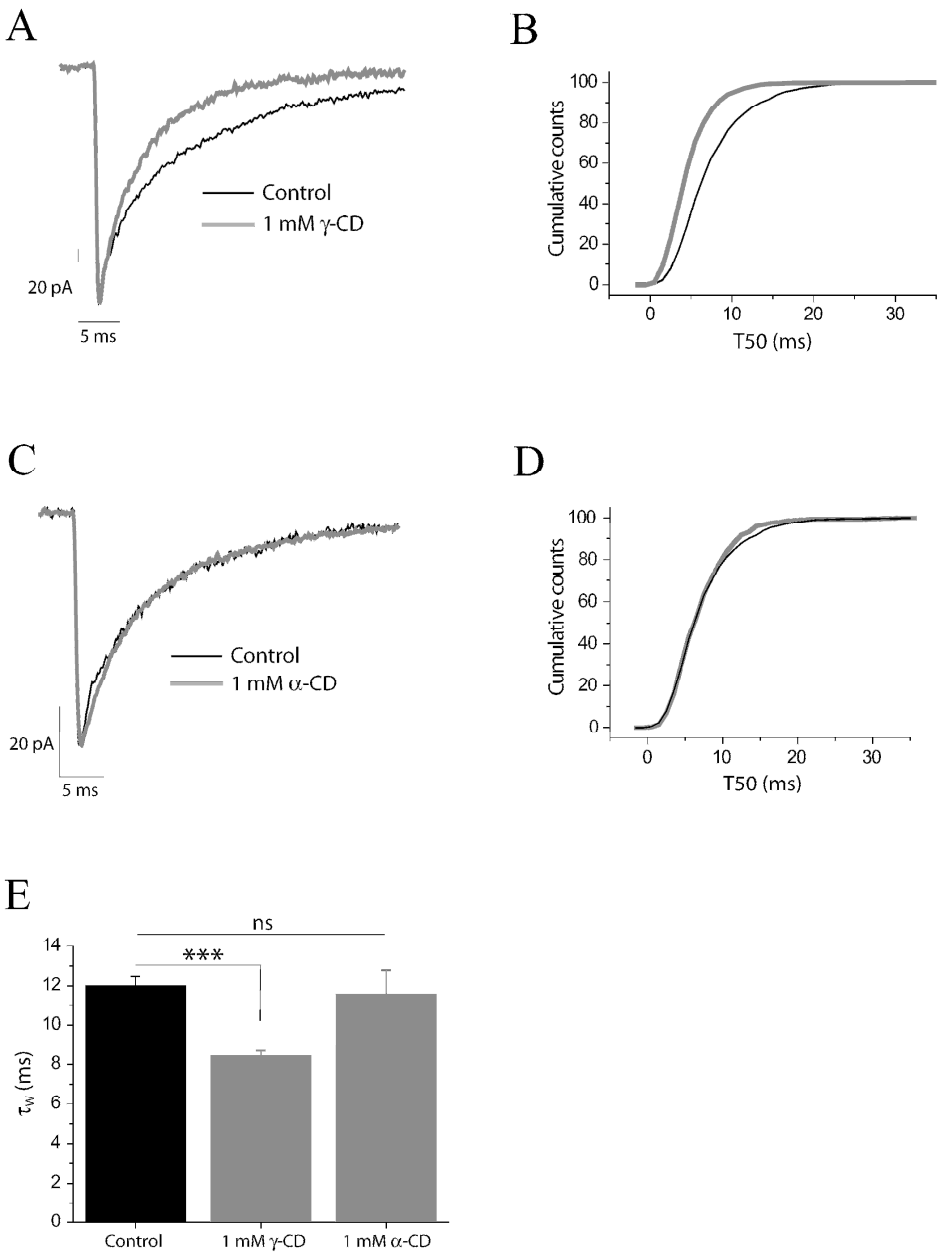

Figure 5.3. The effect of γ- and α-cyclodextrin pre-incubation (1 mM) on the decay kinetics of mIPSCs recorded from P7/8 WT L2/3 pyramidal neurones. **A.** Overlayed, averaged mIPSC normalised with respect to peak amplitude from representative control (black line) and 1 mM γ-CD pre-treated (> 1 hour, grey line) P7 L2/3 neurones. Note that the γ-CD treatment resulted in an average mIPSC with a faster decay time course. **B**. A cumulative probability plot of T50 for 2308 control events (pooled from 42 cells; black line) and 1193 events from P7/8 VB neurones pre-treated with 1 mM γ-CD (pooled from 20 cells; grey line). Note the leftward shift in the T50 distribution indicating that all γ-CD pre-treated cells exhibited faster decay kinetics compared with control ($p < 0.001$, KS-test). **C**. Overlayed, averaged mIPSC normalised with respect to peak amplitude from representative control (black line) and 1 mM α-CD pre-treated (> 1 hour, grey line) P7 L2/3 pyramidal neurones. Compared to γ-CD, pre-incubation with α-CD had no effect on the average mIPSC decay time course. **D**. A cumulative probability plot of T50 for 2308 control events (pooled from 42 cells; black line) and 423 events from P7+8 VB neurones pre-treated with 1 mM α-CD (pooled from 8 cells; grey line). Compared to γ-CD, note the absence of leftward shift in the T50 distribution following α-CD pre-treatment ($p > 0.05$ *vs* control, KS-test). **E**. A bar graph depicting the averaged τ_W of mIPSCs recorded from P7/8 L2/3 pyramidal neurones for control (n = 42 cells), 1 mM γ-CD (n = 20 cells) and 1 mM α-CD (n = 8 cells). Note the significant decrease in τ_W following 1 mM γ-CD, but not α-CD, pre-incubation.

5.4. The effects of γ-CD pre-incubation on mIPSCs recorded from WT L2/3 pyramidal neurones during postnatal development

Experiments performed on VB neurones revealed the mIPSC decay time course to be decreased following γ-CD pre-incubation at P7 and P8 but not at the later developmental stages of P10 and P20. To determine whether L2/3 pyramidal neurones display a γ-CD sensitivity that is also regulated by the developmental stage, mIPSCs were recorded following 1 mM γ-CD pre-incubation of brain slices derived from P7, P8, P9, P10, P15 and P20-24 mice. Following γ-CD pre-incubation, mIPSCs recorded from P7, P8, P9, P10 and P15 displayed faster decay kinetics relative to their respective control mIPSCs (Figure 5.4, for values see Table 5.2). In general, the mIPSC sensitivity to γ-CD decreased with age (Figure 5.4, for values see Table 5.2). A notable exception to this occurred at P10 when a secondary increase in sensitivity to γ-CD was observed (Figure 5.4, Table 5.2). These data indicate that L2/3 pyramidal neurones, in addition to thalamocortical VB neurones, are influenced by a native neurosteroid tone that diminishes as neonatal development progresses. However, mIPSCs recorded from L2/3 pyramidal neurones remain sensitive to γ-CD until at least P15 whereas mIPSCs from VB neurones are insensitive to γ-CD treatment by P10 inferring that the neonatal neurosteroid tone is regulated differentially in a mode that is brain region dependent.

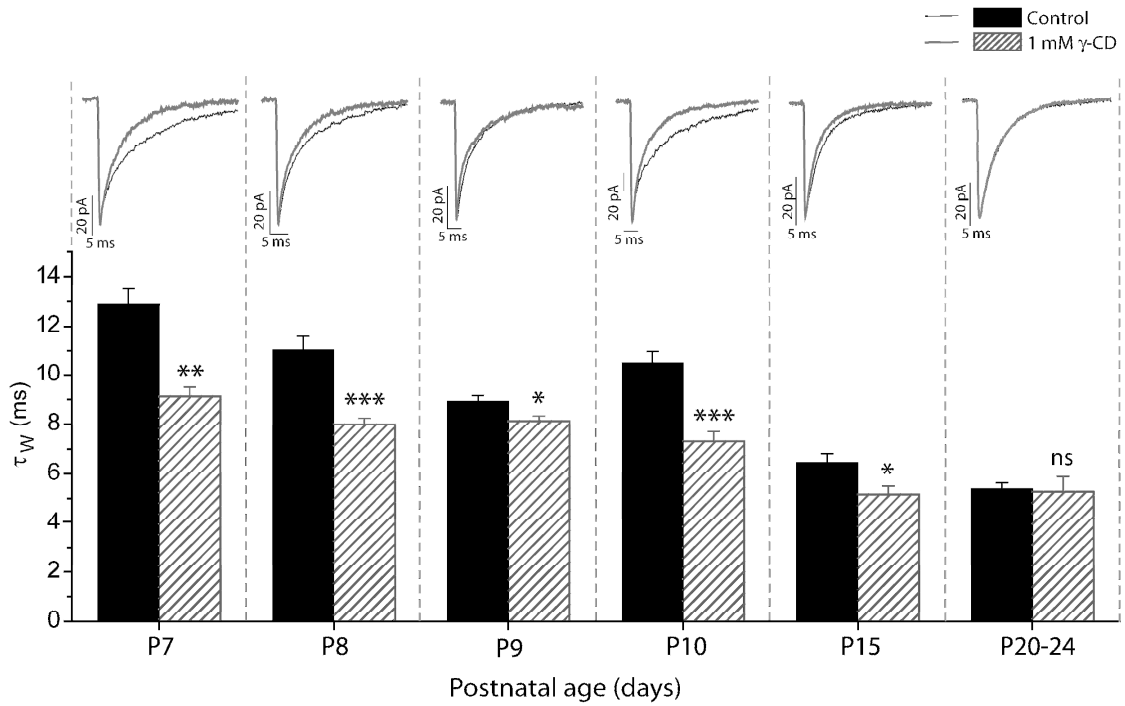

Figure 5.4. The effect of γ-CD pre-incubation (1 mM) on the τ_W of mIPSCs recorded from WT L2/3 pyramidal neurones during development. A bar graph depicting the effect of γ-CD pre-incubation (1 mM) on the τ_W of mIPSCs recorded from WT L2/3 pyramidal neurones at P7, P8, P9, P10, P15 and P20-24. Illustrated above are corresponding averaged and overlayed mIPSCs, normalised with respect to peak amplitude, taken from representative VB neurones in the absence (control, black line) and following 1 mM γ-CD pre-incubation (grey line). Note that at all developmental stages, other than P20-24, γ-CD pre-incubation results in significant reduction in τ_W. * $p < 0.05$, ** $p < 0.01$, *** $p < 0.001$, *vs* control, Student's unpaired t-test.

	P7		P8		P9		P10		P15		P20-24	
	Control (n=23 cells)	1mM γ-CD (n=8 cells)	Control (n=19 cells)	1mM γ-CD (n=12 cells)	Control (n=18 cells)	1mM γ-CD (n=19 cells)	Control (n=20 cells)	1mM γ-CD (n=11 cells)	Control (n=14 cells)	1mM γ-CD (n=12 cells)	Control (n=25 cells)	1mM γ-CD (n=8 cells)
Peak amplitude (pA)	-44 ± 2	-52 ± 6	-46 ± 7	-45 ± 2	-57 ± 3	-50 ± 2*	-46 ± 2	-47 ± 4	-54 ± 3	-45 ± 1*	-42 ± 2	-42 ± 3
Rise time (ms)	0.6 ± 0.1	0.5 ± 0.1	0.6 ± 0.1	0.6 ± 0.1	0.6 ± 0.1	0.6 ± 0.1	0.6 ± 0.1	0.6 ± 0.1	0.5 ± 0.1	0.5 ± 0.1	0.5 ± 0.1	0.5 ± 0.1
τ_W (ms)	12.9 ± 0.6	9.1 ± 0.4**	11.0 ± 0.6	8.0 ± 0.3***	8.9 ± 0.2	8.1 ± 0.2*	10.5 ± 0.5	7.3 ± 0.4***	6.5 ± 0.3	5.2 ± 0.3*	5.4 ± 0.2	5.3 ± 0.6
Frequency (Hz)	0.5 ± 0.1	0.5 ± 0.2	1.4 ± 0.3	1.6 ± 0.3	2.6 ± 0.3	2.9 ± 0.3	2.2 ± 0.3	2.6 ± 0.5	12.9 ± 2.0	12.4 ± 2.8	11.7 ± 1.2	12.6 ± 3.3

Table 5.2. A summary of the impact of development and γ-CD pre-incubation (1 mM) on the properties of mIPSCs recorded from WT L2/3 pyramidal neurones. * $p < 0.05$, ** $p < 0.01$, *** $p < 0.001$, *vs* control, Student's unpaired t-test.

5.5. The effects of intracellular γ-CD application on mIPSCs recorded from WT L2/3 pyramidal neurones during postnatal development

Pre-treatment of P7/8 cortical slices with finasteride (50 μM), or γ-CD (1 mM), resulted in L2/3 pyramidal neurones that displayed mIPSCs with markedly faster decay kinetics compared with those from control recordings. Next, I investigated the effects of γ-CD when applied solely to the intracellular environment *(i.e.* with no pre-incubation period and standard ECS) with a view to assessing the cellular localisation of the perceived neurosteroid tone. Accordingly for such experiments, the ICS was supplemented with 0.5 mM γ-CD (referred to henceforth as γ-CD ICS). Under these conditions P7 mIPSCs presented with faster decay kinetics, as indicated by a reduction in the τ_W (control: 12.9 ± 0.6 ms, n = 23, *vs* γ-CD ICS: 9.5 ± 0.6 ms, n = 7, $p < 0.01$, Student's unpaired t-test, Figure 5.5 A). Moreover, the effect of γ-CD ICS on the mIPSC τ_W was indistinguishable to the effect of γ-CD pre-incubation (γ-CD ICS: 9.5 ± 0.6 ms, n = 7 *vs* γ-CD pre-incubation: 9.1 ± 0.4 ms, n = 8, $p > 0.05$, Student's unpaired t-test, Figure 5.6). As outlined in above, P10 mIPSCs from L2/3 pyramidal neurones exhibit decay times that are prolonged *vs* P9 – an observation that contrasts with the general mIPSC acceleration with development (Figure 5.1). This secondary increase in τ_W was highly sensitive to γ-CD pre-incubation. Following the γ-CD ICS treatment, P10 L2/3 pyramidal neurone mIPSCs were significantly faster decaying *vs* standard ICS controls (τ_W control: 10.5 ± 0.5 ms, n = 19, *vs* 6.7 ± 0.2 ms, n = 10, $p < 0.001$, Student's unpaired t-test, Figure 5.5 B). Moreover, the average mIPSC τ_W at P10 following γ-CD ICS treatment was indistinguishable from that which was obtained following γ-CD pre-incubation (γ-CD ICS: 6.7 ± 0.2 ms, n = 10, *vs* γ-CD pre-incubation: 7.3 ± 0.4 ms, n = 11, $p > 0.05$, Student's unpaired t-test).

These observations confirm that mIPSCs of P7 and P10 L2/3 pyramidal neurones are equally sensitive to intracellular γ-CD application as they are to the γ-CD pre-incubation protocol. Considering that γ-CD is a membrane impermeant molecule, (Shu *et al*., 2007), it appears that extracellular γ-CD does not contribute to the actions observed here on mIPSC decay kinetics.

To assess whether γ-CD ICS is maximally effective at reducing a putative endogenous neurosteroid tone at $GABA_A$Rs, mIPSCs were recorded following incubation with finasteride (50 μM; > 4 hrs) and with the ICS supplemented with γ-CD (0.5 mM). As stated above, pre-incubation of P7/8 cortical slices with finasteride resulted in L2/3 pyramidal cells with mIPSCs that were significantly faster compared to control (τ_W control: 12.0 ± 0.4 ms, n = 42, *vs* τ_W 50 μM finasteride: 8.5 ± 0.3 ms, n = 7, $p < 0.01$, Student's unpaired test, Figure 5.2). When mIPSCs were recorded from finasteride-treated cells with ICS supplemented with 0.5 mM γ-CD, a further reduction in τ_W was observed (50 μM finasteride: 8.5 ± 0.3 ms, n = 7, *vs* 50 μM finasteride + 0.5 mM γ-CD ICS: 7.3 ± 0.2 ms, n = 6, $p < 0.01$, Student's unpaired t-test, Figure 5.6).

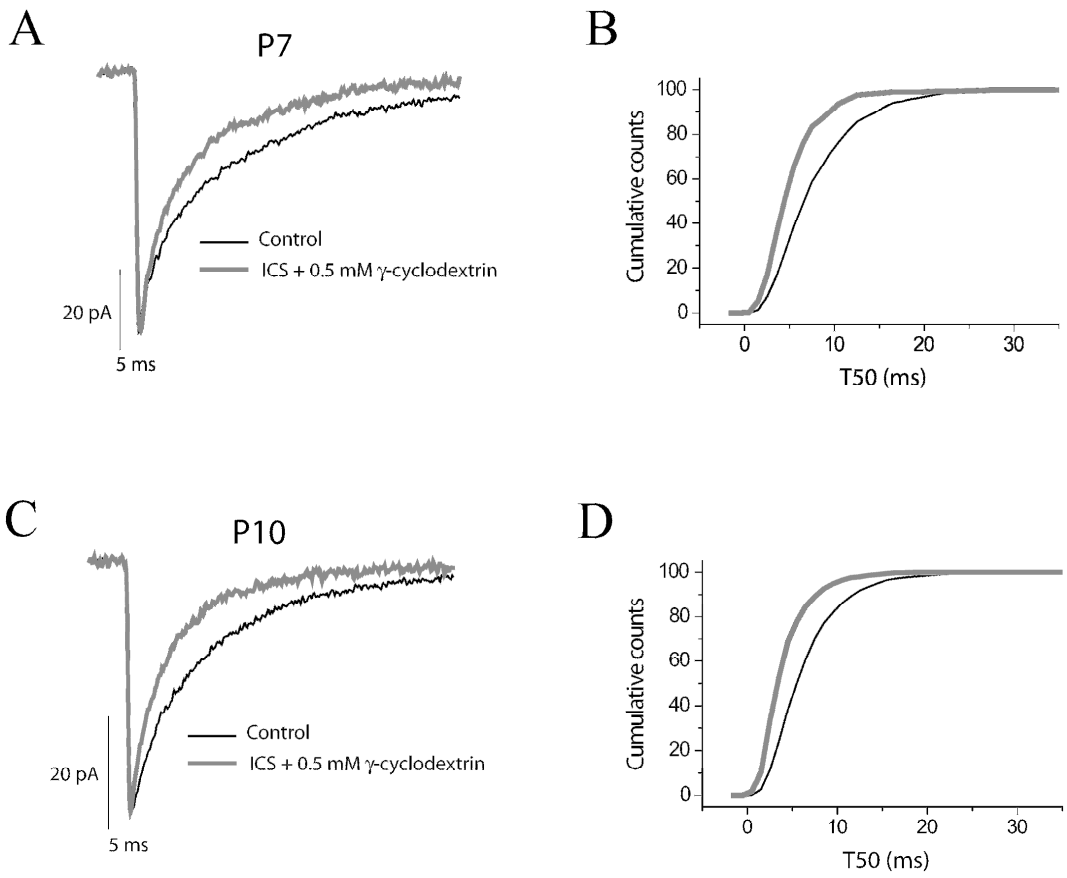

Figure 5.5. The effect of intracellular γ-CD (0.5 mM) on the decay kinetics of mIPSCs recorded from P7 and P10 WT L2/3 cortical pyramidal neurones. A. Overlayed, averaged mIPSC normalised with respect to peak amplitude from representative control P7 WT pyramidal neurone (black line) and a P7 pyramidal neurone in which the intracellular solution contained 0.5 mM γ-CD (grey line). Note that the intracellular γ-CD treatment resulted in an average mIPSC with a faster decay time course compared with control. **B**. A cumulative probability plot of T50 for 1125 control events (pooled from 23 cells; black line) and 581 events from P7 L2/3 pyramidal neurones in which the intracellular solution contained 0.5 mM γ-CD (pooled from 8 cells; grey line). Note the leftward shift in the T50 distribution indicating that all cells treated with intracellular γ-CD exhibited faster decay kinetics compared with control ($p < 0.001$, KS-test). **C**. Overlayed, averaged mIPSC normalised with respect to peak amplitude from a representative control P10 WT pyramidal neurone (black line) and a P10 pyramidal neurone in which the intracellular solution contained 0.5 mM γ-CD (grey line). Note that the intracellular γ-CD treatment resulted in an average mIPSC with a faster decay time course compared with control. **D**. A cumulative probability plot of T50 for 1384 control events (pooled from 20 cells; black line) and 871 events from P10 L2/3 pyramidal neurones in which the intracellular solution contained 0.5 mM γ-CD (pooled from 11 cells; grey line). Note the leftward shift in the T50 distribution indicating that all cells treated with intracellular γ-CD exhibited faster decay kinetics compared with control ($p < 0.001$, KS-test)

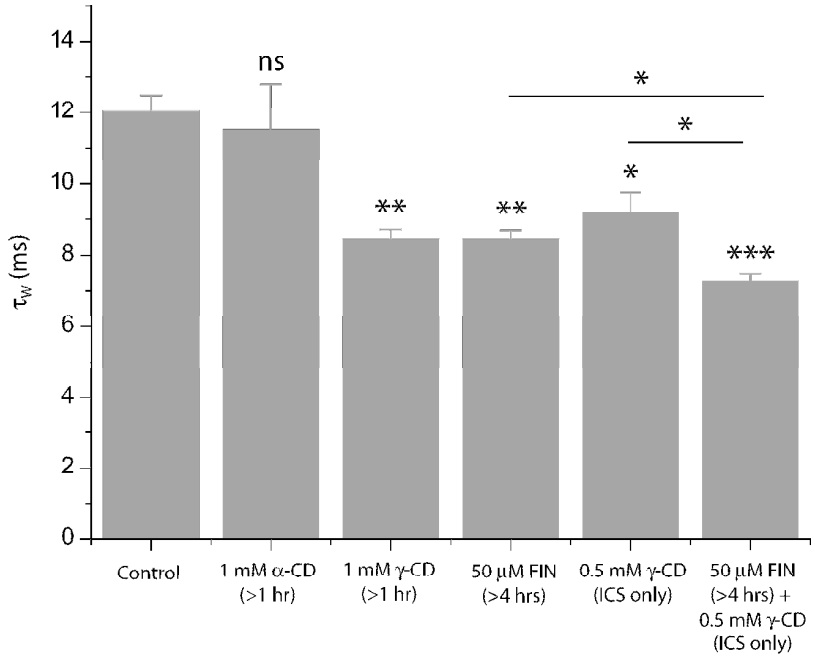

Figure 5.6. The effects of finasteride (50 μM), γ-CD and α-CD on the τ_W of mIPSCs recorded from P7/8 WT L2/3 pyramidal neurones. A bar graph depicting 1) the effects of 1 mM γ/α-CD pre-incubation (>1 hr), 2) the effects of 50 μM finasteride pre-incubation (FIN, >4 hrs), 3) the effects of only supplementing the ICS with 0.5 mM γ-CD and 4) the effects of 50 μM finasteride pre-incubation and intracellular γ-CD (0.5 mM) combined. Note that finasteride and both γ-CD treatments led to a significant and similar reduction in τ_W *vs* control whereas the α-CD treatment was inert in this respect. Moreover, compared to 50 μM finasteride pre-incubation or γ-CD ICS treatment, a further reduction in the τ_W was observed following 50 μM finasteride pre-incubation when combined with intracellular γ-CD (0.5 mM).
* $p < 0.05$, * $p < 0.01$, *** $p < 0.001$, Student's unpaired t-test.

5.6. The effects of γ-CD pre-incubation on mIPSCs from α1$^{0/0}$ L2/3 pyramidal neurones during postnatal development

Several studies have highlighted the α1 subunit to be important in the developmental decrease of the IPSC decay time (Rovira & Ben-Ari 1993; Tia *et al*., 1996; Hollrigel & Soltesz 1997; Dunning *et al*., 1999; Kapur & Macdonald 1999;; Vicini *et al*., 1999, 2001; Okada *et al*., 2000; Ortinski *et al*., 2004). In order to investigate to what extent α1-GABA$_A$Rs influence mIPSC decay kinetics during development of L2/3 pyramidal neurones, cortical brain slices were prepared from mice (P7/8, P10, P15 and P20) in which the α1 subunit had been genetically deleted (α1$^{0/0}$ mice). Under control conditions (*i.e.* standard intra- and extracellular solutions) mIPSCs, although prolonged when compared to those recorded from WT L2/3 pyramidal neurones at corresponding ages, still became more rapidly decaying with development (Figure 5.6, Figure 5.7, Table 5.3). Hence, this conserved developmental trend even in the absence of the α1 subunit is consistent with the proposal that an endogenous neurosteroid tone is retained in α1$^{0/0}$ mice, and may underpin speeding of mIPSC kinetics with development. To test this hypothesis, α1$^{0/0}$ cortical slices from either P7/8, P10, P15 or P20 mice were subjected to the γ-CD pre-incubation protocol. Following γ-CD pre-incubation, mIPSCs from P7/8, P10 and P15 L2/3 pyramidal neurones of α1$^{0/0}$ mice were unchanged with respect to peak amplitude and rise time (in all cases $p > 0.05$ *vs* control, Student's unpaired t-test, Table 5.3) but were significantly faster decaying than their respective controls (in all cases $p < 0.01$ *vs* control, Student's unpaired t-test, Figure 5.7, Figure 5.8, for τ_W values see Table 5.3). However, γ-CD pre-incubation had no effect on the mIPSC decay kinetics by P20-24 (τ_W P20-24 control: 7.9 ± 0.4 ms, n = 13, *vs* τ_W P20-24 γ-CD pre-incubation: 7.9 ± 0.6 ms, n = 11, $p > 0.05$, Student's unpaired t-test, Figure

5.7, Figure 5.8, Table 5.3). Collectively, these observations add weight to the proposal that speeding of mIPSC kinetics during development is not solely governed by a progressive incorporation of α1-$GABA_A$Rs but additionally influenced by the disappearance of an endogenous neurosteroid tone.

.

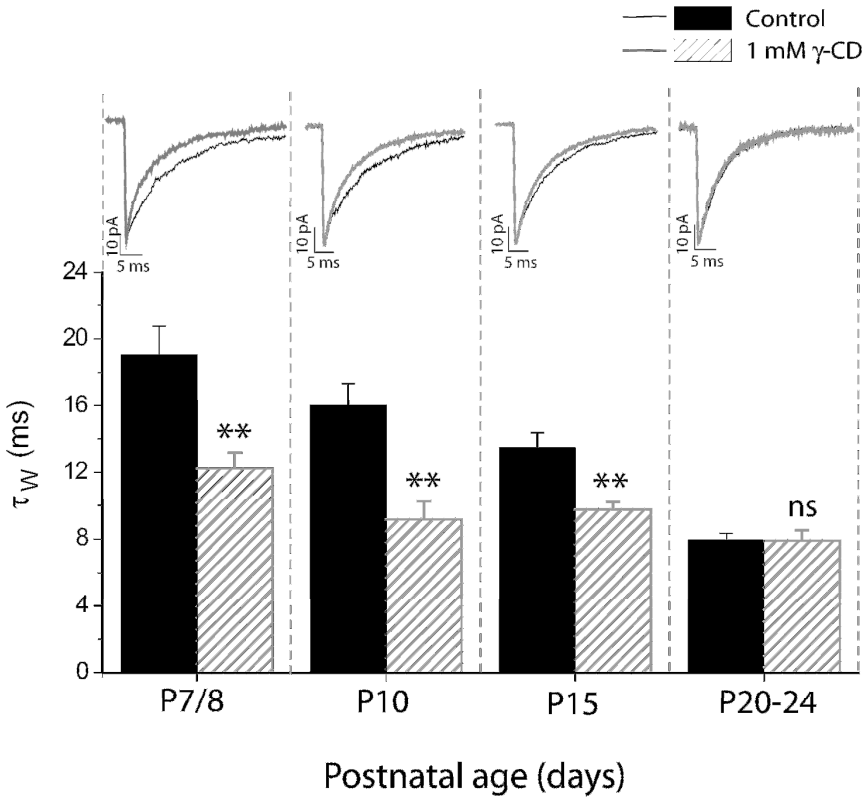

Figure 5.7. The effect of γ-CD pre-incubation (1 mM) on the τ_W of mIPSCs recorded from $\alpha1^{0/0}$ L2/3 pyramidal neurones during development. A bar graph depicting the effect of γ-CD pre-incubation (1 mM) on the τ_W of mIPSCs recorded from $\alpha1^{0/0}$ L2/3 pyramidal neurones at P7/8, P10, P15 and P20-24. Illustrated above are corresponding averaged and overlayed mIPSCs, normalised with respect to peak amplitude, recorded from representative VB neurones in the absence (control, black line) and following 1 mM γ-CD pre-incubation (grey line). Note that at all developmental stages, other than P20-24, γ-CD pre-incubation results in significant reduction in τ_W. ** $p < 0.01$, *vs* control, Student's unpaired t-test.

	P7/8		P10		P15		P20-24	
	Control (n=6 cells)	**1mM γ-CD (n=8 cells)**	**Control (n=4 cells)**	**1mM γ-CD (n=4 cells)**	**Control (n=12 cells)**	**1mM γ-CD (n=9 cells)**	**Control (n=13 cells)**	**1mM γ-CD (n=11 cells)**
Peak amplitude (pA)	-57 ± 2	-52 ± 2	-49 ± 2	-51 ± 6	-41 ± 3	-39 ± 3	-49 ± 3	-47 ± 2
Rise time (ms)	0.5 ±0.1	0.5 ±0.1	0.5 ± 0.1	0.5 ± 0.1	0.5 ± 0.1	0.5 ± 0.1	0.5 ± 0.1	0.5 ± 0.1
τ_W (ms)	19.0 ± 1.7	12.2 ± 1.0**	16.0 ± 1.3	9.2 ± 1.1**	13.5 ± 0.9	9.8 ± 0.4**	7.9 ± 0.4	7.9 ± 0.6

Table 5.3. A summary of the impact of development and γ-CD pre-incubation (1 mM) on the properties of mIPSCs recorded from $\alpha1^{0/0}$ L2/3 pyramidal neurones.
** $p < 0.01$, *vs* control, Student's unpaired t-test.

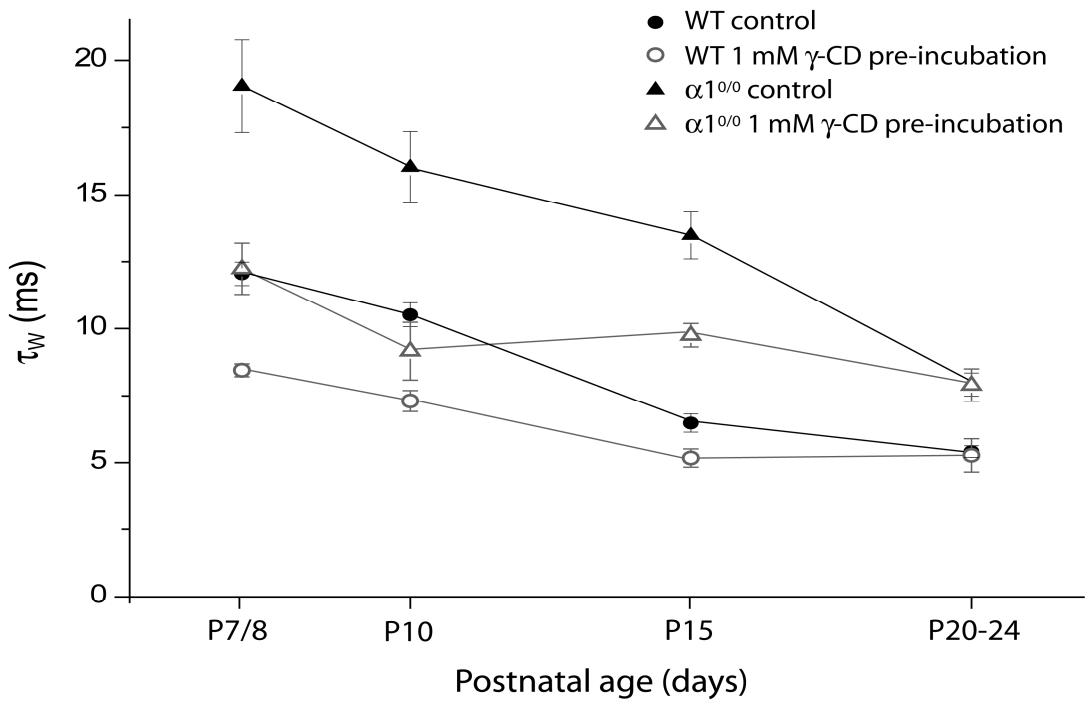

Figure 5.8. The effect of γ-CD pre-incubation (1 mM) on the τ_W of mIPSCs recorded from WT and $\alpha1^{0/0}$ L2/3 pyramidal neurones during development. A line graph depicting the effects of α1 subunit deletion on the τ_W of mIPSCs recorded from L2/3 pyramidal neurones during development. Note that mIPSCs from both WT and $\alpha1^{0/0}$ L2/3 pyramidal neurones become faster with maturity. However, at each developmental stage, mIPSCs recorded from $\alpha1^{0/0}$ neurones are slower decaying compared to those recorded from WT L2/3 pyramidal neurones. Furthermore, in common with WT L2/3 pyramidal neurones, preincubation of $\alpha1^{0/0}$ cortical brain slices with γ-CD (1 mM) results in faster decaying mIPSCs at P7/8, P10 and P15, but not at P20-24.

5.7. The effects of intracellular γ-CD application on mIPSCs recorded from L2/3 GAD67-GFP+ neurones during postnatal development

The experiments described above have highlighted the existence, in two distinct glutamatergic cell types, of a native neurosteroid tone early in neonatal development that prolongs synaptic $GABA_AR$–mediated mIPSCs. One important question regarding this finding concerns the regional specificity of this effect. Is the developmentally regulated neurosteroid tone, as described here in the case of VB and L2/3 pyramidal neurones, experienced globally throughout the brain (and therefore influencing $GABA_AR$ function indiscriminately) or are specific neuronal subsets targeted by a 'tailored' neurosteroid synthesis? A recent immunohistochemical study reported that two key neurosteroidogenic enzymes, 5α-R and 3α-HSD, are expressed in many principal CNS neurones (including L2/3 pyramidal cells), but are apparently absent in GABAergic interneurone populations (Agis-Balboa *et al*., 2006). Thus, investigations were carried out on cortical slices derived from GAD 67 GFP+ mice. This mouse line has been engineered to co-express green fluorescent protein (GFP) with the GABA-synthesising, 67 kDa γ-amino decarboxylase (GAD 67), enzyme (Tamamaki *et al*., 2003). Co-localisation studies confirmed that the three major interneurone classes present in mouse neocortex, (*i.e*. calretinin-, parvalbumin- or somatostatin-expressing) are all GFP-positive (GFP+, Tamamaki *et al*., 2003). Hence, visual identification of L2/3 GFP+ cells, using epifluorescence microscopy, enabled reliable identification of GABAergic interneurones in the cortex and permitted experimental investigation into whether cortical interneurones are similarly influenced by an endogenous steroid tone during development.

In control recordings from P7/8 GFP+ L2/3 neurones, mIPSCs exhibited a fast rise time (0.4 ± 0.1 ms, n = 8), a relatively large peak amplitude (-74 ± 7 pA, n = 8),

occurred at a low frequency (0.3 ± 0.1 Hz, n = 8) and displayed relatively slow decay kinetics as denoted by the determination of the average τ_W (11.7 ± 0.8 ms, n = 8). Moreover, the averaged τ_W was indistinguishable from that determined for mIPSCs recorded from P7/8 L2/3 pyramidal neurones (P7/8 L2/3 pyramidal: 12.0 ± 0.4 ms, n = 42, *vs* P7/8 L2/3 GAD 67 GFP+: 11.7 ± 0.8 ms, n = 8, $p > 0.05$, Student's unpaired t-test). Addition of 0.5 mM γ-CD to the intracellular recording solution had no effect on either the peak amplitude, rise time or mIPSC frequency (in all cases $p > 0.05$ *vs* control, Student's unpaired t-test), but resulted in mIPSCs with a markedly faster decay time course (τ_W control: 11.7 ± 0.8 ms, n = 8, *vs* τ_W ICS + 0.5 mM γ-CD: 7.6 ± 0.2 ms, n = 8, $p < 0.001$, Student's unpaired t-test, Figure 5.9, Table 5.4).

To investigate whether mIPSCs recorded from L2/3 GFP+ neurones remain sensitive to γ-CD at a later developmental time-point, I recorded mIPSCs from P20-24 L2/3 GFP+ neurones with standard ICS (control) or with ICS supplemented with 0.5 mM γ-CD. Under control conditions and relative to P7/8 L2/3 GFP+ neurones, mIPSCs from P20-24 L2/3 GFP+ neurones presented with a similar average peak amplitude (-62 ± 4 pA, n = 14, $p > 0.05$, Student's unpaired t-test, Table 5.4), a similar average rise time (0.4 ± 0.1 ms, n = 14, $p > 0.05$, Student's unpaired t-test), but were more frequent (2.7 ± 0.5 Hz, $p < 0.01$, Student's unpaired t-test) and displayed faster decay kinetics (τ_W: 4.5 ± 0.3 ms, n= 14, $p < 0.001$, Student's unpaired t-test,Figure 5.9, Table 5.4). Following intracellular treatment of P20-24 L2/3 GAD 67 GFP+ neurones with γ-CD (0.5 mM), the mIPSC peak amplitude, rise time, and frequency were unchanged (in all cases $p > 0.05$, Student's unpaired t-test, Table 5.4). Furthermore, in contrast to P7/8, intracellular γ-CD had no effect on the τ_W (control: 4.5 ± 0.3 ms, n = 14, *vs* ICS + 0.5 mM γ-CD: 4.0 ± 0.4, n = 7, $p > 0.05$, Student's unpaired t-test, Figure 5.9, Table 5.4).

Hence, it is apparent that mIPSCs recorded from P7/8 L2/3 GAD 67 GFP+ neurones exhibit similar decay kinetics and show a similar γ-CD sensitivity to those

obtained from P7/8 L2/3 pyramidal neurones. Such facets may reflect a commonality of $GABA_AR$ subtypes at this developmental stage. Further similarities to L2/3 pyramidal neurones are evident at P20-24 for L2/3 GFP+ neurones. The mIPSCs recorded from GFP+ neurones at P20-24 exhibit a significantly faster decay compared to P7/8 ($p < 0.001$, Student's unpaired t-test) and the decay kinetics of such synaptic events are no longer sensitive to intracellular γ-CD treatment. These findings suggest that the neurosteroid tone experienced by synaptic $GABA_ARs$ located on P7/8 L2/3 principal neurones is also experienced by those synaptic $GABA_ARs$ located on interneurone populations. In addition, these observations indicate that the factors responsible for the putative decrease in neurosteroid levels at P20-24, impact on both glutamatergic and GABAergic cell populations of L2/3.

	GFP+ P7/8 control (n = 8 cells)	**GFP+ P7/8 ICS + 0.5 mM γ-CD** (n = 8 cells)	**GFP+ P20-24 control** (n = 14 cells)	**GFP+ P20-24 ICS + 0.5 mM γ-CD** (n = 7 cells)
Peak amplitude (pA)	-74 ± 7	-61 ± 5	-62 ± 4	-59 ± 7
Rise time (ms)	0.4 ± 0.1	0.4 ± 0.1	0.4 ± 0.1	0.4 ± 0.1
τ_W (ms)	11.7 ± 0.8	7.6 ± 0.2***	4.5 ± 0.3	4.0 ± 0.4
Frequency (Hz)	0.3 ± 0.1	0.2 ± 0.1	2.7 ± 0.5	2.1 ± 0.9

Table 5.4. A summary of the effects of intracellular γ-CD (0.5 mM) treatment on the properties of mIPSCs recorded from L2/3 GAD 67 GFP+ neurones. *** $p < 0.001$, *vs* control, Student's unpaired t-test.

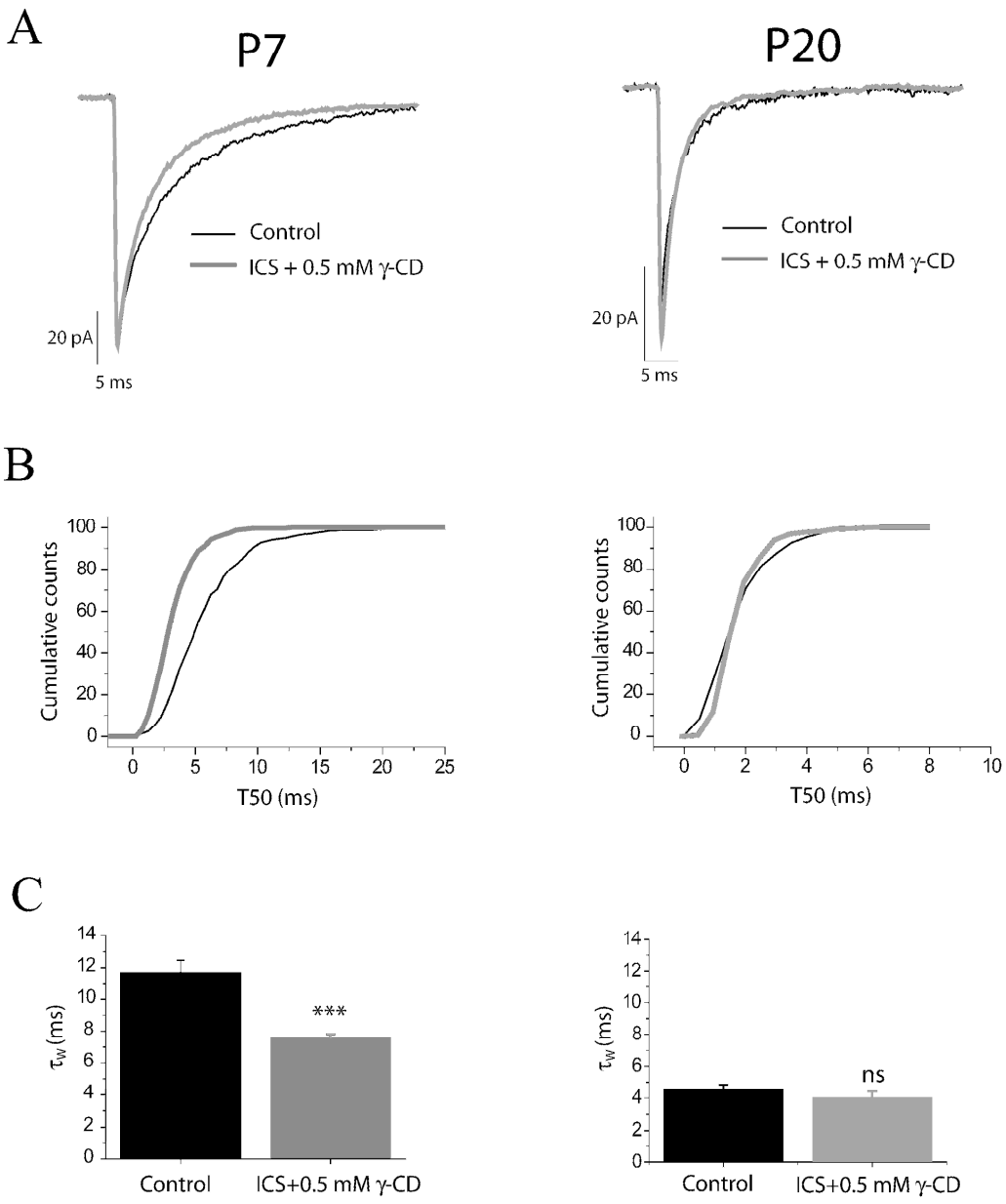

Figure 5.9. The effect of intracellular γ-cyclodextrin (0.5 mM) application on the decay kinetics of mIPSCs recorded from P7/8 and P20-24 L2/3 cortical GAD67 GFP+ neurones. A. Overlayed, averaged mIPSCs normalised with respect to peak amplitude from a representative control L2/3 GAD 67 GFP+ neurone (black line) and a L2/3 GAD 67 GFP+ neurone in which the intracellular solution contained 0.5 mM γ-CD (grey line) at P7 (left) and P20-24 (right). Note that at P7 the intracellular γ-CD treatment resulted in an average mIPSC with a faster decay time course compared with control, an effect absent at P20-24. **B**. Left: a cumulative probability plot of the T50 for 533 control events (pooled from 8 cells; black line) and 311 events from P7/8 L2/3 GAD 67 GFP+ neurones in which the intracellular solution contained 0.5 mM γ-CD (pooled from 8 cells; grey line). Right: a cumulative probability plot of the T50 for 1196 control events (pooled from 14 cells; black line) and 688 events from P20-24 L2/3 GAD 67 GFP+ neurones in which the intracellular solution contained 0.5 mM γ-CD (pooled from 7 cells; grey line). At P7/8, note the leftward shift in the T50 distribution indicating that all cells for which γ-CD was present only in the intracellular environment, exhibited faster decay kinetics compared with control ($p < 0.001$, KS-test). This effect was absent at P20-24. **C**. Left: summary bar graph depicting the significant decrease in the τ_W following intracellular application of γ-CD (0.5 mM). Right: a summary bar graph depicting the lack of effect of intracellular γ-CD (0.5 mM) on the mIPSC τ_W at P20-24. *** $p < 0.001$, Student's unpaired t-test. ns, not significant.

Chapter 6

Discussion

6.1. The properties of mIPSCs recorded from VB neurones

In this study the whole cell voltage clamp technique has been utilised in combination with receptor subunit "knock-out mice" ($\alpha4^{0/0}$ and $\delta^{0/0}$) and pharmacological approaches to investigate inhibitory neurotransmission in P17-24 VB neurones from mouse brain slice preparations. In the presence of TTX (0.5 μM) and kynurenic acid (2 mM) mIPSCs were blocked by the competitive $GABA_AR$ antagonist bicuculline thus identifying these events as $GABA_AR$ mediated. WT mIPSCs exhibited relatively fast rise times, relatively large peak amplitudes and rapid decay kinetics. These properties are consistent with previous reports from studies recording from WT VB neurones of approximately the same age and under similar recording conditions (-60 mV, 35 °C - Belelli *et al*., 2005; Peden *et al*., 2008; Herd *et al*., 2009). Additionally, examination of the distribution of such parameters revealed considerable variation. The mIPSC peak amplitude was particularly variable and exhibited a non-gaussian distribution with a positive rightward skew towards larger values. It is possible that at least a component of this variability (and indeed the variability exhibited by rise- and decay times) may be accounted for by inadequate space clamp. Specifically, mIPSCs originating from distant, dendritic locations relative to the patch clamp pipette at the soma, may undergo dendritic filtering as a result of an imperfect voltage clamp (Copogna & Pearce, 2011). Two lines of evidence obtained from the present study counteract this possibility. First, mIPSCs accepted for analysis were restricted to those events which exhibited rise times < 1 ms. Second, if dendritic filtering is apparent, then a negative correlation between the peak amplitude and rise time is to be expected (*i.e.* larger events will be characterised by slower rise times – Staley & Mody, 1991; Llano & Gerschenfeld, 1993). No such correlation was observed. Moreover, the skewed peak amplitude distribution is a feature shared by many CNS synapses and probably reflects an intrinsic synaptic property

(Edwards *et al*., 1990; Llano & Gerschenfeld, 1993). Indeed, sources of variation that may influence mIPSC properties include multi-vesicular GABA release (Frerking *et al*., 1995; Llano *et al*., 2000), the peak concentration and lifetime of GABA in the cleft (governed by vesicular transmitter concentration, synaptic geometry, diffusion rate and reuptake mechanisms – Nusser *et al*., 2001; Barberis *et al*., 2011) postsynaptic receptor density (Otis *et al*., 1994; Nusser *et al*., 1997), and the stochastic nature of channel openings (Faber *et al*., 1992).

In the vast majority of cases the averaged mIPSC decay time course was well described by a bi-exponential decay function, a finding that is in agreement with the VB neurone IPSP decay profiles reported previously (Zhang *et al*., 1997; Huntsman & Huguenard, 2000; Belelli *et al*., 2005). The bi-exponential decay is in agreement with the current kinetic model developed to describe the mIPSC decay. This model proposes that the fast component of current decay reflects a burst of oscillations between agonist-bound closed and open states of the GABA-activated channel, whereas the slow decay phase reflects clusters of bursts interrupted by transitions to desensitized states (Jones & Westbrook, 1996).

The subunit composition of synaptic $GABA_A$Rs can have a considerable influence on the mIPSC decay kinetics. The VB mIPSC decay kinetics, as described by the average weighted decay time constant, τ_W, was in close agreement with τ_W values reported in previous VB studies conducted on mice of a similar developmental age and under similar recording conditions (-60 mV, 35 °C - Belelli *et al*.,2005; Peden *et al*.,2008; Herd *et al*., 2009). Indeed, the relatively fast kinetics of mIPSCs recorded from VB neurones contrasts with the relatively slow decay kinetics of mIPSCs recorded from nRT neurones (Huntsman *et al*., 1999; Huntsman & Huguenard, 2000; Belelli *et al*., 2005; Cope *et al*., 2005a; Jia *et al*., 2005), a difference that is ascribed to differences in the subunit composition of synaptic $GABA_A$R expression in these neurones.

Specifically, > P20 VB neurones express α1β2γ2 receptors whereas nRT neurones express receptors composed of α3β1/3γ2 (Huntsman *et al*., 1999; Belelli *et al*., 2005; Huntsman & Huguenard, 2006; Peden *et al*., 2008). In this regard, the α subunit isoform is an important determinant of the decay kinetics exhibited by recombinant receptors in response to GABA. Studies utilising rapid GABA application to recombinant $GABA_AR$ subtypes in human endothelial cell lines have reported that the α1 subunit imparts rapid deactivation kinetics and a faster onset of desensitization relative to α2 and α3 containing receptors (discussed further below- Lavoie *et al*., 1997; Picton & Fisher, 2007).

In the present study recordings were made from VB neurones that were derived from P17-24 WT mice of either sex. Whilst gender did not affect any of the mIPSC properties examined, a small but significant decrease was observed in peak amplitude and rise time coupled with a shortening of the mIPSC decay time course, over this developmental period (juvenile to early-adolescent). These observations likely reflect continuing maturational processes regarding synaptic development (Takahashi *et al*., 2005) and are consistent with previous studies (Cohen *et al*., 2000; Peden *et al*., 2008). For example, it is known that VB synapses undergo a considerable program of α subunit reorganization in the first two weeks of life, whereby α1- replaces α2-$GABA_ARs$ at inhibitory synapses (Peden *et al*., 2008). Therefore the small developmental change in mIPSC properties that occurs between P17-24 described here could represent the "tail-end" of the α subunit exchange. In agreement with this notion, Peden *et al*. reported a small decrease in the mIPSC τ_W at P23-27 relative to P15-22 (Peden *et al*., 2008). Although precise measurements of the synaptic GABA transient (*i.e.* the concentration and lifetime of GABA in the synaptic cleft) are hindered by technical limitations, it has been proposed that GABA activation of postsynaptic receptors may occur in conditions of extreme non-equilibrium meaning that saturating concentrations of GABA are rarely

reached (Mozrzymas, 2004; Barberis *et al*., 2011, but see Jones & Westbrook, 1996). Consequently, this situation increases the scope for dynamic modulation of the GABA transient by a variety of modulatory processes including GABA re-uptake mechanisms, synapse geometry, tortuosity and variations in quantal GABA release (Mozyzmas, 2004). The relative impact of these factors on the mIPSC properties was not assessed in this study, however, changes in the synaptic area have been postulated to underlie differences in the mIPSC BDZ sensitivity at adolescent *vs* mature CA1 synapses (Cohen *et al*., 2000) and $GABA_AR$ kinetics have been shown to be influenced by the extent of postsynaptic $GABA_AR$ clustering (Petrini *et al*., 2003). Hence, in addition to $GABA_AR$ subunit changes, it is likely that additional maturational events influence the mIPSC kinetics in VB neurones between P17-24.

A further possibility is that the observed decrease (albeit modest) in mIPSC duration could reflect a developmentally regulated presence of endogenous neurosteroids similar to that described in lamina II neurones in the dorsal horn of the spinal cord (Keller *et al*., 2004b). This proposal is given careful consideration in the following discussion below.

6.2. The properties of the tonic current recorded in VB neurones

A striking feature of whole cell voltage clamp recordings from WT VB neurones was the considerable outward shift in holding current (96 ± 9 pA) coupled with a reduction in baseline noise (RMS) following application of the $GABA_AR$ antagonist bicuculline (30 μM). This finding is in agreement with previous studies reporting these neurones to exhibit a relatively large endogenous $GABA_AR$ mediated tonic current that is preserved even in a well-perfused *in vitro* brain slice preparation (Porcello *et al*., 2003; Belelli *et al*., 2005; Jia *et al*., 2005; Peden *et al*., 2008; Herd *et al*., 2009). In common with the

mIPSCs of VB neurones, the magnitude of the tonic current (as measured by the outward shift in holding current following bicuculline application) was not influenced by gender, but in contrast to the phasic synaptic inhibitory events, was not affected by the somewhat limited developmental age range (P17-24) studied here. Note however, a previous study from the host laboratory investigating the maturation of the tonic current over a longer developmental period (P8-27), has demonstrated that the tonic current greatly increases in magnitude with maturation (Peden *et al*., 2008)

Tonic currents in other brain regions, including dLGN neurones (a thalamic nucleus in close anatomical proximity to the VB) rely on synaptic overspill as a source of GABA (Bright *et al*., 2007). However, the tonic currents in VB neurones observed in this study and in others (Belelli *et al*., 2005; Peden *et al*., 2008; Herd *et a*l., 2009) were recorded in the presence of TTX (0.5 μM) thus excluding action potential drive and the resulting transmitter overspill. Although the source of ambient GABA has not been investigated in the present study, previous reports have implicated GABA re-uptake systems in regulating extracellular GABA levels (Nusser & Mody, 2002; Semyanov *et al*., 2003). The ambient GABA concentration is dynamically determined by the balance between GABA release and GABA re-uptake mechanisms (Glykys & Mody, 2007). In addition to synaptically released GABA, other non-vesicular mechanisms may also contribute to release. These include the reversal of transmitter transport by GATs which may occur following modest depolarisation (Richerson & Wu, 2003). With respect to GABA reuptake, pharmacological blockade of GABA transporters (GATs) has been demonstrated to promote tonic currents in several neuronal types (Nusser & Mody, 2002; Semyanov *et al*., 2003; Keros & Hablitz, 2005) including VB neurones (Peden *et al*., 2008) thus suggesting that reuptake may dominate over GAT-mediated release. In particular, the selective GAT3 inhibitor SNAP5114, and to a lesser extent the GAT1 inhibitor NO711, were recently reported to increase the tonic conductance in mouse VB

neurones (Cope *et al*., 2009). This finding is consistent with evidence indicating a relative abundance of GAT3 *vs* GAT-1 in the VB nucleus (Ikegaki *et al*., 1994). Given that GAT3 expression is predominantly localised to glial cells (Conti *et al*., 2004) and that GAT1 expression is unusually restricted to astrocytes in the thalamus (De Biasi *et al*., 1998) it is likely that glial GABA transporters are endowed with the greatest share of control over the ambient GABA levels experienced by VB neurones.

Recent evidence has indicated that GABA is not the only natural agonist that activates VB tonic currents. Both exogenous taurine application and blockade of taurine transport have been reported to augment the tonic conductance present in VB neurones whilst unaltering synaptic inhibition (Jia *et al*., 2008). Furthermore, taurine was demonstrated to be a more potent agonist at recombinant α4β2δ *cf.* α1βγ2 receptors expressed in host cell lines (Jia *et al*., 2008). Since taurine release is stimulated by hypo-osmotic shock, energy deprivation and membrane depolarization (Oja & Saransaari, 2000), a role in neuronal protection under pathological conditions has been proposed (Jia *et al*., 2008).

6.3. Inhibitory neurotransmisson in VB neurones: relevance to thalamic function

The results from this and previous studies indicate that inhibitory neurotransmission in thalamic VB neurones can be summarised into 1) phasic inhibition, characterized by relatively frequent, large amplitude and fast decaying mIPSCs and 2) tonic inhibition, characterized by a continuous background current that is revealed by $GABA_AR$ antagonists. What is the physiological purpose of these two distinct modes of inhibition in the VB thalamus?

The thalamus is a major subcortical structure with primary roles in sensory processing and motor output (Sherman & Guillery, 2002). Anatomically, the thalamus

is subdivided into a collection of nuclei that were originally characterized according to the type of sensory information they route to cortical regions. The primary role of the VB nucleus, for example, is the relay of somatosensory information to the cortex (Sherman & Guillery, 2002). Thalamocortical (TC) relay neurones, such as those located in the VB nucleus, are able to respond to an excitatory input by one of two distinct firing modes, tonic or bursting (Jahnsen & Llinas, 1984). This functional duality is generated by the presence of voltage dependent T-type Ca^{2+} channels (Crunelli *et al*., 1989; Tscherter *et al*., 2011). At relatively depolarized membrane potentials, these channels are inactivated and therefore have no command over the neurone's firing properties (Crunelli *et al*., 2006; Beenhakker & Huguenard, 2009). Under these conditions the neurone exhibits the tonic firing mode characterized by a continuous and regular "stream" of action potentials that persist for as long as the suprathreshold activation. Alternatively, when the cell is sufficiently hyperpolarized, the T-type Ca^{2+} channels de-inactivate, priming them for the next suprathreshold depolarization (Crunelli *et al*., 1989; Tscherter *et al*., 2011). The activation of these channels leads to an inward Ca^{2+} current that, in turn, causes an all-or-none voltage spike known as a 'low threshold spike' (LTS) . The LTS is often sufficient to trigger a high frequency cluster of action potentials, characteristic of the burst firing mode (Crunelli *et al*., 2006; Beenhakker & Huguenard, 2009). These two firing modes impact differentially on the information being relayed and are implicated in different behavioural states. Generally, the tonic firing mode is prevalent during periods of high vigilance whereas the bursting mode is more evident during drowsiness and periods of slow wave sleep, although both modes can be present in the awake animal (Crunelli *et al*., 2006; Beenhakker & Huguenard, 2009).

Due to the reciprocal excitatory connectivity between sensory, motor and associational cortical areas and related thalamic nuclei, the thalamocortical circuitry can

be considered as an intrinsic oscillatory unit (Huguenard & McCormick, 2007). Excitatory TC cells are reciprocally connected with neurones of the reticular nucleus (nRT), a shell-like structure surrounding the dorsal thalamus and composed entirely of GABAergic neurones (Huguenard & McCormick, 2007). These neurones also exhibit the bi-functional firing properties as described for TC cells and, in concert with relay neurones, a loop is formed that can generate and sustain network oscillations (a processs extensively reviewed in McCormick & Bal, 1997). Synaptic inhibition within thalamic relay nuclei plays an integral role in shaping the thalamocortical oscillatory activity (Steriade, 1997; Sherman & Guillery, 2002). Briefly, spiking nRT neurones with their terminals on TC neurones elicit an IPSP comprising both $GABA_A$ and $GABA_B$ components. The ensuing hyperpolarization de-inactivates the T-type channel priming them for rebound bursting activity. This output, in turn, is routed back to the nRT as synaptic excitation thereby renewing the recurrent network activity (Huguenard & McCormick, 2007; Beenhakker & Huguenard, 2009). This description is, of course, an oversimplification as in order for the network to reach generalized synchrony, synaptic convergence and divergence is required at each stage. Indeed, both TC and nRT cells exhibit a high degree of lateral connectivity so that a localized, point-to-point, oscillatory response between an nRT and TC cell can recruit neighbouring cells into the network (Huguenard & McCormick, 2007; Beenhakker & Huguenard, 2009). Synchronized oscillatory activity of the intrathalamic network occurs *in vivo* and is particularly evident during sleep states when activity of the TC networks are detected on the EEG as 10-15 Hz sleep spindles (Huguenard & McCormick, 2007).

If synaptic inhibition between nRT and TC cells is crucial in sculpting distinct oscillatory activity what role does tonic inhibition play in influencing the network? Tonic inhibition in TC neurones has been proposed to contribute to the shift between

tonic and burst firing modes. Specifically, Cope *et al*. reported that by using gabazine (a competitive $GABA_AR$ antagonist) at a low concentration (50 nM) they were able to "selectively" block the tonic current in VB neurones (Cope *et al*., 2005a). By pharmacologically suppressing this tonic current, under current-clamp conditions this resulted in a small depolarisation together with an increase in the neuronal input resistance. The authors then demonstrated using extracellular single-unit recordings of VB neurones in the presence of 50 nM gabazine, that the selective block of the extrasynaptic conductance caused a switch from the bursting to the tonic firing mode (Cope *et al*., 2005a). Hence, modulation of the tonic conductance in TC neurones may contribute to the shift between distinct thalamic firing modes with the effect of determining certain behavioural states.

Under certain pathological conditions TC networks may exhibit hypersynchronized epileptic discharges that are characteristic of generalized absence epilepsy (GAE - Crunelli & Leresche, 2002). This condition primarily affects children and is characterized behaviourally by a paroxysmal loss of consciousness lasting about 3-10 seconds that has an abrupt onset and termination (Manning *et al*., 2003). Typical absence seizures can be detected *via* EEG recordings as a characteristic 3-4 Hz spike and wave discharge (SWD) that is similar in frequency to EEG oscillations observed seen during slow wave sleep (SWS). Relative to sleep spindles, this form of oscillation is far more synchronous and profound. Together with the nRT, TC cells comprising the ventrobasal nucleus have long been implicated in the maintenance of absence seizures (Manning *et al*., 2003). However, it was recently demonstrated that an enhanced $GABA_AR$ mediated tonic conductance in TC neurones is both necessary and sufficient for the generation of absence seizures (Cope *et al*., 2009). In particular the authors demonstrated that an enhancement of the tonic conductance in TC neurones is evident in several mouse models of GAE and that the SWDs exhibited by these animals could

be mimicked by pharmacological enhancement of δ-$GABA_A$R mediated tonic currents in WT animals (Cope *et al*., 2009). The contribution of δ-$GABA_A$Rs to neuronal inhibition in VB neurones was investigated in the present study by using a combination of $GABA_A$R subunit "knock-out" mice and pharmacological approaches. The results of these investigations are discussed in the accompanying Section.

6.4. Deletion of the α4 subunit disrupts both tonic and synaptic inhibition in VB neurones

Whole cell voltage clamp recordings from VB neurones derived from P17-24 $\alpha4^{0/0}$ mice revealed that deletion of this subunit had a surprising impact on synaptic inhibition. Relative to WT, mIPSCs recorded from $\alpha4^{0/0}$ VB neurones displayed significantly faster decay kinetics, an increased peak amplitude and a greatly increased mIPSC frequency. These findings contrast with the only other description of $\alpha4^{0/0}$ VB mIPSCs in which the authors reported no change in any of the mIPSC parameters (Chandra *et al*., 2006). However, in this study the authors primarily focused on the effects of α4 subunit deletion on the tonic inhibition and provided limited information concerning synaptic inhibition in $\alpha4^{0/0}$ VB neurones. Hence the present study represents the first detailed investigation of synaptic inhibition in VB neurones of $\alpha4^{0/0}$ mice.

A reduced mIPSC decay time in $\alpha4^{0/0}$ VB neurones could reflect an absence of synaptic α4 containing $GABA_A$Rs. Indeed, a proportion of thalamic α4 subunits have been found to co-localise with the γ2 subunit raising the possibility of synaptic α4βγ2 receptors (Sur *et al*. 1999). However, such a scenario is unlikely since recombinant α4βγ2 receptors are known to exhibit rapid decay kinetics relative to α1βγ2 (Picton & Fisher, 2007; Lagrange *et al*., 2007). Hence, if this were the case for native synaptic α4-

$GABA_ARs$ then deletion of this subunit would be expected to produce longer, not shorter, mIPSC decay times.

An alternative interpretation of the shorter decay time of mIPSCs recorded from $\alpha4^{0/0}$ VB neurones may be the absence of peri- or extrasynaptic α4 subunit containing receptors that, following synaptic spillover of GABA, may contribute to the tail of the mIPSC decay. In CGCs and DGGCs, application of TTX to block action potential drive reveals IPSCs with faster decay kinetics, an effect thought to reflect a decrease in perisynaptic $GABA_AR$ activation following reduced GABA spillover (Hamann *et al*., 2002; Wei *et al*., 2003; Bright *et al*., 2011). Direct comparison of these findings with the present study, however, is limited since here recordings were obtained in the presence of TTX (0.5 μM). Nevertheless, it is intriguing to compare the mIPSC duration observed here in $\alpha4^{0/0}$ with those from $\delta^{0/0}$ VB neurones (Herd *et al*., 2009). Compared to $\delta^{+/+}$ VB neurones, Herd *et al*, reported a similarly decreased mIPSC duration following deletion of the δ-subunit (Herd *et al*., 2009). Collectively, the findings reported for both $\alpha4^{0/0}$ and $\delta^{0/0}$ mice suggest that extrasynaptic α4β2δ $GABA_ARs$ may contribute to mIPSC decay time. This proposal has gained credence from recent experiments performed in the host laboratory involving paired whole-cell voltage clamp recordings between neurones of the nRT and VB. In particular, application of the δ-$GABA_AR$ selective modulator DS2 (see below) elicited a robust prolongation of the duration of burst evoked IPSCs in VB neurones (Herd *et al*, unpublished observations). However, in this study and previous studies (Wafford *et al*., 2009) DS2 (10 μM) did not prolong WT VB mIPSC decay kinetics which may be expected if δ-$GABA_ARs$ are involved in the decay of the synaptic currents in these neurones. Moreover, recent investigations of spillover inhibition have added a further tier of complexity. Specifically, it has been proposed that δ-$GABA_ARs$ do not participate in spillover inhibition in CGCs based on the findings that the spillover component of the sIPSC is

eliminated in $\alpha6^{0/0}$ CGCs but not in CGCs derived from $\delta^{0/0}$ mice (Bright *et al*., 2011). It therefore appears that cell-type specific $GABA_AR$ subtypes are involved in sensing GABA overspill. Furthermore, the specialised architecture of the CGC glomerular synapse may serve to increase the lifetime and concentration of GABA at the cleft such that other (non-δ) $GABA_AR$ subtypes are better suited to respond to GABA spillover. In summary, the reasons for the described changes in the $\alpha4^{0/0}$ VB mIPSC properties remain unclear although complex compensatory mechanisms in response to the α4 subunit deletion may be a contributing factor.

The increased mIPSC peak amplitude observed here in $\alpha4^{0/0}$ VB neurones is consistent with the properties of mIPSCs recorded from $\delta^{0/0}$ VB neurones which also displayed a significantly larger peak amplitude (Herd *et al*., 2009). The deletion of the δ subunit has been implicated with an increased co-assembly of α4 with γ2 at the synapse (Korpi *et al*., 2002b) and this has been proposed to underlie the increased peak amplitude of VB mIPSCs recorded from VB neurones of $\delta^{0/0}$ mice (Herd *et al*., 2009). Clearly such a molecular mechanism cannot underpin the increased mIPSC peak amplitude following the deletion of the α4 subunit. Alternatively, the observation that an increase in mIPSC peak amplitude is preserved in both $\alpha4^{0/0}$ and $\delta^{0/0}$ mice suggests that this effect on the properties of mIPSCs may be a crucial compensation in response to a diminished tonic conductance

More generally, an increase in mIPSC peak amplitude may reflect an increased postsynaptic receptor density or an enhancement of the GABA transient by a variety of factors such as an increased quantal size (Otis *et al*., 1994; Mody *et al*., 1994; Barberis *et al*., 2011). Therefore it is tempting to speculate that in order to compensate for the loss of tonic inhibition, the strength of phasic inhibition is increased in the inhibitory synapses of the both the $\alpha4^{0/0}$ and $\delta^{0/0}$ mouse. However, as described above these different forms of inhibition likely serve highly specialised and distinct physiological

roles and it is currently unknown whether synaptic inhibition would be able to deputise efficiently in absence of tonic inhibition.

In this study, a striking feature of synaptic inhibition in $\alpha4^{0/0}$ VB neurones was the greatly increased mIPSC frequency relative to WT recordings. The frequency of mIPSCs in $\alpha4^{0/0}$ VB neurones was twice that of WT VB neurones (24 ± 2 Hz *vs* 12 ± 1 Hz, respectively). It is of interest that in a recent study, $\delta^{0/0}$ VB neurones appear to exhibit an increased mIPSC frequency relative to WT (17 ± 2 Hz *vs* 22 ± 2 Hz) although this effect did not reach statistical significance (Herd *et al*., 2009). An increase in mIPSC frequency is classically associated with an increased probability of presynaptic release (Mody *et al*., 1994; Kullman *et al*., 2005). Although it is conceivable that the observed increase in mIPSC frequency in $\alpha4^{0/0}$ VB neurones is due to the loss of presynaptic α4-$GABA_A$Rs, there is currently no evidence to support this proposal as presynaptic $GABA_A$Rs have scarcely been observed in the higher centres of the CNS (Kullman *et al*., 2005). Alternatively, it is possible that the increased mIPSC frequency observed in $\alpha4^{0/0}$ VB neurones represents complex plasticity changes in order to provide an augmentation of synaptic inhibitory strength in an attempt to compensate for a diminished tonic conductance.

Perhaps a more parsimonious explanation for the marked increase in mIPSC frequency observed in $\alpha4^{0/0}$ VB neurones involves the reduced baseline noise compared to WT recordings. Specifically, P17-24 WT VB neurones exhibited a "noisy" baseline reflecting the continuous "chatter" of extrasynaptic $GABA_A$Rs. This noise is greatly reduced in recordings from $\alpha4^{0/0}$ VB neurones (see below) so it is possible that small amplitude mIPSCs, which are normally masked in recordings made from WT VB neurones, are more readily resolved in recordings from $\alpha4^{0/0}$ neurones. However, if this was the case then a shift in the peak amplitude distribution towards smaller mIPSC values would be anticipated for $\alpha4^{0/0}$ VB mIPSCs. This is clearly not the case, as the

present study found the converse of this *i.e.* an increased mIPSC peak amplitude in $\alpha4^{0/0}$ VB neurones.

Compared to WT VB neurones, $\alpha4^{0/0}$ VB neurones exhibited a reduced baseline noise together with a greatly reduced outward shift in the holding current in response to bicuculline application. Hence, tonic inhibition is severely attenuated in $\alpha4^{0/0}$ VB neurones, a finding that is consistent with previous reports investigating the tonic conductance of VB neurones from $\alpha4^{0/0}$ (Chandra *et al*., 2006) and $\delta^{0/0}$ mice (Porcello *et al*., 2003; Herd *et al*., 2009). Collectively, these findings are in agreement with a co-immunoprecipitation study that reported a co-localisation of α4 and δ subunits in thalamic neurones (Jia *et al*., 2005). Furthermore, VB neurones derived from $\beta2^{0/0}$ mice exhibit a reduced tonic conductance suggesting that extrasynaptic receptors of VB neurones are composed of β2, α4 and δ subunits. In agreement, the tonic-enhancing action of etomidate (a β2/3-$GABA_AR$ selective anaesthetic drug) is attenuated in VB neurones derived from a mouse engineered to express $GABA_ARs$ incorporating an etomidate insensitive β2 subunit (β2N265S; Belelli *et al*., 2005). In conclusion, the results presented here from whole-cell voltage- clamp recordings performed on $\alpha4^{0/0}$ VB neurones are complementary to previous studies and confirm that the α4 subunit, in conjunction with β2 and δ, form receptors that mediate the vast majority of the extrasynaptic, tonic conductance in WT VB neurones.

6.5. THIP selectively enhances tonic inhibiton in WT, but not $\alpha4^{0/0}$, VB neurones

To further investigate $GABA_AR$-mediated neurotransmission in VB neurones, I sought to establish how α4-subunit deletion impacted on the pharmacology of ligands that are commonly regarded to preferentially interact with extrasynaptic $GABA_ARs$

incorporating the δ subunit. These drugs included THIP, DS2 and the neurosteroid 5α3α.

At low concentrations (≤ 1 μM) THIP displays a preferential interaction with δ-$GABA_A$Rs where it acts as a high efficacy GABA-site agonist that (Brown *et al*, 2002). In agreement with this action and with a previous study (Chandra *et al*., 2006), THIP (1 μM) had no effect on the mIPSCs recorded from either WT, or $\alpha4^{0/0}$ VB neurones, whereas this drug evoked a large bicuculline-sensitive tonic current in WT, but not in $\alpha4^{0/0}$ VB neurones. The greatly reduced effect on the tonic conductance seen in $\alpha4^{0/0}$ VB neurones in response to a δ-selective concentration of THIP corroborates the view that the α4 subunit co-assembles with the δ subunit to form extrasynaptic $GABA_A$Rs in VB neurones (Sur *et al*., 1999; Belelli *et al*., 2005; Chandra *et al*., 2006; Herd *et al*., 2009).

6.6. $\alpha4^{0/0}$ VB neurones exhibit a residual tonic conductance that is enhanced by THIP

Interestingly, the deletion of the α4 subunit did not completely abolish the tonic current as evidenced by a residual outward current upon bicuculline application. Although this effect was not reported in a similar study of $\alpha4^{0/0}$ VB neurones (perhaps because of differences in the recording temperature *i.e.* 35°C *vs* room temperature – Chandra *et al*., 2006) the residual tonic current observed here is consistent with that reported for VB neurones derived from $\delta^{0/0}$ mice (in which recordings were performed under identical conditions to the present study - Herd *et al*., 2009). Whether the same $GABA_A$R subtype mediates this residual tonic current in both strains is unknown. Moreover, it also remains to be determined whether this current represents a compensatory attempt by the neurone to restore the tonic current, or whether it represents a component of the WT tonic current. A precedent for the latter scenario has been demonstrated in

hippocampal DGGCs in which the majority of the tonic current is mediated by δ-$GABA_A$Rs with a small contribution from α5-$GABA_A$Rs (Glykys *et al*., 2008). However, there is little if any evidence supporting the expression of α5-$GABA_A$Rs in the VB nucleus (Sur *et al*., 1999; Pirker *et al*., 2000).

Application of the δ-$GABA_A$R preferring agonist THIP (1 μM) evoked a significant enhancement of the residual tonic current in $\alpha4^{0/0}$ VB neurones in this study, in common with equivalent experiments performed on $\delta^{0/0}$ VB neurones (Herd *et al*., 2009). Clearly, the THIP-sensitive residual tonic current is not mediated by α4- or δ-$GABA_A$Rs. Hence it may be speculated that the extrasynaptic $GABA_A$Rs that underlie the THIP-sensitive residual tonic current are composed of αβ isoforms. When expressed recombinantly, such receptors are blocked by low concentrations of Zn^{2+} (Krishhek *et al*., 1998). In hippocampal pyramidal neurones maintained in cell culture, putative receptors composed solely of α and β subunits have been reported based, in part, on the observation that a component of the tonic current in these neurones is blocked by a low concentration of Zn^{2+} (10 μM - Mortensen & Smart, 2006). Furthermore, THIP has been reported to exhibit high efficacy at recombinant α4β3 receptors expressed in *Xenopus* oocytes (Stórustovu & Ebert, 2005). Therefore it is plausible that αβ isoforms may mediate the residual tonic currents observed here in $\alpha4^{0/0}$ and elsewhere in $\delta^{0/0}$ VB neurones (Herd *et al*., 2009), though evidence for the existence of $GABA_A$Rs composed of α and β subunits in these neurones is lacking. To assess this hypothesis, futures studies may seek to investigate the Zn^{2+} sensitivity of the residual tonic conductance in $\alpha4^{0/0}$ (and $\delta^{0/0}$) VB neurones.

6.7. DS2 selectively enhances tonic inhibiton in WT, but not $\delta^{0/0}$, VB neurones

DS2 is a recently developed synthetic ligand that is a selective positive modulator of recombinant δ-$GABA_A$Rs (Wafford *et al*., 2009). Furthermore, DS2 has been shown to augment the tonic conductance of VB neurones whilst having no effect on mIPSCs (Wafford *et al*., 2009). Consistent with this report, 10 μM DS2 had no effect on VB mIPSCs. However, 10 μM DS2 evoked a considerable inward current. To assess whether these effects were mediated by a selective interaction with δ-$GABA_A$Rs, recordings from $\delta^{0/0}$ VB neurones were performed. As with WT recordings, DS2 (10 μM) did not affect any of the properties of mIPSCs recorded from $\delta^{0/0}$ VB neurones. However, in contrast to WT, DS2 did not affect the holding current in VB neurones derived from $\delta^{0/0}$ mice. These findings are consistent with the δ-selective actions of DS2, and confirm this compound as the first synthetic positive allosteric modulator selective for δ-$GABA_A$Rs. The location of the binding site for DS2 on the $GABA_A$R is currently unknown although a recent voltage-clamp study utilising recombinant α4β2/3δ receptors expressed in *Xenopus* oocytes have excluded the possibility of an interaction of this drug at the putative etomidate or neurosteroid binding sites on the receptor (Jensen *et al*., in preparation).

6.8. Low concentrations of 5α3α do not selectively enhance tonic inhibition in VB neurones

Neurosteroids such as the progesterone metabolite 5α3α, are established as being potent endogenous modulators of $GABA_A$R function (Belelli & Lambert 2005; Gunn *et al*., 2011). Here, the actions of 5α3α upon synaptic and tonic inhibition in VB neurones were evaluated in brain slices obtained from both WT and α4-subunit deficient mice. In an initial set of experiments WT VB neurones were treated with 100 nM 5α3α. This

concentration of neurosteroid is considered to be physiologically relevant since brain 5α3α levels are believed to be ~10 nM under normal conditions, but may be elevated following certain physiological conditions (Belelli & Lambert, 2005). For example during pregnancy brain 5α3α levels in excess of 100 nM have been reported (Paul & Purdy, 1992; Concas *et al*., 1998). In WT VB neurones the application of 100 nM 5α3α resulted in a significant prolongation of the mIPSC decay time course, without affecting any of the other mIPSC properties. This is consistent with the widely accepted view that 5α-reduced neurosteroids act as positive allosteric modulators and that for mIPSCs such an action is manifest as a prolongation of the decay time course (Herd *et al*., 2007). Furthermore, the mIPSC prolongation has been resolved at the level of macroscopic kinetics whereby under non-equilibrium conditions, neurosteroids primarily act to slow the recovery of $GABA_A$Rs from desensitization (Zhu & Vicini, 1997). As $GABA_A$Rs exiting desensitized states could re-conduct, this perturbation may elicit a prolongation of the GABA evoked current (Zhu & Vicini, 1997). Moreover, the mIPSC prolonging actions of 5α3α described in this study are consistent with previous studies investigating the actions of both endogenous and synthetic steroids on inhibitory neurotransmission in a variety of CNS locations (for review see Herd *et al*., 2007). More specifically, with respect to this study, the IPSCs recorded in TC neurones have been reported to be sensitive to 5α-THDOC application (100-250 nM - Porcello *et al*., 2003; Cope *et al*., 2005a).

Consistent with recordings from WT VB neurones, the application of 100 nM 5α3α to $\alpha4^{0/0}$ VB neurones resulted in a similar prolongation of the mIPSC decay time course without affecting any of the other mIPSC properties, thus indicating that the genetic deletion of the α4 subunit has little impact on the neurosteroid interaction with synaptic $GABA_A$Rs in VB neurones. Furthermore, this finding argues against the

possibility that the prolongation of WT VB mIPSC decay times by 5α3α (100 nM) is a consequence of a selective potentiation of δ-$GABA_A$Rs.

With respect to the endogenous tonic conductance in WT VB neurones, 100 nM 5α3α evoked a modest inward current that was reversed by bicuculline, an effect that was absent in recordings from $\alpha4^{0/0}$ VB neurones. Furthermore, in recordings of WT neurones a 10 fold greater concentration of the steroid (1 μM 5α3α) produced a similar inward current to that observed with 100 nM. Therefore, in comparison to the actions of THIP (1 μM) and DS2 (10 μM) described above, the tonic-enhancing actions of 100 nM and 1 μM 5α3α were relatively limited. These results on thalamic extrasynaptic $GABA_A$Rs do not support the thesis that δ-$GABA_A$Rs are important molecular targets for low, physiologically relevant concentrations of neurosteroids (Stell *et al*., 2003; Scimemi *et al*., 2005; Shen *et al*., 2007 - see below). Therefore, to further investigate whether thalamic δ-$GABA_A$Rs are neurosteroid-sensitive I investigated the interaction of 5α3α and THIP. I hypothesised that since 5α3α is a positive allosteric modulator of $GABA_A$R function, whereas THIP is a high efficacy agonist at this receptor isoform, it is possible that when THIP is applied in the presence of 5α3α, the THIP response should be augmented due to allosteric modulation. To test the validity of this proposal, initial experiments utilised the δ-$GABA_A$R selective modulator DS2. Indeed, compared to THIP alone, application of THIP (1 μM) in the presence of DS2 (10 μM) resulted in a significant increase in the THIP-induced inward current. However, when this experiment was repeated with 5α3α (100 nM), no difference was observed between the THIP-evoked current in the presence of 5α3α and the THIP-alone evoked current.

These results are perhaps surprising considering the evidence favouring a selective neurosteroid/δ-$GABA_A$R interaction. First, $\delta^{0/0}$ mice exhibit a blunted response to many of the behavioural actions of neurosteroids (Mihalek *et al*., 1999). In addition, studies carried out on recombinant $GABA_A$Rs have uniformly identified that receptors

containing the δ subunit are more sensitive to the GABA-potentiating actions of neurosteroids compared to receptors which contain the γ2 subunit (Belelli *et al*., 2002; Brown *et al*., 2002; Wohlfarth *et al*., 2002; Glykys *et al*., 2007). Subsequently, it was shown that neurosteroids shifted GABA from a low to a high efficacy mode at δ-$GABA_A$Rs thus accounting for the preferential interaction of neurosteroids with these receptors (Bianchi & Macdonald, 2003). At native $GABA_A$Rs in neurones, a selective enhancement of δ-$GABA_A$R mediated tonic inhibition with low concentrations of neurosteroids has been reported (Stell *et al*., 2003; Scimemi *et al*., 2005; Shen *et al*., 2007). For example, the tonic conductance present in DGGCs and CGCs, but not the synaptic events of these neurones, was enhanced by 10 nM 5α-THDOC, an effect blunted in neurones derived from $\delta^{0/0}$ mice (Stell *et al*., 2003). However, other studies performed on thalamic TC neurones have failed to reproduce this selectivity and potency of neurosteroid action on δ-$GABA_A$R tonic currents (Porcello *et al*., 2003; Cope *et al*., 2005a). Hence, whereas 5α-THDOC (250 nM) clearly prolonged the eIPSC decay time course of VB neurones, this concentration of neurosteroid has no effect on the baseline noise (RMS) in these neurones (Porcello *et al*., 2003). Furthermore, in TC neurones of the dLGN, 5α-THDOC (100 nM) produced only a modest enhancement of tonic conductance, although this concentration also impinged on synaptic inhibition as demonstrated by a prolongation of the sIPSC decay time (Cope *et al*., 2005a). These previous findings from studies performed on TC neurones are complementary to those reported here in which 1) 5α3α (100 nM) has only a modest effect on the VB tonic conductance and that this concentration of neurosteroid also prolongs the mIPSC decay time, and 2) that 5α3α (100 nM) does not enhance the THIP evoked current in VB neurones. Importantly therefore, low, physiologically relevant concentrations of 5α3α do not discriminate between tonic and synaptic inhibition in VB neurones. Considering thalamocortical neurones exhibit one of the greatest δ-subunit expression levels in the

brain (Wisden *et al*., 1992; Pirker *et al*., 2000) which is associated with a considerable tonic conductance (Belelli *et al*., 2005; Peden *et al*., 2008; Herd *et al*., 2009), it is surprising that modulation of these receptors by 5α3α is relatively weak. Therefore, it is proposed that future experimental design should caution against the assumption that low neurosteroid concentrations can be used as a pharmacological tool to selectively enhance the function of δ-$GABA_A$Rs in all neurones.

What molecular explanations might account for the discrepancy between neurosteroid sensitivity at δ-$GABA_A$Rs expressed recombinantly and those that are native to VB neurones? As previously described, the phosphorylation status of the $GABA_A$R complex may influence neurosteroid sensitivity of neuronal $GABA_A$Rs (Hodge *et al*., 1999; 2002; Brussaard *et al*., 2000; Fancsik *et al*., 2000; Harney *et al*., 2003; Koksma *et al*., 2003). For example, a critical role for $GABA_A$R phosphorylation in governing neurosteroid sensitivity of sIPSCs has been demonstrated for magnocellular oxytocin releasing neurones of the hypothalamic supraoptic nucleus during pregnancy (Brussaard *et al*., 2000; Koksma *et al*., 2003). Therefore it is plausible that under normal conditions the phosphorylation status of the δ-$GABA_A$Rs in VB neurones renders them relatively insensitive to neurosteroid modulation. However, it is difficult to surmise whether increasing or decreasing receptor phosphorylation in VB neurones would enhance neurosteroid sensitivity because 1) there is a paucity of studies examining the role of phosphorylation on neurosteroid sensitivity at extrasynaptic $GABA_A$R subtypes, and 2) the effects of $GABA_A$R phosphorylation on neurosteroid sensitivity are complex and neurone specific (reviewed in Belelli & Lambert, 2005).

However, findings from a recent investigation into ethanol sensitivity at δ-$GABA_A$Rs may provide an impetus for future research (Choi *et al*., 2008). In this study Choi and colleagues reported that the ethanol enhancement of the tonic current present in TC neurones is regulated by the PKC isoform, δ (PKCδ). Specifically, the tonic

current in TC neurones was found to be less sensitive to enhancement by ethanol (30 mM) in brain slices derived from PKCδ$^{0/0}$ mice. Moreover, behavioural analysis of PKCδ$^{0/0}$ mice revealed them to have a reduced sensitivity to the ataxic effects of 5α3α, but not flunitrazepam (Choi *et al*., 2008). Hence, it remains to be seen whether selectively enhancing PKCδ in VB neurones enhances the sensitivity of the tonic conductance to low neurosteroid concentrations.

An alternative interpretation of the relatively modest effects of 5α3α on the tonic current observed here in VB neurones is that local metabolism converts 5α3α to a GABA-inactive precursor thus diminishing the concentration of 5α3α experienced by δ-$GABA_A$Rs. A similar scenario has been reported in mouse DGGCs where it was found that the relative insensitivity of 5α3α at prolonging the mIPSC decay time was because of the predominance of the membrane bound isoform of 3α-HSD in these cells (*i.e.* the isoform which favours conversion of 5α3α to 5α-DHP - Belelli & Herd, 2003). Indeed, the metabolically stable 5α3α derivative, ganaxolone, elicited a greater effect on the mIPSC decay time relative to 5α3α and blocking 3α-HSD increased the mIPSC prolonging action of 5α3α (Belelli & Herd, 2003). Therefore experiments assessing the relative effect of ganaxolone may prove instructive in determining whether metabolism influences the sensitivity of the tonic conductance to 5α3α in VB neurones

6.9. The developmental speeding of inhibitory synaptic transmission: a role for neurosteroids?

The properties of mIPSCs recorded from VB TC neurones and L2/3 pyramidal neurones have been studied across postnatal development (P7 – P20-24). These studies highlighted two general developmental principles for the mIPSCs recorded from these neurones - namely an increase in mIPSC frequency coupled with a decrease in the

duration of the mIPSC decay time. In addition to previous investigations performed on cortical (Dunning *et al*., 1999; Bosman *et al*., 2005) and TC neurones (Okada *et al*., 2000; Peden *et al*., 2008), these observations are also consistent with studies performed on CGCs (Brickley *et al*., 1996; Tia *et al*., 1996; Vicini *et al*., 2001; Ortinski *et al*., 2004), hippocampal CA3 pyramidal cells (Rovira & Ben-Ari, 1993) and DGGCs (Hollrigel & Soltesz, 1997; Kapur & Macdonald, 1999). An increased mIPSC frequency indicates that the probability of spontaneous GABA release increases with development. The ontogenic mechanisms responsible for the increase in the mIPSC frequency have not been investigated in this study, however insights are provided from previous work. First, the number of synapses increases dramatically during the second postnatal week (Blue & Parnavelas, 1983a; Blue & Parnavelas, 1983b), a time-point which in this study coincided with a substantial increase in mIPSC frequency in both VB and L2/3 neurones. Second, in both cortical neurones and CGCs maintained in cell culture, GAD staining experiments revealed no change in the relative proportion of GABA-ergic cells between 1 and 4 weeks *in vitro* thus indicating that the developmental increase in mIPSC frequency was not due to an increase in the number of GABAergic neurones (Dunning *et al*., 1999; Ortinski *et al*., 2004). Therefore, it appears that the developmental increase in mIPSC frequency observed here and in other studies can be accounted for by an increase in synaptogenesis, particularly towards the end of the second postnatal week, and also by a concomitant increase in the probability of release.

During development the mIPSC decay time decreased in both VB neurones and L2/3 neurones. Several studies on a variety of CNS neuronal types have uniformly reported that an α2/3 to α1 subunit switch most likely underlies the developmental decrease in the duration of IPSCs (Dunning *et al*., 1999; Okada *et al*., 2000; Juttner *et al*., 2001; Bosman *et al*., 2002, 2005; Ortinski *et al*., 2004). In the present study as well as others, cortical L2/3 pyramidal neurones derived from $\alpha1^{0/0}$ mice displayed mIPSCs

with longer decay kinetics compared to WT from early life through to maturity (Bosman *et al*., 2005). However, a finding common to many of these studies is that a significant component of the developmental decrease in IPSC decay kinetics occurs independently of the α1 subunit. A striking example of this phenomenon has been provided by Peden and colleagues. As previously described, the developmental expression of synaptic $GABA_A$Rs in VB neurones involves a near complete change in receptor subtypes such that the immature receptor subtype, α2βγ2 is replaced with the adult subtype α1β2γ2 towards the end of the second postnatal week (Peden *et al*., 2008). However, the authors reported a substantial decrease in mIPSC decay time in VB neurones between P8/9 and P10/11, a time point that preceded α1-subunit protein detection (Peden *et al*., 2008). In agreement, the mIPSCs at P10-11 were insensitive to an α1-$GABA_A$R selective concentration of zolpidem (100 nM) and in experiments performed on VB neurones derived from P8-11 $\alpha1^{0/0}$ mice, mIPSCs presented with decay kinetics that were indistinguishable to those observed in equivalent WT recordings. Collectively, these findings indicate that the α1 subunit is not involved in synaptic inhibition before P11 in VB neurones. This conclusion raises the question of what alternative mechanisms are responsible for the developmental plasticity in the mIPSC decay time observed prior to P11?

One conceivable explanation is a developmental increase in synaptic $GABA_A$Rs containing the α4 subunit since these receptors display relatively rapid decay kinetics (Lagrange *et al*., 2007; Picton & Fisher, 2007). However, immunohistochemical investigation revealed that α4 subunit immunofluorescence did not colocalise with gephyrin, a marker of inhibitory synapses (Peden *et al*., 2008).

Several alternative mechanisms, other than changes in postsynaptic receptor subtype, may also contribute to the decay time course of mIPSCs. These include post-translational modifications of synaptic proteins, alterations of the cytoskeleton, changes

in the kinetics of GABA release and changes in the expression of GATs (Jones & Westbrook, 1996; Petrini *et al*., 2003; Mozrzymas, 2004; Houston *et al*., 2008; Arancibia-Carcámo & Kittler, 2009; Barberis *et al*., 2011). However, evidence presented in this study indicates that early in postnatal development, the mIPSC decay time is greatly influenced by an endogenous neurosteroid presence.

6.10. A developmentally regulated endogenous neurosteroid tone prolongs mIPSCs

Pre-treatment of P6-8 brain slices with the 5α-reductase (5α-R) inhibitor finasteride (50 μM) prior to obtaining whole-cell patch clamp recordings from either VB or L2/3 neurones, resulted in mIPSCs with significantly faster decay kinetics compared to non-treated controls. These results are indicative of a tonic neurosteroid production that is sufficient to prolong the mIPSC decay time course at P6-8. However, these experiments required long (> 4 hr) pre-incubation periods with finasteride before an effect on mIPSC decay time was reliably observed. Presumably, this reflects the time required for the existing levels of neurosteroid to become depleted, either by metabolism, or by diffusion from the slice. With respect to the latter scenario, the long finasteride pre-incubation is perhaps not surprising given the highly lipophilic nature of such steroids (Chisari *et al*., 2010). Therefore, in order to perform a more efficient investigation of how a putative neurosteroid tone may influence synaptic inhibition across postnatal development I utilised the steroid scavenging molecule, γ-cyclodextrin (γ-CD – Shu *et al*., 2007). In these experiments γ-CD (1 mM) was applied in the extracellular (1 mM) and intracellular solutions (0.5 mM) and brain slices were preincubated for a minimum of 1 hr prior to recording in the presence of γ-CD (1 mM). This experimental protocol is referred to henceforward as "γ-CD pre-incubation".

6.10.1. VB neurones

In agreement with a previous study performed in the host laboratory (Peden *et al*, 2008) the decay time of mIPSCs recorded from P7, P8, P10 and P20-24 VB neurones, decreased with development, with the majority of this decrease occurring between P7 and P10. With a clear similarity to the actions of finasteride, γ-CD pre-incubation resulted in VB mIPSCs at P7 and P8 with significantly faster decay times relative to control whereas other mIPSC parameters were largely unaffected (but see below regarding P7 mIPSC frequency). However, at P10 and P20-24 the γ-CD treatment had no effect on the mIPSC decay. Hence, it is proposed that in VB neurones the developmental decrease in mIPSC decay time between P7-P10 observed here and by others (Peden *et al*., 2008) is primarily a consequence of the disappearance of an endogenous neurosteroid action at synaptic $GABA_A$Rs in VB neurones.

Comparison of the action of finasteride and γ-CD pre-incubation revealed both treatments to induce a significant increase in the VB neurone mIPSC frequency at P7 only (Table 4.3). This finding could imply that at P7, endogenous neurosteroids may modulate pre-synaptic $GABA_A$Rs located on nRT neurone boutons with the effect of reducing the frequency of spontaneous vesicular release.

Although there are relatively few reports of presynaptic $GABA_A$Rs in higher centres of the CNS, neurosteroids have previously been demonstrated to influence the frequency of post synaptic events. Specifically, in hippocampal mossy fibre terminals presynaptic $GABA_A$Rs were recently shown to be influenced by a low concentration of the neurosteroid 5α-THDOC (10 nM) indicating that these receptors contain the δ subunit (Ruiz *et al*., 2010). Furthermore, due to localised differences in the transmembarne Cl^- gradient, presynaptic $GABA_A$R activation depolarised the bouton thus facilitating glutamatergic transmission (Ruiz *et al*., 2010). Similarly in neurones of

the rat preoptic nucleus, 5α3α (2 μM) application resulted in an increased frequency of sIPSCs (Haage *et al*., 2002). However, there are currently no indications of presynaptic $GABA_A$Rs at nRT boutons that terminate on to VB neurones. Furthermore, the studies outlined above observed neurosteroid-induced facilitation of release rather than the putative neurosteroid–induced suppression of release proposed here. Nevertheless, the increase in mIPSC frequency at P7 VB neurones described here following neurosteroid depletion/removal may warrant further investigation.

6.10.2. L2/3 pyramidal neurones

The mIPSCs recorded from L2/3 pyramidal neurones of cortical brain slices derived from P7, P8, P9, P10, P15 and P20-24 became progressively faster decaying with development with the exception of P10 when a secondary prolongation of the mIPSC decay time was observed. Subsequent experiments showed that L2/3 mIPSCs also displayed a developmentally regulated sensitivity to γ-CD pre-incubation. However, in comparison to VB recordings, this effect was protracted with mIPSCs at P15 exhibiting faster decay times in response to γ-CD pre-incubation. Moreover, at P10 the effect of γ-CD was greater than that observed for P9 neurones. These findings suggest that the secondary developmental increase in mIPSC decay time observed at P10 is due to an increased production of neurosteroids. This proposal is corroborated by a previous study that used radioimmunoassay to measure the 5α3α concentration in rat cortex during postnatal development (Grobin & Morrow, 2001). The authors demonstrated that 5α3α levels undergo dynamic changes across development whereby relatively high perinatal 5α3α levels decrease following birth and continue to decrease until P10 when a secondary peak in 5α3α levels was observed that persisted until P14 (Grobin & Morrow, 2001).

Compared to VB neurones, L2/3 neurones exhibit a more complex developmental pattern of $GABA_AR$ subtype expression. For example, the α1 subunit protein and mRNA is present in the cortex early in development albeit at low levels, whereas the converse is true for α2/3 subunits which are highly expressed early in life before they decrease to lower, yet significant levels in the mature cortex (Laurie *et al*., 1992b; Fritschy *et al*., 1994; Pirker *et al*., 2000). Thus, considering that a putative tonic neurosteroid production occurs amidst a backdrop of changes in $GABA_AR$ subunit expression, the impact of α1 subunit deletion was investigated. In contrast to mIPSCs recorded from VB neurones which, at P7 and P8, are unaffected by the absence of the α1 subunit (Peden *et al*., 2008), mIPSCs obtained from $\alpha1^{0/0}$ L2/3 neurones at P7/8, P10, P15 and P20-24 exhibited slower decay kinetics compared to WT controls at each developmental time-point. Since α1-$GABA_ARs$ are associated with relatively fast decaying IPSC kinetics (Picton & Fisher, 2007) this finding indicates that a proportion of α1-$GABA_ARs$ are present even at P7/8 in these neurones. However, a developmental decrease in mIPSC decay time in $\alpha1^{0/0}$ L2/3 neurones was still evident implying the presence of additional factors (as has been previously reported – Bosmann *et al*., 2005). Indeed, the mIPSCs from P7/8, P10 and P15 $\alpha1^{0/0}$ L2/3 neurones were not only faster decaying following intracellular γ-CD treatment (0.5 mM – "γ-CD ICS"), but the developmental profile of γ-CD sensitivity was indistinguishable to WT (*i.e*. ≤P15 = γ-CD sensitive; P20-24 = γ-CD insensitive). These results indicate that the endogenous neurosteroid tone occurs irrespective of the $GABA_AR$ subunit composition in L2/3 pyramidal neurones and contributes to the developmental decrease in the duration on mIPSCs.

6.11. γ-CD: the impact of non-specific actions

Clearly, the validity of the findings reported here depends largely on the assumption that γ-CD forms effective inclusion complexes with the endogenous neurosteroid thereby terminating the steroid's interaction with the $GABA_AR$. Manufactured from starch, CDs comprise a series of cyclic oligosaccharides that assume a three-dimensional structure endowing them with useful properties for pharmaceutical applications (Davis & Brewster, 2004). The three most common CDs differ in the number of glucose residues in their structure and are named accordingly: α-CD (pentameric), β-CD (hexameric) and γ-CD (octomeric). Structurally, CDs can be likened to a cup in which the interior cavity is relatively apolar thus creating a hydrophobic micro-environment. This contrasts with the cavity exterior which, due to the large number of hydroxyl groups, is relatively hydrophilic – a facet that makes most CDs readily water soluble (Davis & Brewster, 2004). These properties are responsible for the ability of CDs to form inclusion complexes with hydrophobic guest molecules, such as neurosteroids (Davis & Brewster, 2004; Shu *et al*., 2004, 2007).

Since there are very few reports demonstrating steroid encapsulation by a CD in brain slice tissue (*i.e.* Murayama *et al*., 2006; Izumi *et al*., 2007), it is worthwhile considering the specificity of γ-CD action. For instance, the current responses elicited by ultrafast GABA application to excised patches from rat cultured hippocampal neurones were found to be modulated by β-CD in a concentration dependent manner (0.5-1.5 mM - Pytel *et al*., 2006). Specifically, β-CD increased the current amplitude elicited by saturating GABA concentrations, and induced perturbations of the macroscopic decay kinetics that cumulatively led to an increase in current decay times (Pytel *et al*., 2006). These findings suggest that an increase in the mIPSC decay time might be expected following γ-CD application. However, in both VB and L2/3 neurones

γ-CD induced a marked reduction in the mIPSC decay time early in development and had no effect on this parameter at later developmental time-points (*e.g.* P20-24). Importantly, pre-incubation with α-CD had no effect on any of the mIPSC properties at any age. The simplest and most parsimonious explanation for the effect of γ-CD pre-incubation to decrease the duration of immature L2/3 neurone mIPSCs following γ-CD pre-incubation is that the steroid-sequestering molecule is effective in forming inclusion complexes with endogenous neurosteroids, whereas the observed insensitivity to α-CD reflects the hydrophobic inner cavity being too small to accommodate steroids (Szejtli, 1998; Shu *et al*., 2004).

In agreement with the actions of γ-CD proposed here, other studies have failed to observe any direct interaction between γ-CD and $GABA_A$Rs (Shu *et al*., 2004, 2007). Specifically, for primary hippocampal neurones maintained in cell culture, currents generated by the brief application of GABA were unaffected by 0.5 mM γ-CD application Similarly, this concentration of γ-CD had no effect on GABA evoked currents mediated by α1β2γ2 expressed in *xenopus* oocytes (Shu *et al*., 2004, 2007). Collectively, these findings argue against the idea that a direct interaction between γ-CD and $GABA_A$Rs underpins the decrease in mIPSC decay time observed here early in postnatal development.

To address the issue of γ-CD specificity directly, WT P7 brain slices were pre-incubated in the presence of finasteride (50 μM, ≥ 4 hrs) and mIPSCs recorded from L2/3 pyramidal neurones with γ-CD (0.5 mM) present in the intracellular solution (the effects of intracellular γ-CD treatment are discussed more fully below). Under these conditions mIPSCs presented with decay times that were modestly, but significantly, faster than the mIPSC decay times following finasteride-alone or intracellular γ-CD-alone (Figure 5.6). Nevertheless, due to the relatively modest difference between the actions of finasteride-alone or intracellular γ-CD-alone *vs* finasteride/γ-CD combined, it

is proposed that the combined treatment results in a more complete clearance of the neurosteroid from the brain slice. This view is supported by the fact that finasteride and γ-CD operate *via* distinct mechanisms (*i.e.* depletion *vs* scavenging) to remove the neurosteroid.

However, it remains a possibility that the findings reported in this study concerning the effects of γ-CD were due, in some part, to the non-specific encapsulation of other compatible guest molecules that are important to $GABA_AR$ function. Indeed, it is reasonable to assume that inclusion complexes with other lipophilic molecules do occur *in vitro* since CDs have been used experimentally for a variety of different purposes including extraction of cholesterol from the plasma membrane (Yancey *et al*., 1996), removal of lipophilic fluorescent markers (Kay *et al*., 1999) and for complexing solvents such as DMSO (Aree & Chaichit, 2002). The cholesterol-sequestering action of γ-CD may be of particular relevance to this study considering that this steroid is an important lipid constituent of the plasma membrane. Indeed, it was recently shown in cultured hippocampal CA1 neurones that cholesterol depletion of the synaptic membrane using methyl-β-CD (15 mM) gave rise to an increased probability of spontaneous vesicular release thus raising the possibility that cholesterol acts as an important regulator of this process (Wasser *et al*., 2007). Here, γ-CD pre-incubation did not affect mIPSC frequency (which can be considered a proxy of an increased probability of spontaneous release) in L2/3 pyramidal neurones at any developmental age tested (Table 5.2). For VB neurones, γ-CD pre-incubation had no effect on the mIPSC frequency at P8, P10 or P20-24, however, P7 VB mISPCs were significantly more frequent *vs* control recordings (an effect also observed for finasteride - Table 4.3). Hence, it is unlikely that γ-CD pre-incubation resulted in a gross depletion of plasma membrane cholesterol especially considering that 1) γ-CD is less effective than β-CD in

this regard (Szetji, 1998) and 2) the CD concentration used by Wasser *et al*. far exceeded the concentration used here (15 mM *vs* 1 mM). .

At least two further lines of evidence counteract the possibility of cholesterol removal accounting for the effects of γ-CD. 1) In this study γ-CD had no discernible effect on mIPSCs recorded from P20-24 VB or L2/3 pyramidal neurones. 2) Intracellular γ-CD application (0.5 mM) resulted in a relatively rapid decrease in mIPSC decay time (~75% of the decrease occurred within 3-5 mins of attaining the whole-cell configuration, Table 4.4) which is inconsistent with estimations of the rate of cholesterol removal by 0.5 mM β-CD (~75% of membrane cholesterol required 21 mins - Haynes *et al*., 2000).

In agreement with the proposed action of γ-CD in this study, the ability of γ-CD to remove neurosteroid from a synapse and thereby terminate the steroids modulatory action at $GABA_ARs$ has been demonstrated in autaptic hippocampal neurones maintained in cell culture. In particular, application of γ-CD alone induced only a very modest decrease in the IPSC decay time, possibly due to the presence of endogenous neurosteroids (Shu *et al*., 2007). However, the IPSC potentiating effects of exogenously applied 5α3α (100 nM) were virtually abolished upon 0.5 mM γ-CD application (Shu *et al*., 2007). These results suggest that γ-CD can be used relatively selectively without majorly affecting post-synaptic function.

6.12. The regulation of the neurosteroid tone influencing $GABA_ARs$ during development

A principal finding of this study is that during the second week of life an endogenous neurosteroid production exerts a modulatory influence on synaptic $GABA_ARs$ that is

reflected by a prolongation of the mIPSC decay time course. These findings raise questions concerning the location of neurosteroid synthesis during early development.

One possibility is that the developmentally regulated effects of neurosteroids at synaptic $GABA_ARs$ represent a diminishing supply of maternal neurosteroids following birth. Indeed, neurosteroid levels in pregnant females are relatively high during pregnancy (Concas *et al*., 1998). This explanation is unlikely, however, since the ability of the 5α-R inhibitor finasteride to reduce the mIPSC decay time suggests that the brain slice tissue must be utilizing an intrinsic neurosteroidogenic capacity. On the other hand, this evidence does not exclude the possibility that a portion of the neonatal neurosteroid pool is derived from peripherally imported steroid precursors (*e.g.* progesterone). It has been demonstrated that mIPSCs from P9-15 lamina II neurones of the dorsal horn similarly exhibit a neurosteroid tone that can be blocked by pre-treating the spinal slice with the TSPO inhibitor, PK11195 for > 5 hrs (Inquimbert *et al*., 2008). Since TSPO is the first step in neurosteroidogenesis, this finding suggests that the spinal cord tissue harbours the capacity to manufacture neurosteroids from cholesterol during development (Inquimbert *et al*., 2008). In order to assess whether these findings extend to VB and L2/3 neurones, future experiments in which TSPO activity is pharmacologically manipulated may prove instructive.

The developmental neurosteroid tone described in this study could be a consequence of elevated neurosteroid levels in early postnatal life, changes in the sensitivity of the $GABA_AR$ to neurosteroid modulation, or indeed a combination of the two. It is distinctly plausible that developmental differences in the expression of neurosteroidogenic enzymes contribute to the neurosteroid tone. During development 5α-R is expressed as early as embryonic day 12 (Do Rego *et al*., 2009) and primary neuronal cultures from rat embryo brains express 5α-R mRNA and protein in neurones (Melcangi *et al*., 1993) as well as in glia (Melcangi *et al*., 1994) after 5 days *in vitro*.

Furthermore, during the late embryonic/early neonatal period in rats, 5α-R mRNA was reported to be expressed in the sub-cortical plate and the thalamus (Lauber *et al*., 1996; Poletti *et al*., 1998; Do Rego *et al*., 2009). Hence, 5α-R expression is well established by birth in the rodent brain. Although less information is available regarding the developmental expression of 3α-HSD compared with 5α-R, both these enzymes have been reported to show a high level of activity during the first two postnatal weeks (Eechaute *et al*., 1999; Tsuruo, 2005; Do Rego *et al*., 2009). Furthermore, other studies have confirmed that neonatal 5α3α levels are relatively high around birth and diminish to adult levels towards the end of the second postnatal week (Grobin & Morrow, 2001). As described above the secondary increase in cortical 5α3α levels at P10 (Grobin & Morrow, 2001) is in perfect agreement with the elevated mIPSC decay time at this age described in this study. Together, these findings are consistent with elevated neurosteroid levels early during development.

The sensitivity of $GABA_A$Rs to neurosteroid potentiation may be governed by numerous, aforementioned factors including receptor subunit composition, post translational modification and local neurosteroid metabolism (Belelli & Lambert, 2005). Here, application of exogenous 5α3α (1 μM) to P7 VB neurones elicited a significant prolongation of the mIPSC decay time course. Importantly, the magnitude of this effect was not significantly different to that observed for P20-24 VB mIPSCs following 1 μM 5α3α. However, although it may be tentatively concluded that neurosteroid sensitivity remains constant over this developmental period, it is difficult to draw a firm conclusion because mIPSCs from P7 VB neurones are already under the influence of an endogenous neurosteroid tone. In this respect, future studies in which the sensitivity of exogenous 5α3α is examined in P7 VB neurones following finasteride pre-treatment may be helpful. In summary, the available evidence from this study and others indicates that the developmentally regulated prolongation of mIPSCs from VB and L2/3 neurones

by a native neurosteroid presence is most likely the result of dynamic changes in neurosteroid levels that are governed by the co-ordinated expression of neurosteroidogenic enzymes and the availability of neurosteroid substrates.

5α-dihydroprogesetrone (5α-DHP) is the immediate precursor to 5α3α and this enzymatic conversion is mediated by 3α-HSD (Do Rego *et al*., 2009). Here, acute application or a short pre-incubation period (30-60 mins) with 5α-DHP (3 μM) had no effect on any of the mIPSC properties in P20-24 VB neurones thus confirming this steroid to be inert at $GABA_A$Rs. However, a longer pre-incubation period (> 2 hrs) elicited a striking prolongation of the mIPSC decay time course that was largely blocked by the 3α-HSD inhibitor, indomethacin (30 μM). The molecular reasons for the effectiveness of 5α-DHP treatment relative to exogenous 5α3α are unknown. One possibility is that the 3α-HSD in P20-24 VB neurones strongly favours the forward 5α3α-forming reaction such that the conversion of 5α-DHP is highly efficient. Moreover, it is tempting to speculate on the potential existence of specialized intracellular structures which may preferentially deliver the 5α3α produced by 3α-HSD into the plasma membrane where such steroids may readily access the transmembrane steroid binding sites on the $GABA_A$R.

However, it should be noted that a small component of the 5α-DHP effect remained after incubation with indomethacin (30 μM). It is plausible that this residual action reflects an incomplete inhibition of 3α-HSD, although higher concentrations of indomethacin were not tried. Alternatively, it is possible that genomic actions of 5α-DHP may influence $GABA_A$R subunit expression *via* intracellular PROG receptors (Rupprecht & Holsboer, 1999). Nevertheless, these results suggest that 3α-HSD activity is retained in P20-24 thalamic brain slices. It is therefore likely that the decreased neurosteroid tone observed during development is likely due to a paucity in the supply of the 5α3α precursor, 5α-DHP. A decrease in the level of available 5α-DHP suggests

that one or more steps 'upstream' from 3α-HSD in the neurosteroidogenic pathway are absent or inactive. Unfortunately, the time constraints of the present study prevented further investigations to this end although parallels from other studies are worthwhile considering. In particular, in lamina II (LII) dorsal horn neurones of the spinal cord, a developmentally regulated neurosteroid presence prolongs the mIPSC decay time in neonates, an effect which dissipates completely by maturity (Keller *et al*., 2004b; Poisbeau *et al*., 2005; Inquimbert *et al*., 2008). Co-incubation of > P30 spinal slices with diazepam (1 μM) and flumazenil (10 μM) to selectively activate TSPO prolonged the mIPSC decay time thus demonstrating that the spinal slice preparation retains the ability to manufacture neurosteroids from cholesterol (Keller *et al*., 2004b). Furthermore, TSPO stimulation did not affect the mIPSC decay kinetics of > P30 LIII/IV neurones though 22OH-cholesterol incubation (*i.e.* the next step after translocation of cholesterol by TSPO) resulted in longer mIPSC decay times. Hence, these studies revealed that a full complement of neurosteroidogenic enzymes localised to LII remain active and inducible into adulthood. In contrast, in LIII/IV neurostreoidogenesis is developmentally restricted following either a down regulation or a decreased basal activity of TSPO. Indeed, it was subsequently shown that mIPSCs from both adult LII and LIII/IV neurones were prolonged by a neo-synthesis of neurosteroids following a model of inflammatory pain (Poisbeau *et al*., 2005; Inquimbert *et al*., 2008). Regarding the current study, future experiments may seek to follow a similar pharmacological dissection of the neurosteroidogenic pathway present in brain slice preparations in order to evaluate the limiting-factor in neurosteroid production.

6.13. Intracellular γ-CD treatment

When only the ICS was supplemented with 0.5 mM γ-CD, mIPSCs from P6/7 VB and P7/8, P10 L2/3 neurones exhibited markedly faster decay times compared with the mIPSCs from experiments performed with standard ICS. In fact, in this respect the γ-CD ICS treatment was equally as effective as the γ-CD pre-incubation protocol. To investigate the temporal aspects of these effects, whole cell patch clamp recordings were acquired soon after the whole cell configuration was obtained. This strategy is temporally limited by technical considerations of how quickly the cell's capacitive properties can be compensated for and relies on the whole-cell access resistance to assume a constant value soon after "break-in". Nevertheless, recordings could be reliably obtained ~ 60 secs after acquiring the whole cell mode. These studies showed that the delivery of 0.5 mM γ-CD to the intracellular environment caused a relatively rapid decrease in the mIPSC decay time. The majority (~75 %) of the decrease in decay time was complete after 3-5 minutes, a time scale that is only marginally greater than the predicted dialysis rate before an equilibrium between the intracellular compartment and the pipette is reached (Marty & Neher, 1995). These results provide direct evidence that the γ-CD ICS effect is relatively rapid as perhaps would be expected given 1) the proposed mechanism of action (*i.e*. a neurosteroid "sponge") and 2) previous investigations of the kinetic aspects of steroid sequestration by γ-CD (Shu *et al*., 2004, 2007; Akk *et al*., 2005). Moreover, such a temporal profile precludes the possibility that neurosteroid sequestration by γ-CD prevents steroid-induced gene transcription thereby affecting mIPSC kinetics.

6.14. Putative autocrine actions of neurosteroids

Given that γ-CD is membrane impermeant (Akk *et al*., 2005) it is tempting to speculate that neurosteroidogenesis and neurosteroid-$GABA_AR$ interactions occur in the same neurone. Traditionally, it was believed that neurosteroid production was restricted to glial cell populations based on immunohistochemical studies assessing the brain distribution of steroidogenic enzymes (Pelletier *et al*., 1994; Tsuruo *et al*., 1996; Kiyokage *et al*., 2005). A glial site of production would require neurosteroids to act in a paracrine fashion however there is growing evidence in support of an autocrine mechanism of neurosteroid action. Firstly, a more recent immunohistochemical and *in situ* hybridization study conducted in mouse brain tissue reported that the expression of 5α-R and 3α-HSD (*i.e.* the enzymes required to convert PROG to 5α3α) are primarily restricted to glutamatergic neuronal populations (Agis-Balboa *et al*., 2006). Shortly after, the 5α3α distribution in adult rat brain (investigated using an antibody raised against this neurosteroid) was demonstrated to exhibit a strikingly similar neuronal localisation, with immunostaining for 5α3α restricted predominantly to intracellular and membrane compartments of principal neurone populations (Saalmann *et al*., 2007). With respect to the current study an autocrine neurosteroid action in L2/3 pyramidal neurones is conceivable since these neurones (together with L5 pyramidal neurones) were identified to express relatively high levels of 5α-R and 3α-HSD mRNA and 5α-R protein was found to co-localise with 3α-HSD mRNA in the majority of pyramidal cells. Indeed, only the mitral cells of the olfactory cortex were found to express higher levels of mRNA for these enzymes (Agis-Balboa *et al*., 2006). However, it should be noted that these studies were performed on adult rodents whereas the expression of 5α3α synthesizing enzymes may be different during neonatal development (Do Rego *et al*., 2009).

The concept of an autocrine neurosteroid action has also received support from studies that have investigated the neurosteroid route of access to the $GABA_AR$s (Shu *et al*., 2004, 2006; Akk *et al*., 2005; Chisari *et al*., 2010). These studies have demonstrated that the time taken for the neurosteroid to partition into the plasma membrane is a rate limiting step of $GABA_AR$ potentiation. This was most convincingly demonstrated in voltage clamp experiments performed on dissociated hippocampal neurones and in *xenopus* oocytes recombinantly expressing α1β2γ2L $GABA_AR$s. Specifically, the offset kinetics of steroid potentiation following removal of the free aqueous steroid were markedly hastened by extracellular γ-CD application (Shu *et al*., 2004, 2006; Chisari *et al*., 2009). It was therefore proposed that the slow offset kinetics of neurosteroid action observed under these experimental conditions are due to the slow dissociation of the steroid from the membrane – that is, as opposed to a classical high affinity ligand-receptor interaction which would not render the steroid accessible to γ-CD sequestration (Shu *et al*., 2004, 2006; Chisari *et al*., 2009; Chisari *et al*., 2010).

Numerous studies report low nanomolar concentrations of pregnane steroids such as 5α3α to enhance $GABA_AR$ function suggesting the presence of a relatively high affinity binding site on the receptor (Callachan *et al*., 1987; Harrison *et al*., 1987; Peters *et al*., 1988, for review Lambert *et al*., 1995; Herd *et al*., 2007). However, due to their lipid solubility (5α3α has a LogP of ~ 4.2 – Chisari *et al*., 2009), much greater local concentrations of the neurosteroid, than those present in the aqueous phase, will accumulate in the plasma membrane *i.e.* sited close to the proposed transmembrane binding site(s) on the $GABA_AR$ subunits. In this alternative model, the neurosteroid is considered to have a relatively low absolute affinity for the binding site and consequently only associates briefly with the receptor. However, due to the accumulation of neurosteroid molecules in the membrane, the probability of the receptor

being occupied by the neurosteroid is relatively high and hence low nanomolar aqueous concentrations of neurosteroid are effective.

These studies have collectively indicated that the steroid interaction with the $GABA_AR$ is an inherently low-affinity process, a consequence of which is that in order for neurosteroids to produce their strong modulatory action at $GABA_ARs$, they may have to accumulate in the plasma membrane at much greater concentrations than any given aqueous concentration. Note that experiments utilising a fluorescently-tagged steroid demonstrated strong non-specific membrane accumulation and dissipation of the fluorescence intensity during wash out coincided temporally with a reduction in $GABA_AR$ potentiation (Akk *et al*., 2005). Interestingly, analysis of the fluorescence following application of this steroid revealed a rapid accumulation of steroid in intracellular compartments (Akk *et al*., 2005; Chisari *et al*., 2009) and experiments involving extracellular γ-CD application to "strip" out membrane steroid revealed that this intracellular steroid "reservoir" was in relatively rapid equilibrium with the plasma membrane. Therefore, the lipophilic nature of neurosteroids, the importance of membrane accumulation for steroid access to the $GABA_AR$, and the propensity of steroids to partition into intracellular compartments are all in favour of a spatially restricted neurosteroid action at $GABA_ARs$ (Shu *et al*., 2004, 2007; Akk *et al*., 2005; Chisari *et al*., 2009, 2010). Indeed, the particularly high lipophilicity of 5α3α (LogP ~ 4.2) has led to speculation that this neurosteroid may be trapped in the cell in which it is synthesized such that it becomes a "prisoner" of its own lipohilicity (Chisari *et al*., 2009).

The concept of an exclusive autocrine action for endogenous neurosteroids was considered in the present study. It was hypothesised that if L2/3 pyramidal neurones contain neurosteroidogenic enzymes, whereas GABA-ergic interneurone populations are devoid of these enzymes (Agis-Balboa *et al*., 2006) then mIPSCs recorded from

interneurones may not exhibit γ-CD ICS sensitivity during development. However, the decay times of mIPSCs recorded from P7 and P10 L2/3 interneurones displayed essentially equal sensitivity to γ-CD ICS when compared to recordings from L2/3 pyramidal neurones. Furthermore, in common with mIPSCs recorded from L2/3 pyramidal neurones, interneurone mIPSCs were unaffected by γ-CD ICS treatment by P20-24. These results indicate that $GABA_A$Rs in L2/3 interneurones are also subjected to neurosteroid modulation during development. Whether this is due to a paracrine mode of neurosteroid action or differential enzyme expression in the neonatal brain will require further investigation.

The provenance of the neurosteroid responsible for the mIPSC prolongation in VB neurones during development is also unclear. Although 5α-R and 3α-HSD expression was not evident for adult VB neurones, nRT neurones have been shown to express these enzymes (Agis-Balboa *et al*., 2006). Therefore, VB neurones may receive neurosteroids from the surrounding nRT during development and interestingly, a similar developmentally regulated neurosteroid tone has been confirmed in nRT neurones (S. Humble, unpublished observations). Other observations indicate differences in the regulation of the neurosteroid tone at VB *vs* L2/3 cortical neurones. For example, the neurosteroid presence in L2/3 pyramidal neurones as inferred by mIPSC sensitivity to γ-CD is protracted relative to VB neurones and exhibits a secondary elevation at P10 which may reflect differences in autocrine *vs* paracrine mechanisms in these two neuronal populations.

Clearly, further investigation is required before a better understanding is reached regarding the cellular mechanisms regulating neurosteroid production and action during development. The idea of an autocrine neurosteroid action is particularly appealing as this may afford the glutamatergic cell with a mechanism with which to finely adjust its response to inhibitory input. Interestingly, an elegant mechanism of

autocrine neurosteroid regulation in response to ethanol treatment has recently been described (Tokuda *et al*., 2011). Specifically, the ability of ethanol (60 mM) to inhibit LTP in adult rat CA1 neurones (Izumi *et al*., 2005) was found to involve an activation of unblocked NMDA receptors that subsequently caused a specific enhancement of neurosteroidogenesis within the CA1 neurone (Tokuda *et al*., 2011). Hence, ethanol induced LTP suppression could be blocked by both APV (a broad spectrum competitive NMDA receptor antagonist - 50 μM) and 5α-R inhibitors (finasteride/dutasteride – 1μM). Furthermore, immunohistochemical staining using an antibody against 5α-reduced steroids revealed ethanol to increase staining in a manner that was largely, if not exclusively, confined to CA1 pyramidal neurones - an effect that was mimicked following 1 μM NMDA application and blocked following APV or 5α-R treatment (Tokuda *et al*., 2011). Importantly, this study provides intriguing evidence that, in response to certain stimuli, a neurone may acutely regulate neurosteroidogenesis to induce autocrine effects on neuronal activity.

Immunohistochemical analysis of the cellular localisation of neurosteroid expression during development may prove instructive. Moreover, an alternative approach that may be valuable for assessing an autocrine mechanism of neurosteroid action will be to utilise a preparation in which neurones are dissociated from the brain slice so that they can be studied in isolation. The advantage of this technique, which can be achieved mechanically or enzymatically, is that the presynaptic boutons remain attached to the isolated neurone of interest so that synaptic activity may then be observed using standard whole-cell patch clamp techniques (Jun *et al*., 2011). Hence, by eliminating the influencing factors of surrounding cells, it will be of interest to determine for example whether dissociated P7 VB and L2/3 neurones display sensitivity to γ-CD ICS, or whether more mature neurones (*e.g.* P20-P24) are capable of synthesising $GABA_AR$-active neurosteroids from steroid precursors such as 5α-DHP.

6.15. Physiological implications of a neurosteroid tone influencing mIPSCs during development

A principal and novel finding of this study is that during development, mIPSCs from VB neurones, L2/3 pyramidal neurones and L2/3 interneurones are influenced by a native neurosteroid presence. This finding raises the interesting question: what is the physiological significance of this effect? Although not addressed by the current study, it may be helpful to the design of future endeavours to speculate on possible answers.

Among the myriad of factors that contribute to normal brain development, GABA signalling has emerged as having diverse roles with respect to cell proliferation, differentiation, synaptogenesis, circuit development and circuit function (Represa & Ben-Ari, 2005; Akerman & Cline, 2007; Kuzirian & Paradis, 2011). Indeed, GABA synthesis and signalling begins during mid-gestation, long before the appearance of synaptic communications. At this time GABA acts in a trophic manner and functions through non-vesicular release to tonically activate $GABA_A$Rs expressed on neuronal progenitors thereby influencing the transition from cell proliferation to neuronal differentiation (LoTurco *et al*., 1995; Repressa & Ben-Ari, 2005). A role for neurosteroids during this process has been indicated by the demonstration that 5α3α (0.1-1 μM) significantly increases the rate of proliferation of neuronal progenitors maintained in cell culture (Keller *et al*., 2004a; Wang *et al*., 2005). Migrating neurones may also be influenced by factors which affect GABA signalling (Ben-Ari *et al*., 2007). For instance, administration of 5α3α to neonatal rats resulted in aberrant localisation of parvalbumin-positive interneurones in the adult pre-frontal cortex (Grobin *et al*., 2003). Hence, a neurosteroid/$GABA_A$R interaction is implicated with important developmental actions even at embryonic and perinatal stages.

After birth, GABAergic synapses are established before glutamatergic synapses suggesting a fundamental role for $GABA_AR$ signalling in the regulation of neuronal development (Tyzio *et al*., 1999; Ben-Ari *et al*., 2007). In contrast to mature neurones, $GABA_AR$ activation in many developing neurones elicits a net outward flow of Cl^- ions such that membrane depolarisation ensues. Hence, early in development neuronal excitation is primarily mediated *via* $GABA_ARs$ whereas glutamatergic inputs are relatively weak (Ben-Ari *et al*., 2007). What are the benefits of having an excitatory system mediated by GABA rather than glutamate during neurodevelopment? GABA exerts its excitatory actions with a driving force that is much lower that that of glutamate (~30-40 mV for GABA compared with ~ 80 mV for glutamate) and depolarisation is achieved *via* Cl^- efflux rather than a potentially deleterious Ca^{2+} influx such that collectively, the toxic potential is minimised (Akerman & Cline, 2007; Ben-Ari *et al*., 2007). These intrinsic features are therefore permissive in one respect, allowing depolarisation to occur in "safety mode" such that VGCCs may be activated and primitive network oscillations propagated. On the other hand, it also occludes the necessity, in the immature brain, to have powerful hyperpolarising inhibition to counteract powerful excitation (Ben-Ari *et al*., 2004). Under these conditions activity-dependent plasticity continues and provides the essential functional cues for the temporal and spatial maturation of network activity. Interestingly, the longer the duration of $GABA_AR$ mediated post synaptic currents (PSCs), the greater the likelihood that synaptic currents generated in synapse-sparse neurones will summate. Hence, long PSC kinetics maximise the integrative window of opportunity, a property that could be essential for a neurone to establish excitatory connections and become part of the network (Akerman & Cline, 2007). The findings of the present study may have important implications for this notion. Indeed, the neurosteroid tone described here is most effective at a time when GABA is still depolarising whereas the dissipation of the

neurosteroid effect on mIPSCs coincides with an increasing demand for temporal and spatial precision (Ben-Ari *et al*., 2007; Rheims *et al*., 2008).

A further possibility concerns the timing of the excitation-hyperpolarisation switch. It has been demonstrated in cultured hippocampal neurones that chronic blockade or activation of $GABA_A$Rs delays or accelerates this switch, respectively, thus indicating that the timing of transition is critically dependent of the level of $GABA_A$R activity (Ganguly *et al*., 2001). Therefore, it is conceivable that the enhancement of $GABA_A$R function by endogenous neurosteroids may contribute to the regulation of the depolarising *vs* hyperpolarising GABA. However, it should be noted that subsequent studies have revealed that the GABA switch is maintained even in the absence of GABA (Ludwig *et al*., 2003; Titz *et al*., 2003).

Chapter 7

Summary and Conclusions

The present study initially describes the characterisation of the synaptic and tonic conductances in P17-24 VB neurones derived from either WT of $\alpha4^{0/0}$ mice. WT VB neurones exhibited mIPSCs that are consistent with the proposal that synaptic VB $GABA_ARs$ are primarily composed of α1, β2 and γ2 subunits. Compared with WT, the properties of mIPSCs recorded from $\alpha4^{0/0}$ VB neurones exhibited differences in peak amplitude, decay time and frequency - changes which are speculatively proposed to represent a compensation for the loss of tonic inhibition. WT VB neurones displayed a considerable tonic current which was severely attenuated in $\alpha4^{0/0}$ VB neurones – a result that is in agreement with the proposal that extrasynaptic $GABA_ARs$ in VB neurones are composed of α4, β2/3, and δ subunits. The relative sensitivity of both the synaptic and tonic modes of inhibition in VB neurones to ligands which are reportedly selective for δ-$GABA_ARs$ was also assessed with a view to determining how selective and how potent 5α3α is for the extrasynaptic receptors that mediate the tonic conductance. Whereas THIP (1 μM) and to a lesser extent, DS2 (10 μM), evoked relatively large inward currents in WT VB neurones (but not in $\alpha4^{0/0}/\delta^{0/0}$ VB neurones, respectively), 5α3α (100 nM) elicited only a modest inward current in WT VB neurones (but did not affect the holding current in recordings from $\alpha4^{0/0}$ VB neurones). Moreover, the small inward current evoked by 5α3α (100 nM) in WT VB neurones was concomitant with a prolongation of the mIPSC decay time. These results infer that for P17-24 WT VB neurones, a physiologically relevant concentration of 5α3α (100 nM) acts with relatively low potency at δ-$GABA_ARs$ and that this concentration does not discriminate between synaptic and tonic inhibition.

During development (P7-P24) the decay time course of mIPSCs recorded from VB neurones and L2/3 pyramidal neurones became progressively shorter in duration. To assess a possible role for endogenous neurosteroids in this developmental trend, brain

slices were pre-treated with finasteride or γ-cyclodextrin. These treatments resulted in mIPSCs with markedly faster decay times at P7. However, at subsequent developmental stages (P8-9) sensitivity to γ-CD subsided such that by P20-24, mIPSC decay times were unaffected by γ-CD pre-treatment. These results provide the first evidence that these synaptic $GABA_ARs$ are regulated by an endogenous neurosteroid tone during development. In $\alpha1^{0/0}$ L2/3 neurones, mIPSCs decay more slowly *vs* those recorded from WT at each developmental stage. However, a developmental decrease in mIPSC decay time was still observed in $\alpha1^{0/0}$ recordings. Indeed, the developmental profile of γ-CD sensitivity in $\alpha1^{0/0}$ VB neurones exhibited an identical pattern to WT recordings indicating that $GABA_AR$ subunit plasticity and neurosteroid synthesis are independently regulated. It is therefore proposed here that the developmentally controlled neurosteroid tone plays a physiological role to increase the temporal window over which infrequent synaptic activity may summate - a feature that is important to the activity-dependent aspects of neurodevelopment.

Experiments performed with 5α-DHP show that neurosteroidogenesis may be re-initiated in P20-24 VB neurones thus suggesting that enzymes required for neurosteroid production are present and functional despite the apparently low levels of neurosteroids at this developmental stage. These results present a possible scenario in which neurosteroids are basally maintained at levels that are insufficient to influence synaptic $GABA_AR$ function. However, under certain conditions a local increase in neurosteroid synthesis may provide a way of regulating the strength of neuronal inhibition.

To assess the putative location of cellular neurosteroid synthesis γ-CD was applied to the intracellular compartment *via* the patch pipette. Within a few minutes, this treatment gave rise to P7 mIPSCs with faster decay times – an identical effect to the γ-CD pre-incubation protocol. Hence these results, although not definitive, support an autocrine mechanism of neurosteroid action in VB and L2/3 neurones.

In conclusion, the results presented here provide impetus for further research that may focus on resolving the cellular location of neurosteroid production during development. In addition, future studies may address the mechanisms responsible for the dissipation of the neurosteroid tone with maturity and also whether the enzymatic machinery necessary for *de novo* neurosteroid synthesis is present at later developmental timepoints (*e.g.* P20-24) and if so, under what conditions may it be resumed? Finally, the neurosteroid tone observed here coincides temporally with a period of remarkable change in accordance with an extensive developmental schedule. Therefore it will be important to determine the precise role played by neurosteroids in neurodevelopmental process, for example the transition from excitatory to inhibitory GABA signalling.

References

Ade, K. K., Janssen, M. J., Ortinski, P. I., & Vicini, S. (2008). Differential tonic GABA conductances in striatal medium spiny neurons. *J.Neurosci.* **28**, 1185-1197.

Agis-Balboa, R. C., Pinna, G., Zhubi, A., Maloku, E., Veldic, M., Costa, E., & Guidotti, A. (2006). Characterization of brain neurons that express enzymes mediating neurosteroid biosynthesis. *Proc.Natl.Acad.Sci.U.S.A* **103**, 14602-14607.

Akerman, C. J. & Cline, H. T. (2007). Refining the roles of GABAergic signaling during neural circuit formation. *Trends Neurosci.* **30**, 382-389.

Akk, G., Shu, H. J., Wang, C., Steinbach, J. H., Zorumski, C. F., Covey, D. F., & Mennerick, S. (2005). Neurosteroid access to the $GABA_A$ receptor. *J.Neurosci.* **25**, 11605-11613.

Akk, G., Li, P., Bracamontes, J., Reichert, D. E., Covey, D. F., & Steinbach, J. H. (2008). Mutations of the $GABA_A$ receptor α1 subunit M1 domain reveal unexpected complexity for modulation by neuroactive steroids. *Mol.Pharmacol.* **74**, 614-627.

Akk, G., Covey, D. F., Evers, A. S., Steinbach, J. H., Zorumski, C. F., & Mennerick, S. (2009). The influence of the membrane on neurosteroid actions at $GABA_A$ receptors. *Psychoneuroendocrinology* **34 Suppl 1**, S59-S66.

Akk, G., Covey, D. F., Evers, A. S., Mennerick, S., Zorumski, C. F., & Steinbach, J. H. (2010). Kinetic and structural determinants for GABA-A receptor potentiation by neuroactive steroids. *Curr.Neuropharmacol.* **8**, 18-25.

Albrecht, J. & Schousboe, A. (2005). Taurine interaction with neurotransmitter receptors in the CNS: an update. *Neurochem.Res.* **30**, 1615-1621.

Amin, J. & Weiss, D. S. (1993). $GABA_A$ receptor needs two homologous domains of the β-subunit for activation by GABA but not by pentobarbital. *Nature* **366**, 565-569.

Arancibia-Carcamo, I. L. & Kittler, J. T. (2009). Regulation of $GABA_A$ receptor membrane trafficking and synaptic localization. *Pharmacol.Ther.* **123**, 17-31.

Araki, T., Kiyama, H., & Tohyama, M. (1992). $GABA_A$ receptor subunit messenger RNAs show differential expression during cortical development in the rat brain. *Neuroscience* **51**, 583-591.

Aree, T. & Chaichit, N. (2002). Crystal structure of β-cyclodextrin-dimethylsulfoxide inclusion complex. *Carbohydr.Res.* **337**, 2487-2494.

Atack, J. R. (2005). The benzodiazepine binding site of $GABA_A$ receptors as a target for the development of novel anxiolytics. *Expert.Opin.Investig.Drugs* **14**, 601-618.

Atack, J. R. (2011a). $GABA_A$ receptor subtype-selective modulators. I. α2/α3-selective agonists as non-sedating anxiolytics. *Curr.Top.Med.Chem.* **11**, 1176-1202.

Atack, J. R. (2011b). $GABA_A$ receptor subtype-selective modulators. II. α5-selective inverse agonists for cognition enhancement. *Curr.Top.Med.Chem.* **11**, 1203-1214.

Attwell, D., Barbour, B., & Szatkowski, M. (1993). Nonvesicular release of neurotransmitter. *Neuron* **11**, 401-407.

Awapara, J., Landua, A. J., Fuerst, R., & Seale, B. (1950). Free γ-aminobutyric acid in brain. *J.Biol.Chem.* **187**, 35-39.

Backus, K. H., Arigoni, M., Drescher, U., Scheurer, L., Malherbe, P., Möhler, H., & Benson, J. A. (1993). Stoichiometry of a recombinant $GABA_A$ receptor deduced from mutation-induced rectification. *Neuroreport* **5**, 285-288.

Bai, D., Zhu, G., Pennefather, P., Jackson, M. F., MacDonald, J. F., & Orser, B. A. (2001). Distinct functional and pharmacological properties of tonic and quantal inhibitory postsynaptic currents mediated by γ-aminobutyric $acid_A$ receptors in hippocampal neurons. *Mol.Pharmacol.* **59**, 814-824.

Ballard, T. M., Knoflach, F., Prinssen, E., Borroni, E., Vivian, J. A., Basile, J., Gasser, R., Moreau, J. L., Wettstein, J. G., Buettelmann, B., Knust, H., Thomas, A. W., Trube, G., & Hernandez, M. C. (2009). RO4938581, a novel cognitive enhancer acting at $GABA_A$ α5 subunit-containing receptors. *Psychopharmacology (Berl)* **202**, 207-223.

Bannister, A. P. (2005). Inter- and intra-laminar connections of pyramidal cells in the neocortex. *Neurosci.Res.* **53**, 95-103.

Barberis, A., Petrini, E. M., & Mozrzymas, J. W. (2011). Impact of synaptic neurotransmitter concentration time course on the kinetics and pharmacological modulation of inhibitory synaptic currents. *Front Cell Neurosci.* **5**, 6.

Barker, J. L., Harrison, N. L., Lange, G. D., & Owen, D. G. (1987). Potentiation of γ-aminobutyric-acid-activated chloride conductance by a steroid anaesthetic in cultured rat spinal neurones. *J.Physiol* **386**, 485-501.

Barnes, N. M., Hales, T. G., Lummis, S. C., & Peters, J. A. (2009). The $5\text{-}HT_3$ receptor--the relationship between structure and function. *Neuropharmacology* **56**, 273-284.

Bateson, A. N., Lasham, A., & Darlison, M. G. (1991). γ-Aminobutyric acidA receptor heterogeneity is increased by alternative splicing of a novel β-subunit gene transcript. *J.Neurochem.* **56**, 1437-1440.

Baulieu, E. E., Robel, P., & Schumacher, M. (2001). Neurosteroids: beginning of the story. *Int.Rev.Neurobiol.* **46**, 1-32.

Bazemore, A., Elliot, K. A., & Florey, E. (1956). Factor I and γ-aminobutyric acid. *Nature* **178**, 1052-1053.

Beenhakker, M. P. & Huguenard, J. R. (2009). Neurons that fire together also conspire together: is normal sleep circuitry hijacked to generate epilepsy? *Neuron* **62**, 612-632.

Belelli, D., Bolger, M. B., & Gee, K. W. (1989). Anticonvulsant profile of the progesterone metabolite 5α-pregnan-3α-ol-20-one. *Eur.J.Pharmacol.* **166**, 325-329.

Belelli, D., Lan, N. C., & Gee, K. W. (1990). Anticonvulsant steroids and the GABA/benzodiazepine receptor-chloride ionophore complex. *Neurosci.Biobehav.Rev.* **14**, 315-322.

Belelli, D., Lambert, J. J., Peters, J. A., Gee, K. W., & Lan, N. C. (1996). Modulation of human recombinant $GABA_A$ receptors by pregnanediols. *Neuropharmacology* **35**, 1223-1231.

Belelli, D., Lambert, J. J., Peters, J. A., Wafford, K., & Whiting, P. J. (1997). The interaction of the general anesthetic etomidate with the γ-aminobutyric acid type A receptor is influenced by a single amino acid. *Proc.Natl.Acad.Sci.U.S.A* **94**, 11031-11036.

Belelli, D., Pistis, M., Peters, J. A., & Lambert, J. J. (1999a). General anaesthetic action at transmitter-gated inhibitory amino acid receptors. *Trends Pharmacol.Sci.* **20**, 496-502.

Belelli, D., Pistis, M., Peters, J. A., & Lambert, J. J. (1999b). The interaction of general anaesthetics and neurosteroids with $GABA_A$ and glycine receptors. *Neurochem.Int.* **34**, 447-452.

Belelli, D., Casula, A., Ling, A., & Lambert, J. J. (2002). The influence of subunit composition on the interaction of neurosteroids with $GABA_A$ receptors. *Neuropharmacology* **43**, 651-661.

Belelli, D. & Herd, M. B. (2003). The contraceptive agent Provera enhances $GABA_A$ receptor-mediated inhibitory neurotransmission in the rat hippocampus: evidence for endogenous neurosteroids? *J.Neurosci.* **23**, 10013-10020.

Belelli, D. & Lambert, J. J. (2005). Neurosteroids: endogenous regulators of the $GABA_A$ receptor. *Nat.Rev.Neurosci.* **6**, 565-575.

Belelli, D., Peden, D. R., Rosahl, T. W., Wafford, K. A., & Lambert, J. J. (2005). Extrasynaptic $GABA_A$ receptors of thalamocortical neurons: a molecular target for hypnotics. *J.Neurosci.* **25**, 11513-11520.

Belelli, D., Harrison, N. L., Maguire, J., Macdonald, R. L., Walker, M. C., & Cope, D. W. (2009). Extrasynaptic $GABA_A$ receptors: form, pharmacology, and function. *J.Neurosci.* **29**, 12757-12763.

Ben Ari, Y., Cherubini, E., Corradetti, R., & Gaiarsa, J. L. (1989). Giant synaptic potentials in immature rat CA3 hippocampal neurones. *J.Physiol* **416**, 303-325.

Ben Ari, Y. (2002). Excitatory actions of gaba during development: the nature of the nurture. *Nat.Rev.Neurosci.* **3**, 728-739.

Ben Ari, Y., Khalilov, I., Represa, A., & Gozlan, H. (2004). Interneurons set the tune of developing networks. *Trends Neurosci.* **27**, 422-427.

Ben Ari, Y., Gaiarsa, J. L., Tyzio, R., & Khazipov, R. (2007). GABA: a pioneer transmitter that excites immature neurons and generates primitive oscillations. *Physiol Rev.* **87**, 1215-1284.

Benke, D., Fakitsas, P., Roggenmoser, C., Michel, C., Rudolph, U., & Möhler, H. (2004). Analysis of the presence and abundance of $GABA_A$ receptors containing two different types of α subunits in murine brain using point-mutated α subunits. *J Biol.Chem.* **279** , 43654-43660.

Benson, J. A., Low, K., Keist, R., Möhler, H., & Rudolph, U. (1998). Pharmacology of recombinant γ-aminobutyric $acid_A$ receptors rendered diazepam-insensitive by point-mutated α-subunits. *FEBS Lett.* **431**, 400-404.

Berezhnoy, D., Gibbs, T. T., & Farb, D. H. (2009). Docking of 1,4-benzodiazepines in the α_1/γ_2 $GABA_A$ receptor modulator site. *Mol.Pharmacol.* **76**, 440-450.

Bianchi, M. T. & Macdonald, R. L. (2003). Neurosteroids shift partial agonist activation of $GABA_A$ receptor channels from low- to high-efficacy gating patterns. *J Neurosci.* **23**, 10934-10943.

Birnir, B. & Korpi, E. R. (2007). The impact of sub-cellular location and intracellular neuronal proteins on properties of $GABA_A$ receptors. *Curr.Pharm.Des* **13**, 3169-3177.

Blaesse, P., Airaksinen, M. S., Rivera, C., & Kaila, K. (2009). Cation-chloride cotransporters and neuronal function. *Neuron* **61**, 820-838.

Blair, L. A., Levitan, E. S., Marshall, J., Dionne, V. E., & Barnard, E. A. (1988). Single subunits of the $GABA_A$ receptor form ion channels with properties of the native receptor. *Science* **242**, 577-579.

Blue, M. E. & Parnavelas, J. G. (1983a). The formation and maturation of synapses in the visual cortex of the rat. I. Qualitative analysis. *J.Neurocytol.* **12**, 599-616.

Blue, M. E. & Parnavelas, J. G. (1983b). The formation and maturation of synapses in the visual cortex of the rat. II. Quantitative analysis. *J.Neurocytol.* **12**, 697-712.

Bocquet, N., Prado, d. C., Cartaud, J., Neyton, J., Le Poupon, C., Taly, A., Grutter, T., Changeux, J. P., & Corringer, P. J. (2007). A prokaryotic proton-gated ion channel from the nicotinic acetylcholine receptor family. *Nature* **445**, 116-119.

Bocquet, N., Nury, H., Baaden, M., Le Poupon, C., Changeux, J. P., Delarue, M., & Corringer, P. J. (2009). X-ray structure of a pentameric ligand-gated ion channel in an apparently open conformation. *Nature* **457**, 111-114.

Bogdanov, Y., Michels, G., Armstrong-Gold, C., Haydon, P. G., Lindstrom, J., Pangalos, M., & Moss, S. J. (2006). Synaptic $GABA_A$ receptors are directly recruited from their extrasynaptic counterparts. *EMBO J.* **25**, 4381-4389.

Bohlhalter, S., Weinmann, O., Möhler, H., & Fritschy, J. M. (1996). Laminar compartmentalization of $GABA_A$-receptor subtypes in the spinal cord: an immunohistochemical study. *J.Neurosci.* **16**, 283-297.

Boileau, A. J., Newell, J. G., & Czajkowski, C. (2002). $GABA_A$ receptor β_2 Tyr^{97} and Leu^{99} line the GABA-binding site. Insights into mechanisms of agonist and antagonist actions. *J.Biol.Chem.* **277**, 2931-2937.

Boileau, A. J., Pearce, R. A., & Czajkowski, C. (2010). The short splice variant of the $\gamma 2$ subunit acts as an external modulator of $GABA_A$ receptor function. *J.Neurosci.* **30**, 4895-4903.

Bonin, R. P., Martin, L. J., MacDonald, J. F., & Orser, B. A. (2007). $\alpha 5GABA_A$ receptors regulate the intrinsic excitability of mouse hippocampal pyramidal neurons. *J.Neurophysiol.* **98**, 2244-2254.

Bonin, R. P. & Orser, B. A. (2008). $GABA_A$ receptor subtypes underlying general anesthesia. *Pharmacol.Biochem.Behav.* **90**, 105-112.

Borden, L. A., Smith, K. E., Gustafson, E. L., Branchek, T. A., & Weinshank, R. L. (1995). Cloning and expression of a betaine/GABA transporter from human brain. *J.Neurochem.* **64**, 977-984.

Borden, L. A. (1996). GABA transporter heterogeneity: pharmacology and cellular localization. *Neurochem.Int.* **29**, 335-356.

Bormann, J. (1988). Patch-clamp analysis of GABA- and glycine-gated chloride channels. *Adv.Biochem.Psychopharmacol.* **45**, 47-60.

Bormann, J. (2000). The 'ABC' of GABA receptors. *Trends Pharmacol.Sci.* **21**, 16-19.

Bosman, L. W., Rosahl, T. W., & Brussaard, A. B. (2002). Neonatal development of the rat visual cortex: synaptic function of $GABA_A$ receptor α subunits. *J.Physiol* **545**, 169-181.

Bosman, L. W., Heinen, K., Spijker, S., & Brussaard, A. B. (2005). Mice lacking the major adult $GABA_A$ receptor subtype have normal number of synapses, but retain juvenile IPSC kinetics until adulthood. *J.Neurophysiol.* **94**, 338-346.

Bowery, N. G. & Hudson, A. L. (1979). γ-Aminobutyric acid reduces the evoked release of [^{3}H]-noradrenaline from sympathetic nerve terminals [proceedings]. *Br.J.Pharmacol.* **66**, 108P.

Bowery, N. G., Hill, D. R., Hudson, A. L., Doble, A., Middlemiss, D. N., Shaw, J., & Turnbull, M. (1980). (-)Baclofen decreases neurotransmitter release in the mammalian CNS by an action at a novel GABA receptor. *Nature* **283**, 92-94.

Bowery, N. G. (1993). $GABA_B$ receptor pharmacology. *Annu.Rev.Pharmacol.Toxicol.* **33**, 109-147.

Bowery, N. G. & Enna, S. J. (2000). γ-aminobutyric $acid_B$ receptors: first of the functional metabotropic heterodimers. *J.Pharmacol.Exp.Ther.* **292**, 2-7.

Braestrup, C. & Squires, R. F. (1977). Specific benzodiazepine receptors in rat brain characterized by high-affinity (^{3}H)diazepam binding. *Proc.Natl.Acad.Sci.U.S.A* **74**, 3805-3809.

Braestrup, C. & Squires, R. F. (1978). Pharmacological characterization of benzodiazepine receptors in the brain. *Eur.J.Pharmacol.* **48**, 263-270.

Breitinger, H. G. & Becker, C. M. (2002). The inhibitory glycine receptor-simple views of a complicated channel. *Chembiochem.* **3**, 1042-1052.

Brejc, K., van Dijk, W. J., Klaassen, R. V., Schuurmans, M., van Der, O. J., Smit, A. B., & Sixma, T. K. (2001). Crystal structure of an ACh-binding protein reveals the ligand-binding domain of nicotinic receptors. *Nature* **411**, 269-276.

Brickley, S. G., Cull-Candy, S. G., & Farrant, M. (1996). Development of a tonic form of synaptic inhibition in rat cerebellar granule cells resulting from persistent activation of $GABA_A$ receptors. *J.Physiol* **497 (Pt 3)**, 753-759.

Brickley, S. G., Cull-Candy, S. G., & Farrant, M. (1999). Single-channel properties of synaptic and extrasynaptic $GABA_A$ receptors suggest differential targeting of receptor subtypes. *J.Neurosci.* **19**, 2960-2973.

Brickley, S. G., Revilla, V., Cull-Candy, S. G., Wisden, W., & Farrant, M. (2001). Adaptive regulation of neuronal excitability by a voltage-independent potassium conductance. *Nature* **409**, 88-92.

Bright, D. P., Aller, M. I., & Brickley, S. G. (2007). Synaptic release generates a tonic $GABA_A$ receptor-mediated conductance that modulates burst precision in thalamic relay neurons. *J.Neurosci.* **27**, 2560-2569.

Bright, D. P., Renzi, M., Bartram, J., McGee, T. P., MacKenzie, G., Hosie, A. M., Farrant, M., & Brickley, S. G. (2011). Profound desensitization by ambient GABA limits activation of δ-containing $GABA_A$ receptors during spillover. *J.Neurosci.* **31**, 753-763.

Brinton, R. D. (1994). The neurosteroid 3α-hydroxy-5α-pregnan-20-one induces cytoarchitectural regression in cultured fetal hippocampal neurons. *J.Neurosci.* **14**, 2763-2774.

Brock, L. G., Eccles, J. C., & Rall, W. (1951). Experimental investigations on the afferent fibres in muscle nerves. *Proc.R.Soc.Lond B Biol.Sci.* **138**, 453-475.

Brown, N., Kerby, J., Bonnert, T. P., Whiting, P. J., & Wafford, K. A. (2002). Pharmacological characterization of a novel cell line expressing human $\alpha_4\beta_3\delta$ $GABA_A$ receptors. *Br.J.Pharmacol.* **136**, 965-974.

Brunig, I., Scotti, E., Sidler, C., & Fritschy, J. M. (2002). Intact sorting, targeting, and clustering of γ-aminobutyric acid A receptor subtypes in hippocampal neurons in vitro. *J.Comp Neurol.* **443**, 43-55.

Brussaard, A. B., Kits, K. S., Baker, R. E., Willems, W. P., Leyting-Vermeulen, J. W., Voorn, P., Smit, A. B., Bicknell, R. J., & Herbison, A. E. (1997). Plasticity in fast synaptic inhibition of adult oxytocin neurons caused by switch in $GABA_A$ receptor subunit expression. *Neuron* **19**, 1103-1114.

Brussaard, A. B. & Herbison, A. E. (2000). Long-term plasticity of postsynaptic $GABA_A$-receptor function in the adult brain: insights from the oxytocin neurone. *Trends Neurosci.* **23**, 190-195.

Buhr, A. & Sigel, E. (1997). A point mutation in the γ_2 subunit of γ-aminobutyric acid type A receptors results in altered benzodiazepine binding site specificity. *Proc.Natl.Acad.Sci.U.S.A* **94**, 8824-8829.

Burnham, C. E., Buerk, B., Schmidt, C., & Bucuvalas, J. C. (1996). A liver-specific isoform of the betaine/GABA transporter in the rat: cDNA sequence and organ distribution. *Biochim.Biophys.Acta* **1284**, 4-8.

Callachan, H., Cottrell, G. A., Hather, N. Y., Lambert, J. J., Nooney, J. M., & Peters, J. A. (1987). Modulation of the $GABA_A$ receptor by progesterone metabolites. *Proc.R.Soc.Lond B Biol.Sci.* **231**, 359-369.

Capogna, M. & Pearce, R. A. (2011). $GABA_{A,slow}$: causes and consequences. *Trends Neurosci.* **34**, 101-112.

Caraiscos, V. B., Elliott, E. M., You, T., Cheng, V. Y., Belelli, D., Newell, J. G., Jackson, M. F., Lambert, J. J., Rosahl, T. W., Wafford, K. A., MacDonald, J. F., & Orser, B. A. (2004). Tonic inhibition in mouse hippocampal CA1 pyramidal neurons is mediated by α5 subunit-containing γ-aminobutyric acid type A receptors. *Proc.Natl.Acad.Sci.U.S.A* **101**, 3662-3667.

Carland, J. E., Cooper, M. A., Sugiharto, S., Jeong, H. J., Lewis, T. M., Barry, P. H., Peters, J. A., Lambert, J. J., & Moorhouse, A. J. (2009). Characterization of the effects of charged residues in the intracellular loop on ion permeation in α1 glycine receptor channels. *J.Biol.Chem.* **284**, 2023-2030.

Carter, R. B., Wood, P. L., Wieland, S., Hawkinson, J. E., Belelli, D., Lambert, J. J., White, H. S., Wolf, H. H., Mirsadeghi, S., Tahir, S. H., Bolger, M. B., Lan, N. C., & Gee, K. W. (1997). Characterization of the anticonvulsant properties of ganaxolone (CCD 1042; 3α-hydroxy-3β-methyl-5α-pregnan-20-one), a selective, high-affinity, steroid modulator of the γ-aminobutyric $acid_A$ receptor. *J.Pharmacol.Exp.Ther.* **280**, 1284-1295.

Carter, C. R., Kozuska, J. L., & Dunn, S. M. (2010). Insights into the structure and pharmacology of $GABA_A$ receptors. *Future.Med.Chem.* **2**, 859-875.

Cavelier, P., Hamann, M., Rossi, D., Mobbs, P., & Attwell, D. (2005). Tonic excitation and inhibition of neurons: ambient transmitter sources and computational consequences. *Prog.Biophys.Mol.Biol.* **87**, 3-16.

Chadderton, P., Margrie, T. W., & Hausser, M. (2004). Integration of quanta in cerebellar granule cells during sensory processing. *Nature* **428**, 856-860.

Chalifoux, J. R. & Carter, A. G. (2011). $GABA_B$ receptor modulation of synaptic function. *Curr.Opin.Neurobiol.* **21**, 339-344.

Chandra, D., Jia, F., Liang, J., Peng, Z., Suryanarayanan, A., Werner, D. F., Spigelman, I., Houser, C. R., Olsen, R. W., Harrison, N. L., & Homanics, G. E. (2006). $GABA_A$ receptor α4 subunits mediate extrasynaptic inhibition in thalamus and dentate gyrus and the action of gaboxadol. *Proc.Natl.Acad.Sci.U.S.A* **103**, 15230-15235.

Chattopadhyaya, B., Di Cristo, G., Wu, C. Z., Knott, G., Kuhlman, S., Fu, Y., Palmiter, R. D., & Huang, Z. J. (2007). GAD67-mediated GABA synthesis and signaling regulate inhibitory synaptic innervation in the visual cortex. *Neuron* **54**, 889-903.

Chen, Z. W. & Olsen, R. W. (2007). $GABA_A$ receptor associated proteins: a key factor regulating $GABA_A$ receptor function. *J.Neurochem.* **100**, 279-294.

Cheng, V. Y., Martin, L. J., Elliott, E. M., Kim, J. H., Mount, H. T., Taverna, F. A., Roder, J. C., MacDonald, J. F., Bhambri, A., Collinson, N., Wafford, K. A., & Orser, B. A. (2006). α5$GABA_A$ receptors mediate the amnestic but not sedative-hypnotic effects of the general anesthetic etomidate. *J.Neurosci.* **26**, 3713-3720.

Cherubini, E., Gaiarsa, J. L., & Ben Ari, Y. (1991). GABA: an excitatory transmitter in early postnatal life. *Trends Neurosci.* **14**, 515-519.

Cherubini, E. & Conti, F. (2001). Generating diversity at GABAergic synapses. *Trends Neurosci.* **24**, 155-162.

Chisari, M., Eisenman, L. N., Krishnan, K., Bandyopadhyaya, A. K., Wang, C., Taylor, A., Benz, A., Covey, D. F., Zorumski, C. F., & Mennerick, S. (2009). The influence of neuroactive steroid lipophilicity on $GABA_A$ receptor modulation: evidence for a low-affinity interaction. *J.Neurophysiol.* **102**, 1254-1264.

Chisari, M., Eisenman, L. N., Covey, D. F., Mennerick, S., & Zorumski, C. F. (2010). The sticky issue of neurosteroids and $GABA_A$ receptors. *Trends Neurosci.* **33**, 299-306.

Choh, D. W., Farb, D. H., & Fischbach, G. D. (1977). Chlordiazepoxide selectively augments GABA action in spinal cord cell cultures. *Nature* **269**, 342-344.

Choi, D. S., Wei, W., Deitchman, J. K., Kharazia, V. N., Lesscher, H. M., McMahon, T., Wang, D., Qi, Z. H., Sieghart, W., Zhang, C., Shokat, K. M., Mody, I., & Messing, R. O. (2008). Protein kinase Cδ regulates ethanol intoxication and enhancement of GABA-stimulated tonic current. *J.Neurosci.* **28**, 11890-11899.

Chudomel, O., Herman, H., Nair, K., Moshe, S. L., & Galanopoulou, A. S. (2009). Age- and gender-related differences in $GABA_A$ receptor-mediated postsynaptic currents in GABAergic neurons of the substantia nigra reticulata in the rat. *Neuroscience* **163**, 155-167.

Clausen, R. P., Madsen, K., Larsson, O. M., Frolund, B., Krogsgaard-Larsen, P., & Schousboe, A. (2006). Structure-activity relationship and pharmacology of γ-aminobutyric acid (GABA) transport inhibitors. *Adv.Pharmacol.* **54**, 265-284.

Cobb, S. R., Buhl, E. H., Halasy, K., Paulsen, O., & Somogyi, P. (1995). Synchronization of neuronal activity in hippocampus by individual GABAergic interneurons. *Nature* **378**, 75-78.

Cohen, A. S., Lin, D. D., & Coulter, D. A. (2000). Protracted postnatal development of inhibitory synaptic transmission in rat hippocampal area CA1 neurons. *J.Neurophysiol.* **84**, 2465-2476.

Collinson, N., Kuenzi, F. M., Jarolimek, W., Maubach, K. A., Cothliff, R., Sur, C., Smith, A., Otu, F. M., Howell, O., Atack, J. R., McKernan, R. M., Seabrook, G. R., Dawson, G. R., Whiting, P. J., & Rosahl, T. W. (2002). Enhanced learning and memory and altered GABAergic synaptic transmission in mice lacking the α5 subunit of the $GABA_A$ receptor. *J Neurosci.* **22**, 5572-5580.

Compagnone, N. A. & Mellon, S. H. (2000). Neurosteroids: biosynthesis and function of these novel neuromodulators. *Front Neuroendocrinol.* **21**, 1-56.

Concas, A., Mostallino, M. C., Porcu, P., Follesa, P., Barbaccia, M. L., Trabucchi, M., Purdy, R. H., Grisenti, P., & Biggio, G. (1998). Role of brain allopregnanolone in the plasticity of γ-aminobutyric acid type A receptor in rat brain during pregnancy and after delivery. *Proc.Natl.Acad.Sci.U.S.A* **95**, 13284-13289.

Connolly, C. N. & Wafford, K. A. (2004). The Cys-loop superfamily of ligand-gated ion channels: the impact of receptor structure on function. *Biochem.Soc.Trans.* **32**, 529-534.

Conti, F., Melone, M., De Biasi, S., Minelli, A., Brecha, N. C., & Ducati, A. (1998). Neuronal and glial localization of GAT-1, a high-affinity γ-aminobutyric acid plasma membrane transporter, in human cerebral cortex: with a note on its distribution in monkey cortex. *J.Comp Neurol.* **396**, 51-63.

Conti, F., Minelli, A., & Melone, M. (2004). GABA transporters in the mammalian cerebral cortex: localization, development and pathological implications. *Brain Res.Brain Res.Rev.* **45**, 196-212.

Conti, F., Melone, M., Fattorini, G., Bragina, L., & Ciappelloni, S. (2011). A role for GAT-1 in presynaptic GABA homeostasis? *Front Cell Neurosci.* **5**, 2.

Cooper, E. J., Johnston, G. A., & Edwards, F. A. (1999). Effects of a naturally occurring neurosteroid on $GABA_A$ IPSCs during development in rat hippocampal or cerebellar slices. *J.Physiol* **521 Pt 2**, 437-449.

Cope, D. W., Hughes, S. W., & Crunelli, V. (2005a). $GABA_A$ receptor-mediated tonic inhibition in thalamic neurons. *J.Neurosci.* **25**, 11553-11563.

Cope, D. W., Halbsguth, C., Karayannis, T., Wulff, P., Ferraguti, F., Hoeger, H., Leppa, E., Linden, A. M., Oberto, A., Ogris, W., Korpi, E. R., Sieghart, W., Somogyi, P., Wisden, W., & Capogna, M. (2005b). Loss of zolpidem efficacy in the hippocampus of mice with the $GABA_A$ receptor γ2 F77I point mutation. *Eur.J.Neurosci.* **21**, 3002-3016.

Cope, D. W., Di Giovanni, G., Fyson, S. J., Orban, G., Errington, A. C., Lorincz, M. L., Gould, T. M., Carter, D. A., & Crunelli, V. (2009). Enhanced tonic $GABA_A$ inhibition in typical absence epilepsy. *Nat.Med.* **15**, 1392-1398.

Corpechot, C., Robel, P., Axelson, M., Sjovall, J., & Baulieu, E. E. (1981). Characterization and measurement of dehydroepiandrosterone sulfate in rat brain. *Proc.Natl.Acad.Sci.U.S.A* **78**, 4704-4707.

Corpechot, C., Synguelakis, M., Talha, S., Axelson, M., Sjovall, J., Vihko, R., Baulieu, E. E., & Robel, P. (1983). Pregnenolone and its sulfate ester in the rat brain. *Brain Res.* **270** , 119-125.

Corpechot, C., Leclerc, P., Baulieu, E. E., & Brazeau, P. (1985). Neurosteroids: regulatory mechanisms in male rat brain during heterosexual exposure. *Steroids* **45**, 229-234.

Corpechot, C., Young, J., Calvel, M., Wehrey, C., Veltz, J. N., Touyer, G., Mouren, M., Prasad, V. V., Banner, C., Sjovall, J., & . (1993). Neurosteroids: 3α-hydroxy-5α-pregnan-20-one and its precursors in the brain, plasma, and steroidogenic glands of male and female rats. *Endocrinology* **133**, 1003-1009.

Corringer, P. J., Le Novere, N., & Changeux, J. P. (2000). Nicotinic receptors at the amino acid level. *Annu.Rev.Pharmacol.Toxicol.* **40**, 431-458.

Corringer, P. J., Baaden, M., Bocquet, N., Delarue, M., Dufresne, V., Nury, H., Prevost, M., & Van Renterghem, C. (2010). Atomic structure and dynamics of pentameric ligand-gated ion channels: new insight from bacterial homologues. *J.Physiol* **588**, 565-572.

Crawley, J. N., Glowa, J. R., Majewska, M. D., & Paul, S. M. (1986). Anxiolytic activity of an endogenous adrenal steroid. *Brain Res.* **398**, 382-385.

Crestani, F., Martin, J. R., Möhler, H., & Rudolph, U. (2000). Mechanism of action of the hypnotic zolpidem in vivo. *Br.J.Pharmacol.* **131**, 1251-1254.

Crestani, F., Low, K., Keist, R., Mandelli, M., Möhler, H., & Rudolph, U. (2001). Molecular targets for the myorelaxant action of diazepam. *Mol.Pharmacol.* **59**, 442-445.

Crestani, F., Keist, R., Fritschy, J. M., Benke, D., Vogt, K., Prut, L., Bluthmann, H., Möhler, H., & Rudolph, U. (2002). Trace fear conditioning involves hippocampal α5 $GABA_A$ receptors. *Proc.Natl.Acad.Sci.U.S.A* **99**, 8980-8985.

Cromer, B. A., Morton, C. J., & Parker, M. W. (2002). Anxiety over $GABA_A$ receptor structure relieved by AChBP. *Trends Biochem.Sci.* **27**, 280-287.

Crunelli, V., Lightowler, S., & Pollard, C. E. (1989). A T-type Ca^{2+} current underlies low-threshold Ca^{2+} potentials in cells of the cat and rat lateral geniculate nucleus. *J.Physiol* **413**, 543-561.

Crunelli, V. & Leresche, N. (2002). Childhood absence epilepsy: genes, channels, neurons and networks. *Nat.Rev.Neurosci.* **3**, 371-382.

Crunelli, V., Cope, D. W., & Hughes, S. W. (2006). Thalamic T-type Ca^{2+} channels and NREM sleep. *Cell Calcium* **40**, 175-190.

Curtis, D. R., Phillis, J. W., & Watkins, J. C. (1959). The depression of spinal neurones by γ-amino-*n*-butyric acid and β-alanine. *J.Physiol* **146**, 185-203.

Curtis, D. R., Felix, D., & McLellan, H. (1970). GABA and hippocampal inhibition. *Br.J.Pharmacol.* **40**, 881-883.

Curtis, D. R., Duggan, A. W., Felix, D., & Johnston, G. A. (1970). GABA, bicuculline and central inhibition. *Nature* **226**, 1222-1224.

Cutting, G. R., Lu, L., O'Hara, B. F., Kasch, L. M., Montrose-Rafizadeh, C., Donovan, D. M., Shimada, S., Antonarakis, S. E., Guggino, W. B., Uhl, G. R., & Kazazian Jr, H.H. (1991). Cloning of the γ-aminobutyric acid (GABA) ρ1 cDNA: a GABA receptor subunit highly expressed in the retina. *Proc.Natl.Acad.Sci.U.S.A* **88**, 2673-2677.

D'Hulst, C., Atack, J. R., & Kooy, R. F. (2009). The complexity of the $GABA_A$ receptor shapes unique pharmacological profiles. *Drug Discov.Today* **14**, 866-875.

Darlison, M. G., Pahal, I., & Thode, C. (2005). Consequences of the evolution of the $GABA_A$ receptor gene family. *Cell Mol.Neurobiol.* **25**, 607-624.

Davis, M. E. & Brewster, M. E. (2004). Cyclodextrin-based pharmaceutics: past, present and future. *Nat.Rev.Drug Discov.* **3**, 1023-1035.

Dawson, G. R., Maubach, K. A., Collinson, N., Cobain, M., Everitt, B. J., MacLeod, A. M., Choudhury, H. I., McDonald, L. M., Pillai, G., Rycroft, W., Smith, A. J., Sternfeld, F., Tattersall, F. D., Wafford, K. A., Reynolds, D. S., Seabrook, G. R., & Atack, J. R. (2006). An inverse agonist selective for α5 subunit-containing $GABA_A$ receptors enhances cognition. *J.Pharmacol.Exp.Ther.* **316**, 1335-1345.

De Biasi, S., Vitellaro-Zuccarello, L., & Brecha, N. C. (1998). Immunoreactivity for the GABA transporter-1 and GABA transporter-3 is restricted to astrocytes in the rat thalamus. A light and electron-microscopic immunolocalization. *Neuroscience* **83**, 815-828.

Dellisanti, C. D., Yao, Y., Stroud, J. C., Wang, Z. Z., & Chen, L. (2007). Crystal structure of the extracellular domain of nAChR α1 bound to α-bungarotoxin at 1.94 A resolution. *Nat.Neurosci.* **10**, 953-962.

Di Cristo, G. (2007). Development of cortical GABAergic circuits and its implications for neurodevelopmental disorders. *Clin.Genet.* **72**, 1-8.

Do Rego, J. L., Seong, J. Y., Burel, D., Leprince, J., Luu-The, V., Tsutsui, K., Tonon, M. C., Pelletier, G., & Vaudry, H. (2009). Neurosteroid biosynthesis: enzymatic pathways and neuroendocrine regulation by neurotransmitters and neuropeptides. *Front Neuroendocrinol.* **30**, 259-301.

Draguhn, A., Verdorn, T. A., Ewert, M., Seeburg, P. H., & Sakmann, B. (1990). Functional and molecular distinction between recombinant rat $GABA_A$ receptor subtypes by Zn^{2+}. *Neuron* **5**, 781-788.

Draguhn, A. & Heinemann, U. (1996). Different mechanisms regulate IPSC kinetics in early postnatal and juvenile hippocampal granule cells. *J.Neurophysiol.* **76**, 3983-3993.

Drasbek, K. R. & Jensen, K. (2006). THIP, a hypnotic and antinociceptive drug, enhances an extrasynaptic $GABA_A$ receptor-mediated conductance in mouse neocortex. *Cereb.Cortex* **16**, 1134-1141.

Drasbek, K. R., Hoestgaard-Jensen, K., & Jensen, K. (2007). Modulation of extrasynaptic THIP conductances by $GABA_A$-receptor modulators in mouse neocortex. *J.Neurophysiol.* **97**, 2293-2300.

Dreifuss, J. J., Kelly, J. S., & Krnjevic, K. (1969). Cortical inhibition and γ-aminobutyric acid. *Exp.Brain Res.* **9**, 137-154.

Drew, C. A., Johnston, G. A., & Weatherby, R. P. (1984). Bicuculline-insensitive GABA receptors: studies on the binding of (-)-baclofen to rat cerebellar membranes. *Neurosci.Lett.* **52**, 317-321.

Drexler, B., Antkowiak, B., Engin, E., & Rudolph, U. (2011). Identification and characterization of anesthetic targets by mouse molecular genetics approaches. *Can.J.Anaesth.* **58**, 178-190.

Duggan, M. J., Pollard, S., & Stephenson, F. A. (1991). Immunoaffinity purification of $GABA_A$ receptor α-subunit iso-oligomers. Demonstration of receptor populations containing α1 α2, α1 α3, and α2 α3 subunit pairs. *J.Biol.Chem.* **266**, 24778-24784.

Dunning, D. D., Hoover, C. L., Soltesz, I., Smith, M. A., & O'Dowd, D. K. (1999). $GABA_A$ receptor-mediated miniature postsynaptic currents and α-subunit expression in developing cortical neurons. *J.Neurophysiol.* **82**, 3286-3297.

Durkin, M. M., Smith, K. E., Borden, L. A., Weinshank, R. L., Branchek, T. A., & Gustafson, E. L. (1995). Localization of messenger RNAs encoding three GABA transporters in rat brain: an in situ hybridization study. *Brain Res.Mol.Brain Res.* **33**, 7-21.

Edwards, F. A., Konnerth, A., Sakmann, B., & Takahashi, T. (1989). A thin slice preparation for patch clamp recordings from neurones of the mammalian central nervous system. *Pflugers Arch.* **414**, 600-612.

Edwards, F. A., Konnerth, A., & Sakmann, B. (1990). Quantal analysis of inhibitory synaptic transmission in the dentate gyrus of rat hippocampal slices: a patch-clamp study. *J.Physiol* **430**, 213-249.

Eechaute, W. P., Dhooge, W. S., Gao, C. Q., Calders, P., Rubens, R., Weyne, J., & Kaufman, J. M. (1999). Progesterone-transforming enzyme activity in the hypothalamus of the male rat. *J.Steroid Biochem.Mol.Biol.* **70**, 159-167.

Enz, R. & Cutting, G. R. (1998). Molecular composition of $GABA_C$ receptors. *Vision Res.* **38**, 1431-1441.

Essrich, C., Lorez, M., Benson, J. A., Fritschy, J. M., & Lüscher, B. (1998). Postsynaptic clustering of major $GABA_A$ receptor subtypes requires the γ2 subunit and gephyrin. *Nat.Neurosci.* **1**, 563-571.

Faber, D. S., Young, W. S., Legendre, P., & Korn, H. (1992). Intrinsic quantal variability due to stochastic properties of receptor-transmitter interactions. *Science* **258**, 1494-1498.

Fancsik, A., Linn, D. M., & Tasker, J. G. (2000). Neurosteroid modulation of GABA IPSCs is phosphorylation dependent. *J.Neurosci.* **20**, 3067-3075.

Farrant, M. & Nusser, Z. (2005). Variations on an inhibitory theme: phasic and tonic activation of $GABA_A$ receptors. *Nat.Rev.Neurosci.* **6**, 215-229.

Farrant, M. & Kaila, K. (2007). The cellular, molecular and ionic basis of $GABA_A$ receptor signalling. *Prog.Brain Res.* **160**, 59-87.

Farrar, S. J., Whiting, P. J., Bonnert, T. P., & McKernan, R. M. (1999). Stoichiometry of a ligand-gated ion channel determined by fluorescence energy transfer. *J.Biol.Chem.* **274**, 10100-10104.

Fenalti, G., Law, R. H., Buckle, A. M., Langendorf, C., Tuck, K., Rosado, C. J., Faux, N. G., Mahmood, K., Hampe, C. S., Banga, J. P., Wilce, M., Schmidberger, J., Rossjohn, J., El Kabbani, O., Pike, R. N., Smith, A. I., Mackay, I. R., Rowley, M. J., & Whisstock, J. C. (2007). GABA production by glutamic acid decarboxylase is regulated by a dynamic catalytic loop. *Nat.Struct.Mol.Biol.* **14**, 280-286.

Fenwick, E. M., Marty, A., & Neher, E. (1982). A patch-clamp study of bovine chromaffin cells and of their sensitivity to acetylcholine. *J.Physiol* **331**, 577-597.

Fiumelli, H. & Woodin, M. A. (2007). Role of activity-dependent regulation of neuronal chloride homeostasis in development. *Curr.Opin.Neurobiol.* **17**, 81-86.

Florey, E. (1954). An inhibitory and an excitatory factor of mammalian central nervous system, and their action of a single sensory neuron. *Arch.Int.Physiol* **62**, 33-53.

Flory, E., Mclennan, H. (1959). The effects of Factor 1 and of gamma-amino-butyric acid on smooth muscle preparations. *J. Physiol* **145**, 66-76

Frerking, M. & Wilson, M. (1996). Saturation of postsynaptic receptors at central synapses? *Curr.Opin.Neurobiol.* **6**, 395-403.

Fritschy, J. M., Benke, D., Mertens, S., Oertel, W. H., Bachi, T., & Möhler, H. (1992). Five subtypes of type A γ-aminobutyric acid receptors identified in neurons by double and triple immunofluorescence staining with subunit-specific antibodies. *Proc.Natl.Acad.Sci.U.S.A* **89**, 6726-6730.

Fritschy, J. M., Paysan, J., Enna, A., & Möhler, H. (1994). Switch in the expression of rat $GABA_A$-receptor subtypes during postnatal development: an immunohistochemical study. *J.Neurosci.* **14**, 5302-5324.

Fritschy, J. M. & Möhler, H. (1995). $GABA_A$-receptor heterogeneity in the adult rat brain: differential regional and cellular distribution of seven major subunits. *J.Comp Neurol.* **359**, 154-194.

Gahwiler, B. H. & Brown, D. A. (1985). $GABA_B$-receptor-activated K^+ current in voltage-clamped CA3 pyramidal cells in hippocampal cultures. *Proc.Natl.Acad.Sci.U.S.A* **82**, 1558-1562.

Gambarana, C., Pittman, R., & Siegel, R. E. (1990). Developmental expression of the $GABA_A$ receptor α1 subunit mRNA in the rat brain. *J.Neurobiol.* **21**, 1169-1179.

Gambarana, C., Beattie, C. E., Rodriguez, Z. R., & Siegel, R. E. (1991). Region-specific expression of messenger RNAs encoding $GABA_A$ receptor subunits in the developing rat brain. *Neuroscience* **45**, 423-432.

Ganguly, K., Schinder, A. F., Wong, S. T., & Poo, M. (2001). GABA itself promotes the developmental switch of neuronal GABAergic responses from excitation to inhibition. *Cell* **105**, 521-532.

Gasior, M., Carter, R. B., & Witkin, J. M. (1999). Neuroactive steroids: potential therapeutic use in neurological and psychiatric disorders. *Trends Pharmacol.Sci.* **20**, 107-112.

Gasnier, B. (2004). The SLC32 transporter, a key protein for the synaptic release of inhibitory amino acids. *Pflugers Arch.* **447**, 756-759.

Gee, K. W., Bolger, M. B., Brinton, R. E., Coirini, H., & McEwen, B. S. (1988). Steroid modulation of the chloride ionophore in rat brain: structure-activity requirements, regional dependence and mechanism of action. *J.Pharmacol.Exp.Ther.* **246**, 803-812.

Gingrich, K. J., Roberts, W. A., & Kass, R. S. (1995). Dependence of the $GABA_A$ receptor gating kinetics on the α-subunit isoform: implications for structure-function relations and synaptic transmission. *J.Physiol* **489 (Pt 2)**, 529-543.

Glykys, J. & Mody, I. (2006). Hippocampal network hyperactivity after selective reduction of tonic inhibition in $GABA_A$ receptor α5 subunit-deficient mice. *J.Neurophysiol.* **95**, 2796-2807.

Glykys, J., Peng, Z., Chandra, D., Homanics, G. E., Houser, C. R., & Mody, I. (2007). A new naturally occurring $GABA_A$ receptor subunit partnership with high sensitivity to ethanol. *Nat.Neurosci.* **10**, 40-48.

Glykys, J. & Mody, I. (2007). Activation of $GABA_A$ receptors: views from outside the synaptic cleft. *Neuron* **56**, 763-770.

Glykys, J., Mann, E. O., & Mody, I. (2008). Which $GABA_A$ receptor subunits are necessary for tonic inhibition in the hippocampus? *J.Neurosci.* **28**, 1421-1426.

Goldstein, P. A., Elsen, F. P., Ying, S. W., Ferguson, C., Homanics, G. E., & Harrison, N. L. (2002). Prolongation of hippocampal miniature inhibitory postsynaptic currents in mice lacking the $GABA_A$ receptor α1 subunit. *J Neurophysiol* **88**, 3208-3217.

Griffin, L. D. & Mellon, S. H. (1999). Selective serotonin reuptake inhibitors directly alter activity of neurosteroidogenic enzymes. *Proc.Natl.Acad.Sci.U.S.A* **96**, 13512-13517.

Griffin, L. D., Gong, W., Verot, L., & Mellon, S. H. (2004). Niemann-Pick type C disease involves disrupted neurosteroidogenesis and responds to allopregnanolone. *Nat.Med.* **10**, 704-711.

Grobin, A. C. & Morrow, A. L. (2001). 3A-hydroxy-5α-pregnan-20-one levels and $GABA_A$ receptor-mediated $36Cl^-$ flux across development in rat cerebral cortex. *Brain Res.Dev.Brain Res.* **131**, 31-39.

Grobin, A. C., Heenan, E. J., Lieberman, J. A., & Morrow, A. L. (2003). Perinatal neurosteroid levels influence GABAergic interneuron localization in adult rat prefrontal cortex. *J.Neurosci.* **23**, 1832-1839.

Guidotti, A. & Costa, E. (1998). Can the antidysphoric and anxiolytic profiles of selective serotonin reuptake inhibitors be related to their ability to increase brain 3α,5α-tetrahydroprogesterone (allopregnanolone) availability? *Biol.Psychiatry* **44**, 865-873.

Gunn, B. G., Brown, A.R., Lambert, J.J., & Belelli, D. (2011). Neurosteroids and $GABA_A$ receptor interactions: a focus on stress. *In press.*

Gunther, U., Benson, J., Benke, D., Fritschy, J. M., Reyes, G., Knoflach, F., Crestani, F., Aguzzi, A., Arigoni, M., Lang, Y., Bluethmann, H., Möhler, H., & Lüscher, B. (1995). Benzodiazepine-insensitive mice generated by targeted disruption of the γ_2 subunit gene of γ-aminobutyric acid type A receptors. *Proc.Natl.Acad.Sci.U.S.A* **92**, 7749-7753.

Gutierrez, A., Khan, Z. U., & De Blas, A. L. (1994). Immunocytochemical localization of γ 2 short and γ 2 long subunits of the $GABA_A$ receptor in the rat brain. *J.Neurosci.* **14**, 7168-7179.

Gutierrez, A., Khan, Z. U., Ruano, D., Miralles, C. P., Vitorica, J., & De Blas, A. L. (1996). Aging-related subunit expression changes of the $GABA_A$ receptor in the rat hippocampus. *Neuroscience* **74**, 341-348.

Haage, D. & Johansson, S. (1999). Neurosteroid modulation of synaptic and GABA-evoked currents in neurons from the rat medial preoptic nucleus. *J.Neurophysiol.* **82**, 143-151.

Haage, D., Druzin, M., & Johansson, S. (2002). Allopregnanolone modulates spontaneous GABA release via presynaptic Cl^- permeability in rat preoptic nerve terminals. *Brain Res.* **958**, 405-413.

Haage, D., Backstrom, T., & Johansson, S. (2005). Interaction between allopregnanolone and pregnenolone sulfate in modulating GABA-mediated synaptic currents in neurons from the rat medial preoptic nucleus. *Brain Res.* **1033**, 58-67.

Haas, K. F. & Macdonald, R. L. (1999). $GABA_A$ receptor subunit γ_2 and δ subtypes confer unique kinetic properties on recombinant $GABA_A$ receptor currents in mouse fibroblasts. *J.Physiol* **514 (Pt 1)**, 27-45.

Hales, T. G. & Lambert, J. J. (1991). The actions of propofol on inhibitory amino acid receptors of bovine adrenomedullary chromaffin cells and rodent central neurones. *Br.J.Pharmacol.* **104**, 619-628.

Hales, T.G. & Peters, T.G. (2009). ZAC: IUPHAR database (IUPHAR-DB), http://www.iuphar-db.org/DATABASE/ObjectDisplayForward?objectId=587.

Halonen, L. M., Sinkkonen, S. T., Chandra, D., Homanics, G. E., & Korpi, E. R. (2009). Brain regional distribution of $GABA_A$ receptors exhibiting atypical GABA agonism: roles of receptor subunits. *Neurochem.Int.* **55**, 389-396.

Hamann, M., Rossi, D. J., & Attwell, D. (2002). Tonic and spillover inhibition of granule cells control information flow through cerebellar cortex. *Neuron* **33**, 625-633.

Hamill, O. P., Marty, A., Neher, E., Sakmann, B., & Sigworth, F. J. (1981). Improved patch-clamp techniques for high-resolution current recording from cells and cell-free membrane patches. *Pflugers Arch.* **391**, 85-100.

Hamill, O. P., Bormann, J., & Sakmann, B. (1983). Activation of multiple-conductance state chloride channels in spinal neurones by glycine and GABA. *Nature* **305**, 805-808.

Hansen, S. B., Sulzenbacher, G., Huxford, T., Marchot, P., Taylor, P., & Bourne, Y. (2005). Structures of Aplysia AChBP complexes with nicotinic agonists and antagonists reveal distinctive binding interfaces and conformations. *EMBO J.* **24**, 3635-3646.

Harney, S. C., Frenguelli, B. G., & Lambert, J. J. (2003). Phosphorylation influences neurosteroid modulation of synaptic $GABA_A$ receptors in rat CA1 and dentate gyrus neurones. *Neuropharmacology* **45**, 873-883.

Harrison, N. L. & Simmonds, M. A. (1984). Modulation of the GABA receptor complex by a steroid anaesthetic. *Brain Res.* **323**, 287-292.

Harrison, N. L., Vicini, S., & Barker, J. L. (1987). A steroid anesthetic prolongs inhibitory postsynaptic currents in cultured rat hippocampal neurons. *J.Neurosci.* **7**, 604-609.

Hartmann, K., Stief, F., Draguhn, A., & Frahm, C. (2004). Ionotropic GABA receptors with mixed pharmacological properties of $GABA_A$ and $GABA_C$ receptors. *Eur.J.Pharmacol.* **497**, 139-146.

Harvey, V. L., Duguid, I. C., Krasel, C., & Stephens, G. J. (2006). Evidence that GABA ρ subunits contribute to functional ionotropic GABA receptors in mouse cerebellar Purkinje cells. *J.Physiol* **577**, 127-139.

Haynes, M. P., Phillips, M. C., & Rothblat, G. H. (2000). Efflux of cholesterol from different cellular pools. *Biochemistry* **39**, 4508-4517.

Herd, M. B., Belelli, D., & Lambert, J. J. (2007). Neurosteroid modulation of synaptic and extrasynaptic $GABA_A$ receptors. *Pharmacol.Ther.* **116**, 20-34.

Herd, M. B., Haythornthwaite, A. R., Rosahl, T. W., Wafford, K. A., Homanics, G. E., Lambert, J. J., & Belelli, D. (2008). The expression of $GABA_A$ β subunit isoforms in synaptic and extrasynaptic receptor populations of mouse dentate gyrus granule cells. *J.Physiol* **586**, 989-1004.

Herd, M. B., Foister, N., Chandra, D., Peden, D. R., Homanics, G. E., Brown, V. J., Balfour, D. J., Lambert, J. J., & Belelli, D. (2009). Inhibition of thalamic excitability by 4,5,6,7-tetrahydroisoxazolo[4,5-c]pyridine-3-ol: a selective role for δ-$GABA_A$ receptors. *Eur.J.Neurosci.* **29**, 1177-1187.

Hevers, W. & Lüddens, H. (1998). The diversity of $GABA_A$ receptors. Pharmacological and electrophysiological properties of $GABA_A$ channel subtypes. *Mol.Neurobiol.* **18**, 35-86.

Hibbs, R. E. & Gouaux, E. (2011). Principles of activation and permeation in an anion-selective Cys-loop receptor. *Nature* **474**, 54-60.

Hill-Venning, C., Belelli, D., Peters, J. A., & Lambert, J. J. (1997). Subunit-dependent interaction of the general anaesthetic etomidate with the γ-aminobutyric acid type A receptor. *Br.J.Pharmacol.* **120**, 749-756.

Hill, D. R. & Bowery, N. G. (1981). ^{3}H-baclofen and ^{3}H-GABA bind to bicuculline-insensitive $GABA_B$ sites in rat brain. *Nature* **290**, 149-152.

Hinkle, D. J. & Macdonald, R. L. (2003). β subunit phosphorylation selectively increases fast desensitization and prolongs deactivation of α1β1γ2L and α1β3γ2L $GABA_A$ receptor currents. *J Neurosci.* **23**, 11698-11710.

Hodge, C. W., Mehmert, K. K., Kelley, S. P., McMahon, T., Haywood, A., Olive, M. F., Wang, D., Sanchez-Perez, A. M., & Messing, R. O. (1999). Supersensitivity to allosteric $GABA_A$ receptor modulators and alcohol in mice lacking PKCε. *Nat.Neurosci.* **2**, 997-1002.

Hodge, C. W., Raber, J., McMahon, T., Walter, H., Sanchez-Perez, A. M., Olive, M. F., Mehmert, K., Morrow, A. L., & Messing, R. O. (2002). Decreased anxiety-like behavior, reduced stress hormones, and neurosteroid supersensitivity in mice lacking protein kinase Cε. *J.Clin.Invest* **110**, 1003-1010.

Hollrigel, G. S. & Soltesz, I. (1997). Slow kinetics of miniature IPSCs during early postnatal development in granule cells of the dentate gyrus. *J.Neurosci.* **17**, 5119-5128.

Hornung, J. P. & Fritschy, J. M. (1996). Developmental profile of $GABA_A$-receptors in the marmoset monkey: expression of distinct subtypes in pre- and postnatal brain. *J.Comp Neurol.* **367**, 413-430.

Hosie, A. M., Dunne, E. L., Harvey, R. J., & Smart, T. G. (2003). Zinc-mediated inhibition of $GABA_A$ receptors: discrete binding sites underlie subtype specificity. *Nat.Neurosci.* **6**, 362-369.

Hosie, A. M., Wilkins, M. E., da Silva, H. M., & Smart, T. G. (2006). Endogenous neurosteroids regulate $GABA_A$ receptors through two discrete transmembrane sites. *Nature* **444**, 486-489.

Hosie, A. M., Wilkins, M. E., & Smart, T. G. (2007). Neurosteroid binding sites on $GABA_A$ receptors. *Pharmacol.Ther.* **116**, 7-19.

Houston, C. M., Hosie, A. M., & Smart, T. G. (2008). Distinct regulation of β2 and β3 subunit-containing cerebellar synaptic $GABA_A$ receptors by calcium/calmodulin-dependent protein kinase II. *J.Neurosci.* **28**, 7574-7584.

Huang, Z. J. (2009). Activity-dependent development of inhibitory synapses and innervation pattern: role of GABA signalling and beyond. *J.Physiol* **587**, 1881-1888.

Huguenard, J. R. & McCormick, D. A. (2007). Thalamic synchrony and dynamic regulation of global forebrain oscillations. *Trends Neurosci.* **30**, 350-356.

Huh, K. H., Endo, S., & Olsen, R. W. (1996). Diazepam-insensitive $GABA_A$ receptors in rat cerebellum and thalamus. *Eur.J.Pharmacol.* **310**, 225-233.

Huntsman, M. M., Leggio, M. G., & Jones, E. G. (1996). Nucleus-specific expression of $GABA_A$ receptor subunit mRNAs in monkey thalamus. *J.Neurosci.* **16**, 3571-3589.

Huntsman, M. M., Munoz, A., & Jones, E. G. (1999). Temporal modulation of $GABA_A$ receptor subunit gene expression in developing monkey cerebral cortex. *Neuroscience* **91**, 1223-1245.

Huntsman, M. M., Porcello, D. M., Homanics, G. E., DeLorey, T. M., & Huguenard, J. R. (1999). Reciprocal inhibitory connections and network synchrony in the mammalian thalamus. *Science* **283**, 541-543.

Huntsman, M. M. & Huguenard, J. R. (2000). Nucleus-specific differences in $GABA_A$-receptor-mediated inhibition are enhanced during thalamic development. *J.Neurophysiol.* **83**, 350-358.

Huntsman, M. M. & Huguenard, J. R. (2006). Fast IPSCs in rat thalamic reticular nucleus require the $GABA_A$ receptor β1 subunit. *J.Physiol* **572**, 459-475.

Ikegaki, N., Saito, N., Hashima, M., & Tanaka, C. (1994). Production of specific antibodies against GABA transporter subtypes (GAT1, GAT2, GAT3) and their application to immunocytochemistry. *Brain Res.Mol.Brain Res.* **26**, 47-54.

Im, W. B., Pregenzer, J. F., Binder, J. A., Dillon, G. H., & Alberts, G. L. (1995). Chloride channel expression with the tandem construct of α_6-β_2 $GABA_A$ receptor subunit requires a monomeric subunit of α6 or γ_2. *J.Biol.Chem.* **270**, 26063-26066.

Inquimbert, P., Rodeau, J. L., & Schlichter, R. (2007). Differential contribution of GABAergic and glycinergic components to inhibitory synaptic transmission in lamina II and laminae III-IV of the young rat spinal cord. *Eur.J.Neurosci.* **26**, 2940-2949.

Iversen, L. L. & Neal, M. J. (1968). The uptake of [^{3}H]GABA by slices of rat cerebral cortex. *J.Neurochem.* **15**, 1141-1149.

Iwama, K. & Jasper, H. H. (1957). The action of γ aminobutyric acid upon cortical electrical activity in the cat. *J.Physiol* **138**, 365-380.

Izumi, Y., Nagashima, K., Murayama, K., & Zorumski, C. F. (2005). Acute effects of ethanol on hippocampal long-term potentiation and long-term depression are mediated by different mechanisms. *Neuroscience* **136**, 509-517.

Izumi, Y., Murayama, K., Tokuda, K., Krishnan, K., Covey, D. F., & Zorumski, C. F. (2007). GABAergic neurosteroids mediate the effects of ethanol on long-term potentiation in rat hippocampal slices. *Eur.J.Neurosci.* **26**, 1881-1888.

Jacob, T. C., Moss, S. J., & Jurd, R. (2008). $GABA_A$ receptor trafficking and its role in the dynamic modulation of neuronal inhibition. *Nat.Rev.Neurosci.* **9**, 331-343.

Jahn, R. & Scheller, R. H. (2006). SNAREs--engines for membrane fusion. *Nat.Rev.Mol.Cell Biol.* **7**, 631-643.

Jahnsen, H. & Llinas, R. (1984). Voltage-dependent burst-to-tonic switching of thalamic cell activity: an in vitro study. *Arch.Ital.Biol.* **122**, 73-82.

Janssen, M. J., Ade, K. K., Fu, Z., & Vicini, S. (2009). Dopamine modulation of GABA tonic conductance in striatal output neurons. *J.Neurosci.* **29**, 5116-5126.

Jechlinger, M., Pelz, R., Tretter, V., Klausberger, T., & Sieghart, W. (1998). Subunit composition and quantitative importance of hetero-oligomeric receptors: $GABA_A$ receptors containing α_6 subunits. *J.Neurosci.* **18**, 2449-2457.

Jensen, K., Chiu, C. S., Sokolova, I., Lester, H. A., & Mody, I. (2003). GABA transporter-1 (GAT1)-deficient mice: differential tonic activation of $GABA_A$ versus $GABA_B$ receptors in the hippocampus. *J.Neurophysiol.* **90**, 2690-2701.

Jia, F., Pignataro, L., Schofield, C. M., Yue, M., Harrison, N. L., & Goldstein, P. A. (2005). An extrasynaptic $GABA_A$ receptor mediates tonic inhibition in thalamic VB neurons. *J.Neurophysiol.* **94**, 4491-4501.

Jia, F., Yue, M., Chandra, D., Keramidas, A., Goldstein, P. A., Homanics, G. E., & Harrison, N. L. (2008). Taurine is a potent activator of extrasynaptic $GABA_A$ receptors in the thalamus. *J.Neurosci.* **28**, 106-115.

Johnston, G. A. (2005). $GABA_A$ receptor channel pharmacology. *Curr.Pharm.Des* **11**, 1867-1885.

Jones, M. V. & Westbrook, G. L. (1996). The impact of receptor desensitization on fast synaptic transmission. *Trends Neurosci.* **19**, 96-101.

Jones, M. V. & Westbrook, G. L. (1997). Shaping of IPSCs by endogenous calcineurin activity. *J.Neurosci.* **17**, 7626-7633.

Jun, S. B., Cuzon, C., V, Ikeda, S., & Lovinger, D. (2011). Vibrodissociation of neurons from rodent brain slices to study synaptic transmission and image presynaptic terminals. *J.Vis.Exp.*

Jurd, R., Arras, M., Lambert, S., Drexler, B., Siegwart, R., Crestani, F., Zaugg, M., Vogt, K. E., Ledermann, B., Antkowiak, B., & Rudolph, U. (2003). General anesthetic actions in vivo strongly attenuated by a point mutation in the $GABA_A$ receptor β_3 subunit. *FASEB J* **17**, 250-252.

Juttner, R., Meier, J., & Grantyn, R. (2001). Slow IPSC kinetics, low levels of α_1 subunit expression and paired-pulse depression are distinct properties of neonatal inhibitory GABAergic synaptic connections in the mouse superior colliculus. *Eur.J.Neurosci.* **13**, 2088-2098.

Kaneda, M., Farrant, M., & Cull-Candy, S. G. (1995). Whole-cell and single-channel currents activated by GABA and glycine in granule cells of the rat cerebellum. *J.Physiol* **485 (Pt 2)** , 419-435.

Kanner, B. I. (2006). Structure and function of sodium-coupled GABA and glutamate transporters. *J.Membr.Biol.* **213**, 89-100.

Kapur, J. & MacDonald, R. L. (1999). Postnatal development of hippocampal dentate granule cell γ-aminobutyric acidA receptor pharmacological properties. *Mol.Pharmacol.* **55**, 444-452

Kasugai, Y., Swinny, J. D., Roberts, J. D., Dalezios, Y., Fukazawa, Y., Sieghart, W., Shigemoto, R., & Somogyi, P. (2010). Quantitative localisation of synaptic and extrasynaptic $GABA_A$ receptor subunits on hippocampal pyramidal cells by freeze-fracture replica immunolabelling. *Eur.J.Neurosci.* **32**, 1868-1888.

Katz, B. & Miledi, R. (1972). The statistical nature of the acetycholine potential and its molecular components. *J.Physiol* **224**, 665-699.

Kaufman, D. L., Houser, C. R., & Tobin, A. J. (1991). Two forms of the γ-aminobutyric acid synthetic enzyme glutamate decarboxylase have distinct intraneuronal distributions and cofactor interactions. *J.Neurochem.* **56**, 720-723.

Kavaliers, M. & Wiebe, J. P. (1987). Analgesic effects of the progesterone metabolite, 3α-hydroxy-5α-pregnan-20-one, and possible modes of action in mice. *Brain Res.* **415**, 393-398.

Kay, A. R., Alfonso, A., Alford, S., Cline, H. T., Holgado, A. M., Sakmann, B., Snitsarev, V. A., Stricker, T. P., Takahashi, M., & Wu, L. G. (1999). Imaging synaptic activity in intact brain and slices with FM1-43 in C. elegans, lamprey, and rat. *Neuron* **24**, 809-817.

Keller, A. F., Coull, J. A., Chery, N., Poisbeau, P., & De Koninck, Y. (2001). Region-specific developmental specialization of GABA-glycine cosynapses in laminas I-II of the rat spinal dorsal horn. *J.Neurosci.* **21**, 7871-7880.

Keller, A. F., Breton, J. D., Schlichter, R., & Poisbeau, P. (2004b). Production of 5α-reduced neurosteroids is developmentally regulated and shapes $GABA_A$ miniature IPSCs in lamina II of the spinal cord. *J.Neurosci.* **24**, 907-915.

Keller, E. A., Zamparini, A., Borodinsky, L. N., Gravielle, M. C., & Fiszman, M. L. (2004a). Role of allopregnanolone on cerebellar granule cells neurogenesis. *Brain Res.Dev.Brain Res.* **153**, 13-17.

Kellogg, C. K. & Frye, C. A. (1999). Endogenous levels of 5α-reduced progestins and androgens in fetal vs. adult rat brains. *Brain Res.Dev.Brain Res.* **115**, 17-24.

Kennedy, R. T., Thompson, J. E., & Vickroy, T. W. (2002). In vivo monitoring of amino acids by direct sampling of brain extracellular fluid at ultralow flow rates and capillary electrophoresis. *J.Neurosci.Methods* **114**, 39-49.

Keros, S. & Hablitz, J. J. (2005). Subtype-specific GABA transporter antagonists synergistically modulate phasic and tonic $GABA_A$ conductances in rat neocortex. *J.Neurophysiol.* **94**, 2073-2085.

Keynan, S. & Kanner, B. I. (1988). γ-Aminobutyric acid transport in reconstituted preparations from rat brain: coupled sodium and chloride fluxes. *Biochemistry* **27**, 12-17.

Khan, Z. U., Gutierrez, A., Miralles, C. P., & De Blas, A. L. (1996). The γ subunits of the native $GABA_A$/benzodiazepine receptors. *Neurochem.Res.* **21**, 147-159.

Khatri, A. & Weiss, D. S. (2010). The role of Loop F in the activation of the GABA receptor. *J.Physiol* **588**, 59-66.

Kirmse, K., Dvorzhak, A., Kirischuk, S., & Grantyn, R. (2008). GABA transporter 1 tunes GABAergic synaptic transmission at output neurons of the mouse neostriatum. *J.Physiol* **586**, 5665-5678.

Kittler, J. T. & Moss, S. J. (2003). Modulation of $GABA_A$ receptor activity by phosphorylation and receptor trafficking: implications for the efficacy of synaptic inhibition. *Curr.Opin.Neurobiol.* **13**, 341-347.

Kiyokage, E., Toida, K., Suzuki-Yamamoto, T., & Ishimura, K. (2005). Localization of 5α-reductase in the rat main olfactory bulb. *J.Comp Neurol.* **493**, 381-395.

Klausberger, T., Roberts, J. D., & Somogyi, P. (2002). Cell type- and input-specific differences in the number and subtypes of synaptic $GABA_A$ receptors in the hippocampus. *J.Neurosci.* **22**, 2513-2521.

Klausberger, T. & Somogyi, P. (2008). Neuronal diversity and temporal dynamics: the unity of hippocampal circuit operations. *Science* **321**, 53-57.

Knabl, J., Witschi, R., Hosl, K., Reinold, H., Zeilhofer, U. B., Ahmadi, S., Brockhaus, J., Sergejeva, M., Hess, A., Brune, K., Fritschy, J. M., Rudolph, U., Möhler, H., & Zeilhofer, H. U. (2008). Reversal of pathological pain through specific spinal $GABA_A$ receptor subtypes. *Nature* **451**, 330-334.

Knoflach, F., Benke, D., Wang, Y., Scheurer, L., Luddens, H., Hamilton, B. J., Carter, D. B., Mohler, H., & Benson, J. A. (1996). Pharmacological modulation of the diazepam-insensitive recombinant gamma-aminobutyric acidA receptors $\alpha_4\beta_2\gamma_2$ and $\alpha_6\beta_2\gamma_2$. *Mol.Pharmacol.* **50**, 1253-1261.

Kofuji, P., Wang, J. B., Moss, S. J., Huganir, R. L., & Burt, D. R. (1991). Generation of two forms of the γ-aminobutyric acidA receptor γ_2-subunit in mice by alternative splicing. *J.Neurochem.* **56**, 713-715.

Koksma, J. J., Van Kesteren, R. E., Rosahl, T. W., Zwart, R., Smit, A. B., Lüddens, H., & Brussaard, A. B. (2003). Oxytocin regulates neurosteroid modulation of $GABA_A$ receptors in supraoptic nucleus around parturition. *J.Neurosci.* **23**, 788-797.

Korpi, E. R., Grunder, G., & Lüddens, H. (2002a). Drug interactions at $GABA_A$ receptors. *Prog.Neurobiol.* **67**, 113-159.

Korpi, E. R., Mihalek, R. M., Sinkkonen, S. T., Hauer, B., Hevers, W., Homanics, G. E., Sieghart, W., & Luddens, H. (2002b). Altered receptor subtypes in the forebrain of

$GABA_A$ receptor δ subunit-deficient mice: recruitment of γ_2 subunits. *Neuroscience* **109**, 733-743.

Korpi, E. R. & Sinkkonen, S. T. (2006). $GABA_A$ receptor subtypes as targets for neuropsychiatric drug development. *Pharmacol.Ther.* **109**, 12-32.

Kragler, A., Hofner, G., & Wanner, K. T. (2005). Novel parent structures for inhibitors of the murine GABA transporters mGAT3 and mGAT4. *Eur.J.Pharmacol.* **519**, 43-47.

Krishek B.J., Moss S.J., & Smart T.G. (1998). Interaction of H^+ and Zn^{2+} on recombinant and native rat neuronal $GABA_A$ receptors. *J Physiol* **507**, 639–665

Krnjevic, K. & Schwartz, S. (1966). Is γ-aminobutyric acid an inhibitory transmitter? *Nature* **211**, 1372-1374.

Krnjevic, K. & Schwartz, S. (1967). The action of γ-aminobutyric acid on cortical neurones. *Exp.Brain Res.* **3**, 320-336.

Krnjevic, K. (2005). From 'soup physiology' to normal brain science. *J.Physiol* **569**, 1-2.

Krogsgaard-Larsen, P., Frolund, B., Liljefors, T., & Ebert, B. (2004). $GABA_A$ agonists and partial agonists: THIP (Gaboxadol) as a non-opioid analgesic and a novel type of hypnotic. *Biochem.Pharmacol.* **68**, 1573-1580.

Krook-Magnuson, E. I. & Huntsman, M. M. (2005). Excitability of cortical neurons depends upon a powerful tonic conductance in inhibitory networks. *Thalamus.Relat Syst.* **3**, 115-120.

Kuffler, S. W. & Edwards, C. (1958). Mechanism of γ aminobutyric acid (GABA) action and its relation to synaptic inhibition. *J.Neurophysiol.* **21**, 589-610.

Kullmann, D. M., Ruiz, A., Rusakov, D. M., Scott, R., Semyanov, A., & Walker, M. C. (2005). Presynaptic, extrasynaptic and axonal $GABA_A$ receptors in the CNS: where and why? *Prog.Biophys.Mol.Biol.* **87**, 33-46.

Kuzirian, M. S. & Paradis, S. (2011). Emerging themes in GABAergic synapse development. *Prog.Neurobiol.* **95**, 68-87.

Lagrange, A. H., Botzolakis, E. J., & Macdonald, R. L. (2007). Enhanced macroscopic desensitization shapes the response of α_4 subtype-containing $GABA_A$ receptors to synaptic and extrasynaptic GABA. *J.Physiol* **578**, 655-676.

Lambert, J. J., Belelli, D., Hill-Venning, C., & Peters, J. A. (1995). Neurosteroids and $GABA_A$ receptor function. *Trends Pharmacol.Sci.* **16**, 295-303.

Lambert, J. J., Belelli, D., Peden, D. R., Vardy, A. W., & Peters, J. A. (2003). Neurosteroid modulation of $GABA_A$ receptors. *Prog.Neurobiol.* **71**, 67-80.

Lauber, M. E. & Lichtensteiger, W. (1996). Ontogeny of 5α-reductase (type 1) messenger ribonucleic acid expression in rat brain: early presence in germinal zones. *Endocrinology* **137**, 2718-2730.

Laurie, D. J., Seeburg, P. H., & Wisden, W. (1992a). The distribution of 13 $GABA_A$ receptor subunit mRNAs in the rat brain. II. Olfactory bulb and cerebellum. *J.Neurosci.* **12**, 1063-1076.

Laurie, D. J., Wisden, W., & Seeburg, P. H. (1992b). The distribution of thirteen $GABA_A$ receptor subunit mRNAs in the rat brain. III. Embryonic and postnatal development. *J Neurosci.* **12**, 4151-4172.

Lavoie, A. M., Tingey, J. J., Harrison, N. L., Pritchett, D. B., & Twyman, R. E. (1997). Activation and deactivation rates of recombinant $GABA_A$ receptor channels are dependent on α-subunit isoform. *Biophys.J.* **73**, 2518-2526.

Lee, A. K., Manns, I. D., Sakmann, B., & Brecht, M. (2006). Whole-cell recordings in freely moving rats. *Neuron* **51**, 399-407.

Lerma, J., Herranz, A. S., Herreras, O., Abraira, V., & Martin, d. R. (1986). In vivo determination of extracellular concentration of amino acids in the rat hippocampus. A method based on brain dialysis and computerized analysis. *Brain Res.* **384**, 145-155.

Levitan, E. S., Schofield, P. R., Burt, D. R., Rhee, L. M., Wisden, W., Kohler, M., Fujita, N., Rodriguez, H. F., Stephenson, A., Darlison, M. G., & . (1988). Structural and functional basis for $GABA_A$ receptor heterogeneity. *Nature* **335**, 76-79.

Li, P., Covey, D. F., Steinbach, J. H., & Akk, G. (2006). Dual potentiating and inhibitory actions of a benz[*e*]indene neurosteroid analog on recombinant α1β2γ2 $GABA_A$ receptors. *Mol.Pharmacol.* **69**, 2015-2026.

Li, M. & De Blas, A. L. (1997). Coexistence of two β subunit isoforms in the same γ-aminobutyric acid type A receptor. *J.Biol.Chem.* **272**, 16564-16569.

Li, W., Jin, X., Covey, D. F., & Steinbach, J. H. (2007). Neuroactive steroids and human recombinant ρ1 $GABA_C$ receptors. *J.Pharmacol.Exp.Ther.* **323**, 236-247.

Li, X., Bertics, P. J., & Karavolas, H. J. (1997). Regional distribution of cytosolic and particulate 5α-dihydroprogesterone 3α-hydroxysteroid oxidoreductases in female rat brain. *J.Steroid Biochem.Mol.Biol.* **60**, 311-318.

Liu, Q. R., Lopez-Corcuera, B., Nelson, H., Mandiyan, S., & Nelson, N. (1992). Cloning and expression of a cDNA encoding the transporter of taurine and β-alanine in mouse brain. *Proc.Natl.Acad.Sci.U.S.A* **89**, 12145-12149.

Liu, Q. R., Lopez-Corcuera, B., Mandiyan, S., Nelson, H., & Nelson, N. (1993). Molecular characterization of four pharmacologically distinct γ-aminobutyric acid transporters in mouse brain [corrected]. *J.Biol.Chem.* **268**, 2106-2112.

Llano, I. & Gerschenfeld, H. M. (1993). Inhibitory synaptic currents in stellate cells of rat cerebellar slices. *J.Physiol* **468**, 177-200.

Llano, I., Gonzalez, J., Caputo, C., Lai, F. A., Blayney, L. M., Tan, Y. P., & Marty, A. (2000). Presynaptic calcium stores underlie large-amplitude miniature IPSCs and spontaneous calcium transients. *Nat.Neurosci.* **3**, 1256-1265.

LoTurco, J. J., Owens, D. F., Heath, M.J., Davis, M. B., & Kriegstein, A. R. (1995). GABA and glutamate depolarize cortical progenitor cells and inhibit DNA synthesis. *Neuron* **15**, 1287-1298.

Low, K., Crestani, F., Keist, R., Benke, D., Brunig, I., Benson, J. A., Fritschy, J. M., Rulicke, T., Bluethmann, H., Möhler, H., & Rudolph, U. (2000). Molecular and neuronal substrate for the selective attenuation of anxiety. *Science* **290**, 131-134.

Luchetti, S., Huitinga, I., & Swaab, D. F. (2011). Neurosteroid and GABA-A receptor alterations in Alzheimer's disease, Parkinson's disease and multiple sclerosis. *Neuroscience* **191**, 6-21.

Lüddens, H., Killisch, I., & Seeburg, P. H. (1991). More than one α variant may exist in a $GABA_A$/benzodiazepine receptor complex. *J.Recept.Res.* **11**, 535-551.

Ludwig, A., Li, H., Saarma, M., Kaila, K., & Rivera, C. (2003). Developmental up-regulation of KCC2 in the absence of GABAergic and glutamatergic transmission. *Eur.J.Neurosci.* **18**, 3199-3206.

Lüscher, B., Fuchs, T., & Kilpatrick, C. L. (2011). $GABA_A$ receptor trafficking-mediated plasticity of inhibitory synapses. *Neuron* **70**, 385-409.

Ma, W., Saunders, P. A., Somogyi, R., Poulter, M. O., & Barker, J. L. (1993). Ontogeny of $GABA_A$ receptor subunit mRNAs in rat spinal cord and dorsal root ganglia. *J.Comp Neurol.* **338**, 337-359.

Macdonald, R. L. & Barker, J. L. (1977). Pentylenetetrazol and penicillin are selective antagonists of GABA-mediated post-synaptic inhibition in cultured mammalian neurones. *Nature* **267**, 720-721.

Macdonald, R. L. & Barker, J. L. (1978a). Different actions of anticonvulsant and anesthetic barbiturates revealed by use of cultured mammalian neurons. *Science* **200**, 775-777.

Macdonald, R. L. & Barker, J. L. (1978b). Specific antagonism of GABA-mediated postsynaptic inhibition in cultured mammalian spinal cord neurons: a common mode of convulsant action. *Neurology* **28**, 325-330.

Macdonald, R. & Barker, J. L. (1978c). Benzodiazepines specifically modulate GABA-mediated postsynaptic inhibition in cultured mammalian neurones. *Nature* **271**, 563-564.

Macdonald, R. L. & Barker, J. L. (1979a). Enhancement of GABA-mediated postsynaptic inhibition in cultured mammalian spinal cord neurons: a common mode of anticonvulsant action. *Brain Res.* **167**, 323-336.

Macdonald, R. L. & Barker, J. L. (1979b). Anticonvulsant and anesthetic barbiturates: different postsynaptic actions in cultured mammalian neurons. *Neurology* **29**, 432-447.

Macdonald, R. L. & Twyman, R. E. (1992). Kinetic properties and regulation of $GABA_A$ receptor channels. *Ion Channels* **3**, 315-343.

Macdonald, R. L. & Olsen, R. W. (1994). $GABA_A$ receptor channels. *Annu.Rev.Neurosci.* **17**, 569-602.

MacLennan, A. J., Brecha, N., Khrestchatisky, M., Sternini, C., Tillakaratne, N. J., Chiang, M. Y., Anderson, K., Lai, M., & Tobin, A. J. (1991). Independent cellular and ontogenetic expression of mRNAs encoding three α polypeptides of the rat $GABA_A$ receptor. *Neuroscience* **43**, 369-380.

Madsen, K. K., Larsson, O. M., & Schousboe, A. (2008). Regulation of excitation by GABA neurotransmission: focus on metabolism and transport. *Results Probl.Cell Differ.* **44**, 201-221.

Madsen, K. K., White, H. S., & Schousboe, A. (2010). Neuronal and non-neuronal GABA transporters as targets for antiepileptic drugs. *Pharmacol.Ther.* **125**, 394-401.

Majewska, M. D., Harrison, N. L., Schwartz, R. D., Barker, J. L., & Paul, S. M. (1986). Steroid hormone metabolites are barbiturate-like modulators of the GABA receptor. *Science* **232**, 1004-1007.

Mann, E. O. & Mody, I. (2010). Control of hippocampal γ oscillation frequency by tonic inhibition and excitation of interneurons. *Nat.Neurosci.* **13**, 205-212.

Manning, J. P., Richards, D. A., & Bowery, N. G. (2003). Pharmacology of absence epilepsy. *Trends Pharmacol.Sci.* **24**, 542-549.

Martens, S. & McMahon, H. T. (2008). Mechanisms of membrane fusion: disparate players and common principles. *Nat.Rev.Mol.Cell Biol.* **9**, 543-556.

Martin, D. L., Martin, S. B., Wu, S. J., & Espina, N. (1991). Regulatory properties of brain glutamate decarboxylase (GAD): the apoenzyme of GAD is present principally as the smaller of two molecular forms of GAD in brain. *J.Neurosci.* **11**, 2725-2731.

Martin, D. L. & Rimvall, K. (1993). Regulation of γ-aminobutyric acid synthesis in the brain. *J.Neurochem.* **60**, 395-407.

Martin, L. J., Zurek, A. A., MacDonald, J. F., Roder, J. C., Jackson, M. F., & Orser, B. A. (2010). α5$GABA_A$ receptor activity sets the threshold for long-term potentiation and constrains hippocampus-dependent memory. *J.Neurosci.* **30**, 5269-5282.

Marty, A. & Neher, E. (1995). The whole-cell recording configuration from a chemical point of view. In *Single-Channel Recording*, eds. Sakmann, B. & Neher, E., pp. 42-45. Plennum Press, New York.

Matsumoto, K., Puia, G., Dong, E., & Pinna, G. (2007). $GABA_A$ receptor neurotransmission dysfunction in a mouse model of social isolation-induced stress: possible insights into a non-serotonergic mechanism of action of SSRIs in mood and anxiety disorders. *Stress.* **10**, 3-12.

McCartney, M. R., Deeb, T. Z., Henderson, T. N., & Hales, T. G. (2007). Tonically active $GABA_A$ receptors in hippocampal pyramidal neurons exhibit constitutive GABA-independent gating. *Mol.Pharmacol.* **71**, 539-548.

McCormick, D. A. & Bal, T. (1997). Sleep and arousal: thalamocortical mechanisms. *Annu.Rev.Neurosci.* **20** , 185-215.

McIntire, S. L., Reimer, R. J., Schuske, K., Edwards, R. H., & Jorgensen, E. M. (1997). Identification and characterization of the vesicular GABA transporter. *Nature* **389**, 870-876.

McKernan, R. M. & Whiting, P. J. (1996). Which $GABA_A$-receptor subtypes really occur in the brain? *Trends Neurosci.* **19**, 139-143.

McKernan, R. M., Rosahl, T. W., Reynolds, D. S., Sur, C., Wafford, K. A., Atack, J. R., Farrar, S., Myers, J., Cook, G., Ferris, P., Garrett, L., Bristow, L., Marshall, G., Macaulay, A., Brown, N., Howell, O., Moore, K. W., Carling, R. W., Street, L. J., Castro, J. L., Ragan, C. I., Dawson, G. R., & Whiting, P. J. (2000). Sedative but not anxiolytic properties of benzodiazepines are mediated by the $GABA_A$ receptor α1 subtype. *Nat.Neurosci.* **3**, 587-592.

McLennan, H. (1958). Absence of γ-aminobutyric acid from brain extracts containing factor I. *Nature* **181**, 1807.

Meier, J. & Grantyn, R. (2004). Preferential accumulation of $GABA_A$ receptor γ2L, not γ2S, cytoplasmic loops at rat spinal cord inhibitory synapses. *J.Physiol* **559**, 355-365.

Melcangi, R. C., Celotti, F., Castano, P., & Martini, L. (1993). Differential localization of the 5α-reductase and the 3α-hydroxysteroid dehydrogenase in neuronal and glial cultures. *Endocrinology* **132**, 1252-1259.

Melcangi, R. C., Celotti, F., & Martini, L. (1994). Progesterone 5-α-reduction in neuronal and in different types of glial cell cultures: type 1 and 2 astrocytes and oligodendrocytes. *Brain Res.* **639**, 202-206.

Melcangi, R. C., Poletti, A., Cavarretta, I., Celotti, F., Colciago, A., Magnaghi, V., Motta, M., Negri-Cesi, P., & Martini, L. (1998). The 5α-reductase in the central nervous system: expression and modes of control. *J.Steroid Biochem.Mol.Biol.* **65**, 295-299.

Melcangi, R. C., Panzica, G., & Garcia-Segura, L. M. (2011). Neuroactive steroids: focus on human brain. *Neuroscience* **191**, 1-5.

Mellon, S. H., Griffin, L. D., & Compagnone, N. A. (2001). Biosynthesis and action of neurosteroids. *Brain Res.Brain Res.Rev.* **37**, 3-12.

Mellon, S. H. & Vaudry, H. (2001). Biosynthesis of neurosteroids and regulation of their synthesis. *Int.Rev.Neurobiol.* **46**, 33-78.

Mellon, S. H. & Griffin, L. D. (2002). Neurosteroids: biochemistry and clinical significance. *Trends Endocrinol.Metab* **13**, 35-43.

Mellon, S. H. (2007). Neurosteroid regulation of central nervous system development. *Pharmacol.Ther.* **116**, 107-124.

Mertens, S., Benke, D., & Möhler, H. (1993). $GABA_A$ receptor populations with novel subunit combinations and drug binding profiles identified in brain by α5- and δ-subunit-specific immunopurification. *J.Biol.Chem.* **268**, 5965-5973.

Michels, G. & Moss, S. J. (2007). $GABA_A$ receptors: properties and trafficking. *Crit Rev.Biochem.Mol.Biol.* **42**, 3-14.

Mihalek, R. M., Banerjee, P. K., Korpi, E. R., Quinlan, J. J., Firestone, L. L., Mi, Z. P., Lagenaur, C., Tretter, V., Sieghart, W., Anagnostaras, S. G., Sage, J. R., Fanselow, M. S., Guidotti, A., Spigelman, I., Li, Z., DeLorey, T. M., Olsen, R. W., & Homanics, G. E. (1999). Attenuated sensitivity to neuroactive steroids in γ-aminobutyrate type A receptor δ subunit knockout mice. *Proc.Natl.Acad.Sci.U.S.A* **96**, 12905-12910.

Miller, P. S. & Smart, T. G. (2010). Binding, activation and modulation of Cys-loop receptors. *Trends Pharmacol.Sci.* **31**, 161-174.

Milligan, C. J., Buckley, N. J., Garret, M., Deuchars, J., & Deuchars, S. A. (2004). Evidence for inhibition mediated by coassembly of $GABA_A$ and $GABA_C$ receptor subunits in native central neurons. *J.Neurosci.* **24**, 7241-7250.

Minelli, A., DeBiasi, S., Brecha, N. C., Zuccarello, L. V., & Conti, F. (1996). GAT-3, a high-affinity GABA plasma membrane transporter, is localized to astrocytic processes, and it is not confined to the vicinity of GABAergic synapses in the cerebral cortex. *J.Neurosci.* **16**, 6255-6264.

Minier, F. & Sigel, E. (2004). Positioning of the α-subunit isoforms confers a functional signature to γ-aminobutyric acid type A receptors. *Proc.Natl.Acad.Sci.U.S.A* **101**, 7769-7774.

Mintz, I. M. & Bean, B. P. (1993). $GABA_B$ receptor inhibition of P-type Ca^{2+} channels in central neurons. *Neuron* **10**, 889-898.

Mirza, N. R., Larsen, J. S., Mathiasen, C., Jacobsen, T. A., Munro, G., Erichsen, H. K., Nielsen, A. N., Troelsen, K. B., Nielsen, E. O., & Ahring, P. K. (2008). NS11394 [3'-[5-(1-hydroxy-1-methyl-ethyl)-benzoimidazol-1-yl]-biphenyl-2-carbonitr ile], a unique subtype-selective $GABA_A$ receptor positive allosteric modulator: in vitro actions, pharmacokinetic properties and in vivo anxiolytic efficacy. *J.Pharmacol.Exp.Ther.* **327**, 954-968.

Mitchell, E. A., Herd, M. B., Gunn, B. G., Lambert, J. J., & Belelli, D. (2008). Neurosteroid modulation of $GABA_A$ receptors: molecular determinants and significance in health and disease. *Neurochem.Int.* **52**, 588-595.

Miyazawa, A., Fujiyoshi, Y., & Unwin, N. (2003). Structure and gating mechanism of the acetylcholine receptor pore. *Nature* **423**, 949-955.

Mody, I., De Koninck, Y., Otis, T. S., & Soltesz, I. (1994). Bridging the cleft at GABA synapses in the brain. *Trends Neurosci.* **17**, 517-525.

Möhler, H. & Okada, T. (1977). GABA receptor binding with $^{3}H^{+}$ bicuculline-methiodide in rat CNS. *Nature* **267**, 65-67.

Möhler, H. (2006). $GABA_A$ receptor diversity and pharmacology. *Cell Tissue Res.* **326**, 505-516.

Möhler, H. (2011). The rise of a new GABA pharmacology. *Neuropharmacology* **60**, 1042-1049.

Mortensen, M. & Smart, T. G. (2006). Extrasynaptic αβ subunit $GABA_A$ receptors on rat hippocampal pyramidal neurons. *J.Physiol* **577**, 841-856.

Moss, S. J., Doherty, C. A., & Huganir, R. L. (1992). Identification of the cAMP-dependent protein kinase and protein kinase C phosphorylation sites within the major intracellular domains of the β_1, γ_2S, and γ_2L subunits of the γ-aminobutyric acid type A receptor. *J.Biol.Chem.* **267**, 14470-14476.

Mozrzymas, J. W., Barberis, A., Mercik, K., & Zarnowska, E. D. (2003). Binding sites, singly bound states, and conformation coupling shape GABA-evoked currents. *J.Neurophysiol.* **89**, 871-883.

Mozrzymas, J. W. (2004). Dynamism of $GABA_A$ receptor activation shapes the "personality" of inhibitory synapses. *Neuropharmacology* **47**, 945-960.

Mtchedlishvili, Z. & Kapur, J. (2006). High-affinity, slowly desensitizing $GABA_A$ receptors mediate tonic inhibition in hippocampal dentate granule cells. *Mol.Pharmacol.* **69**, 564-575.

Murayama, K., Zorumski, C. F., & Izumi, Y. (2006). Effects of neurosteroid 3α-hydroxy-5α-pregnan-20-one on ethanol-mediated paired-pulse depression of population spikes in the CA1 region of rat hippocampal slices. *Neurosci.Lett.* **394**, 28-32.

Nayeem, N., Green, T. P., Martin, I. L., & Barnard, E. A. (1994). Quaternary structure of the native $GABA_A$ receptor determined by electron microscopic image analysis. *J Neurochem.* **62**, 815-818.

Neher, E. & Sakmann, B. (1976). Single-channel currents recorded from membrane of denervated frog muscle fibres. *Nature* **260**, 799-802.

Neher, E. & Sakmann, B. (1992). The patch clamp technique. *Sci.Am.* **266**, 44-51.

Neher, E. (1992). Nobel lecture. Ion channels for communication between and within cells. *Neuron* **8**, 605-612.

Nelson, N. (1998). The family of Na^+/Cl^- neurotransmitter transporters. *J.Neurochem.* **71**, 1785-1803.

Nicholls, J. G., Martin, A.R., Wallace, B.G., & Fuchs, P.A. (2001). Cellular and molecular biochemistry of synaptic transmission. In *From Neuron to Brain*, eds. Nicholls, J. G., Martin, A.R., Wallace, B.G., & Fuchs, P.A., pp. 252-253. Sinauer Associates, inc, Massachusetts

The whole-cell recording configuration form a chemical point of view. In *Single-Channel Recording*, eds. Sakmann, B. & Neher, E., pp. 42-45. Plennum Press, New York.

Nusser, Z., Roberts, J. D., Baude, A., Richards, J. G., & Somogyi, P. (1995). Relative densities of synaptic and extrasynaptic $GABA_A$ receptors on cerebellar granule cells as determined by a quantitative immunogold method. *J.Neurosci.* **15**, 2948-2960.

Nusser, Z., Sieghart, W., Benke, D., Fritschy, J. M., & Somogyi, P. (1996b). Differential synaptic localization of two major γ-aminobutyric acid type A receptor α subunits on hippocampal pyramidal cells. *Proc.Natl.Acad.Sci.U.S.A* **93**, 11939-11944.

Nusser, Z., Sieghart, W., Stephenson, F. A., & Somogyi, P. (1996a). The α6 subunit of the $GABA_A$ receptor is concentrated in both inhibitory and excitatory synapses on cerebellar granule cells. *J.Neurosci.* **16**, 103-114.

Nusser, Z., Cull-Candy, S., & Farrant, M. (1997). Differences in synaptic $GABA_A$ receptor number underlie variation in GABA mini amplitude. *Neuron* **19**, 697-709.

Nusser, Z., Sieghart, W., & Somogyi, P. (1998a). Segregation of different $GABA_A$ receptors to synaptic and extrasynaptic membranes of cerebellar granule cells. *J Neurosci.* **18**, 1693-1703.

Nusser, Z., Hajos, N., Somogyi, P., & Mody, I. (1998b). Increased number of synaptic $GABA_A$ receptors underlies potentiation at hippocampal inhibitory synapses. *Nature* **395**, 172-177.

Nusser, Z., Naylor, D., & Mody, I. (2001). Synapse-specific contribution of the variation of transmitter concentration to the decay of inhibitory postsynaptic currents. *Biophys.J.* **80**, 1251-1261.

Nusser, Z. & Mody, I. (2002). Selective modulation of tonic and phasic inhibitions in dentate gyrus granule cells. *J.Neurophysiol.* **87**, 2624-2628.

Nyitrai, G., Kekesi, K. A., & Juhasz, G. (2006). Extracellular level of GABA and Glu: in vivo microdialysis-HPLC measurements. *Curr.Top.Med.Chem.* **6**, 935-940.

Obata, K., Ito, M., Ochi, R., & Sato, N. (1967). Pharmacological properties of the postsynaptic inhibition by Purkinje cell axons and the action of γ-aminobutyric acid on deiters neurones. *Exp.Brain Res.* **4**, 43-57.

Oja, S. S. & Saransaari, P. (2000). Modulation of taurine release by glutamate receptors and nitric oxide. *Prog.Neurobiol.* **62**, 407-425.

Okada, M., Onodera, K., Van Renterghem, C., Sieghart, W., & Takahashi, T. (2000). Functional correlation of $GABA_A$ receptor α subunits expression with the properties of IPSCs in the developing thalamus. *J.Neurosci.* **20**, 2202-2208.

Olah, S., Fule, M., Komlosi, G., Varga, C., Baldi, R., Barzo, P., & Tamas, G. (2009). Regulation of cortical microcircuits by unitary GABA-mediated volume transmission. *Nature* **461**, 1278-1281.

Olsen, R. W. & Sieghart, W. (2008). International Union of Pharmacology. LXX. Subtypes of γ-aminobutyric $acid_A$ receptors: classification on the basis of subunit composition, pharmacology, and function. Update. *Pharmacol.Rev.* **60**, 243-260.

Olsen, R. W. & Li, G. D. (2011). $GABA_A$ receptors as molecular targets of general anesthetics: identification of binding sites provides clues to allosteric modulation. *Can.J.Anaesth.* **58**, 206-215.

Ortinski, P. I., Lu, C., Takagaki, K., Fu, Z., & Vicini, S. (2004). Expression of distinct α subunits of $GABA_A$ receptor regulates inhibitory synaptic strength. *J.Neurophysiol.* **92**, 1718-1727.

Otis, T. S. & Mody, I. (1992). Modulation of decay kinetics and frequency of $GABA_A$ receptor-mediated spontaneous inhibitory postsynaptic currents in hippocampal neurons. *Neuroscience* **49**, 13-32.

Otis, T. S., De Koninck, Y., & Mody, I. (1994). Lasting potentiation of inhibition is associated with an increased number of γ-aminobutyric acid type A receptors activated during miniature inhibitory postsynaptic currents. *Proc.Natl.Acad.Sci.U.S.A* **91**, 7698-7702.

Owens, D. F. & Kriegstein, A. R. (2002). Is there more to GABA than synaptic inhibition? *Nat.Rev.Neurosci.* **3**, 715-727.

Pan, Y. & Qian, H. (2005). Interactions between rho and γ2 subunits of the GABA receptor. *J.Neurochem.* **94**, 482-490.

Panzanelli, P., Gunn, B. G., Schlatter, M. C., Benke, D., Tyagarajan, S. K., Scheiffele, P., Belelli, D., Lambert, J. J., Rudolph, U., & Fritschy, J. M. (2011). Distinct

mechanisms regulate $GABA_A$ receptor and gephyrin clustering at perisomatic and axo-axonic synapses on CA1 pyramidal cells. *J.Physiol*.

Park, J. S., Higashi, H., Nagata, K., & Yoshimura, M. (1999). Bicuculline-resistant, Cl^- dependent GABA response in the rat spinal dorsal horn. *Neurosci.Res.* **33**, 261-268.

Paul, S. M. & Purdy, R. H. (1992). Neuroactive steroids. *FASEB J.* **6**, 2311-2322.

Pavlov, I., Savtchenko, L. P., Kullmann, D. M., Semyanov, A., & Walker, M. C. (2009). Outwardly rectifying tonically active $GABA_A$ receptors in pyramidal cells modulate neuronal offset, not gain. *J.Neurosci.* **29**, 15341-15350.

Paysan, J., Kossel, A., Bolz, J., & Fritschy, J. M. (1997). Area-specific regulation of γ-aminobutyric acid type A receptor subtypes by thalamic afferents in developing rat neocortex. *Proc.Natl.Acad.Sci.U.S.A* **94**, 6995-7000.

Peden, D. R., Petitjean, C. M., Herd, M. B., Durakoglugil, M. S., Rosahl, T. W., Wafford, K., Homanics, G. E., Belelli, D., Fritschy, J. M., & Lambert, J. J. (2008). Developmental maturation of synaptic and extrasynaptic $GABA_A$ receptors in mouse thalamic ventrobasal neurones. *J.Physiol* **586**, 965-987.

Pelletier, G., Luu-The, V., & Labrie, F. (1994). Immunocytochemical localization of 5α-reductase in rat brain. *Mol.Cell Neurosci.* **5**, 394-399.

Peng, Z., Huang, C. S., Stell, B. M., Mody, I., & Houser, C. R. (2004). Altered expression of the δ subunit of the $GABA_A$ receptor in a mouse model of temporal lobe epilepsy. *J Neurosci.* **24**, 8629-8639.

Perrais, D. & Ropert, N. (1999). Effect of zolpidem on miniature IPSCs and occupancy of postsynaptic $GABA_A$ receptors in central synapses. *J.Neurosci.* **19**, 578-588.

Persohn, E., Malherbe, P., & Richards, J. G. (1992). Comparative molecular neuroanatomy of cloned $GABA_A$ receptor subunits in the rat CNS. *J.Comp Neurol.* **326**, 193-216.

Peters, J. A., Kirkness, E. F., Callachan, H., Lambert, J. J., & Turner, A. J. (1988). Modulation of the $GABA_A$ receptor by depressant barbiturates and pregnane steroids. *Br.J.Pharmacol.* **94**, 1257-1269.

Peters, J. A., Hales, T. G., & Lambert, J. J. (2005). Molecular determinants of single-channel conductance and ion selectivity in the Cys-loop family: insights from the $5\text{-}HT_3$ receptor. *Trends Pharmacol.Sci.* **26**, 587-594.

Petrini, E. M., Zacchi, P., Barberis, A., Mozrzymas, J. W., & Cherubini, E. (2003). Declusterization of $GABA_A$ receptors affects the kinetic properties of GABAergic currents in cultured hippocampal neurons. *J.Biol.Chem.* **278**, 16271-16279.

Picton, A. J. & Fisher, J. L. (2007). Effect of the α subunit subtype on the macroscopic kinetic properties of recombinant $GABA_A$ receptors. *Brain Res.* **1165**, 40-49.

Pinna, G., Uzunova, V., Matsumoto, K., Puia, G., Mienville, J. M., Costa, E., & Guidotti, A. (2000). Brain allopregnanolone regulates the potency of the $GABA_A$ receptor agonist muscimol. *Neuropharmacology* **39**, 440-448.

Pinna, G., Costa, E., & Guidotti, A. (2004). Fluoxetine and norfluoxetine stereospecifically facilitate pentobarbital sedation by increasing neurosteroids. *Proc.Natl.Acad.Sci.U.S.A* **101**, 6222-6225.

Pinna, G. (2010). In a mouse model relevant for post-traumatic stress disorder, selective brain steroidogenic stimulants (SBSS) improve behavioral deficits by normalizing allopregnanolone biosynthesis. *Behav.Pharmacol.* **21**, 438-450.

Pirker, S., Schwarzer, C., Wieselthaler, A., Sieghart, W., & Sperk, G. (2000). $GABA_A$ receptors: immunocytochemical distribution of 13 subunits in the adult rat brain. *Neuroscience* **101**, 815-850.

Pistis, M., Belelli, D., Peters, J. A., & Lambert, J. J. (1997). The interaction of general anaesthetics with recombinant $GABA_A$ and glycine receptors expressed in Xenopus laevis oocytes: a comparative study. *Br.J.Pharmacol.* **122**, 1707-1719.

Poisbeau, P., Patte-Mensah, C., Keller, A. F., Barrot, M., Breton, J. D., Luis-Delgado, O. E., Freund-Mercier, M. J., Mensah-Nyagan, A. G., & Schlichter, R. (2005). Inflammatory pain upregulates spinal inhibition via endogenous neurosteroid production. *J.Neurosci.* **25**, 11768-11776.

Polc, P., Möhler, H., & Haefely, W. (1974). The effect of diazepam on spinal cord activities: possible sites and mechanisms of action. *Naunyn Schmiedebergs Arch.Pharmacol.* **284**, 319-337.

Polc, P. & Haefely, W. (1976). Effects of two benzodiazepines, phenobarbitone, and baclofen on synaptic transmission in the cat cuneate nucleus. *Naunyn Schmiedebergs Arch.Pharmacol.* **294**, 121-131.

Polenzani, L., Woodward, R. M., & Miledi, R. (1991). Expression of mammalian γ-aminobutyric acid receptors with distinct pharmacology in Xenopus oocytes. *Proc.Natl.Acad.Sci.U.S.A* **88**, 4318-4322.

Poletti, A., Negri-Cesi, P., Rabuffetti, M., Colciago, A., Celotti, F., & Martini, L. (1998). Transient expression of the 5α-reductase type 2 isozyme in the rat brain in late fetal and early postnatal life. *Endocrinology* **139**, 2171-2178.

Pomata, P. E., Colman-Lerner, A. A., Baranao, J. L., & Fiszman, M. L. (2000). In vivo evidences of early neurosteroid synthesis in the developing rat central nervous system and placenta. *Brain Res.Dev.Brain Res.* **120**, 83-86.

Porcello, D. M., Huntsman, M. M., Mihalek, R. M., Homanics, G. E., & Huguenard, J. R. (2003). Intact synaptic GABAergic inhibition and altered neurosteroid modulation of thalamic relay neurons in mice lacking δ subunit. *J.Neurophysiol.* **89**, 1378-1386.

Poulter, M. O., Barker, J. L., O'Carroll, A. M., Lolait, S. J., & Mahan, L. C. (1992). Differential and transient expression of $GABA_A$ receptor α-subunit mRNAs in the developing rat CNS. *J.Neurosci.* **12**, 2888-2900.

Poulter, M. O., Barker, J. L., O'Carroll, A. M., Lolait, S. J., & Mahan, L. C. (1993). Co-existent expression of $GABA_A$ receptor β2, β3 and γ2 subunit messenger RNAs during embryogenesis and early postnatal development of the rat central nervous system. *Neuroscience* **53**, 1019-1033.

Pouzat, C. & Hestrin, S. (1997). Developmental regulation of basket/stellate cell→Purkinje cell synapses in the cerebellum. *J.Neurosci.* **17**, 9104-9112.

Prenosil, G. A., Schneider Gasser, E. M., Rudolph, U., Keist, R., Fritschy, J. M., & Vogt, K. E. (2006). Specific subtypes of $GABA_A$ receptors mediate phasic and tonic forms of inhibition in hippocampal pyramidal neurons. *J.Neurophysiol.* **96**, 846-857.

Pritchett, D. B., Sontheimer, H., Shivers, B. D., Ymer, S., Kettenmann, H., Schofield, P. R., & Seeburg, P. H. (1989). Importance of a novel $GABA_A$ receptor subunit for benzodiazepine pharmacology. *Nature* **338**, 582-585.

Pritchett, D. B. & Seeburg, P. H. (1990). γ-aminobutyric $acid_A$ receptor α_5-subunit creates novel type II benzodiazepine receptor pharmacology. *J.Neurochem.* **54**, 1802-1804.

Puia, G., Mienville, J. M., Matsumoto, K., Takahata, H., Watanabe, H., Costa, E., & Guidotti, A. (2003). On the putative physiological role of allopregnanolone on $GABA_A$ receptor function. *Neuropharmacology* **44**, 49-55.

Purdy, R. H., Morrow, A. L., Moore, P. H., Jr., & Paul, S. M. (1991). Stress-induced elevations of γ-aminobutyric acid type A receptor-active steroids in the rat brain. *Proc.Natl.Acad.Sci.U.S.A* **88**, 4553-4557.

Purpura, D. P., Girado, M., & Grundfest, H. (1957). Selective blockade of excitatory synapses in the cat brain by γ-aminobutyric acid. *Science* **125**, 1200-1202.

Pytel, M., Mercik, K., & Mozrzymas, J. W. (2006). Interaction between cyclodextrin and neuronal membrane results in modulation of $GABA_A$ receptor conformational transitions. *Br.J.Pharmacol.* **148**, 413-422.

Quirk, K., Whiting, P. J., Ragan, C. I., & McKernan, R. M. (1995). Characterisation of δ-subunit containing $GABA_A$ receptors from rat brain. *Eur.J.Pharmacol.* **290**, 175-181.

Ramadan, E., Fu, Z., Losi, G., Homanics, G. E., Neale, J. H., & Vicini, S. (2003). $GABA_A$ receptor β3 subunit deletion decreases α2/3 subunits and IPSC duration. *J Neurophysiol* **89**, 128-134.

Rancz, E. A., Ishikawa, T., Duguid, I., Chadderton, P., Mahon, S., & Hausser, M. (2007). High-fidelity transmission of sensory information by single cerebellar mossy fibre boutons. *Nature* **450**, 1245-1248.

Reddy, D. S. (2010). Neurosteroids: endogenous role in the human brain and therapeutic potentials. *Prog.Brain Res.* **186**, 113-137.

Represa, A. & Ben Ari, Y. (2005). Trophic actions of GABA on neuronal development. *Trends Neurosci.* **28**, 278-283.

Reynolds, D. S., Rosahl, T. W., Cirone, J., O'Meara, G. F., Haythornthwaite, A., Newman, R. J., Myers, J., Sur, C., Howell, O., Rutter, A. R., Atack, J., Macaulay, A. J., Hadingham, K. L., Hutson, P. H., Belelli, D., Lambert, J. J., Dawson, G. R., McKernan, R., Whiting, P. J., &

Rudolph, U. & Mohler, H. (2004). Analysis of $GABA_A$ receptor function and dissection of the pharmacology of benzodiazepines and general anesthetics through mouse genetics. *Annu.Rev.Pharmacol.Toxicol.* **44**, 475-498.

Rudolph, U. & Knoflach, F. (2011). Beyond classical benzodiazepines: novel therapeutic potential of $GABA_A$ receptor subtypes. *Nat.Rev.Drug Discov.* **10**, 685-697.

Wafford, K. A. (2003). Sedation and anesthesia mediated by distinct $GABA_A$ receptor isoforms. *J. Neurosci.* **23**, 8608-8617.

Rheims, S., Minlebaev, M., Ivanov, A., Represa, A., Khazipov, R., Holmes, G. L., Ben Ari, Y., & Zilberter, Y. (2008). Excitatory GABA in rodent developing neocortex in vitro. *J.Neurophysiol.* **100**, 609-619.

Richerson, G. B. & Wu, Y. (2003). Dynamic equilibrium of neurotransmitter transporters: not just for reuptake anymore. *J.Neurophysiol.* **90**, 1363-1374.

Rick, C. E., Ye, Q., Finn, S. E., & Harrison, N. L. (1998). Neurosteroids act on the $GABA_A$ receptor at sites on the N-terminal side of the middle of TM2. *Neuroreport* **9**, 379-383.

Robel, P., Synguelakis, M., Halberg, F., & Baulieu, E. E. (1986). Persistence of the circadian rhythm of dehydroepiandrosterone in the brain, but not in the plasma, of castrated and adrenalectomized rats. *C.R.Acad.Sci.III* **303**, 235-238.

Roberts, E. & Frankel, S. (1950). γ-Aminobutyric acid in brain: its formation from glutamic acid. *J.Biol.Chem.* **187**, 55-63.

Roberts, E., Kuriyama, K., & Haber, B. (1970). Biochemistry of synaptic inhibition at the cellular level: the GABA system. *Adv.Biochem.Psychopharmacol.* **2**, 139-161.

Rossi, D. J. & Hamann, M. (1998). Spillover-mediated transmission at inhibitory synapses promoted by high affinity α_6 subunit $GABA_A$ receptors and glomerular geometry. *Neuron* **20**, 783-795.

Rovira, C. & Ben Ari, Y. (1993). Developmental study of benzodiazepine effects on monosynaptic $GABA_A$-mediated IPSPs of rat hippocampal neurons. *J.Neurophysiol.* **70**, 1076-1085.

Rozzo, A., Armellin, M., Franzot, J., Chiaruttini, C., Nistri, A., & Tongiorgi, E. (2002). Expression and dendritic mRNA localization of $GABA_C$ receptor rho1 and ρ2 subunits in developing rat brain and spinal cord. *Eur.J.Neurosci.* **15**, 1747-1758.

Rudolph, U., Crestani, F., Benke, D., Brunig, I., Benson, J. A., Fritschy, J. M., Martin, J. R., Bluethmann, H., & Möhler, H. (1999). Benzodiazepine actions mediated by specific γ-aminobutyric acid(A) receptor subtypes. *Nature* **401**, 796-800.

Rudolph, U. & Antkowiak, B. (2004). Molecular and neuronal substrates for general anaesthetics. *Nat.Rev.Neurosci.* **5**, 709-720.

Ruiz, A., Campanac, E., Scott, R. S., Rusakov, D. A., & Kullmann, D. M. (2010). Presynaptic $GABA_A$ receptors enhance transmission and LTP induction at hippocampal mossy fiber synapses. *Nat.Neurosci.* **13**, 431-438.

Rupprecht, R. & Holsboer, F. (1999). Neuroactive steroids: mechanisms of action and neuropsychopharmacological perspectives. *Trends Neurosci.* **22**, 410-416.

Rupprecht, R. (2003). Neuroactive steroids: mechanisms of action and neuropsychopharmacological properties. *Psychoneuroendocrinology* **28**, 139-168.

Rupprecht, R., Rammes, G., Eser, D., Baghai, T. C., Schule, C., Nothdurfter, C., Troxler, T., Gentsch, C., Kalkman, H. O., Chaperon, F., Uzunov, V., McAllister, K. H., Bertaina-Anglade, V., La Rochelle, C. D., Tuerck, D., Floesser, A., Kiese, B., Schumacher, M., Landgraf, R., Holsboer, F., & Kucher, K. (2009). Translocator protein (18 kD) as target for anxiolytics without benzodiazepine-like side effects. *Science* **325**, 490-493.

Rupprecht, R., Papadopoulos, V., Rammes, G., Baghai, T. C., Fan, J., Akula, N., Groyer, G., Adams, D., & Schumacher, M. (2010). Translocator protein (18 kDa) (TSPO) as a therapeutic target for neurological and psychiatric disorders. *Nat.Rev.Drug Discov.* **9**, 971-988.

Saalmann, Y. B., Kirkcaldie, M. T., Waldron, S., & Calford, M. B. (2007). Cellular distribution of the $GABA_A$ receptor-modulating 3α-hydroxy, 5α-reduced pregnane steroids in the adult rat brain. *J.Neuroendocrinol.* **19**, 272-284.

Sakmann, B. & Brenner, H. R. (1978). Change in synaptic channel gating during neuromuscular development. *Nature* **276**, 401-402.

Sakmann, B., Hamill, O. P., & Bormann, J. (1983). Patch-clamp measurements of elementary chloride currents activated by the putative inhibitory transmitter GABA and glycine in mammalian spinal neurons. *J.Neural Transm.Suppl* **18**, 83-95.

Sakmann, B. (1992). Nobel Lecture. Elementary steps in synaptic transmission revealed by currents through single ion channels. *Neuron* **8**, 613-629.

Salin, P. A. & Prince, D. A. (1996). Spontaneous $GABA_A$ receptor-mediated inhibitory currents in adult rat somatosensory cortex. *J.Neurophysiol.* **75**, 1573-1588.

Sanna, E., Mascia, M. P., Klein, R. L., Whiting, P. J., Biggio, G., & Harris, R. A. (1995). Actions of the general anesthetic propofol on recombinant human $GABA_A$ receptors: influence of receptor subunits. *J.Pharmacol.Exp.Ther.* **274**, 353-360.

Sanna, E., Talani, G., Busonero, F., Pisu, M. G., Purdy, R. H., Serra, M., & Biggio, G. (2004). Brain steroidogenesis mediates ethanol modulation of $GABA_A$ receptor activity in rat hippocampus. *J.Neurosci.* **24**, 6521-6530.

Santhakumar, V., Jones, R. T., & Mody, I. (2010). Developmental regulation and neuroprotective effects of striatal tonic $GABA_A$ currents. *Neuroscience* **167**, 644-655.

Saxena, N. C. & Macdonald, R. L. (1994). Assembly of $GABA_A$ receptor subunits: role of the δ subunit. *J.Neurosci.* **14**, 7077-7086.

Schlichter, R., Keller, A. F., De Roo, M., Breton, J. D., Inquimbert, P., & Poisbeau, P. (2006). Fast nongenomic effects of steroids on synaptic transmission and role of endogenous neurosteroids in spinal pain pathways. *J.Mol.Neurosci.* **28**, 33-51.

Schofield, P. R., Darlison, M. G., Fujita, N., Burt, D. R., Stephenson, F. A., Rodriguez, H., Rhee, L. M., Ramachandran, J., Reale, V., Glencorse, T. A., Seeburg, P. H., Barnard, E. A. (1987). Sequence and functional expression of the $GABA_A$ receptor shows a ligand-gated receptor super-family. *Nature* **328**, 221-227.

Scimemi, A., Semyanov, A., Sperk, G., Kullmann, D. M., & Walker, M. C. (2005). Multiple and plastic receptors mediate tonic $GABA_A$ receptor currents in the hippocampus. *J.Neurosci.* **25**, 10016-10024.

Sebe, J. Y., Looke-Stewart, E. C., Estrada, R. C., & Baraban, S. C. (2010). Robust tonic GABA currents can inhibit cell firing in mouse newborn neocortical pyramidal cells. *Eur.J.Neurosci.* **32**, 1310-1318.

Selye, H. (1941). Anaesthetic effects of steroid hormones. *Proc. Soc. Exp. Biol. Med.* **46**, 116-121.

Semyanov, A., Walker, M. C., & Kullmann, D. M. (2003). GABA uptake regulates cortical excitability via cell type-specific tonic inhibition. *Nat.Neurosci.* **6**, 484-490.

Semyanov, A., Walker, M. C., Kullmann, D. M., & Silver, R. A. (2004). Tonically active $GABA_A$ receptors: modulating gain and maintaining the tone. *Trends Neurosci.* **27**, 262-269.

Serwanski, D. R., Miralles, C. P., Christie, S. B., Mehta, A. K., Li, X., & De Blas, A. L. (2006). Synaptic and nonsynaptic localization of $GABA_A$ receptors containing the α5 subunit in the rat brain. *J.Comp Neurol.* **499**, 458-470.

Shen, H., Gong, Q. H., Aoki, C., Yuan, M., Ruderman, Y., Dattilo, M., Williams, K., & Smith, S. S. (2007). Reversal of neurosteroid effects at α4β2δ $GABA_A$ receptors triggers anxiety at puberty. *Nat.Neurosci.* **10**, 469-477.

Sherman, S. M. & Guillery, R. W. (2002). The role of the thalamus in the flow of information to the cortex. *Philos.Trans.R.Soc.Lond B Biol.Sci.* **357**, 1695-1708.

Shimada, S., Cutting, G., & Uhl, G. R. (1992). γ-Aminobutyric acid A or C receptor? γ-Aminobutyric acid ρ1 receptor RNA induces bicuculline-, barbiturate-, and

benzodiazepine-insensitive γ-aminobutyric acid responses in Xenopus oocytes. *Mol.Pharmacol.* **41**, 683-687.

Shu, H. J., Eisenman, L. N., Jinadasa, D., Covey, D. F., Zorumski, C. F., & Mennerick, S. (2004). Slow actions of neuroactive steroids at $GABA_A$ receptors. *J.Neurosci.* **24**, 6667-6675.

Shu, H. J., Zeng, C. M., Wang, C., Covey, D. F., Zorumski, C. F., & Mennerick, S. (2007). Cyclodextrins sequester neuroactive steroids and differentiate mechanisms that rate limit steroid actions. *Br.J.Pharmacol.* **150**, 164-175.

Sieghart, W. & Sperk, G. (2002). Subunit composition, distribution and function of $GABA_A$ receptor subtypes. *Curr.Top.Med.Chem.* **2**, 795-816.

Siegwart, R., Jurd, R., & Rudolph, U. (2002). Molecular determinants for the action of general anesthetics at recombinant $\alpha_2\beta_3\gamma_2$ γ-aminobutyric $acid_A$ receptors. *J.Neurochem.* **80**, 140-148.

Sierra, A. (2004). Neurosteroids: the StAR protein in the brain. *J.Neuroendocrinol.* **16**, 787-793.

Sigel, E., Stephenson, F. A., Mamalaki, C., & Barnard, E. A. (1983). A γ-aminobutyric acid/benzodiazepine receptor complex of bovine cerebral cortex. *J.Biol.Chem.* **258**, 6965-6971.

Sigel, E. & Buhr, A. (1997). The benzodiazepine binding site of $GABA_A$ receptors. *Trends Pharmacol.Sci.* **18**, 425-429.

Sigel, E. & Lüscher, B. P. (2011). A closer look at the high affinity benzodiazepine binding site on $GABA_A$ receptors. *Curr.Top.Med.Chem.* **11**, 241-246.

Sigworth, F. J. & Neher, E. (1980). Single Na^+ channel currents observed in cultured rat muscle cells. *Nature* **287**, 447-449.

Simon, J., Wakimoto, H., Fujita, N., Lalande, M., & Barnard, E. A. (2004). Analysis of the set of $GABA_A$ receptor genes in the human genome. *J.Biol.Chem.* **279**, 41422-41435.

Sixma, T. K. & Smit, A. B. (2003). Acetylcholine binding protein (AChBP): a secreted glial protein that provides a high-resolution model for the extracellular domain of pentameric ligand-gated ion channels. *Annu.Rev.Biophys.Biomol.Struct.* **32**, 311-334.

Skerritt, J. H., Willow, M., & Johnston, G. A. (1982). Diazepam enhancement of low affinity GABA binding to rat brain membranes. *Neurosci.Lett.* **29**, 63-66.

Smith, K. E., Borden, L. A., Wang, C. H., Hartig, P. R., Branchek, T. A., & Weinshank, R. L. (1992). Cloning and expression of a high affinity taurine transporter from rat brain. *Mol.Pharmacol.* **42**, 563-569.

Sohal, V. S. & Huguenard, J. R. (2003). Inhibitory interconnections control burst pattern and emergent network synchrony in reticular thalamus. *J.Neurosci.* **23**, 8978-8988.

Somogyi, P., Fritschy, J. M., Benke, D., Roberts, J. D., & Sieghart, W. (1996). The γ_2 subunit of the $GABA_A$ receptor is concentrated in synaptic junctions containing the α_1 and $\beta_{2/3}$ subunits in hippocampus, cerebellum and globus pallidus. *Neuropharmacology* **35**, 1425-1444.

Song, I., Savtchenko, L., & Semyanov, A. (2011). Tonic excitation or inhibition is set by $GABA_A$ conductance in hippocampal interneurons. *Nat.Commun.* **2**, 376.

Spigelman, I., Li, Z., Liang, J., Cagetti, E., Samzadeh, S., Mihalek, R. M., Homanics, G. E., & Olsen, R. W. (2003). Reduced inhibition and sensitivity to neurosteroids in hippocampus of mice lacking the $GABA_A$ receptor δ subunit. *J Neurophysiol* **90**, 903-910.

Staley, K. J. & Mody, I. (1991). Integrity of perforant path fibers and the frequency of action potential independent excitatory and inhibitory synaptic events in dentate gyrus granule cells. *Synapse* **9**, 219-224.

Stell, B. M., Brickley, S. G., Tang, C. Y., Farrant, M., & Mody, I. (2003). Neuroactive steroids reduce neuronal excitability by selectively enhancing tonic inhibition mediated by δ subunit-containing $GABA_A$ receptors. *Proc.Natl.Acad.Sci.U.S.A* **100**, 14439-14444.

Steriade, M. (1997). Synchronized activities of coupled oscillators in the cerebral cortex and thalamus at different levels of vigilance. *Cereb.Cortex* **7**, 583-604.

Storustovu, S. I. & Ebert, B. (2006). Pharmacological characterization of agonists at δ-containing $GABA_A$ receptors: Functional selectivity for extrasynaptic receptors is dependent on the absence of γ_2. *J.Pharmacol.Exp.Ther.* **316**, 1351-1359.

Study, R. E. & Barker, J. L. (1981). Diazepam and (--)-pentobarbital: fluctuation analysis reveals different mechanisms for potentiation of γ-aminobutyric acid responses in cultured central neurons. *Proc.Natl.Acad.Sci.U.S.A* **78**, 7180-7184.

Sucher, N. J. & Deitcher, D. L. (1995). PCR and patch-clamp analysis of single neurons. *Neuron* **14**, 1095-1100.

Sudhof, T. C. (2004). The synaptic vesicle cycle. *Annu.Rev.Neurosci.* **27**, 509-547.

Sur, C., Farrar, S. J., Kerby, J., Whiting, P. J., Atack, J. R., & McKernan, R. M. (1999). Preferential coassembly of α_4 and δ subunits of the γ-aminobutyric acidA receptor in rat thalamus. *Mol.Pharmacol.* **56**, 110-115.

Sur, C., Wafford, K. A., Reynolds, D. S., Hadingham, K. L., Bromidge, F., Macaulay, A., Collinson, N., O'Meara, G., Howell, O., Newman, R., Myers, J., Atack, J. R., Dawson, G. R., McKernan, R. M., Whiting, P. J., & Rosahl, T. W. (2001). Loss of the major $GABA_A$ receptor subtype in the brain is not lethal in mice. *J.Neurosci.* **21**, 3409-3418.

Suter, K. J., Song, W. J., Sampson, T. L., Wuarin, J. P., Saunders, J. T., Dudek, F. E., & Moenter, S. M. (2000). Genetic targeting of green fluorescent protein to gonadotropin-releasing hormone neurons: characterization of whole-cell electrophysiological properties and morphology. *Endocrinology* **141**, 412-419.

Synguelakis, M., Halberg, F., Baulieu, E. E., & Robel, P. (1985). Circadian course of δ 5,3 β-hydroxysteroids and glucocorticosteroids in the plasma and brain of rats. *C.R.Acad.Sci.III* **301**, 823-826.

Szejtli, J. (1998). Introduction and general overview of cyclodextrin chemistry. *Chem.Rev.* **98**, 1743-1754.

Takahashi, T., Momiyama, A., Hirai, K., Hishinuma, F., & Akagi, H. (1992). Functional correlation of fetal and adult forms of glycine receptors with developmental changes in inhibitory synaptic receptor channels. *Neuron* **9**, 1155-1161.

Takahashi, T., Feldmeyer, D., Suzuki, N., Onodera, K., Cull-Candy, S. G., Sakimura, K., & Mishina, M. (1996). Functional correlation of NMDA receptor epsilon subunits expression with the properties of single-channel and synaptic currents in the developing cerebellum. *J.Neurosci.* **16**, 4376-4382.

Takahashi, T. (2005). Postsynaptic receptor mechanisms underlying developmental speeding of synaptic transmission. *Neurosci.Res.* **53**, 229-240.

Tallman, J. F. & Gallager, D. W. (1985). The GABA-ergic system: a locus of benzodiazepine action. *Annu.Rev.Neurosci.* **8**, 21-44.

Tamamaki, N., Yanagawa, Y., Tomioka, R., Miyazaki, J., Obata, K., & Kaneko, T. (2003). Green fluorescent protein expression and colocalization with calretinin,

parvalbumin, and somatostatin in the GAD67-GFP knock-in mouse. *J.Comp Neurol.* **467**, 60-79.

Tang, Z. Q., Dinh, E. H., Shi, W., & Lu, Y. (2011). Ambient GABA-activated tonic inhibition sharpens auditory coincidence detection via a depolarizing shunting mechanism. *J.Neurosci.* **31**, 6121-6131.

Taschenberger, H. & von Gersdorff, H. (2000). Fine-tuning an auditory synapse for speed and fidelity: developmental changes in presynaptic waveform, EPSC kinetics, and synaptic plasticity. *J.Neurosci.* **20**, 9162-9173.

Tasneem, A., Iyer, L. M., Jakobsson, E., & Aravind, L. (2005). Identification of the prokaryotic ligand-gated ion channels and their implications for the mechanisms and origins of animal Cys-loop ion channels. *Genome Biol.* **6**, R4.

Telgkamp, P., Padgett, D. E., Ledoux, V. A., Woolley, C. S., & Raman, I. M. (2004). Maintenance of high-frequency transmission at purkinje to cerebellar nuclear synapses by spillover from boutons with multiple release sites. *Neuron* **41**, 113-126.

Thompson, S. A., Whiting, P. J., & Wafford, K. A. (1996). Barbiturate interactions at the human $GABA_A$ receptor: dependence on receptor subunit combination. *Br.J.Pharmacol.* **117**, 521-527.

Tia, S., Wang, J. F., Kotchabhakdi, N., & Vicini, S. (1996). Developmental changes of inhibitory synaptic currents in cerebellar granule neurons: role of $GABA_A$ receptor α_6 subunit. *J.Neurosci.* **16**, 3630-3640.

Tian, N., Petersen, C., Kash, S., Baekkeskov, S., Copenhagen, D., & Nicoll, R. (1999). The role of the synthetic enzyme GAD65 in the control of neuronal γ-aminobutyric acid release. *Proc.Natl.Acad.Sci.U.S.A* **96**, 12911-12916.

Titz, S., Hans, M., Kelsch, W., Lewen, A., Swandulla, D., & Misgeld, U. (2003). Hyperpolarizing inhibition develops without trophic support by GABA in cultured rat midbrain neurons. *J.Physiol* **550**, 719-730.

Tokuda, K., Izumi, Y., & Zorumski, C. F. (2011). Ethanol enhances neurosteroidogenesis in hippocampal pyramidal neurons by paradoxical NMDA receptor activation. *J.Neurosci.* **31**, 9905-9909.

Torres, V. I. & Weiss, D. S. (2002). Identification of a tyrosine in the agonist binding site of the homomeric ρ1 γ-aminobutyric acid (GABA) receptor that, when mutated, produces spontaneous opening. *J.Biol.Chem.* **277**, 43741-43748.

Tossman, U., Segovia, J., & Ungerstedt, U. (1986). Extracellular levels of amino acids in striatum and globus pallidus of 6-hydroxydopamine-lesioned rats measured with microdialysis. *Acta Physiol Scand.* **127**, 547-551.

Toyoshima, C. & Unwin, N. (1988). Ion channel of acetylcholine receptor reconstructed from images of postsynaptic membranes. *Nature* **336**, 247-250.

Tretter, V., Ehya, N., Fuchs, K., & Sieghart, W. (1997). Stoichiometry and assembly of a recombinant $GABA_A$ receptor subtype. *J.Neurosci.* **17**, 2728-2737.

Tretter, V., Hauer, B., Nusser, Z., Mihalek, R. M., Hoger, H., Homanics, G. E., Somogyi, P., & Sieghart, W. (2001). Targeted disruption of the $GABA_A$ receptor δ subunit gene leads to an up-regulation of γ2 subunit-containing receptors in cerebellar granule cells. *J.Biol.Chem.* **276**, 10532-10538.

Tretter, V., Jacob, T. C., Mukherjee, J., Fritschy, J. M., Pangalos, M. N., & Moss, S. J. (2008). The clustering of $GABA_A$ receptor subtypes at inhibitory synapses is facilitated via the direct binding of receptor α2 subunits to gephyrin. *J.Neurosci.* **28**, 1356-1365.

Trigo, F. F., Marty, A., & Stell, B. M. (2008). Axonal $GABA_A$ receptors. *Eur.J.Neurosci.* **28**, 841-848.

Tscherter, A., David, F., Ivanova, T., Deleuze, C., Renger, J. J., Uebele, V. N., Shin, H. S., Bal, T., Leresche, N., & Lambert, R. C. (2011). Minimal alterations in T-type calcium channel gating markedly modify physiological firing dynamics. *J.Physiol* **589**, 1707-1724.

Tsuruo, Y., Miyamoto, T., Yokoi, H., Kitagawa, K., Futaki, S., & Ishimura, K. (1996). Immunohistochemical presence of 5α-reductase rat type 1-containing cells in the rat brain. *Brain Res.* **722**, 207-211.

Tsuruo, Y. (2005). Topography and function of androgen-metabolizing enzymes in the central nervous system. *Anat.Sci.Int.* **80**, 1-11.

Tsutsui, K. (2008). Neurosteroids in the Purkinje cell: biosynthesis, mode of action and functional significance. *Mol.Neurobiol.* **37**, 116-125.

Twyman, R. E. & Macdonald, R. L. (1992). Neurosteroid regulation of $GABA_A$ receptor single-channel kinetic properties of mouse spinal cord neurons in culture. *J.Physiol* **456**, 215-245.

Tyzio, R., Represa, A., Jorquera, I., Ben Ari, Y., Gozlan, H., & Aniksztejn, L. (1999). The establishment of GABAergic and glutamatergic synapses on CA1 pyramidal

neurons is sequential and correlates with the development of the apical dendrite. *J.Neurosci.* **19**, 10372-10382.

Udenfriend, S. (1950). Identification of γ-aminobutyric acid in brain by the isotope derivative method. *J.Biol.Chem.* **187**, 65-69.

Ulrich, D. & Bettler, B. (2007). $GABA_B$ receptors: synaptic functions and mechanisms of diversity. *Curr.Opin.Neurobiol.* **17**, 298-303.

Unwin, N. (1993). Nicotinic acetylcholine receptor at 9Å resolution. *J.Mol.Biol.* **229**, 1101-1124.

Unwin, N. (2003). Structure and action of the nicotinic acetylcholine receptor explored by electron microscopy. *FEBS Lett.* **555**, 91-95.

Unwin, N. (2005). Refined structure of the nicotinic acetylcholine receptor at 4Å resolution. *J.Mol.Biol.* **346**, 967-989.

Uzunova, V., Sheline, Y., Davis, J. M., Rasmusson, A., Uzunov, D. P., Costa, E., & Guidotti, A. (1998). Increase in the cerebrospinal fluid content of neurosteroids in patients with unipolar major depression who are receiving fluoxetine or fluvoxamine. *Proc.Natl.Acad.Sci.U.S.A* **95**, 3239-3244.

Van Eden, C. G., Parmar, R., Lichtensteiger, W., & Schlumpf, M. (1995). Laminar distribution of $GABA_A$ receptor α1, β2, and γ2 subunit mRNAs in the granular and agranular frontal cortex of the rat during pre- and postnatal development. *Cereb.Cortex* **5** , 234-246.

Vautrin, J., Schaffner, A. E., Fontas, B., & Barker, J. L. (1993). Frequency modulation of transmitter release. *J.Physiol Paris* **87**, 51-73.

Verdoorn, T. A. (1994). Formation of heteromeric γ-aminobutyric acid type A receptors containing two different α subunits. *Mol.Pharmacol.* **45**, 475-480.

Verleye, M., Akwa, Y., Liere, P., Ladurelle, N., Pianos, A., Eychenne, B., Schumacher, M., & Gillardin, J. M. (2005). The anxiolytic etifoxine activates the peripheral benzodiazepine receptor and increases the neurosteroid levels in rat brain. *Pharmacol.Biochem.Behav.* **82**, 712-720.

Vicini, S., Ferguson, C., Prybylowski, K., Kralic, J., Morrow, A. L., & Homanics, G. E. (2001). $GABA_A$ receptor α1 subunit deletion prevents developmental changes of inhibitory synaptic currents in cerebellar neurons. *J Neurosci.* **21**, 3009-3016.

Vicini, S., Losi, G., & Homanics, G. E. (2002). $GABA_A$ receptor δ subunit deletion prevents neurosteroid modulation of inhibitory synaptic currents in cerebellar neurons. *Neuropharmacology* **43**, 646-650.

Vinnakota, S., Qian, X., Egal, H., Sarthy, V., & Sarkar, H. K. (1997). Molecular characterization and in situ localization of a mouse retinal taurine transporter. *J.Neurochem.* **69**, 2238-2250.

Vithlani, M., Terunuma, M., & Moss, S. J. (2011). The dynamic modulation of $GABA_A$ receptor trafficking and its role in regulating the plasticity of inhibitory synapses. *Physiol Rev.* **91**, 1009-1022.

Wafford, K. A., Thompson, S. A., Thomas, D., Sikela, J., Wilcox, A. S., & Whiting, P. J. (1996). Functional characterization of human γ-aminobutyric acidA receptors containing the α_4 subunit. *Mol.Pharmacol.* **50**, 670-678.

Wafford, K. A., van Niel, M. B., Ma, Q. P., Horridge, E., Herd, M. B., Peden, D. R., Belelli, D., & Lambert, J. J. (2009). Novel compounds selectively enhance δ subunit containing $GABA_A$ receptors and increase tonic currents in thalamus. *Neuropharmacology* **56**, 182-189.

Wall, M. J. & Usowicz, M. M. (1997). Development of action potential-dependent and independent spontaneous $GABA_A$ receptor-mediated currents in granule cells of postnatal rat cerebellum. *Eur.J.Neurosci.* **9**, 533-548.

Wallner, M., Hanchar, H. J., & Olsen, R. W. (2003). Ethanol enhances $\alpha_4\beta_3\delta$ and $\alpha_6\beta_3\delta$ γ-aminobutyric acid type A receptors at low concentrations known to affect humans. *Proc.Natl.Acad.Sci.U.S.A* **100**, 15218-15223.

Wang, D. S. & Orser, B. A. (2011). Inhibition of learning and memory by general anesthetics. *Can.J.Anaesth.* **58**, 167-177.

Wang, J. M., Johnston, P. B., Ball, B. G., & Brinton, R. D. (2005). The neurosteroid allopregnanolone promotes proliferation of rodent and human neural progenitor cells and regulates cell-cycle gene and protein expression. *J.Neurosci.* **25**, 4706-4718.

Wang, J. M. & Brinton, R. D. (2008). Allopregnanolone-induced rise in intracellular calcium in embryonic hippocampal neurons parallels their proliferative potential. *BMC.Neurosci.* **9 Suppl 2**, S11.

Wasser, C. R., Ertunc, M., Liu, X., & Kavalali, E. T. (2007). Cholesterol-dependent balance between evoked and spontaneous synaptic vesicle recycling. *J.Physiol* **579**, 413-429.

Wei, W., Zhang, N., Peng, Z., Houser, C. R., & Mody, I. (2003). Perisynaptic localization of delta subunit-containing $GABA_A$ receptors and their activation by GABA spillover in the mouse dentate gyrus. *J.Neurosci.* **23**, 10650-10661.

Wei, J. & Wu, J. Y. (2008). Post-translational regulation of L-glutamic acid decarboxylase in the brain. *Neurochem.Res.* **33**, 1459-1465.

White, G. (1992). Heterogeneity in EC50 and nH of $GABA_A$ receptors on dorsal root ganglion neurons freshly isolated from adult rats. *Brain Res.* **585**, 56-62.

Whiting, P., McKernan, R. M., & Iversen, L. L. (1990). Another mechanism for creating diversity in γ-aminobutyrate type A receptors: RNA splicing directs expression of two forms of γ_2 phosphorylation site. *Proc.Natl.Acad.Sci.U.S.A* **87**, 9966-9970.

Whiting, P. J. (2003). $GABA_A$ receptor subtypes in the brain: a paradigm for CNS drug discovery? *Drug Discov.Today* **8**, 445-450.

Wick, M. J., Radcliffe, R. A., Bowers, B. J., Mascia, M. P., Lüscher, B., Harris, R. A., & Wehner, J. M. (2000). Behavioural changes produced by transgenic overexpression of γ_2L and γ_2S subunits of the $GABA_A$ receptor. *Eur.J.Neurosci.* **12**, 2634-2638.

Wieland, H. A., Lüddens, H., & Seeburg, P. H. (1992). A single histidine in $GABA_A$ receptors is essential for benzodiazepine agonist binding. *J. Biol.Chem.* **267**, 1426-1429.

Wingrove, P. B., Wafford, K. A., Bain, C., & Whiting, P. J. (1994). The modulatory action of loreclezole at the γ-aminobutyric acid type A receptor is determined by a single amino acid in the β_2 and β_3 subunit. *Proc.Natl.Acad.Sci.U.S.A* **91**, 4569-4573.

Wisden, W., Laurie, D. J., Monyer, H., & Seeburg, P. H. (1992). The distribution of 13 $GABA_A$ receptor subunit mRNAs in the rat brain. I. Telencephalon, diencephalon, mesencephalon. *J.Neurosci.* **12**, 1040-1062.

Wittmer, L. L., Hu, Y., Kalkbrenner, M., Evers, A. S., Zorumski, C. F., & Covey, D. F. (1996). Enantioselectivity of steroid-induced γ-aminobutyric acidA receptor modulation and anesthesia. *Mol.Pharmacol.* **50**, 1581-1586.

Wohlfarth, K. M., Bianchi, M. T., & Macdonald, R. L. (2002). Enhanced neurosteroid potentiation of ternary $GABA_A$ receptors containing the δ subunit. *J.Neurosci.* **22**, 1541-1549.

Wu, Y., Wang, W., Diez-Sampedro, A., & Richerson, G. B. (2007). Nonvesicular inhibitory neurotransmission via reversal of the GABA transporter GAT-1. *Neuron* **56**, 851-865.

Wu, Z. Y. & Xu, T. L. (2003). Taurine-evoked chloride current and its potentiation by intracellular Ca^{2+} in immature rat hippocampal CA1 neurons. *Amino.Acids* **24**, 155-161.

Xi, Z. X., Ramamoorthy, S., Shen, H., Lake, R., Samuvel, D. J., & Kalivas, P. W. (2003). GABA transmission in the nucleus accumbens is altered after withdrawal from repeated cocaine. *J.Neurosci.* **23**, 3498-3505.

Xu, J. & Wojcik, W. J. (1986). *Gamma* aminobutyric acid B receptor-mediated inhibition of adenylate cyclase in cultured cerebellar granule cells: blockade by islet-activating protein. *J.Pharmacol.Exp.Ther.* **239**, 568-573.

Yamauchi, A., Uchida, S., Kwon, H. M., Preston, A. S., Robey, R. B., Garcia-Perez, A., Burg, M. B., & Handler, J. S. (1992). Cloning of a Na^+- and Cl^--dependent betaine transporter that is regulated by hypertonicity. *J.Biol.Chem.* **267**, 649-652.

Yancey, P. G., Rodrigueza, W. V., Kilsdonk, E. P., Stoudt, G. W., Johnson, W. J., Phillips, M. C., & Rothblat, G. H. (1996). Cellular cholesterol efflux mediated by cyclodextrins. Demonstration of kinetic pools and mechanism of efflux. *J.Biol.Chem.* **271**, 16026-16034.

Yuste, R. & Katz, L. C. (1991). Control of postsynaptic Ca^{2+} influx in developing neocortex by excitatory and inhibitory neurotransmitters. *Neuron* **6**, 333-344.

Zeilhofer, H. U., Witschi, R., & Hosl, K. (2009). Subtype-selective $GABA_A$ receptor mimetics--novel antihyperalgesic agents? *J.Mol.Med.(Berl)* **87**, 465-469.

Zeller, A., Arras, M., Jurd, R., & Rudolph, U. (2007). Mapping the contribution of β3-containing $GABA_A$ receptors to volatile and intravenous general anesthetic actions. *BMC.Pharmacol.* **7**, 2.

Zhang, N., Wei, W., Mody, I., & Houser, C. R. (2007). Altered localization of $GABA_A$ receptor subunits on dentate granule cell dendrites influences tonic and phasic inhibition in a mouse model of epilepsy. *J.Neurosci.* **27**, 7520-7531.

Zhang, S. J., Huguenard, J. R., & Prince, D. A. (1997). $GABA_A$ receptor-mediated Cl^- currents in rat thalamic reticular and relay neurons. *J.Neurophysiol.* **78**, 2280-2286.

Zhu, W. J. & Vicini, S. (1997). Neurosteroid prolongs $GABA_A$ channel deactivation by altering kinetics of desensitized states. *J Neurosci.* **17**, 4022-4031.

Zhu, X. M. & Ong, W. Y. (2004). A light and electron microscopic study of betaine/GABA transporter distribution in the monkey cerebral neocortex and hippocampus. *J.Neurocytol.* **33**, 233-240.

Zimprich, F., Zezula, J., Sieghart, W., & Lassmann, H. (1991). Immunohistochemical localization of the α_1, α_2 and α_3 subunit of the $GABA_A$ receptor in the rat brain. *Neurosci.Lett.* **127**, 125-128.